Authors are requested to submit three copies of manuscripts and illustrations to the Editorial Department, Institute of Radio Engineers, 1 East 79 St., New York 21, N. Y.

Responsibility for the contents of papers published in the PROCEEDINGS OF THE IRE rests upon the authors. Statements made in papers are not binding on the IRE or its members.

Change of address (with 15 days advance notice) and letters regarding subscriptions and payments should be mailed to the Secretary of the IRE, 1 East 79 Street, New York 21, N. Y.

PROCEEDINGS OF THE IRE®

Published Monthly by

The Institute of Radio Engineers, Inc.

VOLUME 45 — *October, 1957* — NUMBER 10

CONTENTS

ADVERTISING SECTION

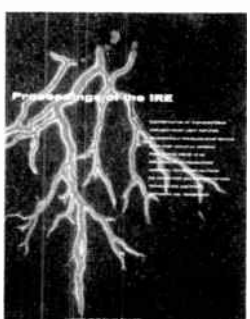

THE COVER—The release of hundreds of kilowatt hours of electrical energy in a single stroke of lightning is a major source of noise in radio communications systems. Although the physics of this discharge is simple in concept, its detailed description is so complex that even today the processes by which lightning is generated are not fully understood. An excellent review of the presently available facts and most recent authoritative conclusions concerning this phenomenon is presented in the article on page 1331.

Scanning the Issue

The Electrification of Precipitation and Thunderstorms (Gunn, p. 1331)—Despite the fact that lightning is one of nature's most commonplace spectacles, the mechanisms by which it is produced has remained one of the major puzzles of science. It is evident that a predominance of electrical charges of a like sign builds up in a rain cloud until the electric field intensity exceeds the dielectric strength of the atmosphere. At this moment, it is estimated, the cloud potential exceeds 100 million volts and the lightning discharge that follows will probably expend 500 killowatt hours of energy. But by what processes is this enormous store of electrical energy accumulated? The importance of static in radio communications and an avid curiosity about its origin prompted the PROCEEDINGS editors to find out. They turned to one of the world's leading authorities for an explanation of the basic physical processes involved. The result is a paper which all readers will find rewarding and stimulating. Despite the complexity of the subject, the author unravels in a clear fashion much of the mystery surrounding this awesome phenomenon. Starting with the generation of ion pairs in the atmosphere by cosmic rays and other mechanisms, the reader is taken through the steps by which rain drops become selectively electrified and a final gross separation of positive and negative charges occurs. The discussion discloses new facts as well as reviewing old ones in what is probably the most complete and authoritative explanation of the generation of atmospheric electricity that has yet been published.

An Improved High-Gain Panel Light Amplifier (Kazan, p. 1358)—The panel light amplifier is a relatively new device which has many interesting potential uses. In essence, it consists of a layer of photoconductive material (cadmium sulfide powder) followed by a layer of electroluminescent phosphor, with an ac voltage applied across the two layers. In the dark the high impedance of the CdS layer permits only a negligible fraction of the ac voltage to be applied across the phosphor layer. When light falls on the CdS, its resistance decreases and a greater exciting voltage appears across the phosphor layer, resulting in the emission of light at a greater intensity than the input light falling on the CdS layer. This paper reports on some substantial improvements that have been made since the first experimental model was announced two years ago. These improvements have to do with the method of connecting the individual photoconductive elements in the panel to the rest of the circuit so as to enable a more efficient type of operation, and the development of a more sensitive CdS powder. The result is a much improved light amplifier whose gain is 10 times greater than any previous amplifier and whose threshold for input light is greatly reduced. The high gains and long persistence of the device make it potentially useful in intensifying the low-light-level images that are common to slow-scan TV and certain radar screens. Moreover, the device is sensitive to infrared and, especially, X-ray radiation. In the latter case the light amplifier can convert an X-ray image into a visible picture 100 times brighter than a fluoroscope screen which, until now, has been the primary means of direct viewing of X-rays.

The Large-Signal Behavior of Crossed-Field Traveling-Wave Devices (Feinstein and Kino, p. 1364)—This paper considers a class of traveling-wave devices in which the electron beam flow is perpendicular to both the dc electric and magnetic fields. After developing a large-signal theory of operation, the authors employ an analog computer to analyze the operating characteristics of a forward-wave amplifier, backward-wave amplifier and backward-wave oscillator. The results show clearly the relative merits and limitations of these devices with respect to gain and efficiency. This is the first large-signal analysis that has been made of crossed-field tubes, and as such represents an important, original contribution to the microwave tube field.

A Versatile Multiport Biconical Antenna (Honey and Jones, p. 1374)—A novel antenna system has been developed which can be used as a new type of direction finder or as a multiplexer at microwave frequencies. The antenna itself consists of two flared cones mounted in tandem so that the neck of one points down the mouth of the one behind. The antenna feeds into a coaxial line, each quadrant of which is channelled off into a separate waveguide. The direction of arrival of an inconing signal is given by the relative amplitudes of the signals in the four waveguides. Alternatively, with additional waveguide circuitry the propagation modes in the system can be separated and brought out to three separate ports. The phase difference between two of them again gives the angle of arrival of a received signal. Because the three ports are well isolated from each other, this latter arrangement can be turned around and used as a multiplexing system and omnidirectional transmitting antenna. The novelty and versatility of the system will make it of considerable interest in the fields of antennas, microwave communications and navigational electronics.

Radio Propagation Above 40 MC Over Irregular Terrain (Egli, p. 1383)—Radio transmission above 40 mc usually takes place over terrain which is dotted with trees, buildings and other irregularities so that the standard formulas for calculating propagation attenuation under idealized conditions become unsatisfactory. In this paper the author analyzes a large number of propagation measurements, made in the past by various organizations, in an effort to derive empirically relations for terrain effects versus frequency, antenna height, polarization and distance. His results, presented in the form of nomographs and correction curves, will be very useful to those dealing with the service area of vhf and uhf broadcasting stations and mobile communication systems covering distances up to 40 miles. In particular, this study will find direct application to problems of systems design, frequency allocation, and interference evaluation.

Design Theory for Depletion Layer Transistors (Gärtner, p. 1392)—The continuing effort to increase the operating frequencies of transistors is aimed primarily at two problems: increasing the speed with which carriers travel from the emitter to the collector junction, and reducing the values of the internal RC combinations in the transistor. Because very high electric fields may be created in the depletion layer of a reverse-biased p-n junction, it has been proposed that injecting carriers into this region would result in maximum attainable carrier speeds, thus meeting the first problem. At the same time, careful design would, it is felt, keep the RC values low enough to insure operation up to microwave frequencies. This paper takes a theoretical excursion into the design of this new type of transistor, presenting valuable information on the behavior of one form of the device and suggesting other forms and modes of operation for future study.

A Note on Numerical Transform Calculus (Boxer, p. 1401)—Over the past ten years several numerical transform techniques have been developed for solving integro-differential equations of a type that arise in problems involving linear and nonlinear systems. These techniques have proved valuable in analyzing the behavior of networks and in using digital computers in the solution of problems. This paper modifies and extends previous methods by overcoming the difficulty of including the initial conditions in the working of the problem and by increasing the accuracy of the solution.

Poles and Zeros

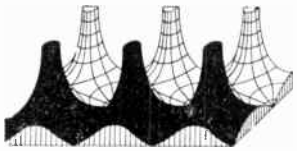

Questions. Two issues ago, in announcing the recent formation of the Professional Group on Education, we expressed the hope that this group would quickly uncover problems peculiar to education in electronics and the allied arts. Now, from another source, comes a proposal that would appear to be proper grist for the PGE mill.

Writing in a recent issue of *Harper's Magazine* ("Can We Grow Geniuses in Science?," June, 1957), Lancelot Law Whyte asks in effect: How can outstanding students of science and engineering be inspired to original thinking, to the synthesis of new and embracing concepts? How can they be turned away from preoccupation with mere elaboration or refinement of past art?

Mr. Whyte's answer* is: "Ask the right question. . . . It is a commonplace that fertile scientific activity results from posing of the right questions. But they must not only be posed, the attention of the young must be called to them as a deliberate policy. . . . We cannot produce genius at will, but if it is there we can provoke it. We cannot say whether America will produce an Einstein tomorrow, but we can at least plant flags in the unknown." Whyte proposes that faculties concerned with scientific education should proclaim each year "ten unsolved fundamental problems lying in the broad field of the faculties . . . and let these problems be collected in a master Book of Problems, lying open to all on the reference desk of every scientific library."

Why, indeed, should not the PGE Administrative Committee set up as one of its immediate objectives the compilation of an IRE Book of Problems and give it wide circulation among students and teachers in science and engineering? The other Professional Groups could act as expert advisers in choosing the questions and phrasing them incisively, to stimulate rather than to baffle. Some questions would be of the fundamental type proposed by Mr. Whyte; others might relate to more immediate concerns, such as improvements in the design and application of devices and components.

Examples readily come to mind. In the fundamental realm, the PG on Information Theory has been wrestling in the pages of its *TRANSACTIONS* with the conceptual difficulties associated with the word entropy. Originally devised for thermodynamics, this term has been adopted by students of information theory because there is an engaging similarity between the disorder of a thermodynamical system and the disorder of an information transmission system. But the analogy is by no means exact, and use of one word to cover the two situations may in fact generate more confusion than understanding. An IRE Problem posed to bring out the subtle distinctions in the disorder states of communication systems, versus other disorderly disciplines, might well be on the list.

As a second example, closer to home, the PG on Electron Devices might well draw attention to the wide gulf separating our understanding of semiconductors as used in the cathodes of vacuum tubes, as contrasted with their use as the base material in transistors. The former is still cook-book artistry after 40 years; the latter has become almost an exact science in a decade. What insight, what controls and measurements are needed to take oxide cathodes out of the kitchen? As a third example, if we want to uncover a second Einstein, the PG on Antennas and Propagation might wish to pose the problem of the propagation velocity of the field of gravity, its detection and measurement.

Participation. The educational matters discussed above are just as much the concern of the non-educational members of IRE as they are of the professors. In fact, one of our most prominent educators has been heard to observe that, if you leave such matters to the likes of him without industry drive behind them, not much concrete progress can be expected. So the constitution of the PG on Education wisely provides that half the membership of the Administrative Committee shall be from the teaching profession and half from industry. Practicing engineers and scientists in industry who have ideas to offer or axes to grind in the educational sphere are therefore urged to join this group and to make themselves available to assist in its management. Write HQ for the application blank; the assessment is $3.00 per year.

Reminder. We hope to close the books on the IRE Editorial Survey at the end of next month. So, if you have not participated in the survey, consult the PROCEEDINGS for June 1957, pages 737 and 884. Then write your Section Chairman.—D.G.F.

*Quoted by permission. Copyright 1957 by Harper & Brothers.

Frank A. Polkinghorn

DIRECTOR, 1957–1958

Frank A. Polkinghorn was born in Massachusetts and received his education in California, graduating from the University of California (Berkeley) in 1922 with honors in electrical engineering and membership in Eta Kappa Nu, Tau Beta Pi, Sigma Xi and Phi Beta Kappa.

From 1922 to 1924 he was employed in the Radio Laboratory of the Mare Island Navy Yard. In 1924 he became Chief Engineer of the A-P Radio Laboratories, successors to the Moorhead Laboratories, one of the early manufacturers of vacuum tubes. In 1925 he entered the employ of the Pacific Telephone & Telegraph Co. in San Francisco as a transmission engineer, transferring to the Radio Research Department of the Bell Telephone Laboratories in 1927.

From 1928 to 1948 he had a prominent part in the establishment of the high frequency transoceanic radiotelephone circuits of the A. T. & T. Co., including pioneer work in the use of single sideband operation. He was also active in the early applications of frequencies above this range to point-to-point applications. During World War II he did work on the Loran system, various radar systems, and bombsight and communication projects.

From 1948 to 1950 he was on loan to the Army in Japan, where he was Director of the Research and Development Division, Civil Communications Section, Supreme Command for Allied Powers, in which position he had supervision of all communications research, development, and manufacturing in Japan. In appreciation for this work he was elected an Honorary Member of Denki Tsushin Gakkai, the Japanese counterpart of the IRE.

He served on several receiver committees in the 1930's; his participation on the High Frequency Receiver Committee resulted in the IRE standardization in 1932 of the use of resistance noise for the rating of radio receivers. He was a member of the Admissions Committee from 1941 to 1948 and was largely responsible for the writing of the Admissions Manual. He has also served on the Sections and National Convention Committees and is presently a member of the Policy Advisory Committee. He held various offices in the Northern New Jersey Subsection and became the first full-term Chairman of the Northern New Jersey Section in 1954.

He is a member of the AIEE, AAAS, Montclair Society of Engineers, Armed Forces Communication & Electronics Association and is a licensed professional engineer of the State of New York. In addition, he rose from IRE Associate in 1925 to Fellow in 1938.

The Electrification of Precipitation and Thunderstorms*

ROSS GUNN†, FELLOW, IRE

The following paper is one of a planned series of invited papers, in which men of recognized standing will review recent developments in, and the present status of, various fields in which noteworthy progress has been made.—*The Editor*

Summary—**The fundamental physical processes responsible for the observed electrification of ordinary precipitating clouds, as well as thunderstorms, is considered in quantitative terms and new facts are emphasized. Cosmic rays and radioactivity, sometimes supplemented by corona and photoionization, produce ion pairs in the atmosphere. These ions are transferred to cloud droplets or ice crystals by diffusion or by electric fields and thereby establish a droplet charge distribution. This distribution is profoundly influenced by the observed differences between the positive and negative light ion conductivities in the atmosphere. Electrification by induction frequently supplements these processes. Rain formed by the association of these cloud elements may be highly electrified and a mixture of positive and negative drops is usually produced. Experimentally well-established processes are considered that can selectively charge such rain or selectively discharge it. It is shown that either process can establish a free space charge distribution that is transferred toward the ground by gravity, and may be large enough to develop electric fields exceeding the dielectric strength of air. Lightning then intervenes. The conditions necessary to establish gross free charge distributions by regeneration are specified and shown to be met under frequently occurring meteorological situations. Many of the observed characteristics of thunderstorms are traceable to the nonuniform semiconducting nature of the lower atmosphere and its nonohmic behavior. The analysis reflects the results of earlier work.**

Introduction

THE instantaneous release of some hundreds of kilowatt hours of electrical energy by a lightning discharge is one of nature's most awesome spectacles. Although the lightning discharge has excited the wonder of many men, the complexities of weather processes have obscured the fundamental electromechanics and delayed the collection of data necessary to illuminate the basic physical processes. Urgently required data on the distribution of free electric charge within a thundercloud are still missing, although flights through some 25 active thunderstorms by the highly instrumented laboratory aircraft of the Army-Navy Precipitation Static Project [11] have provided a number of highly valuable samples. These samples may not represent all the thunderstorms distributed over the world and in too many cases the measurements are contradictory. This writer is sensitive to the fact that the observations are still incomplete and not always consistent or accurate, but our critics may notice that flying in active thunderstorms is somewhat hazardous and that our small store of data was obtained only after the highly instrumented project airplanes had been intentionally flown through some 25 active thunderstorms and been struck by lightning three times! The author, accordingly, bequeaths to an unsympathetic critic the job of collecting many more facts. We trust that he will be lucky.

The object of the present review is to bring together the presently available and reliable physical data on thunderstorms and attempt to synthesize from them as complete a quantitative description of the electrified thundercloud as these data permit. The principal problem of thunderstorm electricity is to describe those processes responsible for establishing the over-all free charge distribution just before lightning is initiated. The physics of the actual discharge is simple in concept, but its detailed description is complex. A discussion of its characteristics, therefore, are reserved for separate analysis.

The electrostatic state established inside a thundercloud by meteorological processes can usually be represented by a steady state. Accordingly, if one had a complete space-wide description of the electrostatic potential, electric field, or free space charge at any given instant, he could immediately calculate most of the required physical quantities. Actually, such data are far beyond the reach of present measurement techniques and one must be content with samples of the above quantities and use these as a framework to support a consistent quantitative description. In general, the potential differences cannot be measured and our knowledge of the electrostatic state is based primarily upon electric field measurements, and the charges carried toward the ground on the precipitation particles inside active thunderstorms. Valuable clues to the basic processes can be inferred from the measured charges deposited on the earth by rain.

An improved understanding of the fundamental processes has resulted from the invention and development of new instruments for measuring the electrical state and the important physical characteristics of falling rain. The development of adequate instruments has absorbed much of the writer's effort but their description will be found elsewhere [14, 15, 21, 42]. It is sufficient to notice that out of the instrument development program has emerged electric field meters capable of

* Original manuscript received by the IRE, May 17, 1957.
† U. S. Weather Bureau, Washington, D.C.

operating continuously in very heavy rain both on the ground and on aircraft. These instruments measure continuously both the sign and magnitude of the electric field and have a response time of about one second. Such data are of the utmost importance in assessing thunderstorm electrification processes.

Supplementing the above have been instruments which permit the determination of the sign and magnitude of the free charge carried on falling rain. It is sometimes possible to measure simultaneously the mass of the drop by means of an instrument which has been particularly valuable on aircraft in providing specific information on the drop charges and their approximate distribution. Other devices, such as a small wind tunnel employing ionized air as the moving fluid, have been of great value in the laboratory. Descriptions of some of the above instruments will be found in the Bibliography [14, 15, 21, 42].

As a direct result of efforts to develop new and better instruments, we have the largest store of coherent measurements yet made in the field of atmospheric electricity; their availability is reflected in the conclusions and references cited herein. The emphasis in the present review has been largely determined by these measured data. Theoretical estimates have been invoked primarily to bridge some of the present gaps in the measurements and to guide the interpretation.

The common active thunderstorm is a veritable museum of atmospheric phenomena. Clouds, heavy rain, snow, and hail are commonly produced and intermixed in a typical active storm and the whole matrix is bathed in turbulence and vertical air currents of great complexity. It is inevitable, therefore, that the electrical phenomena will be extremely difficult to interpret and describe in quantitative terms. Thunderstorms commonly develop in thermally disturbed air masses during the summer months or whenever large amounts of water vapor are present in the atmosphere. The typical summer thunderstorm is approximately 20 kilometers in diameter, although the cloud mass itself may be somewhat more extensive. It commonly extends vertically about 12 km but occasionally may develop to 15 km with an increased probability for the production of hail. The complexity of typical thunderstorms suggests that many processes contribute to the observed state [1, 10, 47] and therefore, it is particularly necessary to separate those that are most energetic for quantitative discussion. These selections will doubtless lead to differences of opinion but as long as one clings steadfastly to the observed data, these differences need not be serious.

Characteristics of Active Thunderstorms as Observed on the Ground

As far as this writer is aware, normal lightning activity has never been observed in clear air *except in the vicinity* of falling precipitation. There is much additional evidence showing that the principal electrical effects accompanying a thunderstorm are closely related to the production and fall of precipitation. Precipitation is necessary but is not always sufficient to induce visible electrical activity. The free electrical charges brought to the earth by rain may vary over a wide range; it has been observed that electrical activity may be produced even with moderate precipitation. Conversely, heavy precipitation like that frequently encountered in a mature hurricane sometimes develops surprisingly little lightning activity. The connection between precipitation and lightning activity, therefore, is not a direct one.

The Electrification and Energetics

The electrification observed in thunderstorms implies the gross separation of free electrical charge with a consequent expenditure of large amounts of energy. It is important to understand this process. The electrification is usually established by a three-stage mechanism whereby positive and negative ions are first generated from neutral molecules by cosmic rays and radioactivity, or in special cases by corona or photoelectric effects. The ions are transferred to cloud droplets by diffusion and conduction. The cloud droplets, in turn, unite to form a mixture of positively and negatively electrified raindrops. The rain is then selectively electrified to permit a final gross separation of positive and negative charge. Under special conditions, charge is separated by the more efficient processes of induction.

Cosmic rays produce about 10 ion pairs per cubic centimeter per second in the lower atmosphere and this increases, more or less uniformly, to 45 at an altitude of about 14 km. Extensive measurements show that when cloud droplets are present, the ions produced by cosmic rays normally diffuse onto the cloud droplets to establish an equilibrium charge. For a typical cloud containing 400 droplets per cubic centimeter, all having a radius of 6 microns, it is found that the droplets in every cubic kilometer of cloud normally accumulate a total charge of the order of one coulomb. Cosmic rays will separate this much charge in about five minutes. The above clouds are nearly neutral and half of the droplets carry positive charges while the other half carry negative charges. These two first stages of thunderstorm electrification are perfectly clear and capable of quantitative formulation. However, when the cloud droplets grow into raindrops and these fall in the atmosphere in the presence of electric fields, the electrical processes become enormously complex. Many data are available describing the probable subsequent course of events and these will be considered in later sections.

The energy necessary to separate the free charges carried by the raindrops is derived from gravitational forces and it is necessary to show that they are adequate. The electric field throughout a typical thunderstorm is frequently observed to be about 150 volt/cm or 0.5 statvolt/cm, although fields 20 times this are known to occur [12]. The energy density required to establish the field is $(\frac{1}{8}\pi)E^2$ erg/cm^3 so that at a given instant the total electrostatic energy W of the storm is

$$W = \frac{1}{8\pi}\int E^2 dU = 10^{-2}U = 2 \times 10^{16}\ \text{erg}$$
$$= 550\ \text{kilowatt hours}, \quad (1)$$

where dU is the element of volume U. In a typical storm this volume approaches 2×10^{18} cm³. Perhaps most of this calculated energy is expended in a single lightning stroke whose energy is specified by the product of the effective potential and the transferred quantity of electricity. Therefore, because we will show presently that a typical stroke neutralizes some 17 coulombs, one may estimate that the initial cloud potential *exceeds* 10^8 volts. It is not surprising, therefore, that lightning sparks 5 to 10 km long are frequently produced in the free atmosphere.

Consider a precipitating thundercloud in which the liquid or crystalline water content (LWC) is a representative 10^{-6}gm/cm³. The work that the free water in this unit volume can do in falling towards the ground a distance h is (LWC) gh. where g is the acceleration due to gravity. This energy must necessarily exceed the electrostatic energy stored in the same unit volume or $(1/8\pi)E^2$. Thus, if E approximates 0.5 statvolt/cm the electrostatic energy may be derived from the available condensed water falling a distance of only 10 cm. Since raindrops normally fall many kilometers, the available gravitational energy is thousands of times more than that necessary to establish a typical electric field. Therefore, fairly inefficient electrical processes are entirely capable of describing a common thunderstorm. It is worthy of note in passing that the free water transferred to the high levels in the atmosphere ultimately derives its energy from the sun which originally evaporated the water from the earth.

It is clear that the precipitation must always be electrified if active lightning is to be produced. Many suggestions have been made as to the basic electrification processes [4, 10, 22, 24, 36, 47]. Perhaps most processes invoke the transfer of ions to the drops by diffusion, by conduction, or by differential convection. Others, of a more energetic type, such as direct induction or selective conduction induced by polarization, play an important role. Still others attributing the charge to systematically oriented surface layers have their special advocates. Irrespective of the particular process, the charges on raindrops may be greatly enhanced whenever large numbers of electrified droplets associate to form larger raindrops [24, 25, 32].

Electric Field

Perhaps the most important index of thunderstorm activity is the electric field measured both at the ground and inside the active cloud high above. A vertically upward surface electric field corresponding to a positive surface charge is adopted as positive. This is the definition used by physicists and mathematicians and is opposite in sign to that used by a number of workers in atmospheric electricity. In fair weather the surface electric field intensity is negative and approximates -1.5 volt/cm. The development of clouds over a given observing station usually has little influence on the fair weather field until 10 or 20 minutes before precipitation is observed at the ground. The electrification of the droplets permits a selective electrification of the cloud as a whole that thereby produces measurable electric fields at the surface. In a typical stable cloud the electric field is less than 10 volt/cm and probably less than 1 volt/cm. When the cloud becomes unstable and produces slight precipitation, the electric field measured on the ground commonly approximates $+10$ to $+25$ volt/cm and may fluctuate or even reverse sign. Frequently this electric field is quite steady and as the precipitation rate or vertical convection within the cloud increases, the electric field may increase to ± 50 or more volts per centimeter at which time discontinuities in the electric field are sometimes observed [13]. These discontinuities normally accompany a lightning or invisible static discharge. In the presence of sufficient cloud instability and vertical convection, a typical thunderstorm is produced and the electric field at the ground may then increase to about ± 100 volt/cm with maxima up to ± 140 volt/cm. Marked discontinuities in the field are observed at the instant of nearly every lightning discharge and reversals of sign are common. In an active storm the electric field may be either positive or negative but the basic charging processes, once the thunderstorm is well started, are such as to produce predominantly positive electric fields at the earth's surface.

A network of eight electric field meters was installed in Kansas during the thunderstorm season of 1955. We have complete records of the electric field established at these stations by an active thunderstorm throughout a three-hour period just prior to and after a disastrous tornado passed through Udall, Kan. One station within a mile or two of the funnel lost the door of the barn in which it was housed. Excerpts from these records are given in [30] and in Fig. 1. Their analysis shows that, in general, the electric field may be built towards negative electric field values for the first and last 10 to 20-minute period as shown in Fig. 1, part 3. During the *main part* of the thunderstorm, however, the electric field is positive 61 per cent of the time but *builds towards positive* electric fields more than 90 per cent of the time as in Fig. 1, part 1, and Fig. 1, part 2. Such a field implies that an excess negative charge systematically accumulates in the clouds overhead. The main problem of thunderstorm electricity is to describe the processes whereby this charge and the associated electric field are produced and show how to calculate their magnitude.

In the above thunderstorm, the measurements show that the electric field *just prior* to the lightning discharge was positive in 88 per cent of some 2600 events. Moreover, the electric field immediately after the discharge was negative in 65 per cent of the cases. This implies, and the records clearly show, that the typical lightning discharge not only neutralizes the free charges accumu-

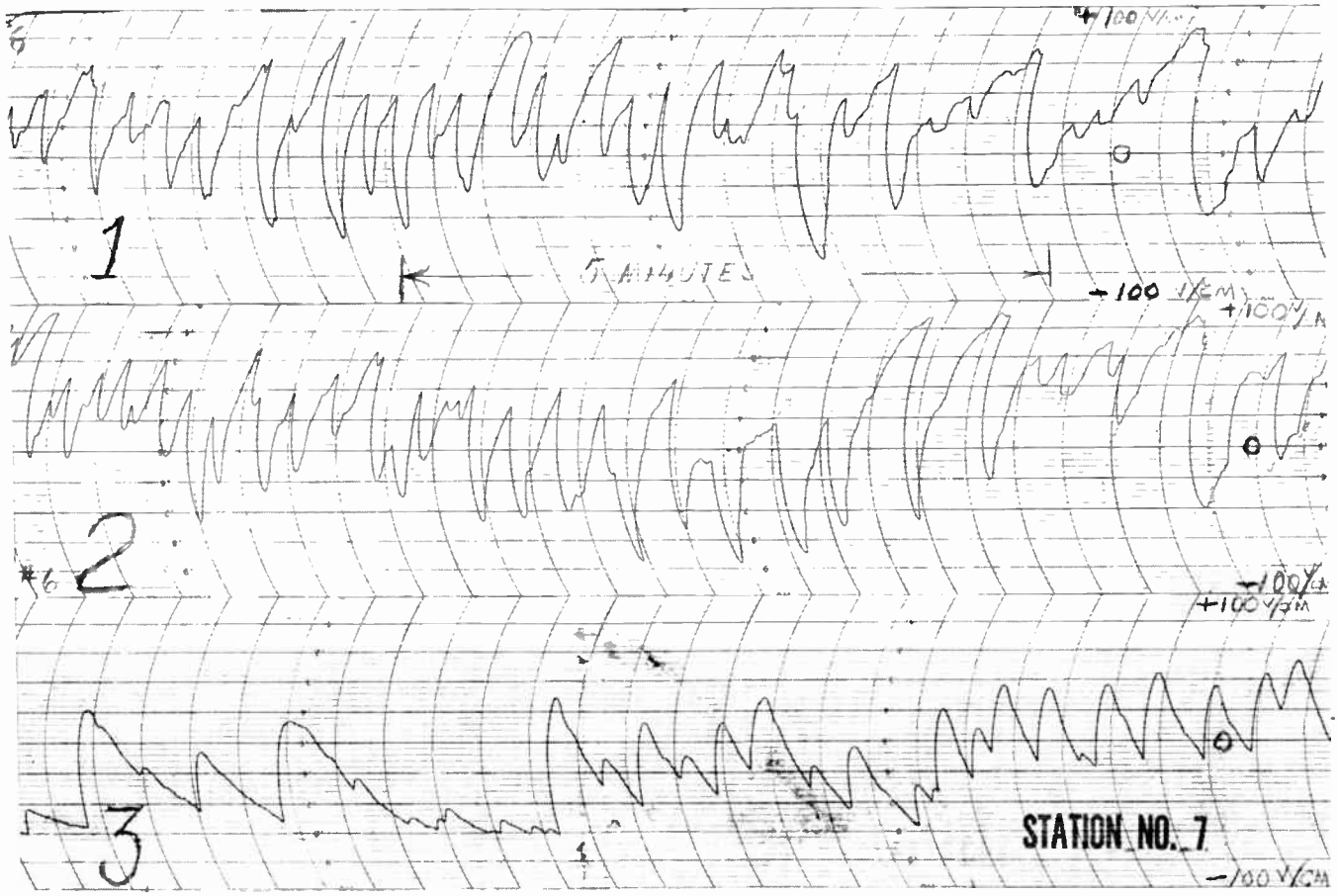

Fig. 1—Extracts from electric field intensity records measured at ground. Active Kansas thunderstorm, May 25, 1955. Electric fields in two top records build toward positive fields. The lower record builds toward negative fields. The measured discontinuities are always accompanied by a lightning discharge.

lated overhead but, in the majority of cases, apparently overneutralizes the charge and develops an electric field which is usually of opposite sign to that existing prior to the lightning stroke. To be more specific, it is found that the average electric field is this active Kansas thunderstorm just prior to a lightning discharge was +41 volt/cm and after the discharge was −10.4 volt/cm. The number of discharges, wherein negative charge was neutralized overhead, was more than 10 times the number of events when positive charge was neutralized, and the average measured *change* of electric field was −50.2 volt/cm or 0.16 statvolt/cm. The largest electric field measured by the writer on the ground was +140 volt/cm, which we will see is less than 1/10 of the maximum electric fields commonly measured on aircraft well *inside* an active thundercloud.

The mean charges neutralized by lightning as summarized in the above data may be immediately calculated by noticing that the electric field observing stations were probably only two or three kilometers below the free charge distributions and therefore these may be assumed to approximate a horizontal sheet. Neglecting the fringing near the edges of these clouds one may write that

$$E = 4\pi\sigma = 0.16 \text{ statvolt/cm} \qquad (2)$$

where E is the observed electric field and σ is the free charge per unit area of the cloud. Now if one considers only the change in the electric field, it is clear that the change in σ corresponds to the discharge of the cloud. Now analysis of many thunderstorms shows that a typical storm has dimensions of 20 km×20 km so that by (2) one finds that the average charge neutralized for more than 2600 measurements approximates 17 coulombs. This value is in good agreement with earlier estimates by other investigators.

Further analysis of the same thunderstorm shows that as the thunderstorm increases in intensity the number of lightning strokes per minute steadily increase to an average maximum value of 4.4 strokes per minute. At the particular station closest to the passage of the tornado funnel the lightning rate increased to an average maximum of 7.2 strokes per minute.

The electric fields measured at the top of mountains exhibit generally the same characteristics as the Kansas storm except that the electric fields are commonly much larger. A program of measurements on mountain tops is currently underway and more data will shortly be available. On top of a mountain nearly 6600 feet high, maximum electric fields of more than 1000 volt/cm have been measured.

Raindrop Charges

Important clues as to the fundamental electrical processes inside an active thunderstorm may be discovered by a careful study of the electrical charges brought to the earth by rain. It was found long ago that quietly falling rain is weakly electrified whereas raindrops falling from active thunderstorms are usually highly charged.

Gschwend [8] observed that the charges brought down on typical thunderstorm raindrops were seldom of a single sign and that a mixture of positive and negative charged drops was characteristic of almost all storms. This fact has been verified many times and has an important bearing on the interpretation of thunderstorm phenomena. Gunn and Devin [19] measured and analyzed the characteristics of some 7000 raindrops that represented a continuous sample of the drops falling to the ground from an active thunderstorm. The distribution of the number of drops in relation to the sign and magnitude of the free charge they carried is given in Fig. 2. This shows clearly that save for a slight preference for small positive charges the distribution is nearly symmetrical and does not appreciably depend upon the sign of the surface electric field. The mixture of positive and negative drops usually observed and the independence of drop charge and the sign of the electric field show that the origin of these charges is to be found in mechanisms taking place far above the earth's surface.

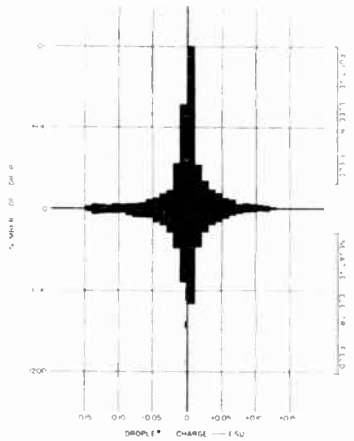

Fig. 2—Number of drops measured at the ground in free charge intervals of 0.01 esu for active thunderstorms of May 5 and June 10, 1950. Total positive charge brought to the ground was 83 per cent of the total negative charge.

Summarizing the data of Fig. 2, it was found that the average charge for positive drops in the above thunderstorm was 0.022 esu/drop and for the negative drops the charge was 0.031 esu/drop. Moreover, the ratio of the sums of all the positive to negative charges brought down on this thunderstorm rain was 0.83. Related sets of data on the charge carried by rain have been given by Scrase [44], by Chalmers and Pasquill [3], and by Banerji and Lele [2]. Average values for raindrop charges are summarized in Table 1.

TABLE I

AVERAGE FREE ELECTRICAL CHARGE ON INDIVIDUAL DROPLETS (ESU×10³)

Observer	Altitude (feet)	Charge	Quiet rain	Shower rain	Electrical storm rain	Quiet snowfall	Squall snowfall
Gschwend (1921)	surface	+	0.24	1.75	8.11	0.09	5.64
		−	0.53	5.43	5.88	0.06	4.78
Banerji and Lele (1932)	surface	+		6.4	6.9		
		−		6.7	7.3		
Chalmers and Pasquill (1938)	surface	+	2.2	1.3	3.7*		10.5
		−	3.0	2.3	9.2*		5.7
Gunn (1947)	4000	+		ϕ			
		−		24			
	12,000	+		41			
		−		100			
	20,000	+		63			
		−		ϕ			
Gunn (1949)	surface	+			15	0.67	
		−			19	1.0	
Gunn (1950)	5000	+			81		
		−			63		
	10,000	+			148		
		−			112		
	15,000	+			123		
		−			76		
	20,000	+			52		
		−			62		
Gunn and Devin (1953)	surface	+			22		
		−			31		

* Actual lightning activity doubtful.
ϕ No droplets of this sign were observed at the indicated level.

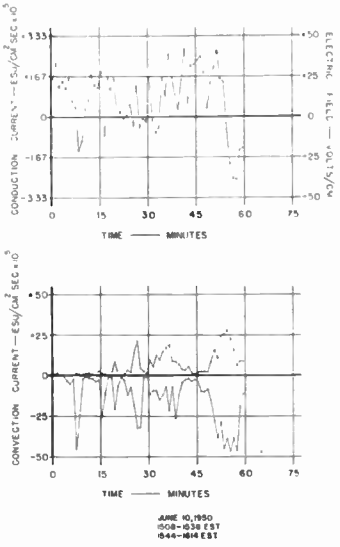

Fig. 3—Top: Electric field and estimated conduction current averaged over one-minute intervals for storm of May 5, 1950 Bottom: The convected current density for positive drops is plotted above the axis. Below the axis is the negative drop current density. The net current density is their sum.

Convected Current Density

When the charges on falling rain are directly measured together with their size and numbers per unit volume it is possible to calculate the convected current density i through

$$i = \sum NQV \tag{3}$$

where N is the number of drops per unit volume, Q is their free charge, and V is their velocity of fall. Since the raindrops all fall towards the ground, the contribution of the positively charged and negatively charged drops are of opposite sign. Accordingly, it is expedient to calculate and plot separately the charge per unit area transferred per unit time to the earth by both the positive and negative drops. Such data [19] are summarized in Fig. 3 and are placed adjacent to simultaneously collected data for the electric field and the presumed conduction current density. The convected current densities for the positive drops are plotted above the axis while those for the negative charges are plotted below. It may be noticed in Fig. 3 that the convected current densities for the positive and negative drops are seldom of the same magnitude and, therefore, rather large fluctuations of the free drop space charge density are generally encountered. These irregularities produce associated fluctuations in the local electric field. Further, since the net convection current density is notably larger than the conduction current of opposite sign, a surplus free charge necessarily accumulates on the ground and this in turn modifies the electric field. One may notice particularly from the observed curve that the excess droplet convected current density is sometimes as much as 4×10^{-4} esu/cm²sec. These direct measurements permit one to infer, through a simple analysis, that the observed electric fields in the free atmosphere can be excited and maintained by the observed charges on falling rain.

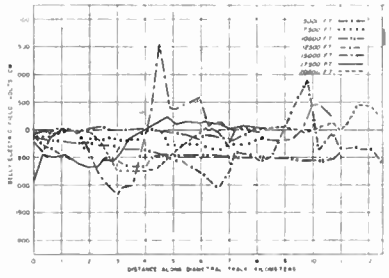

Fig. 4—Electric field intensity measured on belly of B17 airplane during successive passages through active thunderstorm of July 24, 1945 at different levels. Positive fields correspond to positive surface charges at the field meter site.

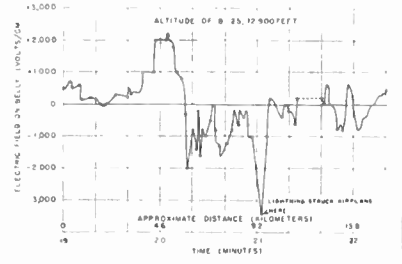

Fig. 5—Electric field intensity at belly of B25 airplane during a lightning strike at 13,000 feet on August 5, 1944.

Electrical Characteristics Measured Inside Active Thunderclouds by Aircraft

Although important guide posts for the development of an adequate description of thunderstorm electricity are established by surface data, yet there are many important facts that can be determined only by flying through active thunderstorms. The highly instrumented airplanes of the Army-Navy Precipitation Static Project, which the writer directed during World War II, intentionally flew through some 25 active thunderstorms and succeeded in collecting valuable data. These measurements still provide the best available cross section of thunderstorm electrification phenomena. Many more data are urgently required. The laboratory airplanes were equipped with induction-type electric field meters, both on the top and bottom of the main cabin. A drop charge apparatus was installed under one wing and simultaneous measurements could be made of the electric fields, drop charges, and other more obvious meteorological factors [11, 12, 17].

Observed Electric Fields

Repeated flights through active thunderstorms showed that the electric field at low levels approaches that commonly measured at the surface and that these fields generally increase to a maximum in the vicinity of the freezing level. Somewhat typical data for a number of passes through the active thunderstorm of July 24, 1945, are summarized in Fig. 4. The measurements show that at altitudes near the freezing level the electric fields frequently exceed a thousand volts per centimeter. In a total of nine thunderstorms examined in 1944 by repeated flights through each, the average measured maximum field was 1300 volt/cm [13]. One flight through an

TABLE II*

Altitude	Temp.	Positive drops		Negative drops		Particle space-charge density		Measured drop density	Mean drop mass for liquid water content of 0.5 gm/m³	$(Q/m)_{ext}$	
		Number	Charge	Number	Charge	Positive	Negative			Positive drops	Negative drops
Feet	°C		esu/drop		esu/drop	esu/cm³	esu/cm³	drop/cm³	grams	esu/gm	esu/gm
5,000	+14.7	89	+0.081	171	−0.063	5.6×10^{-5}	3.1×10^{-5}	4.8×10^{-4}	1.0×10^{-3}	81.0	63.0
7,500	+10.3	43	+0.280	47	−0.267	14.5×10^{-5}	15.6×10^{-5}	3.2×10^{-4}	1.5×10^{-3}	185.0	178.0
10,000	+6.7	71	+0.148	133	−0.112	4.9×10^{-5}	2.9×10^{-5}	2.5×10^{-4}	2.0×10^{-3}	74.0	56.0
12,500	+2.4	0	—	196	−0.135	—	7.0×10^{-5}	4.4×10^{-4}	1.1×10^{-3}	—	123.0
15,000	−0.7	130	+0.123	150	−0.077	8.5×10^{-5}	4.8×10^{-5}	5.7×10^{-4}	0.8×10^{-3}	153.0	95.0
17,500	−5.5	45	+0.036	79	−0.041	1.5×10^{-5}	1.6×10^{-5}	4.1×10^{-4}	1.2×10^{-3}	30.0	34.0
20,000	−9.9	76	+0.052	74	−0.062	1.1×10^{-5}	3.6×10^{-5}	3.4×10^{-4}	1.4×10^{-3}	37.0	44.0
									Mean	93.0	85.0

* Summarized data for drops measured inside active thunderstorm of July 24, 1954. The particle space charge densities are estimated from the drop charges actually observed and, therefore, ignore the smaller and possibly more numerous charges carried by the cloud droplets or very small raindrops. The specific charges, or charges per unit mass, are considered rough.

active storm encountered both positive and negative fields of 2000 volt/cm and a half minute later the field increased to 3400 volt/cm at which time the lightning struck the airplane and damaged some of our instruments [12, 13]. The electric field intensity throughout this interval is shown in Fig. 5. All aircraft electric field measurements are subject to a possible correction of the order of unity because of the unknown orientation of the electric field in relation to that of the aircraft. It is a significant observed fact that 65 per cent of all lightning strikes to operating aircraft occur at outside air temperatures within the narrow range of from 0° to +5°C. Although air traffic at these levels is high, the facts still suggest that the layer of maximum electrical activity can hardly exceed a thickness of 2 or 3 km.

One characteristic of the electric field distribution in thunderstorms is worthy of emphasis. The free charge in the thundercloud is distributed over a large volume and it was originally anticipated that the electric fields would gradually build up as the thundercloud was approached. Actually it was found that the electric field outside the cloud approximated only 150 to 200 volt/cm in the clear air even through the towering cumulus overhead suggested that one was very close to the electrically active centers.

However, just as soon as the aircraft entered the cloud, the electric fields increased rather rapidly and in a matter of 15 seconds the field might increase to ±1000 volt/cm. Inside the cloud large values of field, both positive and negative, were commonly encountered, although the geometrical position of the aircraft in relation to the active center of the thundercloud had changed very little [11, 17]. This observed fact emphasizes the importance of space charge layers near the boundary of thunderclouds. The important role of such layers will be discussed in another section.

Observed Raindrop Electrification

The raindrops inside an active thunderstorm are highly electrified. The writer pointed out long ago that the measured charges were frequently so large that the electric field at the surface of the drop might approach the dielectric strength of air [14]. This implies that increased charges on the larger drops might initiate corona discharge and thus limit the electrification [14]. The measured electric charges in an active Minnesota thunderstorm are summarized in Table II (above) and show clearly that not only are the electric fields a maximum near the freezing level but the drop charges also. Table II gives not only the measured values of the drop charges, but also a rough estimate of the specific charge or charge per unit mass. A plot of the average free charge carried by the precipitation particles at different positions within the thundercloud at a given level is given in Fig. 6. Many more data of this nature may be found [17]. It is observed that frequently a mixture of positive and negative drops exists but occasionally regions 1 or 2 km in linear dimension contain raindrops of *only a single sign* [17]. This statement applies only to the measured drops and does not imply that there may not be relatively large numbers of much smaller cloud droplets carrying charges of opposite sign. It is clear, however, that these large rapidly falling drops are primarily responsible for the convective transport of free charge towards the ground by gravitational action and are, indeed, the active agents in separating the free charge within the cloud.

The available data on the electricity transferred to the earth by rain show that the charges are overwhelmingly positive for very light rain and low precipitation rates. But, this decreases with increasing precipitation until in almost all thunderstorms the free charge brought to the ground is predominantly negative [44]. These data probably imply that raindrops become more negative at higher levels and, indeed, this is just what is measured in aircraft flights both in the mild cold front and in thunderstorms which show that at rain-forming levels the total negative charge on the rain is some 60 per cent larger than the total positive charge [12, 17]. This excess may be directly attributed to the differential discharge resulting from the observed differences in the positive and negative light ion conductivities at flight altitudes or to the selective electrification of cloud droplets when $\lambda_+ \neq \lambda_-$.

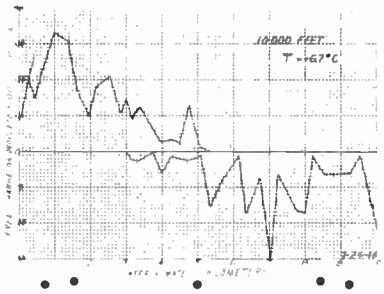

Fig. 6—Measured free charges carried by individual raindrops at various positions inside thunderstorm of July 24, 1945. This curve for 10,000 feet. For additional data, see Gunn [17].

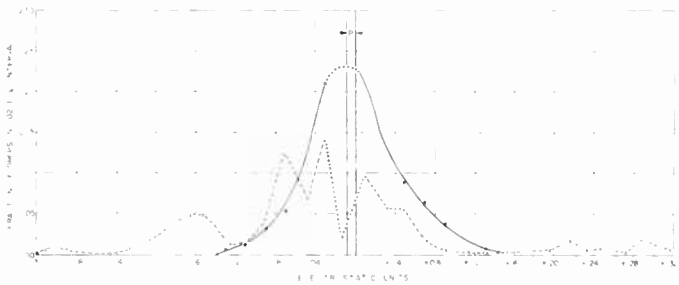

Fig. 7—Distribution of fractional numbers of charged drops in 0.02-esu intervals. Solid curve for mild cold front of July 27, 1945. Dashed curve for active thunderstorm of July 24, 1945. The dotted sections imply that weakly charged drops may have been missed.

Comparison of Electrification Inside an Active Thunderstorm with that Observed in a Mild Cold Front

It is of considerable interest to compare the electrical properties of heavy precipitation produced within a mild cold front with those observed inside an active thunderstorm. The laboratory airplane flew through a mild cold front that crossed Minnesota on July 27, 1945. Precipitation was moderate to heavy; no lightning activity was observed. The charges measured on the individual raindrops falling at various levels are summarized in Table III (opposite). A comparison with the thunderstorm data of Table II shows that the measured drop charges on the rain within the cold front were roughly one half of the charge measured on the drops falling within the active thunderstorm. The charges on the raindrops at all levels gave a nearly smooth distribution like that of the solid curve in Fig. 7. This distribution was nearly symmetrical about the axis of zero charge and was roughly Gaussian. On the other hand, the distribution of charges in the thunderstorm suggested great complexity and there were large numbers of drops carrying both positive and negative charges of considerable magnitude, as shown in the dashed curve of Fig. 7. At any given level the data were insufficient to provide representative statistical data, but did show that in both types of storm large volumes sometimes existed wherein the charge on the larger precipitation particles is *all of one sign*. The data of Tables I and III permit one to estimate the total free charge carried by all the rain drops if they are assumed to be distributed uniformly over a sphere of radius 1 km. One may verify that if the charges are all of one sign, electric fields over the surface of the assumed sphere are great enough to initiate lightning discharges that are not observed. Thus, the summarized data show that charges of opposite sign, presumably on the smaller cloud droplets or the air, are usually intermixed with the charges measured on the large raindrops and that only a partial separation of the measured charges is necessary to establish active lightning. One concludes from a comparison of the thunderstorm and mild cold front regimes that heavily precipitating regions exhibiting modest measured electric fields are intrinsically capable of establishing a charge distribution adequate to produce lightning, and that the differences between a mild cold front and a thunderstorm are probably related principally to the selective separation of charges already present on the rain. These seemingly minor differences between the thunderstorm and nonthunderstorm regimes must be objectively considered in formulating a quantitative description of thunderstorm phenomena.

Electrical Properties of the Semiconducting Lower Atmosphere

The earth's lower atmosphere is essentially a high grade insulator in which ion pairs are continuously formed principally by cosmic rays and radioactivity. Because of the decrease in density of the atmosphere with increasing altitude and because most of the radioactive material is concentrated near the surface, the produced ionization changes markedly with altitude. In addition to the observed variation of ionic density, the ionic mobility regularly increases with altitude, and is somewhat greater for the negative ion than for the positive ion.

The number of ions per unit volume established in the atmosphere at equilibrium depends not only upon the rate of ion production but also upon their rate of disappearance. In clean air the rate of disappearance is determined by the recombination coefficient; but, in ordinary air containing various types of pollution and cloud droplets, the rate of disappearance is determined by a number of factors that have been discussed adequately in earlier communications [22, 23, 31].

The most important factors controlling the electrical state of the atmosphere are the electrical conductivities for the positive and negative light ions and their ratio. By ignoring a number of secondary processes which may be important under special conditions, one may summarize present views regarding the atmospheric conductivity under two headings.

Clean Air Conductivity

In the absence of suspended particulate matter the rate of recombination of the positive and negative ions is given by

TABLE III*

Altitude	Temp.	Positive drops		Negative drops		Particle space charge density		Measured drop density	Mean drop mass for liquid water content of 0.5 gm/m³	$(Q/m)_{est.}$	
		Number	Charge	Number	Charge	Positive	Negative			Positive drops	Negative drops
Feet	°C		esu/drop		esu/drop	esu/cm³	esu/cm³	drop/cm³	grams	esu/gm	esu/gm
4000	+12.0	—	—	72	−0.029	—	-0.9×10^{-5}	2.7×10^{-4}	1.8×10^{-3}	—	−16
6000	+ 8.5	—	—	59	−0.027	—	-0.6×10^{-5}	2.2×10^{-4}	2.2×10^{-3}	—	−12
8000	+ 6.0	—	—	157	−0.033	—	-1.3×10^{-5}	4.4×10^{-4}	1.1×10^{-3}	—	−29
10,000	+ 3.0	—	—	78	−0.032	—	-1.0×10^{-5}	2.9×10^{-4}	1.7×10^{-3}	—	−18
12,000	0.0	84	+0.042	130	−0.100	$+1.0\times10^{-5}$	-4.6×10^{-5}	7.5×10^{-4}	0.65×10^{-3}	+64	−150
14,000	− 1.0	8	+0.037	171	−0.037	$+0.15\times10^{-5}$	-1.5×10^{-5}	4.1×10^{-4}	1.2×10^{-3}	+31	−31
16,000	− 4.5	—	—	120	−0.034	—	-1.3×10^{-5}	3.8×10^{-4}	1.3×10^{-3}	—	−26
18,000	− 7.1	200	+0.051	12	−0.032	$+2.2\times10^{-5}$	-0.1×10^{-5}	6.6×10^{-4}	0.76×10^{-3}	+67	−42
20,000	−11.0	129	+0.067	—	—	$+2.7\times10^{-5}$	—	5.1×10^{-4}	1.0×10^{-3}	+67	—
22,000	−15.5	80	+0.037	—	—	$+1.1\times10^{-5}$	—	3.1×10^{-4}	1.6×10^{-3}	+23	—
24,000	—	—	—	—	—	—	—	—	—	—	—
26,000	−23	18	+0.028	—	—	$+0.3\times10^{-5}$	—	1.2×10^{-4}	4.2×10^{-3}	+ 7	—
									Mean	43	40

* Summarized data for drops measured inside mild cold front of July 27, 1945. The particle space charge densities are estimated from the drop charges actually observed and therefore ignores the smaller and possibly more numerous charges carried by the cloud droplets or on the small raindrops. The specific charges, or the charges per unit mass are considered rough.

$$-\frac{dn_+}{dt} = \alpha n_+ n_- = -\frac{dn_-}{dt} \tag{4}$$

where n is the number of ions per unit volume and the subscript denotes their sign, e is the elementary ionic charge, and α is the recombination coefficient. Now if q ion pairs per unit volume per unit time are produced, then the equilibrium electrical conductivities for the positive ions λ_+ and for the negative ions λ_- become

$$\lambda_\pm = \left[\frac{q}{\alpha}\right]^{1/2} e u_\pm \tag{5}$$

where u is the mobility of the appropriate ion and λ is defined by

$$\lambda = \lambda_+ + \lambda_- = \left[\frac{q}{\alpha}\right]^{1/2} e(u_+ + u_-) \tag{6}$$

so that the ratio of the conductivities is

$$\frac{\lambda_+}{\lambda_-} = \frac{u_+}{u_-} \doteqdot 0.8 \tag{7}$$

These expressions are, in general, not applicable near the earth's surface but are somewhat descriptive of the conductivities between 3 and 20 km.

Cloudy or Polluted Air Conductivity

Whenever cloud droplets or other suspended nuclei are present in the atmosphere the positive and negative ions not only recombine with each other but are also transferred to the pollution particles or cloud droplets by diffusion. The droplets thereby develop an equilibrium charge which systematically modifies the diffusion of other ions onto the particle and in this way the ionic density of the mobile conducting ions in the air proper is controlled [41]. The rate of combination of positive and negative ions with the suspended particles of mean population density N_0 and radius a is given approximately by [22]:

$$-\frac{dn_+}{dt} = \frac{4\pi akTu_+n_+N_0}{e\left[1 + \dfrac{Qe}{2akT} + \cdots\right]} = \frac{4\pi akTu_+n_+N_0}{e\left[1 + \dfrac{1}{2}\ln\dfrac{\lambda_+}{\lambda_-} + \cdots\right]} \tag{8}$$

and

$$-\frac{dn_-}{dt} = \frac{4\pi akTu_-n_-N_0}{e\left[1 - \dfrac{Qe}{2akT} + \cdots\right]} = \frac{4\pi akTu_-n_-N_0}{e\left[1 - \dfrac{1}{2}\ln\dfrac{\lambda_+}{\lambda_-} + \cdots\right]} \tag{9}$$

where k is the Boltzmann constant, T is the absolute temperature, and Q is the average charge carried by each droplet. When the number of suspended particles per unit volume corresponds to typical clouds the disappearence of ions by diffusion is much larger than by recombination. In this case, one may equate the rate of disappearance to the rate of production and thus calculate the conductivity due to the light ions moving within the cloud droplet space. The conductivity is then nearly the same for positive and negative ions and is much less than in clear air as suggested by (6). Carrying out the substitution it is found for stable clouds that

$$\lambda = \lambda_+ + \lambda_- = n_+u_+e + n_-u_-e = \frac{qe^2}{2\pi akTN_0}\left[1 + \frac{1}{6}\left(\frac{Qe}{akT}\right)^2 + \cdots\right]. \tag{10}$$

Unless N_0 is very large or very small it is necessary to combine the effects of ionic recombination and ion disappearance by diffusion onto the suspended particulate matter. This has been found possible, although awkward, because the ratio of the positive and negative light ion conductivities measures the particulate matter suspended in the air and this ratio can be estimated from $N_0^2a^2/q$, as shown in Fig. 15. Thus by the aid of this curve and expressions in [31], one may estimate the conductivities for any specified atmosphere.

Accordingly it is clear that while the conductivity of the atmosphere is largely determined by the rate of ion production by cosmic rays, radioactivity, and in some cases by corona or photoionization, the cleanliness of the air plays a major role in determining the measured values and their ratio.

Observed Electrical Conductivity and the Altitude

The electrical conductivity of the lower atmosphere has been measured by many investigators and is known to increase notably with increasing altitude. Gish and Wait [7] have measured the positive and negative light ion conductivities to an altitude of 40,000 feet using aircraft, and found that the positive light ion conductivity was represented by

$$\lambda_+ = 1.5 \times 10^{-4}[1 + 0.13 \times 10^{-10}Z^2]\text{esu}. \quad (11)$$

Moreover, the negative conductivity is given by

$$\lambda_- = 0.4 \times 10^{-4}[1 + 0.42 \times 10^{-10}Z^2]\text{esu} \quad (12)$$

where Z is the altitude in centimeters.

Extensive new measurements at this laboratory extending up to altitudes of 20 km, show that the positive and negative conductivities are generally different. At low levels the positive conductivity is normally in excess and at the "crossover point" the conductivities are equal but above this point the negative conductivity is in excess. The "crossover point" according to (11) and (12) is at 7 km, but our measurements show that it frequently is as low as 3 or 4 km, the exact level depending in an important way upon the cleanliness of the lower atmosphere. We have found that the conductivity λ at an altitude Z may be represented by an improved expression of the form $\lambda = \lambda_0 \exp [fZ - gZ^2]$ where the constants f, g, and λ_0 are considerably different for positive and negative ions. The new measurements and the magnitude of the controlling constants will be reported elsewhere by Woessner and Cobb. Their results clearly show that at a level above 3 or 6 km the conductivity due to the negative ions is considerably larger than that due to the positive ions.

The author is persuaded that these observed differences in the conductivities are an important and controlling factor in determining many basic features of the free charge distribution in the atmosphere.

Discharge of Electrified Clouds and Raindrops

Consider any closed surface in the free atmosphere which contains within its boundaries a total free charge Q. If the distribution of the conductivity λ over the surface is known, one may write that the time rate of charge decay is

$$-\frac{dQ}{dt} = \int E\lambda dS \quad (13)$$

where the integration is carried out over the entire surface. Now if λ is nearly constant over the boundary, it may be placed outside of the integral sign so that one may, by the use of Gauss' law, integrate the equation to show that [10]

$$Q = Q_0 \exp [-4\pi\lambda t] \quad (14)$$

where Q_0 is the initial free charge. This expression is quite general and shows that any free charge is dissipated logarithmically and that it degrades to $1/\epsilon$ in a time known as the *relaxation time* or

$$\tau = \frac{1}{4\pi\lambda}. \quad (15)$$

Since the conductivity of air increases rapidly with altitude, it is evident that the *time to discharge clouds at high level is notably less* than the time to discharge clouds located *nearer the earth's surface.* This effect plays an important role in converting double layer distributions of free charge into unipolar distributions much like those frequently observed [10]. Fig. 8 gives a plot of the total conductivity and relaxation times for free charges located at various altitudes in the atmosphere.

It may be noticed from (13) that the rate of discharge depends on the conductivity over the surface where the electric field is measured. Because the atmosphere is, in general, a poor conductor and because the electric fields established in it by thunderclouds are frequently quite large, there is a marked tendency for ions, of a sign opposite to that enclosed by the surface, to accumulate at the surface while ions of the same sign are repelled. Thus, a space charge layer of considerable magnitude may surround the free charge and notably modify the conductivity of the surface region. The rate at which a cloud discharges, therefore, usually depends somewhat on the sign of the charge.

The accumulation of space charge in the semiconducting atmosphere depends both on the electric field and the local conductivity. To emphasize this fact consider the vertical conduction current flowing through a prism extending from the earth to the ionosphere. When a steady state is established, the current density i in the column is a constant. Accordingly,

$$i = \lambda E = \text{constant} \quad (16)$$

where E is the vertical electric field intensity and λ is the conductivity. If this expression is differentiated

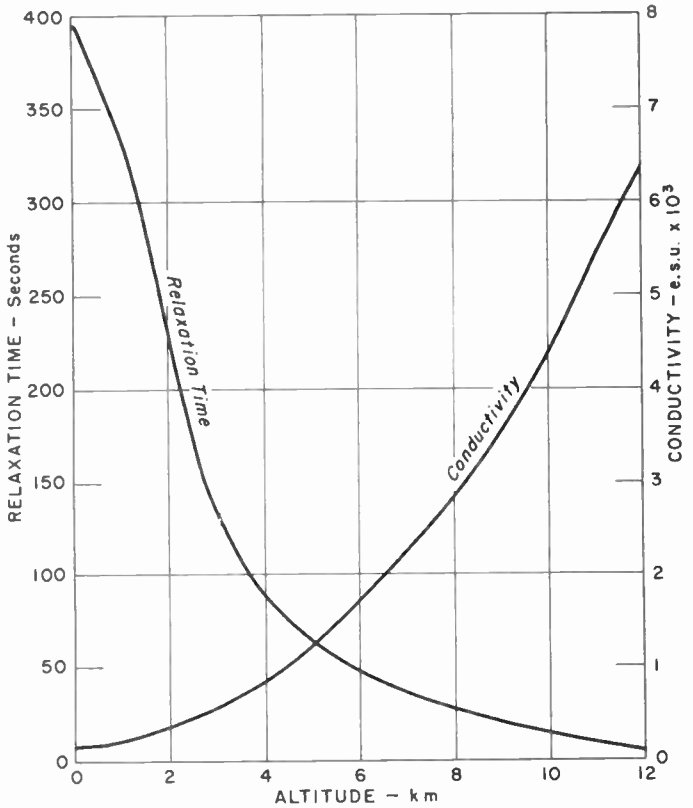

Fig. 8—Estimated electrical conductivity and relaxation time as a function of the altitude.

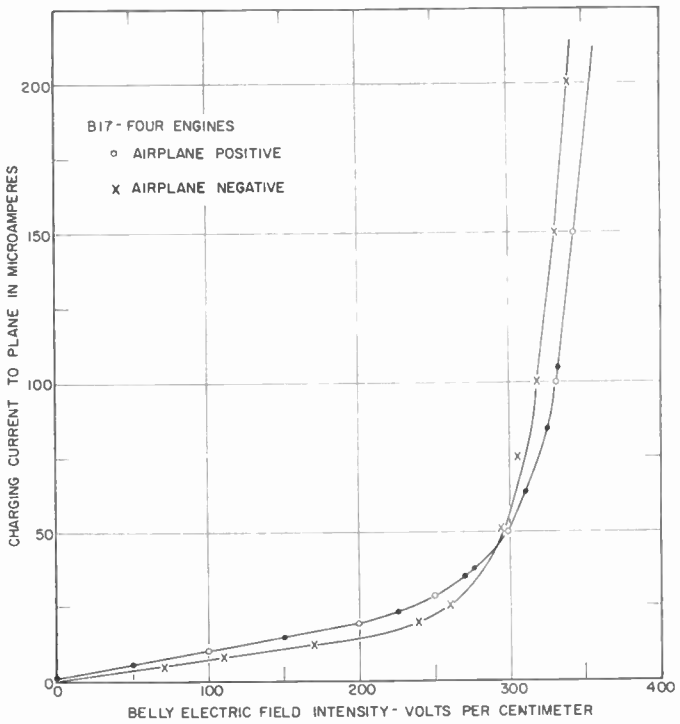

Fig. 9—Unipolar charging currents required to maintain the measured belly electric fields on B17 flying laboratory. Note that more current is required to maintain an assigned positive charge on the airplane than a negative one of the same magnitude. Note that beyond the ohmic region the discharge regime is reversed.

with respect to the altitude Z, it is found by employing a one dimensional Poisson's equation, that

$$\frac{dE}{dZ} = -\frac{E}{\lambda}\frac{d\lambda}{dZ} = 4\pi\rho. \qquad (17)$$

Thus the accumulated free space charge ρ normally increases with the electric field and decreases as the conductivity becomes large. Substitution of numerical values will show that near the earth's surface space charge effects are likely to be large but at great altitudes they are not so important.

The accumulation of a space charge just outside a highly charged body and its influence on the discharge rate was particularly evident in our experimental work with the laboratory airplane of the Precipitation Static Project. An artificial charging device was invented that could place any selected *unipolar* charge on the airplane *in flight* and the current to maintain the charge could be determined as a function of the electric field [11]. We observed very early in our experimental program that the airplane charging characteristics depended on the sign of its free charge. This phenomena is well illustrated by Fig. 9, which shows that the charging current to the airplane is greatest when the airplane is positive and least when it is negative. One may notice further from Fig. 9 that as soon as the belly electric field on the airplane exceeds 300 volt/cm which corresponds to the onset of corona at the wing tips, the discharge regime is completely reversed. These observed data show very clearly that the conductivity near any surface enclosing a free charge depends on its sign. At the level of highly electrified clouds the conductivity due to the negative ions normally exceeds that due to the positive ions and therefore free positive charge commonly disappears more rapidly than free negative charge. Although such sign selective discharge effects are quite evident in charged raindrops and electrified clouds, it is still improper to conclude from this analysis and Fig. 9 that the relative discharge rates always depend *only* on the conductivities. Frequently, the discharge circuits extend both to the ground and to the ionosphere and therefore the whole electrical discharge path outside the cloud must then be considered in the over-all determination of the rates.

Highly charged raindrops of both signs commonly are observed in precipitating areas. When the conductivities due to the positive and negative ions are identical, the drops will discharge at the same rate. However, when the conductivities are different as suggested by (11) and (12), the drops of opposite sign are likely to discharge at different rates. This selective discharge process has been shown to develop free space charge distributions in the atmosphere having a considerable magnitude [27]. By using the clear air conductivity values given by (11) and (12) to illustrate the magnitudes, one may calculate how far a raindrop must fall to reduce its charge to any selected fraction of its initial value. Thus, when the

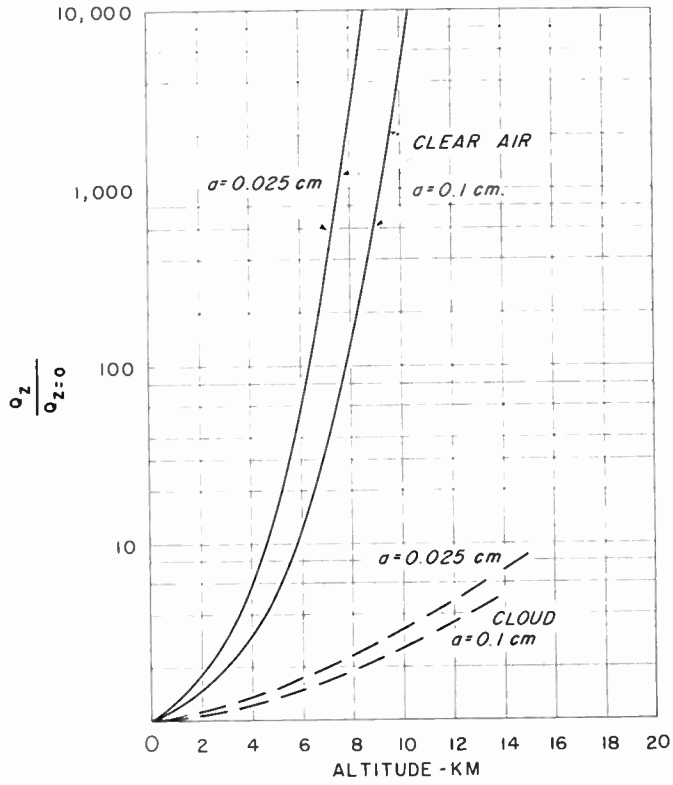

Fig. 10—Ratio of the free charge Q_z on a raindrop at level Z to its value Q_0 after falling to earth through clear air, and through stable clouds.

electrical conductivities are equal one may plot the solid curve of Fig. 10 showing the charges carried by a drop at altitude Z relative to the charge at the ground after falling through clear air. Because the conductivities inside a cloud are much less, the discharge rates are less and the estimated relative charges may be read from the dashed curve of Fig. 10. Now when the conductivities are different, one must calculate a pair of curves similar to that of Fig. 10 for positively charged and negatively charged drops [27]. The pair of curves so plotted will differ from, but still approximate, Fig. 10.

Although (11) and (12) above suggest that the positive and negative conductivities are equal at the 7-km level, we have data showing that this level sometimes is as low as 3 or 4 km. Accordingly selective charging and discharging will be evident at most rain-forming levels and there will be a marked tendency for the positive drops to discharge somewhat faster than the negative drops. Unfortunately, conditions inside a thundercloud are not quite as simple as in the clear air outside and the positive and negative conductivities inside clouds are generally unknown. However, there is accumulating evidence, for example the work of Mathias and Grenet [37], Rossmann [43], Nolan and Nolan [39], and others, all suggesting that the conductivities within a cloud or precipitating regions are much different. The differential discharge of the positive and negative drops would then be very important. The question of selective discharge in thunderstorms can only be finally settled by further measurements. Present data suggest that it plays a vital role in the establishment of free charge distributions.

Space Charge Layers and Their Effects

It has been emphasized in one of the author's articles that the discontinuity in an electrical conductivity that necessarily occurs at a cloud boundary results in the development of a space charge layer whenever the boundary is traversed by electric fields [29]. The conductivity inside a stable cloud is commonly one tenth that in the clear air just outside. Whenever free charge develops inside a cloud electrical currents flow across the boundary. Continuity requires that the equilibrium current density inside the cloud be the same as it is outside. It then follows that there is a discontinuity in the electric field at the cloud boundary just as shown by aircraft flights into thunderclouds [13, 17]. The layer of discontinuity invariably contains free space charge of a sign opposite to the charge inside the cloud. Further, since the ions produced in the atmosphere recombine or are continually deposited on the cloud droplets, an average free charge density ρ is commonly established whose magnitude is [29]

$$\rho = \frac{qe}{4\pi}\left[\frac{1}{\lambda_0} - \frac{1}{\lambda_i}\right] \tag{18}$$

where λ_0 and λ_i are the conductivities outside and inside the transition layer. Assuming that the ions in the region are produced principally by cosmic rays (*i.e.*, $q = 10$ ion/cm³sec) one may estimate that the space charge density is the order of 2×10^{-5} esu/cm³. The thickness of this space charge layer is directly proportional to the electric field, although it does not explicitly appear in (18) [29]. Within a highly electrified thundercloud the thickness of the transition layer is both calculated and observed to approximate 1 or 2 km.

The space charges accumulated near cloud boundaries are at first transferred to these regions by ions but if there are cloud droplets or raindrops in this region these ions shortly are deposited on the droplets and the space charge finally resides, for the most part, on the hyperelectrified rain. This special mechanism which communicates *systematic* charges to the drops approximating $3E_0a^2$ will be discussed in another section.

The free charges inside a thundercloud always attract ions of opposite sign toward the cloud. This means that space charge established by electrical conduction will always play a secondary but clearly evident role in determining the over-all electric field configuration. For example, the character of the branching from lightning strokes shows rather clearly that free charge opposite to that inside the cloud is commonly present below most thunderclouds. This accumulated free charge is always less than the charge on the main cloud but if the principal cloud charges are suddenly annihilated by lightning, the space charge may still persist. In this event the

Fig. 11—Branching feeder strokes showing partial discharge from low clouds having same sign of charge as that induced on the earth. (Photo courtesy of Albert Ford.)

sign of the resultant charge in the overhead regions is reversed. Reference to the records of Fig. 1 will clearly show this residual charge. The residual charge manifests its presence by an *apparent over-neutralization* of the charge overhead whenever lightning discharges the main cloud. This space charge accumulated by conduction is discharged by the lightning as evidenced by the brush-like feeders to the main stroke as shown in Fig. 11, but it seems clear from the records that the discharge is commonly *incomplete.*

The Layer of Maximum Resistance at Low Levels

Because of the contamination and suspended matter in the lower 3 or 4 km of the atmosphere and its relatively high gaseous density, the conductivity of these lower layers is unusually low. Space charge is then readily developed [as suggested by (17)] and is frequently large enough to modify the electric fields and currents flowing across the layer. By the use of observed conductivity data one may show that the total resistance offered to the flow of current from the earth to the high atmosphere is located principally in these lower layers. Now if high voltages are developed between the ionosphere and the earth the ensuing currents will be independent of altitude and a large fraction of the potential difference is necessarily found across the lowest layers. The potential differences established between the top and bottom of a thundercloud are frequently in excess of 10^8 volts. This potential is applied to a closed circuit extending from the top of a cloud to the ionosphere where the charge is distributed more or less uniformly over the earth and the current flows back to the earth in the fair weather regions of the world. The rest of the circuit to the lower parts of the original thundercloud is completed through the conducting earth and through the high resistance layer between the earth and the cloud. Thus, much of the generated cloud potential difference is frequently applied across the low lying layers of high resistance. In this event lightning strokes to the ground may occur and thus, instantaneously transfer charge to the ground. Stated another way, one may notice that the ohmic resistance of these special lower layers is oftentimes so large that nature finds other auxiliary ways to transfer the rapidly accumulating free charge in the clouds to the ground. This process is suggested by Fig. 18.

It is important to notice that the mountainous areas of the earth frequently extend well above the high resistance lower layers and thus effectively provide a low resistance bypass to the high conductivity regions in the atmosphere. Electrification effects and charge transfer in mountainous areas, accordingly, play a larger role proportionately than do the oceanic areas. Eq. (17) suggests and observation shows that space charge phenomena on the tops of mountains play a somewhat lesser role than in low level layers and the distribution of charges is somewhat easier of interpretation. The study of thunderstorm phenomena in mountainous areas is, therefore, unusually important.

Electrification of Cloud Droplets

Since most raindrops are formed by the association of small melted snow crystals or cloud droplets it is important to discover the basic processes responsible for their electrification. During the last few years our laboratory has made tremendous strides in understanding these processes. These electrification mechanisms are of the greatest importance. The diffusion of ions onto the cloud droplets represents a universal process [22, 23, 26]. On the other hand, hyperelectrification and simple induction processes are of controlling importance whenever electric fields are present. Because induction and hyperelectrification [29] both depend on the presence of appreciable electric fields, they play a minor role in describing the initial phases of thundercloud electricity but may become all important after the electric field is once fully established by other electrifying mechanisms.

Laboratory clouds produced in the Weather Bureau's giant expansion chamber have provided much valuable information as to the nature of cloud electrification. The experiments show that when the cloud droplets are first formed by condensation they are all essentially neutral [46]. However, as the cloud ages, atmospheric ions diffuse onto the droplets and after an hour or so it is found that the average droplet carries about 10 elementary ions, half of the droplets being positively charged and the others negatively charged [46]. In order to establish the nature of the electrifying process studies were made of a number of different aerosols dispersed in the air by different methods [28, 46]. For example, cloud droplets formed by sudden expansion from moist air are initially neutral. A sulphur aerosol formed by the condensation of sulphur vapor is similarly neutral. On the other hand, a finely divided cloud of silica particles blown into the air by an air blast are found to be highly electrified both positively and negatively [46]. Water droplets atomized by an air blast are also highly electrified. In spite of the complexities suggested by the above differences in initial behavior of newly formed dust and water clouds, we have discovered that for droplets of the same size the electric charge magnitude and distribution are

TABLE IV*

Number of Collisions	Number of Unit Charges q																			
	−10	−9	−8	−7	−6	−5	−4	−3	−2	−1	0	+1	+2	+3	+4	+5	+6	+7	+8	+9	+10
0											1000										
1										500		500									
2									250		500		250								
3								125		375		375		125							
4							62.5		250		375		250		62.5						
5						31.2		156		312		312		156		31.2					
6					15.6		93.7		234		312		234		93.7		15.6				
7				7.8		54.6		164		273		273		164		54.6		7.8			
8			3.9		31.2		109.0		218		273		218		109.0		31.2		3.9		
9		1.9		17.5		70.3		164		246		246		164		70.3		17.5		1.9	
10	0.9		9.7		43.9		117.0		205		246		205		117.0		43.9		9.7		0.9

* Beginning with 1000 neutral drops, the table gives the probable number of drops carrying the assigned numbers of unit charges indicated in the top horizontal line, after suffering the number of unit charge transferring collisions shown in the left-hand column. Note that the distribution after a number of collisions is nearly Gaussian.

finally exactly the same no matter how the cloud is first produced *provided the aerosol is aged by exposure to copious ionization* [46]. This ionization may be produced by cosmic rays, X rays, or any other suitable ionizer. Since the final equilibrium charge distribution of an aerosol is the same irrespective of the original neutral or highly electrified condition and since the equilibrium depends on the presence of ionization, it is clear that the atmospheric ions are responsible for their charges. The time required to establish the charge equilibrium on cloud droplets is comparable to the value given in (15). But it may be noticed that the potential of the typical cloud particle does not finally approach zero as suggested by (14) but rather a value something less than kT/e. Thus each cloud droplet in the semiconducting atmosphere acts as though it were a tiny electrical concentration cell [10].

The electrification of cloud droplets by diffusion plays an important role in the mechanics of precipitation. When the cloud droplets are electrified like those in Figs. 14 and 16 the establishment of electric fields throughout the cloud may profoundly modify the collision processes and the resulting stability. For example, we have shown that when the electric field exceeds about 2 statvolt/cm the electrical forces may sometimes be as effective as gravity in promoting precipitation [24]. Thus, in the presence of high fields the rate of precipitation may be greatly increased. Indeed, there is evidence to suggest that this process is responsible for the so-called "rain gush" sometimes observed in thunderstorms.

The Diffusion Charging of Droplets in an Ionized Atmosphere

It has been found possible to show from the ordinary classical diffusion equations that the bombardment of droplets by ions describing free paths as a result of their thermal kinetic energy, act to establish a Gaussian-like distribution of positive and negative drops just like that observed. The fundamental mechanisms may be understood by reference to Table IV. Suppose that cloud droplets are suspended in the air where there are n_+ positive ions and n_- negative ions per unit volume, and suppose further that their mobilities are u_+ and u_- respectively. Because of the thermal motions of the ions, the ratio of the probability of a positive ion striking a droplet as compared to the probability of a strike by a negative ion is n_+u_+/n_-u_-. For illustration, suppose that the probability of a droplet acquiring a positive ion is exactly the same as the probability of it capturing a negative ion. Now, if there are a thousand droplets initially, after one ionic collision, 500 droplets will acquire a positive ion and 500 will pick up a negative one. When these electrified droplets capture a second ion, half of the droplets in each new group will acquire a positive ionic charge and the other half a negative charge. Thus, after two collisions 250 droplets will have two negative charges, 500 will be neutral, and 250 will have two positive charges. By carrying out this procedure for each succeeding collision one may show as in Table IV that a distribution is established in which equal numbers of positive and negative cloud droplets are present and the Gaussian-like distribution will be symmetrical about the axis of zero charge. It is especially important to notice from Table IV that the mean charge on the cloud droplets is many times the charge on the parent ions.

It frequently happens that the number of positive and negative ions or their mobilities are different, and this modifies the relative probability of collision. One may easily construct another table in which the probabilities of collision for the positive and negative ions are different [32]. The reader may verify that a distribution is established here also, but the maximum is displaced systematically towards the sign of the droplet charge having the highest probability of collisions.

It should be emphasized here that Table IV describes only the initial phases of the electrification and one may show that as the number of collisions increases to large values, sufficient charge is transferred to the mean drop to reduce the probability of collision with ions of the same sign and increase the probability of collision with ions of the opposite sign. Under such conditions an equilibrium charge is established. This conclusion is

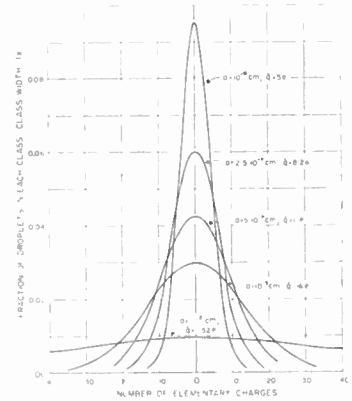

Fig. 12—Distribution of the fractional number of cloud droplets carrying assigned numbers of elementary charges and having different radii. The mean charge, $\bar{q}$, irrespective of sign, is indicated on each curve. Distribution calculated from (19) with $\lambda_+/\lambda_-=1$.

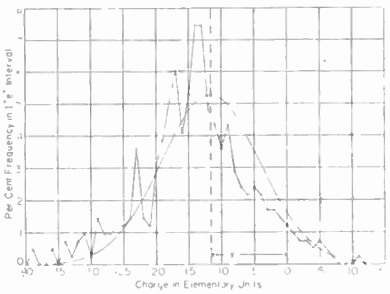

Fig. 13—Measured fractional number of water droplets carrying assigned numbers of elementary charges. Average radius 3.3μ. Measured conductivity ratio $\lambda_-/\lambda_-=0.82$ so that average free charge is -11.7 elementary units. Smooth curve is calculated from (19).

based on a careful analysis of the dynamical equilibrium established by diffusion as recently worked out by the author [22, 23]. It is sufficient to mention here that by applying well-established laws describing the motion of particles subject to electric fields and diffusion, one may work out the rate at which ions are transferred and accumulated on a spherical droplet. From these relations it is possible to determine the resulting distribution through a theorem on detailed balancing at equilibrium [23]. In an assemblage of a large number of droplets of common radius a immersed in an environment wherein the ratio of the positive and negative light ion conductivities is λ_+/λ_- we have shown that

$$\frac{F_x}{F_t}=\frac{e}{(2\pi akT)^{1/2}}\exp\left\{\frac{-\left(x-\frac{akT}{e^2}\ln\frac{\lambda_+}{\lambda_-}\right)^2}{\frac{2akT}{e^2}}\right\} \tag{19}$$

where F_x is the number of droplets carrying x elementary charges of magnitude e, F_t is the total number of droplets, k is the Boltzmann constant, T is the absolute temperature, and e is the elementary electronic charge. *This is the fundamental electrification equation for aerosols* [23], and includes both the statistical and systematic charging. The distribution calculated from (19) for a number of different droplet sizes is shown in Fig. 12 when $\lambda_+/\lambda_-=1$. By integration of (19) one may determine an average number of elementary charges, irrespective of sign, carried by the aerosol particles. From this it is found that [23]:

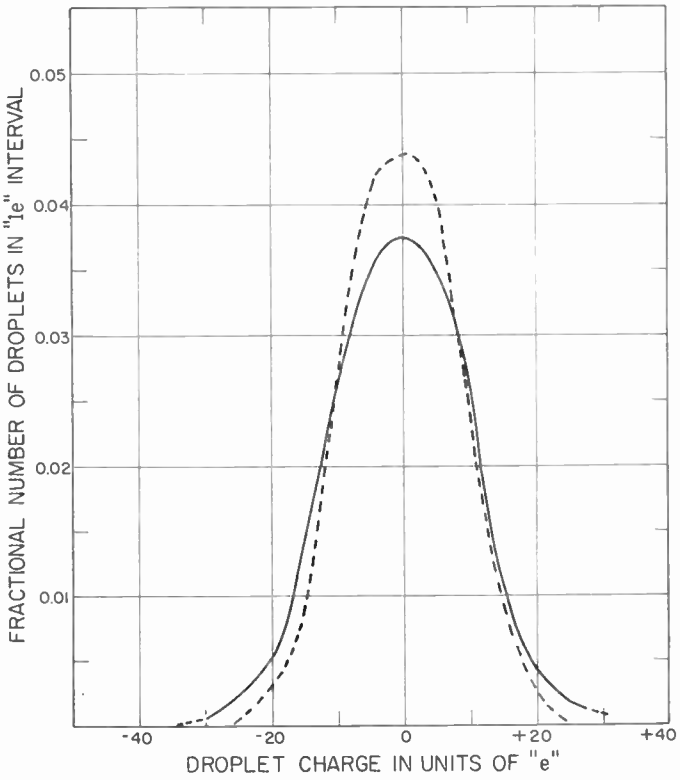

Fig. 14—Observed droplet charge distribution in natural cloud. Radius=4μ. Electric field small. Dotted curve calculated from (19).

$$\frac{\bar{q}^2}{2a}=\frac{\pi}{4}kT \tag{20}$$

where $\bar{q}$ is a previously defined mean charge, averaged without respect to sign [23]. Now since a is essentially the electrical capacity of the droplet, the terms on the left-hand side represent the stored electrical energy, while kT is the probable thermal kinetic energy. Thus an *equipartition* is established between the *electrical* and *thermal energies* of the droplets when equilibrium is finally reached.

The fundamental electrification expression of (19) has been well tested in the laboratory. It may be noticed particularly that when the ratio of the probabilities for capture of positive and negative ions or λ_+/λ_- is different from unity, then the curves in Fig. 12 are systematically displaced [28]. An experimental measurement of the distribution under carefully controlled conditions with $\lambda_+\neq\lambda_-$ is shown in Fig. 13. The measurements are fully consistent with the basic equation.

For the purpose of comparison with the analysis just indicated, one shows in Fig. 14 the distribution ob-

served in a *natural cloud* on the top of Clingman's Peak, N. C. This cloud was relatively stable and the electric field at the point of measurement was negligible. Thus, in accordance with (19), the distribution would be expected to correspond to $\lambda_+=\lambda_-$ and be symmetrical about the zero charge axis.

Systematic Electrification by Ionic Diffusion $\lambda_+\neq\lambda_-$

Droplets maintained in an environment wherein the electrical conductivities for the positive and negative ions are different all develop a systematic electrification of preferred sign. This phenomenon is illustrated in Fig. 13. When the cloud particles are sufficiently small the distribution coincides with (19) above, but whenever there is appreciable relative motion between the droplet and its ionized environment this motion modifies the ionic density gradient around the droplet and increases the systematic charge. It may be shown that under these circumstances the falling droplet acquires a mean systematic charge [22] given by

$$Q=\left[1+F\frac{aVe}{2\pi kTu_{\pm}}\right]^{1/2}\frac{akT}{e}\ln\frac{n_+u_+}{n_-u_-} \qquad (21)$$

where F is a numerical constant of the order of unity, V is the velocity of fall of the droplet, $u_{\pm}$ is the mobility of the mean ion in the transition layer next to the droplet, and $n_+u_+/n_-u_-=\lambda_+/\lambda_-$. The enhanced electrification due to the motion of the droplet is by no means negligible, because large raindrops falling in a field free region can easily accumulate 20 times the charge that would be developed were the drop maintained at rest. The essential correctness of (21) has been verified by laboratory measurements employing a small wind tunnel supplied with ionized air [42].

It is clear from (19) and (21) that no *systematic* charge is transferred to the droplets whenever the positive and negative light ion conductivities are equal. According to an earlier investigation this conductivity ratio depends notably upon the number of particles suspended in the air and their radius [31]. The relationship is specified in Fig. 15. Thus, in a typical stable cloud where $N_0^2a^2/q$ is large the droplet charges are distributed at random and no systematic electrification is produced. However, in those special regions where there are relatively few droplets or snow flakes per unit volume the conductivity ratio may be much different from unity and considerable systematic electrification produced. (See Fig. 13.) Recent work has shown that rain is initiated in typical warm clouds when parcels of nearly nuclei free air are lifted near the tops of clouds [33]. The droplets then formed by direct condensation are abnormally large and examination shows that the conditions for their production are just those required systematically to electrify them. In the presence of sufficient cooling these droplets may grow to produce raindrops carrying charges of moderate size. Such systematic droplet electrification plays a part in the *initiation*

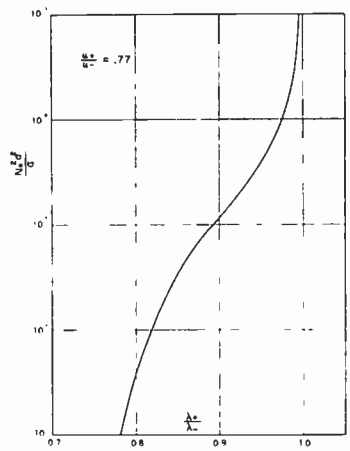

Fig. 15—Calculated relation between $N_0^2a^2/q$ and the ratio of the light ion conductivities λ_+/λ_-.

of electric fields. Since the process can electrify either snow flakes or droplets it is clear that even warm clouds may develop lightning [6, 24, 25].

Hyperelectrification of Cloud Droplets in an Electric Field

Many suggestions have been made as to ways that cloud and raindrops might acquire their charge [36, 47]. Space does not permit a general discussion of this interesting problem and one considers here only those electrification processes that are thought to be so energetic that they probably control the basic phenomena. As emphasized above, ionic diffusion is a universal phenomenon and it is, therefore, particularly important whenever electric fields are not present. However, it is well known that electric fields are commonly generated by precipitation and in their presence very energetic droplet electrification is produced by other processes.

Consider a slightly conducting sphere immersed in an electric field. It becomes polarized and free charges of opposite sign are induced on the opposite polar surfaces. When this polarized sphere is maintained in a conducting atmosphere, the positive ions migrate to the negatively charged areas and the negative ions migrate toward the positive. A careful analysis of this process shows that if the conductivities of the positive and negative ions are equal the sphere accumulates no net charge. On the other hand if the conductivities are notably different the sphere acquires a free charge comparable to the charge induced near its poles or $\pm 3E_0a^2$ [29]. This process might not be particularly important were it not for the fact that atmospheric electric fields invariably sweep ions of a single sign into extensive space charge or transition layers that mark gross discontinuities in the electrical conductivity. In such transition layers the conductivity ratios may be very large and all the droplets maintained in this region become highly electrified and all have the *same sign*. On the other hand, a cloud composed of several parts, each separated by clear air, will produce drops of opposite signs on the adjacent faces of the juxtaposed sections. A mixture of charges may then

be anticipated. The magnitude and reality of this process which we have called *hyperelectrification* has been established in the laboratory [29]. The magnitude of the charge transferred to such polarized spheres is [29]

$$Q = 3E_0a^2\left[\frac{(\lambda_+/\lambda_-)^{1/2} - 1}{(\lambda_+/\lambda_-)^{1/2} + 1}\right]. \tag{22}$$

The specific charge is therefore

$$\frac{Q}{M} = \frac{9E_0}{4\pi ad}\left[\frac{(\lambda_+/\lambda_-)^{1/2} - 1}{(\lambda_+/\lambda_-)^{1/2} + 1}\right] \tag{23}$$

where d is the bulk density of the drops. As an example of hyperelectrification consider Fig. 16 representing the charge distribution on natural cloud droplets observed on top of Clingman's Peak when the cloud droplets were exposed to measured electric fields. It may be noticed that all of the droplets are highly electrified and carry only a negative charge. The observed distribution may be related to variations in droplet size but their mean value is indicated in the caption of the figure. The new data of Figs. 14 and 16 were kindly made available through Dr. Gilbert D. Kinzer.

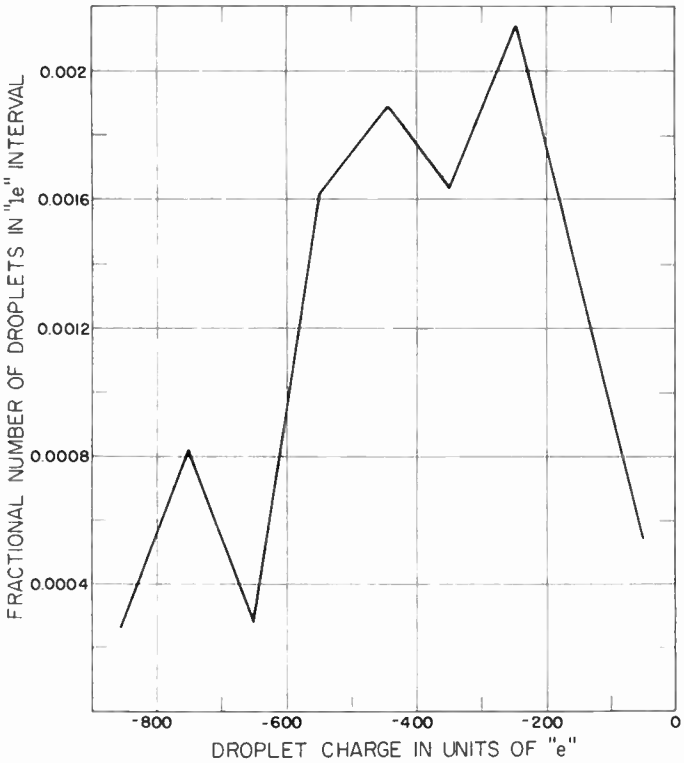

Fig. 16—Droplet charge distribution observed in natural cloud. Radius 8μ. Electric field $\neq 0$. An example of hyperelectrification.

Electrification by Induction of Colliding but Nonassociating Snow Flakes and Raindrops $E \neq 0$

Some of the following sections emphasize the enhanced electrification that may be transferred to falling rain as a result of the association of large numbers of electrified cloud droplets. There is, however, a special case of considerable importance wherein electrical effects are produced *because the particles do not associate* or because they breakup in an electric field. Ice crystals and individual snow flakes are commonly formed at high levels where the temperature is below freezing and these grow to appreciable size by direct condensation of the water vapor. These snow flakes fall at different velocities and frequently collide but thereafter may immediately separate because no surface tension forces promote association as in water droplets. Whenever an electric field is present the snow flakes are polarized and on contact may exchange charge. It is clear that if the colliding particle are favorably oriented with respect to the electric field their separation may produce a highly charged positive and negative pair. In a somewhat similar way raindrops that collide and immediately separate instead of associating will have opposite charges on the separated drops. It is well known that raindrops having a radius greater than about 0.25 cm, commonly break up. Large charges of opposite sign will then be produced by induction on the resulting smaller drops.

Recently Müller-Hillebrand [38] has revived the well-known Elster and Geitel [5] mechanism by showing that ice crystals in collision with graupel possess sufficient conductivity to permit an exchange of charge and thus become systematically electrified. The Müller-Hillebrand processes may very well contribute to the electrification but the simple induction processes are much more energetic.

Consider a large number of snow flakes falling in the cold high atmosphere. These flakes are of different sizes and have different aerodynamic properties so that there is relative motion between all the particles and collisions are moderately frequent. Suppose that any two flakes or any two nonassociating raindrops may be thought of as two similar polarized slightly conducting spheres. Now if they collide in such a way that the line joining their centers is in the direction of the electric field, then one may show that the free charge induced on each sphere has a magnitude given by

$$Q = \frac{\pi^2}{3} E_0a^2 \tag{24}$$

where E_0 is the impressed electric field and a is the radius of the spheres. Upon separation one sphere will carry a positive charge and the other a negative charge of the same magnitude. When the orientation is random, the average charge will be some appreciable fraction of (24). Because the separating components are of opposite sign they will attract each other and in some cases the initial relative kinetic energy between the particles will be insufficient to separate them. Accordingly, the induction process will be important only when the relative kinetic energy is greater than $Q^2/2a$. It can be shown that such a requirement is met in most cases and perhaps most snow or ice crystal collisions and

nonassociating raindrop collisions result in oppositely charged *pairs* of magnitude comparable to (24). Such simple induction processes have a marked advantage over other mechanisms because the charging is instantaneous and does not depend either on the generation or on the capture of ions. The mechanism is believed to be of considerable importance. From (24) it follows that the charge per unit mass or the specific charge irrespective of the sign is $Q/M = \pi E_0/4ad$.

Electrification by induction is highly efficient and energetic so that when this process is common, a mixture of snow flakes or raindrops carrying *nearly equal positive and negative charges will be found in the atmosphere.* Because the charges transferred to each particle are proportional to the electric field, flakes falling near the freezing level where the field is normally large are likely to be highly electrified and if they further associate to form rain *after they melt*, extraordinary high drop charges may be anticipated. The Graupel forming stage, therefore, is likely to transfer excessively large free charges to the drops. Indeed, calculations suggest that corona will be discharged from a small percentage of them [32].

Attention is drawn to the fact that the free water necessary to produce a snow flake is only about 1/50 that for a spherical water drop of the same size [34]. Since the charge induced on each separating flake is proportional to the square of its linear dimensions, it is clear that snow crystals electrified by induction in an appreciable electric field may produce relatively *large free charges per unit mass.* In the next section we will consider the electrical effects produced when such highly electrified snow flakes melt to form droplets and these further associate to produce enhanced electrification.

Enhanced Electrification by the Association of Electrified Droplets to Form Rain

Enhanced electrification is always produced whenever electrified cloud or rain droplets collide and associate to form rain [24, 25, 32]. Analysis shows that if the cloud droplets are all of one sign the association simply concentrates these free charges on the raindrops and the free charge is conserved. On the other hand, if the parent cloud droplets are composed of a mixture of positive and negative charges the association processes neutralize some of the available free charge. However, the statistics of the processes are such as to establish a mixture that effectively preserves an appreciable fraction. (See Table IV.) This charge is distributed more or less equally among a large number of drops each of which may sometimes carry thousands of the original cloud droplet charges [24, 25, 32].

According to the results of earlier sections a typical cloud consists of large numbers of droplets in which about half of the droplets carry a positive charge that is typically 11 elementary units while the other half typically carries 11 negative units. Normally 4 per cent or less of the droplets are uncharged. Suppose that a small raindrop falls down through such a cloud and grows by association thus consolidating the charges carried by the cloud droplets. The falling raindrop is accordingly bombarded in a purely random manner by the cloud droplets which it successively intercepts. If there are equal numbers of positively and negatively charged droplets the probability of the drop colliding with a positive droplet is the same as the probability of it colliding with a negative droplet. The statistical distribution of charge may, therefore, be worked out in a manner precisely like that used to determine the charge on the cloud droplet when it was bombarded by ions. The exact process is well illustrated by Table IV. The fundamental difference between the electrification of the cloud droplet and the raindrop is that the cloud droplet encounters ions by virtue of their thermal agitation, whereas the raindrop is bombarded as a result of the relative gravitational motions of the large raindrop and the small electrified droplets.

Two raindrop electrifying regimes by droplet association are evident. The initial or nonequilibrium regime describes the early stages of electrification and is descriptive as long as the probability of collision of a droplet with a charged drop in constant. This regime is gradually converted into the equilibrium regime which is established whenever accumulated raindrop charges become large enough to control the probability of collision.

The Initial or Nonequilibrium Regime

Whenever the number of collisions between the raindrop and the cloud droplets is limited and the probability of collision is constant, the *average* charges *for the distributions* illustrated by Table IV may be estimated by use of the binomial point equation of statistical theory. It has been shown [32] that the mean nonequilibrium charge accumulated on raindrops $\hat{Q}$, *averaged without regard to sign*, is nearly

$$\hat{Q} = \left[\frac{2K}{\pi}\right]^{1/2} \bar{q} \tag{25}$$

where K is the number of collisions that establish the charge on the raindrop and $\bar{q}$ is the mean charge on the parent droplets, irrespective of their sign. The value of $\bar{q}$ may be given by (20) or by (24). Since K may be large it is clear that very large drop charges may sometimes accumulate.

In the special case where there are more cloud droplets carrying one kind of charge than the other, and their numbers per unit volume are C_+ and C_-, it is found [32] that the mean *systematic* charge $\overline{Q}$ accumulated on the raindrops *averaged with respect to sign* is

$$\overline{Q} = \left[\frac{\frac{C_+}{C_-} - 1}{\frac{C_+}{C_-} + 1}\right] K\bar{q} = \frac{K\bar{q}}{2} \ln\left(\frac{C_+}{C_-}\right) \tag{26}$$

where the logarithmic form is applicable only when C_+ and C_- are not too different. The above nonequilibrium expressions for the raindrop charges are of value only when the number of collisions can be specified. Although other assumptions are possible, it is illuminating to suppose that the number of collisions is determined only by the ratio of the mass of the final drop to the mass of the average colliding cloud particle. Under this condition the random specific charge or the charge per unit mass accumulated on the falling rain, when averaged without regard to sign [32], is given by

$$\frac{\hat{Q}}{m_2} = \left[\frac{2fm_1}{\pi m_2}\right]^{1/2} \frac{\bar{q}}{m_1} \tag{27}$$

where $\bar{q}/m_1$ is the random specific charge carried on the parent droplets, m_1 and m_2 are the masses of the cloud and raindrops, respectively, and f is an unknown factor that measures the evaporation, breakup of the drop, etc., and approaches unity when these factors are negligible. In a similar way the systematic specific charge transferred to the falling rain is [32]:

$$\frac{\bar{Q}}{m_2} = \left[\frac{C_+ - C_-}{C_+ - C_-}\right] f \frac{\bar{q}}{m_1}. \tag{28}$$

This expression shows that the systematic *specific free charge is conserved* during drop growth.

The Equilibrium Electrification of Raindrops

When there are sufficiently large numbers of collisions with the cloud droplets or when the cloud droplets are highly electrified an equilibrium distribution much like that given in (19) may be established. The fractional number of raindrops carrying integral multiples of the mean cloud droplet charge $\bar{q}$ is essentially a Gaussian distribution. This distribution is normally symmetrical about the zero charge axis whenever equal numbers of positive and negative cloud droplets are encountered, but may be radically skewed towards positive or negative charges when the population densities C_+ and C_- of the positive and negative parent cloud droplets are appreciably different. When equilibrium is established one may show [24, 25] from the mathematical analysis that

$$D_{\Omega\bar{q}} = \frac{D_t \bar{q}}{\left[\dfrac{\pi(r_1 + r_2)U_R^2}{2\left(\dfrac{1}{m_1} + \dfrac{1}{m_2}\right)}\right]^{1/2}} \cdot \exp\left\{\frac{-\left[\Omega\bar{q} - \dfrac{(r_1 + r_2)U_R^2 \ln (C_+/C_-)}{4\bar{q}(\{1/m_1\} + \{1/m_2\})}\right]^2}{\dfrac{(r_1 + r_2)U_R^2}{2\left(\dfrac{1}{m_1} + \dfrac{1}{m_2}\right)}}\right\}. \tag{29}$$

In this expression D_t is the total number of raindrops per unit volume, $D_{\Omega q}$ is the number per unit volume carrying a charge $\Omega\bar{q}$, $\bar{q}$ is the mean parent droplet charge, irrespective of sign, Ω is an integral number, m_1, m_2 and r_1 and r_2 are the masses and radii of the cloud and raindrop respectively and U_r is the relative velocity of the two types of drops. The ratio of the number of parent positive cloud droplets to those carrying negative charges is C_+/C_-. It may be noticed that this expression is similar in form to (19) and analogous to it in many ways. Thus one may calculate the mean charge on both the positive and negative *fractions* of the falling rain and show that this charge is given [25] by

$$Q_+ = \left[\frac{\pi(r_1 + r_2)U_R^2}{8\left(\dfrac{1}{m_1} + \dfrac{1}{m_2}\right)}\right]^{1/2} = \bar{Q}_-. \tag{30}$$

Like (19) this may also be rewritten to show that an approximate *equipartition* is established wherein the electrical potential energy carried by the average falling raindrop is equal to the energy of bombardment by the smaller cloud particles.

One may emphasize that the equilibrium charge described by the above equations is not always established in ordinary rain because of the limited distance of fall or limited numbers of collisions. This is particularly true when the cloud droplets are weakly electrified as by ionic diffusion. As a rough guide, the equilibrium distribution of (29) and (30) may be used whenever a mixture of highly electrified droplets is produced as by induction. The nonequilibrium expressions of (27) and (28) are used when the droplets are weakly electrified as by the diffusion processes. No general rule is applicable and a special examination must be made in doubtful cases [32].

Maximum Accumulated Drop Charges

In an earlier analysis of the electrical charges measured on the ground and on aircraft flying through active thunderstorms, it was pointed out that the raindrop electrification processes must be extremely energetic because large numbers of drops of both signs were observed, each of which carried charges so large that the electric field at their surface was an appreciable fraction of the dielectric strength of air [14]. Reference to Table II will show that direct measurement of the charge on thunderstorm rain suggests charges approximating ± 0.1 esu/drop. Now, if the drop corresponds to "medium rain," its radius will approximate 5×10^{-2} cm. The electric field at the drop's surface, therefore, is about 40 statvolt/cm or 12,000 volt/cm. When one reflects that such drops approach small conducting cloud particles that may locally concentrate the electric field, and notes further that the drop is frequently deformed as a result of aerodynamic forces, it is clear that adequate fields may exist at the drop surface to produce a corona discharge. Actually, the conditions necessary to induce

corona are more complex than the above statement implies. It has been long known that a certain minimum voltage is necessary as well as a large electric field. In small droplets the voltage is so low that electric fields exceeding the normal dielectric strength of air will not cause discharge but drops as large as the example used above may very well exceed the critical value and transfer by corona discharge any excess charge to the surrounding air [14]. It seems clear from the data in Table II and from other measurements made in active thunderstorms near the rain-forming levels, that many of the larger raindrops are "fully charged" by the acting electrification processes.

Free Charge Distributions and Their Separation

Whenever equal amounts of positive and negative electricity are found within a given volume, it is neutral and no systematic electric fields are produced. In a thundercloud consisting of a mixture of highly charged raindrops, electrified cloud droplets, and ions, it is *not likely* that such a condition of exact neutrality will long persist. Consider a great neutral sheet of rain and cloud droplets. The rain falls faster than the cloud particles and an initial neutrality is shortly replaced by a free charge distribution. For example, negative charges largely carried by rain generally appear near the bottom of high level clouds while positive charges are likely to remain above. By considering a vertical prism of unit cross section extending from the ground through the thundercloud one may calculate the electric field E and the total charge per unit area within the prism by integrating Poisson's equation

$$E = 4\pi \int \rho dz = 4\pi\sigma + E' \qquad (31)$$

where ρ is the free charge per unit volume, σ is the integrated free charge per unit area, and E' is the constant of integration determined by the surface charge. In this way one may formally determine the field in terms of the separated free charges on the precipitation and on the ground [10].

In addition to the free charges carried inside the cloud there are invariably charges induced on the conducting ionosphere and on the earth below. These induced charges play an important role in transferring electricity to the earth. The induced and free charge per unit areas within the prism are usually so adjusted that the total is approximately zero. In typical cases the electric field within the active region of the thundercloud is downward. But near the ground and above the cloud, the field is positive and outward. Sometimes the whole configuration is reversed. Usually the separation of free charge establishes fields that not only induce charges on the high atmosphere and the ground but simultaneously transport ions towards charge centers and thus establish space charge sheets that act to limit the intensity of the electric field as measured at the earth's surface. This effect is prominent in the observed reversal of the field after a lightning stroke (Fig. 1).

According to the direct measurements reported in Table II above, the rain inside an active thunderstorm may consist of nearly equal numbers of positively and negatively charged drops or in some cases drops carrying a single sign are observed. When a matrix consisting of equal numbers of equally charged positive and negative drops are present in the air and both types fall at the same velocities, it is clear that no free charge separation or electric fields are produced. On the other hand, if the larger raindrops carry predominantly charge of one sign, neutrality of any given volume of space cannot be maintained and the big drops carrying their selected charge will fall, leaving their neutralizing charges of opposite sign to fall at a slower rate. A progressive separation of free charge by this means steadily increases the electric field. The accumulation of separated free charge cannot continue for long, because according to (31) electric fields of progressively greater intensity are immediately established and these fields interacting with the charge on the droplets produce electrical forces that act to oppose and limit the separation. In some cases these forces are adequate to support many of the raindrops against the forces of gravity [10].

One may emphasize that in most cases the free positive charges are never completely separated from the free negative charges. For example, in a mild cold front exhibiting charges like those summarized in Table III, it was found that the free charges corresponding to those measured on the large drops and distributed through a spherical volume a kilometer or so in radius would establish electric fields at the surface of the sphere many times as large as that actually measured. This shows that the charge separation is incomplete and that, in nature, there is always a mixture of positive and negative charges. However, one sign may be somewhat in excess [17]. This same conclusion is reached by calculatint the approximate free space charge density from the observed space gradients of the electric field values, and comparing this value with the free charges directly measured on the precipitation. The charge on the precipitation alone is again several times the net space charge showing that neutralizing charges, not measured by the raindrop analyzing equipment are present and mixed with the highly charged rain. Thus it is always necessary to distinguish carefully between the drop space charge density and the net space charge density [12].

According to the foregoing observations made inside actual storms one is brought to the view that a typical thunderstorm cloud is composed of large amounts of free charge of both signs carried partly by large raindrops, partly by small cloud droplets, and partly by ions. In this matrix, the heavily charged raindrops always fall towards the earth and when they carry charge

predominantly of a single sign, then a convective or transport current is produced carrying charge towards the ground and separating free charge. The magnitude of this convective current density [18] is given by

$$i = \Sigma N_+ Q_+ V_+ + \Sigma N_- Q_- V_- = \rho \overline{V} \qquad (32)$$

where N_+ and N_- are the numbers of large raindrops per unit volume carrying positive and negative charges respectively. Q is the charge on each, $V_\pm$ is the velocity of fall of the drops; ρ is the net free space charge density; and V is its effective falling velocity. The velocities of fall for large drops is primarily determined by the aerodynamic forces and by gravity. But the smaller drops develop lower velocities that may be somewhat influenced by the electric fields.

It is clear from the foregoing paragraphs that gross electrification is not likely to be established within a cloud unless some mechanism selectively transfers free charge to the larger raindrops. One has, therefore, to examine the possible processes which can transfer free charge to rain. That such selective charging frequently occurs is fully demonstrated [12, 17, 19] by detailed plots of the summarized data. For example, in both the thunderstorm in the mild cold front mentioned above, *regions were observed wherein the large precipitation elements all carried charges of the same sign.* Neutralizing charges doubtless were associated with these but were attached to the smaller particles that would fall at a very much slower speed. Thus, according to (32) a net convective current is established.

Hyperelectrification provides an energetic mechanism for placing charges, all of one sign on large number of raindrops. We have shown that near the boundaries of electrified clouds, ions of a selected sign are concentrated; these ions are transferred to the polarized raindrops immersed in the layer and selectively charge them to a value given by (22). Now within the boundary space charge layer the positive and negative light ion conductivities are normally much different so that the drop charges are generally of one sign.

The number of raindrops or snow flakes in unit volume is determined by the liquid or crystalline water content (LWC) of the cloud and the droplet mass, so that the convected current density i of (32) in the case where all drops carry the same sign of charge, as for example, in hyperelectrification, is

$$i = (\mathrm{LWC}) \frac{Q}{M} V \qquad (33)$$

where the velocities of fall V may be determined nearly enough from available Tables of terminal velocities [16].

Earlier paragraphs have noticed that a mixture of highly charged positive and negative raindrops can be established either by induction in an electric field or by the association of large numbers of oppositely electrified cloud or rain droplets. Irrespective of the processes whereby such a mixture is produced, drops, falling down through an atmosphere wherein the positive and negative light ion conductivities are different, will selectively discharge drops of one sign more rapidly than they will discharge those of the opposite sign. This process results in the accumulation of raindrops at lower levels having a predominant free charge [27]. Whenever the initial specific charge of the mixed raindrops is sufficiently large and the differences in electrical conductivity are considerable, the convected current densities are large enough to establish measurable electrical activity [27]. The difference in conductivities between the positive and negative ions is established only for clear air as shown by (11) and (12) but there is accumulating evidence [37, 39, 43] to show that the conductivities are frequently much different inside natural clouds or in precipitating regions. Whenever the raindrops fall some kilometers in an atmosphere wherein $\lambda_+ \neq \lambda_-$ we have been able to show that the current density established by the above differential discharge processes is given roughly by [27]:

$$i = \frac{\mathrm{LWC}}{2} \left(\frac{Q}{M}\right) V \left[\exp(-1) - \exp\left(\frac{-\lambda_+}{\lambda_-}\right)\right] \qquad (34)$$

where λ_+/λ_- is the ratio of the conductivities of the environment through which the drops fall.

It is convenient to recognize that the product of the liquid water content and its effective velocity of fall corresponds to the mass precipitation rate P expressed in terms of grams per square centimeter per second and therefore the convected current density may always be represented by an expression of form

$$i = (\mathrm{LWC}) \frac{Q}{M} V \phi(\lambda_+/\lambda_-) = P \left(\frac{Q}{M}\right)' \phi(\lambda_+/\lambda_-) \qquad (35)$$

where the function $\phi(\lambda_+/\lambda_-)$ measures the fraction of the total drop charge Q that is preserved as a free or systematic charge. This fraction depends on the particular drop electrifying mechanism and commonly approximates values from 0.05 to 1.0.

The energetic processes capable of highly electrifying rain that is exposed to electric fields have been emphasized above. There are, in addition, other electrification means that may contribute to the establishment of thunderstorm activity. For example, melting hail may place an excess positive charge of more than 1 esu on each gram that melts and falls to lower levels [4]. Similarly, the selective transport of ions to cloud droplets in regions where the positive and negative light ion conductivities are notably different can, according to (21), produce specific charges of 1.0 esu/gm under favorable conditions [26]. This latter process is of some importance in describing the initial electrification induced by low level nonthunderstorm rain.

Equilibrium Electric Fields and the Regeneration Time

Because electric fields are easily measured, it seems important to express the charge transferring processes in terms of the established field. Consider for example the downward transfer of a horizontal sheet of negatively charged raindrops and assume that the positive charge remains essentially fixed on the smaller cloud droplets above. Earlier articles [18, 20] considered the equilibrium in a vertical prism of unit cross section extending from the earth through the thundercloud. It was shown that in this prism

$$\frac{1}{4\pi}\frac{dE}{dt} + \lambda E = \Sigma NQV = \rho\overline{V} = i. \tag{36}$$

The first term expresses the accumulation of free charge per unit area below a selected reference plane, the second term the conduction current density, and these are equal to the convective current density i. The solution of (36) is

$$E = \frac{\rho\overline{V}}{\lambda}\left[1 - \exp\left(-4\pi\lambda t\right)\right] + E_1 \exp\left(-4\pi\lambda t\right) \tag{37}$$

where E is the generated electric field at the reference plane, E_1 the field at the plane when $t=0$, λ the total electrical conductivity of the environment, ρ the net free charge density carried by the large raindrops, and $\overline{V}$ is the fall velocity of the heavy drops relative to the much smaller ones that carry the neutralizing or partially neutralizing charges. It is clear from (36) that when an equilibrium electric field is established, the charge accumulating below the reference plane approaches zero and the downward convected current density is just balanced by the upward conduction current density. Thus the equilibrium electric field approximates

$$E_e = i/\lambda = \frac{\rho\overline{V}}{\lambda}. \tag{38}$$

Now immediately after a lightning discharge, E_1 is small and therefore by (37) one has approximately

$$\left(\frac{dE}{dt}\right)_0 = 4\pi\rho\overline{V} = 4\pi i. \tag{39}$$

Here $[dE/dt]_0$ is the *initial* rate of increase of the electric field just after the thundercloud has been neutralized by a lightning discharge. Thus, if the electric field recovers logarithmically as suggested by (37), the time τ_R it will take the convection current to raise the electric field to a value E_e is given by [20]:

$$\tau_R = \frac{E_e}{4\pi i} = \frac{E_e}{4\pi\rho V}. \tag{40}$$

It is illuminating to identify this critical field E_e with the dielectric strength of air and then τ_R may be identified with the time to regenerate an electrical state capable of producing a lightning discharge. By the use of this expression one may formally express the lightning discharge frequency as a function of the net convected current density and the critical dielectric strength of air. In this way one may plot Fig. 17 giving the discharge frequency as a function of the activity index defined as $\rho\overline{V}/\lambda E_e$ [20].

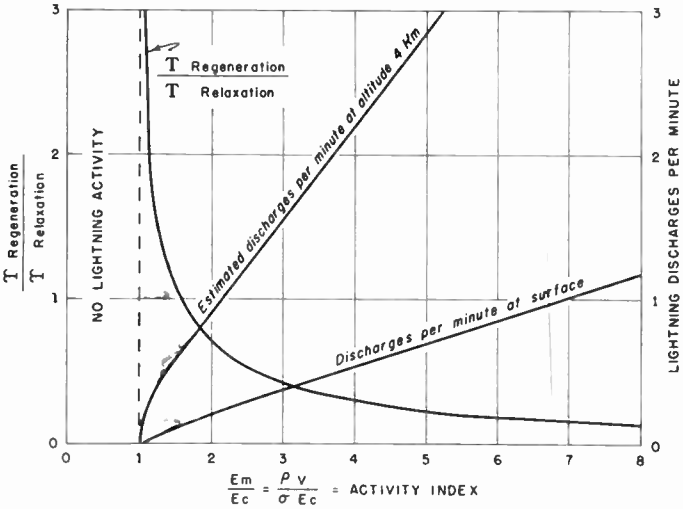

Fig. 17—Estimated relation between the electrical activity index, the lightning recurrence frequency, and the ratio of the regeneration to relaxation times.

For short discharge paths it is well known that the dielectric strength of air is something like 20,000 volt/cm but as the path length increases and electron avalanches develop the dielectric strength steadily decreases to about 4500 volt/cm at ground levels [40]. At higher levels it is systematically less. This value of E_e has been adopted in calculating Fig. 17.

If the atmosphere were a perfect insulator with an extremely high dielectric strength, only selectively charged raindrops would fall, and thus separate free charge until an electric field was established that would either drag downward the lighter particles left overhead or the raindrops would be supported by the field. One may calculate the electric field required to support the droplets and it is found that the required field is in excess of 25,000 volt/cm and greatly exceeds any gradient that can continuously be maintained in ordinary air [18]. This means, in general, that true equilibrium fields seldom fully mature in heavy rain regimes because lightning discharges intervene.

The Initial Electrification of All Precipitating Clouds

The crucial problem of precipitation electricity is to describe how light rain falling from a neutral cloud usually initiates electric fields of from +10 to +30 volt/cm at the earth's surface. It is true that an all pervading fair weather electric field exists over the earth

and presumably has appreciable values at all levels even within a neutral cloud. Therefore, if regenerative mechanisms are invoked to describe the high, subsequently developed fields, this residual field may be of theoretical significance. Actually the presence or absence of a small initial field is not considered important since electric fields may be established in a cloud which is at first entirely neutral and by other straightforward energetic processes.

It is emphasized again that ions are always produced in *pairs* and that the mobility of the negative ion in *clean* air is some 40 per cent larger than that for the positive ion. This provides a fundamental mechanism for establishing a higher conductivity for the negative ions than for the positives, in those regions where suspended particulate matter is a minimum. Observations clearly show that the condensation and sublimation nuclei density normally decreases very rapidly with altitude [35]. Therefore, at rain and snow forming levels, one might anticipate that the number of precipitation particles per unit volume would be low and the negative conductivity would be notably larger than the positive conductivity. This difference has been observed by a number of investigators in clear air and therefore, according to (21), one would expect snow flakes or water droplets at high levels to carry an excess negative free charge.

Now it has been possible to determine the ratio of the positive and negative ionic conductivities from a knowledge of the number of cloud droplets per unit volume, their radius, and the rate of ion pair production. This ratio determines the free charge carried on the droplets through (21). Thus, in the special case when the cloud droplet or snow flake density is low, appreciable net electrification is induced by the difference in ionic conductivities. To illustrate the initial electrification processes, consider an example. Published data on the size of falling snow flakes show that a typical snow flake radius is 0.05 cm and its mass approximates 8×10^{-6} gms [34]. Now when the condensed water content approximates a typical 10^{-6} gm/cm^3, the number of snow flakes per unit volume is 0.12 so that Na approximates 0.006. Thus, at snow forming levels N^2a^2/q approximates 3.6×10^{-6} and by Fig. 15, $\ln \lambda_+/\lambda_- = -0.12$. By use of (21) it is found that the systematic negative charge transferred to the typical snow flakes by ionic diffusion is $Q = -5.2\times10^{-7}$ esu and the specific charge approximates $Q/M = -0.065$ esu/gm. In a similar way one may show that the large rain initiating droplets produced by condensation at levels where the air is relatively free of pollution will produce specific charges of comparable but somewhat larger magnitude. As noted in (26), the *systematic* specific free charge is conserved when the melted or newly formed droplets associate to form larger raindrops. Accordingly, it is evident that, when these droplets coalesce and fall towards the ground, they will transfer negative charge downward. It remains only to determine the magnitude of the electric field that these electrified drops may produce.

By substituting the values suggested in the above paragraph in (21), assuming that liquid or crystalline water content is 10^{-6} gm/cm^3, and that the drops grow large enough to fall at a velocity of 400 cm/sec, then it is found by (33) and (38) that at 2-km altitude where $\lambda = 4.10^{-4}$ esu, that $E_c = +0.06$ statvolt/cm $= +20$ volt/cm. Such an electric field is the same sign and approximate magnitude as the field commonly observed whenever stratus clouds of modest depth precipitate. The field is more than an order of magnitude larger than the fair weather field and is in the direction of commonly observed electric fields in thunderstorms just prior to a discharge. We consider it adequate to excite all the induction and hyperelectrification effects mentioned in the foregoing paragraphs and thus initiate through further regeneration full scale lightning activity.

Electrification of drops by the above process also takes place in the lower levels of the atmosphere but the charges here are predominantly positive because of the excess conductivity of the positive ions. This special case has been considered [26].

Criteria for the Establishment of High Electric Fields by Regeneration

The foregoing section has shown how the diffusion of ions onto falling precipitation may sometimes establish initial electric fields approximating +20 volt/cm. Such a field does not depend on the presence of an initial electric field or upon influence effects.

According to (22) and (24), large charges are transferred to raindrops whenever electric fields are present and these charges are proportional to the impressed electric field. It is important to determine whether the charge so produced can maintain or actually increase an initial field of moderate intensity.

Let the charges transferred to rain by the various influence processes considered above be represented by

$$Q = 3BE_0a^2 \text{ esu} \tag{41}$$

where B is a numerical constant of the order of unity which depends upon the specific electrifying process and upon the relative values of the average and maximum charges actually produced. The charge per unit mass, accordingly, is given by

$$\frac{Q}{M} = \frac{9BE_0}{4\pi ad} \text{ esu/gm.} \tag{42}$$

Thus, by (35), (38), and (41) one finds that

$$\frac{E_e}{E_0} = \frac{(\text{LWC})VB\phi\left(\frac{\lambda_+}{\lambda_-}\right)}{4\pi da\lambda} = \frac{9B\left[\phi\left(\frac{\lambda_+}{\lambda_-}\right)\right]P}{4\pi da\lambda} \tag{43}$$

where P is the mass precipitation rate in gm/cm^{2}sec and $\phi(\lambda_+/\lambda_-)$ represents the functional dependence of

(22) or (24) on the conductivity ratio. This function is also dependent upon the drop radius a.

It is clear that if the generated electric field E_e is greater than the electric field E_0 which transfers charge to the raindrops, then the drop charges will increase and the electric field can steadily increase or regenerate until the dielectric strength of air is surpassed. Accordingly, the criterion for the regeneration and establishment of large fields within a thundercloud from a small initial intensity is that (43) be greater than unity, or that

$$\frac{(\mathrm{LWC})V}{\lambda a}\,\phi\left(\frac{\lambda_+}{\lambda_-}\right)=\frac{P\phi(\lambda_+/\lambda_-)}{a\lambda}\geq\frac{4\pi d}{9B}\doteq 2.8. \quad (44)$$

For the purpose of illustration, it is convenient to adopt numbers that describe the *critical case;* note that precipitation rates and free charges *larger* than this critical value will permit regeneration while lesser values will degenerate. Thus, in this critical case one may adopt as representative $B/d=0.5$, $\phi[\lambda_+/\lambda_-]=0.5$, λ at 2 km $=4\times10^{-4}$ esu, so that $P=0.0022a$ gm/cm² sec. Thus if $a=0.05$ cm corresponding to "medium rain" then $P=0.4$ gm/cm²hr $=0.4$ cm of H_2O/hr. Such precipitation rates and liquid water contents (LWC) are frequently exceeded. It is clear from these figures that regeneration and build up to high electric fields cannot occur unless the precipitation rate exceeds that of typical "medium rain" and unless $\phi[\lambda_+/\lambda_-]$ is some appreciable fraction. The writer believes that this is a proper conclusion because the data clearly show that heavy precipitation is not always accompanied by lightning. It is noteworthy that large precipitation rates act to accentuate any electrical activity already present.

It would be improper to conclude that gross electrification phenomena can only develop through influence effects, but since these are clearly regenerative under certain conditions and are especially energetic we consider them to be of some importance.

The Estimated Electrification in Active Thunderstorms

The foregoing sections have outlined some of the basic electrical phenomena taking place in the earth's lower atmosphere. The differences in conductivities of the positive and negative ions contribute to differential discharge and electrifying processes that ultimately develop free charges on the falling rain. One now considers the over-all behavior and electrical magnitudes within an active thunderstorm.

It has been shown how an initiating positive electric field of about +20 volt/cm could be established by light rain falling to the ground. This initial field is capable of being regenerated and built up by influence effects operating on the falling rain. To illustrate the basic processes, one considers two examples of charge transfer and electric field production that are so energetic that they probably play a major role in establishing the observed electrical state. These processes and possibly others frequently act simultaneously so the electrification of a thundercloud as a whole is likely to be complex.

Consider first a vertical prism of unit cross section extending to high levels where snow flakes and ice crystals are formed and fall towards the melting level. At these high levels the suspended contamination is normally small and some systematic electrification due to ionic diffusion will be produced just as suggested previously. However, quite independent of these diffusion processes the snow crystals will frequently collide and separate. When the separation takes place in an electric field we have seen that large charges of opposite sign are produced on the separated snow crystals. For the purpose of estimation suppose that the ice crystals have a radius that is typically 0.05 cm and that they are favorably oriented with respect to an electric field E_0 at the time of their separation. The magnitude of the positive and negative induced charges by (24) is then 8×10^{-3} E_0 esu. Now when this mixture of highly charged ice crystals carrying both positive and negative charges fall to the melting level and are there converted into water droplets *further collisions will result in association* to form a distribution of highly charged *raindrops* related to that shown in Table IV. It is estimated that some 65 associations between such small *melted* ice crystals will take place before they grow into a "medium raindrop" having a radius of 0.05 cm [34]. Thus, by use of (25), one may calculate the mean multiplied drop charge, averaged without respect to sign, as 5.1×10^2 E_0 esu. The specific charge carried by such associated raindrops is 96 E_0 esu/gm. A short calculation will show that the ratio of the electric field at the surface of the drop to the exciting field E_0 is 20. Thus, if the exciting field E_0 is as much as 2 statvolt/cm the field at the drop surface will approximate 12,000 volt/cm. Any additional charge may well induce corona and thereby limit the drop charges. This example suggests that the electrification by induction and their subsequent association will "fully electrify" the produced droplets whenever the original induced electric field much exceeds 2 statvolt/cm. Attention is drawn to the fact that nearly equal numbers of positive and negative drops are produced by this process. However, as this mixture of positive and negative drops falls in the atmosphere the conductivity measurements [7, 37, 39, 43] together with the measurements on the discharge characteristics of our flying laboratory, Fig. 9, show that they will discharge selectively. Thus when the mixture of drops falls some 2 or 3 km an excess free charge is established having a sign corresponding to the ions exhibiting the larger conductivity [27]. At levels above 3 or 5 km the negative ion conductivity is in excess and drops falling through this region would accumulate a negative free charge. Below 3 or 5 km there would be a marked tendency for the drops to accumulate a positive free charge [26]. Now when the ratio of the conductivities λ_+/λ_- approximates

0.9 the differential discharge of the raindrops will establish thereby an excess negative free charge that is transferred toward the earth with a velocity corresponding to the terminal velocity of "medium rain," or 400 cm. Thus when LWC $= 10^{-6}$ gm/cm^3 one may calculate the convected current density by (34) and it is found to approximate $7\times10^{-4}\ E_0$ esu/cm^2. The reader may verify that such a current density summed up over the entire area of a typical thunderstorm will establish a total convection current of more than one ampere if $E_0 = 2$ statvolt/cm. Such a current approximates the measured currents [7].

One may estimate from (38) the equilibrium electric field that will be established as a result of the convected charge moving towards the ground. At a selected height of 2 km one may adopt a conductivity for clear air of 4×10^{-4} esu or 4×10^{-5} esu within a typical stable cloud. Thus by (38) the established equilibrium electric field would approximate 1000 volt/cm in clear air or 10,000 volt/cm within a cloud. Because of uncertainties in the conductivity and the physical properties of the falling rain exact numerical values are unimportant, but one may notice that the charge transferring processes are adequate 1) to regenerate the initial field and 2) to establish electric fields and gross currents within the thunderstorm that are descriptive of the available observations. Whenever the electric field exceeds about 4500 volt/cm at the earth's surface or something less than this value over an extensive path, observations show rather clearly that a disruptive lightning discharge will be initiated [40]. Accordingly, one may understand in quantitative terms one of the basic mechanisms that is capable of establishing lightning.

Consider another energetic mechanism of somewhat different type and suppose that some free charge already exists within the thundercloud. We have seen that hyperelectrification is important at the boundary of discontinuity between the thundercloud and the clear air outside. This mechanism has been discussed in some detail [29] and leads to drop charges of magnitude given by (22). According to this expression, high charges all of one sign are transferred to the raindrops in the transition layer. To illustrate the process, assume that the precipitation is characterized by "medium rain" and the drop radii approximate 0.05 cm. Thus, the charge on each drop by (22) is $7.5\times10^{-3}\ E_0$ esu. When E_0 is large enough the drops may again carry charges comparable to the maximum as discussed previously. Further assuming that the liquid water content is a typical 10^{-6} gm/cm^3, the space charge density will be $1.5\times10^{-5}\ E_0$ esu/cm^3 and this falls towards the earth at the velocity of fall for "medium rain." Therefore, the convected current density is $6\times10^{-3}\ E_0$ esu/cm^2 and the total current for a typical thunderstorm may be several amperes. The precipitation charge in the above example is all of one sign and could have been calculated directly from (33). Again noticing that the equilibrium electric field is determined by the convected current density and the conductivity one may again substitute the conductivity at 2 km or 4×10^{-4} esu to show that the equilibrium field is 15 E_0 statvolt/cm or 4500 E_0 volt/cm. Thus if E_0 has typical values the falling rain is capable of establishing an electric field, even in clear air, which is greater than the dielectric strength of air. Further, one may notice that if a lower conductivity, characteristic of stable clouds, is employed the equilibrium field would be much larger than that just calculated and the field would then far exceed the dielectric strength of air. In any event, lightning is likely to intervene, which will equalize the separated charges.

The above electrification processes are exceedingly energetic and are thought to be principally responsible for the observed separation of free charge in a thunderstorm. It is important to recognize that the sign of the charges produced by hyperelectrification depends on the direction of the electric field at the cloud boundary. When the cloud boundary sees positive charge within the cloud the drops are likely to be negatively charged but if the boundary sees negative charge within the cloud the drops will be positively electrified. It is clear, therefore, that some thunderstorm regions will be characterized by highly charged drops of one sign while other regions will contain highly charged drops of the opposite sign, just as Fig. 6 and our other aircraft measurements clearly show [17]. These aircraft measurements show that negative charges normally predominate on precipitation at the high rain forming levels. The excessive negative ionic conductivity commonly observed at such levels where the suspended pollution is a minimum suggests strongly that perhaps most of the marked sign selective processes considered in the foregoing sections may be fundamentally traceable to the superior mobility of the negative ion. This general view has influenced the interpretation of atmospheric electric problems since the classical measurements of ionic mobilities were first made in 1900 by Dr. John Zeleny.

Relation of Thunderstorm Electricity to the Earth's Fair Weather Field and to the Cleanliness of the Earth's Atmosphere

It is well known that the surface of the earth in all fair weather regions carries a negative charge of about 4×10^{-4} esu/cm^2, and that this maintains an inward electric field of about 1.5 volt/cm. Wilson suggested long ago [45] that the maintenance of the observed fair weather charge and field was probably related to the presence of thunderstorms somewhere else on the earth. Probably most workers in the field of atmospheric electricity accept this explanation as correct because there are worldwide fluctuations of the fair weather field which appear to be in phase with the abundance of thunderstorms averaged over the earth. Gish and Wait [7] have estimated the current at the top of a thunder-

cloud where the current density measurements were not complicated by the convective transport of charge on rain, and they found currents approximating 1 ampere per thunderstorm. Since the current to the high atmosphere and the ground must be continuous a negative current of similar magnitude usually flows towards the ground just as we have estimated in the foregoing section. However, because of the relatively high resistance of these lower layers the transfer of charge across this layer is frequently augmented by lightning discharge. We have seen that typically 17 coulombs is transferred to the earth by each lightning discharge. This transfer is frequently supplemented by conduction currents and the charges on the falling rain so that the determination of exact quantities is rather difficult.

We have evidence suggesting that the transfer of charge from the clouds to the earth takes place with greater ease in mountainous regions because such mountains frequently extend well into the conducting atmosphere at high levels. The total currents transferred in mountainous regions is unknown but preliminary measurements suggest that it may be large and the matter deserves careful investigation. The general character of the equivalent electrical circuit in the atmosphere is outlined in Fig. 18.

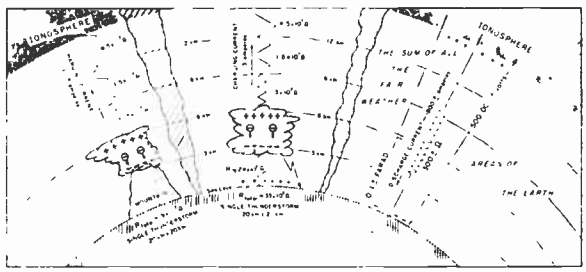

Fig. 18—Equivalent electrical circuit of the atmosphere. From 1000 to 2000 thunderstorms in constant operation are required to maintain the currents in the fair weather areas of the earth. Notice that charged raindrops transport the free charge through the cloud and provide the energy to establish the current.

One aspect of the maintenance of the earth's charge requires special consideration. Fig. 1 shows that in active thunderstorms the impressed electric field is more or less alternating in character and positive and negative fields are common. We have seen that space charge always accumulates in the lower atmosphere which is opposite in sign to the charge on the earth. An analysis shows that whenever time is available to accumulate space charge a positively charged surface will discharge more rapidly than a negatively charged surface. Thus, alternating electric fields impressed on the lower atmosphere will result in the transfer of more negative charge to the earth than positive. That is to say, the lower atmosphere has rectifying properties [9]. Even if the acting charge separating processes in the atmosphere were purely random in nature, it is clear that this earthly condenser would accumulate and maintain a negative charge. The magnitude of the rectified current would not fully account for the observed field unless thunderstorms are more general and cover more area than we now believe [9].

The fundamental importance of thunderstorm activity and the maintenance of the earth's fair weather electric field has never been adequately emphasized. It is clear that it plays no direct part in the over-all weather process but its secondary role in sweeping the atmosphere clear of fine particulate matter can hardly be overestimated. It is well known that the number of condensation nuclei decrease rather rapidly with increasing altitude and this has generally been attributed to gravitational fallout. With the advent of nuclear bombs the problem of cleansing the stratosphere of its suspended particulate matter is a very practical one. One may easily show that a particle of radius 10^{-6} cm and carrying one elementary charge will experience a force, produced by the fair weather electric field in the stratosphere, that is roughly ten times as large as the gravitational force. Near thunderclouds the relative forces will be proportionately much greater. Accordingly, in the presence of clouds, or indeed in clear air, the superimposed systematic electrical motions communicated to the particles acts to precipitate out the very fine particles onto cloud droplets and on the ground. We do not suggest that the mechanism is important for particles as large as a micron because here gravity plays probably the major role but it is extremely difficult to understand how the tremendous numbers of very fine particles of the size of many condensation nuclei suspended in the atmosphere are purged unless electrical phenomena are invoked. Accordingly, this author believes that the role of thunderstorm electricity is an important one in making this earth a habitable abode for man.

Conclusion

The foregoing sections have summarized probably the most important phenomena responsible for the electrification of precipitation and thunderstorms. We have attempted to emphasize that thunderstorm electrification is but an extreme manifestation of the charges commonly produced on all precipitation. It seems clear from the data that large, newly formed raindrops are usually electrified but do not always produce lightning. Thus, one infers that there are secondary relationships related to the rate of precipitation and to the character of the cloud development which somewhat determine the electrical activity of the cloud. These relationships are specified by (44).

According to the above analysis the electrification is principally associated with: 1) Droplets or ice crystals formed in clean air at high levels. The process here is primarily one of selective diffusion. 2) Special phe-

nomena in the transition layer between a cloud and its clear air environment. In this layer, ions of a single sign from outside the cloud, are commonly concentrated and are deposited on cloud droplets and raindrops by hyperelectrification. 3) Electrical induction by the contact and separation of ice crystals or raindrops exposed to an electric field. The mechanism is such as to produce a mixture of positive and negative drops carrying roughly the same charge magnitudes. 4) The selective discharge of mixtures of positive and negative drops as they fall down through an environment wherein the positive and negative conductivities are different. All of these processes are energetically capable of contributing to the over-all electrification of a thundercloud. Some of these processes are evident in light rain and drizzle formed at low levels which is known to be weakly electrified [26].

It seems clear from the analysis that rapid regeneration and build up of the electric field accompanied by frequent lightning discharges can hardly be anticipated unless the precipitation rate *exceeds* that characteristic of "medium rain." All of these requirements appear consistent with the available knowledge on the meteorological characteristics of thunderstorms. Thus, the above quantitative description of thunderstorms is adequate to account not only for active thunderclouds extending to high freezing levels, but also in very clean air when the storm cloud fully develops below the freezing level. Moreover, the description does not require that lightning be produced by every heavily precipitating cloud. This summary attempts to discuss only the outstanding features of thunderstorms and because of their complexity exceptions must be anticipated.

Many of the processes which we have examined in this communication are directly applicable to the generation of volcanic lightning. The main requirement is that particulate matter collide, separate, and fall in a semiconducting ionized atmosphere. It is anticipated that lightning storms much like those observed on the earth will develop on other planets or on stars.

The analysis of atmospheric electric phenomena in precipitating regions has necessarily ignored a number of processes that have been considered adequately by other writers. Our research team has examined a number of suggested electrifying processes to determine roughly their relative importance in atmospheric electricity. Some of these processes doubtless contribute to the overall electrification under especially favorable conditions. But the mechanisms we have considered above all prove to be energetic and electrically active in the laboratory. Much more work needs to be done in this field of research and there is a large number of stimulating problems yet to be solved. This review is intended to emphasize those mechanisms that appear to the writer to be most important and to stimulate further work in this specialized area of basic physics.

Bibliography

[1] Banerji, S. K. "The Electric Field of Overhead Thunderclouds," *Philosophical Transactions*, Vol. 231 (1932), pp. 1–28.

[2] Banerji, S. K., and Lele, S. R. "Electric Charges on Raindrops," *Nature*, Vol. 130 (1932), pp. 998–999.

[3] Chalmers, J. A., and Pasquill, F. "The Electric Charges on Single Raindrops and Snowflakes," *Proceedings of Physical Society*, London, Vol. 50, (1938), pp. 1–15.

[4] Dinger, J. E., and Gunn, R. "Electrical Effects Associated With a Change of State of Water," *Terrestrial Magnetism and Atmospheric Electricity*, Vol. 51 (1946), pp. 447–494.

[5] Elster, J., and Geitel, H. "Zur Influenztheorie der niederschags.-Elektrizitat," *Physikalische Zeitschrift*, Vol. 14, (1913), p. 1287.

[6] Foster, H. "An Unusual Observation of Lightning," *Bulletin of the American Meteorological Society*, Vol. 31, (1950), p. 140.

[7] Gish, O. H., and Wait, G. R. "Thunderstorms and The Earth's General Electrification," *Journal of Geophysical Research*, Vol. 55, (1950), pp. 473–484.

[8] Gschwend, P. "Beobachtungen Uber Die Elektrischen Ladungen Einzelner Regentropfen und Schneeflocken," *Jahrbuch der Radioaktivität und Elektronik*, Vol. 17 (1920), pp. 62–79.

[9] Gunn, R. "On Electrical Rectification by the Earth's Lower Atmosphere," *Terrestrial Magnetism and Atmospheric Electricity*, Vol. 38 (1933), pp. 303–308.

[10] Gunn, R. "Electricity of Rain and Thunderstorms," *Terrestrial Magnetism and Atmospheric Electricity*, Vol. 40 (1935), pp. 79–106.

[11] Gunn, R., Hall, W. C., Kinzer, G. D., *et al.* "Technical Reports, Army-Navy Precipitation Static Project," Proceedings of the IRE, Vol. 34 (April, 1946), pp. 156–177, (May, 1946), pp. 234–254.

[12] Gunn, R. "The Electrical Charge on Precipitation at Various Altitudes and its Relation to Thunderstorms," *Physical Review*, Vol. 71 (1947), pp. 181–186.

[13] Gunn, R. "Electric Field Intensity Inside of Natural Clouds," *Journal of Applied Physics*, Vol. 19 (1948) pp. 481–484.

[14] Gunn, R. "The Free Electrical Charge on Thunderstorm Rain and Its Relation to Droplet Size," *Journal of Geophysical Research*, Vol. 54 (1949), pp. 57–63.

[15] Gunn, R. "Electronic Apparatus for the Determination of The Physical Properties of Freely Falling Raindrops," *Review of Scientific Instruments*, Vol. 20 (1949), pp. 291–296.

[16] Gunn, R., and Kinzer, G. D. "Terminal Velocity of Fall of Water Droplets in Stagnant Air," *Journal of Meteorology*, Vol. 6 (1949), pp. 243–248.

[17] Gunn, R. "The Free Electrical Charge on Precipitation Inside an Active Thunderstorm," *Journal of Geophysical Research*, Vol. 55 (1950), pp. 171–178.

[18] Gunn, R. "Precipitation Electricity," *Compendium of Meteorology, American Meteorological Society*, (1951), pp. 128–135.

[19] Gunn, R., and Devin, C., Jr. "Raindrop Charge and Electric Field in Active Thunderstorms," *Journal of Meteorology*, Vol. 10 (1953), pp. 279–284.

[20] Gunn, R. "Electric-Field Regeneration in Thunderstorms," *Journal of Meteorology*, Vol. 11 (1954), pp. 130–138.

[21] Gunn, R. "Electric Field Meters," *Review of Scientific Instruments*, Vol. 25 (1954), pp. 432–437.

[22] Gunn, R. "Diffusion Charging of Atmospheric Droplets by Ions, and The Resulting Combination Coefficients," *Journal of Meteorology*, Vol. 11 (1954), pp. 339–347.

[23] Gunn, R. "The Statistical Electrification of Aerosols by Ionic Diffusion," *Journal of Colloid Science*, Vol. 10 (1955), pp. 107–119.

[24] Gunn, R. "Droplet Electrification Processes and Coagulation in Stable and Unstable Clouds," *Journal of Meteorology*, Vol. 12 (1955), pp. 511–518.

[25] Gunn, R. "Raindrop Electrification by the Association of Randomly Charged Cloud Droplets," *Journal of Meteorology*, Vol. 12 (1955) pp. 562–568.

[26] Gunn, R. "The Systematic Electrification of Mist and Light Rain in the Lower Atmosphere," *Journal of Geophysical Research*, Vol. 60 (1955), pp. 23–27.

[27] Gunn, R. "Initial Electrification Processes in Thunderstorms," *Journal of Meteorology*, Vol. 13 (1956), pp. 21–29.

[28] Gunn, R., and Woessner, R. H. "Measurements of the Systematic Electrification of Aerosols," *Journal of Colloid Science*, Vol. 11 (1956), pp. 254–259.

[29] Gunn, R. "The Hyperelectrification of Raindrops by Atmospheric Electric Fields," *Journal of Meteorology*, Vol. 13 (1956) pp. 283–288.

[30] Gunn, R. "Electric Field Intensity at the Ground Under Active Thunderstorms and Tornadoes," *Journal of Meteorology*, Vol. 13 (1956), pp. 269–273.
[31] Gunn, R. "The Ratio of The Positive and Negative Light Ion Conductivities Within a Neutral Aerosol Space," *Journal of Colloid Science*, Vol. 11 (1956), pp. 691–698.
[32] Gunn, R. "The Non-Equilibrium Electrification of Raindrops by the Association of Charged Cloud Droplets," *Journal of Meteorology*, Vol. 14 (1957).
[33] Gunn, R. and Phillips, B. B. "Experimental Investigation of The Effects of Air Pollution on the Initiation of Rain," *Journal of Meteorology*, Vol. 14, (1957), pp. 272–280.
[34] Higuchi, K. "A New Method for the Simultaneous Observations of Shape and Size of a Large Number of Falling Snow Particles," *Journal of Meteorology*, Vol. 13 (1956), pp. 274–287.
[35] Landsberg, H. "Atmospheric Condensation Nucleii," *Beiträge zur Geophysique*, (Suppl.,) Vol. 103 (1938), pp. 155–252.
[36] Mason, B. J. "A Critical Examination of Theories of Charge Generation in Thunderstorms," *Tellus* Vol. 5 (1953), pp. 446–460.
[37] Mathias, E., and Grenet, G. "Conductabilite Electrique de L'air au Sommet Du Puy de Dome," *Congr. Sav.*, Vol. 64 (1931), pp. 220.
[38] Müller-Hillebrand, D. "Charge Generation in Thunderstorms by Collision of Ice Crystals with Graupel, Falling through a Vertical Field," *Tellus*, Vol. 6 (1954), pp. 367–381.
[39] Nolan, J. J., and Nolan, P. J. "Further Observations on Atmospheric Ionization at Glencree," *Proceedings of the Royal Irish Academy*, Vol. 61 (1933), pp. 111–128.
[40] Norinder, H., and Salka, O. "Mechanism of Positive Spark Discharges with Long Gaps in Air at Atmospheric Pressure," *Arkiv Fysik*, Vol. 3 (1951), pp. 347–386.
[41] Phillips, B. B., Allee, P. A., Pales, J. C., and Woessner, R. H. "An Experimental Analysis of the Effect of Air Pollution on the Conductivity and Ion Balance of the Atmosphere," *Journal of Geophysical Research*, Vol. 60 (1955), pp. 289–296.
[42] Phillips, B. B., and Gunn, R. "Measurements of the Electrification of Spheres by Moving Ionized Air," *Journal of Meteorology*, Vol. 11 (1954), pp. 348–351.
[43] Rossmann, F. "Luftelektrische Messungen mittels Segelflugzeugan," *Ber. Deut. Wetterd.*, US-Zone, No. 15 (1950), pp. 3–54.
[44] Scrase, F. J. "Electricity On Rain," *Geophysics Mem.*, Vol. 9 (1938), p. 20.
[45] Wilson, C. T. R. "Investigations on Lightning Discharges and on the Electric Field of Thunderstorms," *Transactions of the Royal Society*, Vol. A221 (1920), pp. 73–115.
[46] Woessner, R. H., and Gunn, R. "Measurements Related to The Fundamental Processes of Aerosol Electrification," *Journal of Colloid Science*, Vol. 11 (1955), pp. 69–76.
[47] Wormell, T. W. "Atmospheric Electricity—Some Recent Trends and Problems," *Royal Meteorological Quarterly Journal*, Vol. 79 (1953), pp. 3–38.

An Improved High-Gain Panel Light Amplifier*

B. KAZAN†, SENIOR MEMBER, IRE

Summary—**A grooved photoconductor light-amplifying picture panel is described, whose gain is more than 10 times greater than any previous amplifier and whose threshold for input light is reduced. These improvements have been obtained with a new electrode structure which enables a more efficient type of operation and by the use of a more sensitive photoconductive powder. Measured input-output characteristics are shown comparing the new and earlier types of operation and also indicating the effects of different supply frequencies. The time-integrated energy gain for a one-second excitation is of the order of 100 with input light of the same spectral distribution as the output. The asymptotic energy gain after a longer excitation interval is about 800 with optimum spectral matching of the photoconductor. Although the decay time is of the order of seconds, as with early amplifiers, the shape of the decay curves and the rate of decay are changed by the new method of operation.**

Introduction

THE basic design of the original panel light amplifier[1] is shown in cross section in Fig. 1. The principal layers are the electroluminescent phosphor layer which produces the output image and the photoconductive layer which varies its resistance in accordance with the input radiation. Since the photoconductive layer in the dark must be many times higher in impedance than the electroluminescent layer, it is made much thicker. To efficiently illuminate the thick photoconductor, it is grooved. In operation, the incident light is absorbed on the surfaces of the photoconductor so that photocurrents flow down the sides of the ridges and converge at the bottom of the grooves. To efficiently utilize the entire phosphor area, a resistive current-diffusing layer is placed below the photoconductor. This spreads the photocurrents slightly, approximately one groove width. To prevent feedback of output light, an opaque insulating layer is provided on the back surface of the phosphor layer.

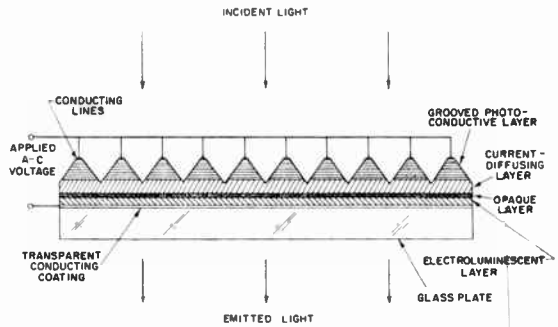

Fig. 1—Basic design of grooved photoconductor light amplifier.

* Original manuscript received by the IRE, May 6, 1957.
† RCA, Princeton, N. J.
[1] B. Kazan and F. H. Nicoll, "An electroluminescent light-amplifying picture panel," PROC. IRE, vol. 43, pp. 1888–1897; December, 1955. (Some of the results of this work were also described in *Radio Age*, vol. 14, p. 6; January, 1955 and by D. W. Epstein in *RCA Eng.*, vol. 1, pp. 42–44; June July, 1955.)

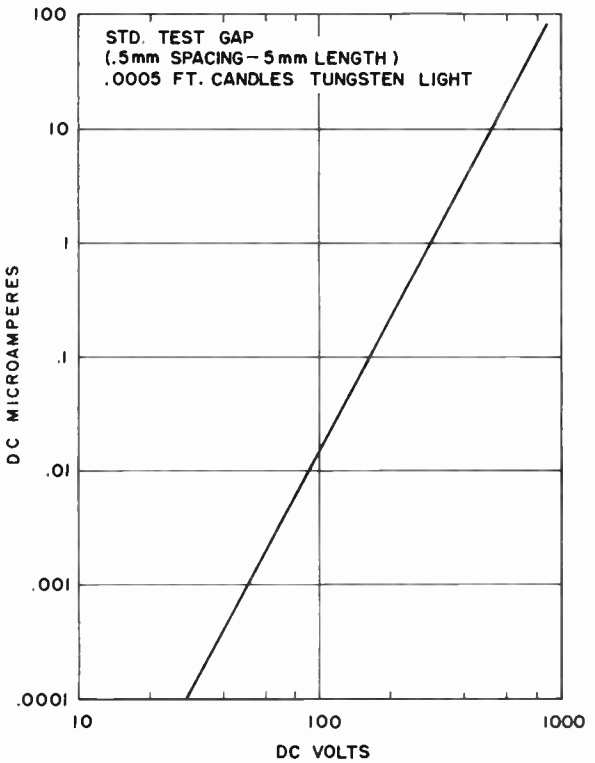

Fig. 2—DC photocurrent vs voltage of photoconductive powder.

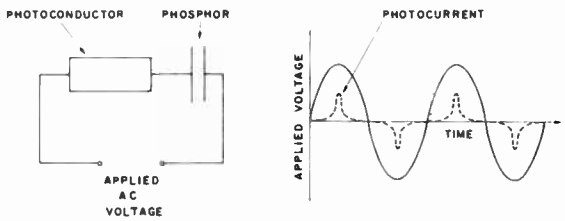

Fig. 3—AC operation of single element.

Conventional Method of Operation

The photoconductive material employed is an improved CdS powder bonded with plastic. The current-voltage characteristic of this material is very nonlinear.[2] Fig. 2 shows a log-log plot of dc current vs voltage for a fixed light level, indicating the current to vary approximately as the fourth power of the voltage over many orders of magnitude of current. One effect of the nonlinearity is a reduction in amplifier gain when operated in the usual manner with ac voltage. Fig. 3 shows a single amplifier element with sine-wave excitation. Because of the nonlinearity of the photoconductor, most of the current flows during a small portion of the cycle when the voltage is near its peak. Compared to a linear photoconductor with equal peak current, there is a reduction in average current for the nonlinear CdS powder with a corresponding reduction in output light from the phosphor layer. In operation, the peak voltage which can be applied to the photoconductor is limited by breakdown. With a given peak voltage level some improvement in operation is possible with the nonlinear CdS by using rectangular wave shapes which increase the average ac current. However, a much larger increase in current can be obtained by a different method as next indicated.

[2] F. H. Nicoll and B. Kazan, "Large area high-current photoconductive cells using cadmium sulfide powder," *J. Opt. Soc. Amer.*, vol. 45, pp. 647–650; August, 1955.

New Methods of Operation

If a dc voltage equal to the peak ac voltage is applied to the photoconductor, it is found that the dc photocurrent is usually many times greater than the peak ac photocurrent.[1] This dc increase of photocurrent is a particular property of the CdS photoconductive powder. At the low-light levels used with the amplifier the increase in photosensitivity may be as high as 10 times.

While the photoconductor requires dc voltage for best operation, the electroluminescent phosphor layer requires ac voltage, being inoperative with dc. This difference cannot be reconciled by the simple series circuit which has been the basis of light amplifier operation until now.

One method of overcoming the problem is shown in Fig. 4, representing a single amplifier element. Instead of a single photoconductive element, two smaller photoconductors are used, both of which are assumed to be equally illuminated. In series with each photoconductor is a diode so that a half-wave rectified voltage of opposite polarity and phase is applied to the two photoconductors. The voltage polarity and phase are shown by the solid lines to the right, with the photocurrent pulses as dashed lines. In operation during a positive half cycle, the current pulse through photoconductor A charges the phosphor element positive. During the next half cycle, the current pulse of opposite direction through photoconductor B charges the phosphor element negative, developing ac voltage across the phosphor. Although pulsed dc voltage is applied to the photoconductors instead of steady dc, it is found that the peak photocurrent obtained is almost as great as with steady dc. This type of operation produces a large increase in ac voltage across the phosphor element for a given light flux in lumens falling on the photoconductive elements.

Using the basic principle of the rectified ac operation, further improvement is obtained with the circuit of Fig. 5. Here, instead of diodes, dc bias voltages of opposite polarity are inserted in series with the two photoconductive elements. By setting the bias voltage equal to the peak ac voltage, pulsating dc voltages of opposite polarity and phase are applied to the photoconductors. Since the width of the voltage pulses between half-value points is greater than for the rectified ac operation, the photocurrent pulses are wider than with rectified ac. Therefore, the average ac current through the phosphor is increased, and more output light is produced. Although the voltage applied to one photoconductor rises

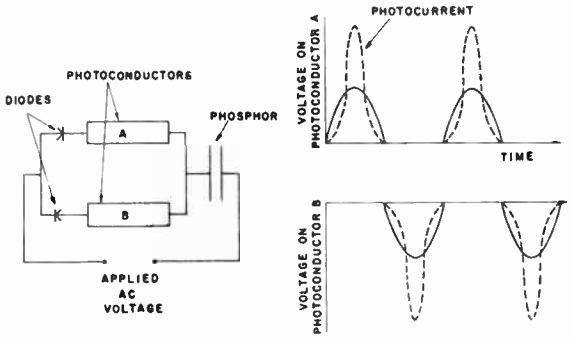

Fig. 4—Rectified ac operation of single element.

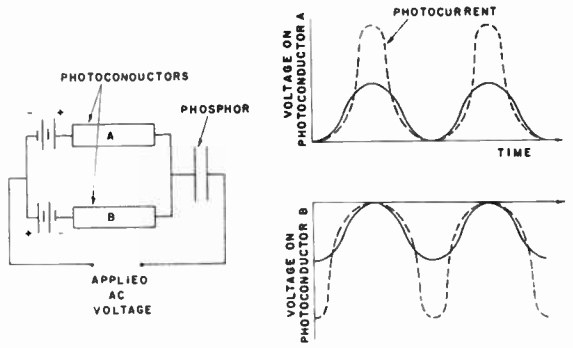

Fig. 5—Biased ac operation of single element.

before the voltage on the other photoconductor falls to zero, the current flow when the instantaneous voltage is low can be neglected for most input levels because of the nonlinear property of the photoconductors.

To apply the rectified ac or biased ac method of operation to the light amplifier requires a modification of the electrode system. Fig. 6 shows the cross section of the modified amplifier operated with biased ac. The conducting lines on the grooved photoconductor are separated into two interdigital sets, each set being connected to one of the two bias supplies. If light strikes the photoconductive layer, as shown, conductivity results on the surfaces of the grooves at the local area illuminated. The portions of the photoconductor and phosphor area corresponding to the single picture element of the previous figure are shown by the heavy lines.

Comparison of Operating Methods

The different modes of amplifier operation can be compared by means of the corresponding input-output characteristics. These cannot be measured, however, as static characteristics because of the build-up properties of the photoconductor. Fig. 7 shows a log-log plot of dc photocurrent vs time for different light levels using the grooved photoconductive layer of the amplifier with interdigital electrodes as a photocell. The procedure used before measuring each curve was to initially flood the photoconductor with a high light level and then allow it to decay. At the moment the dark current reached a specified level (approximately 4 μamp), the input light for the measurement was switched on and the curve

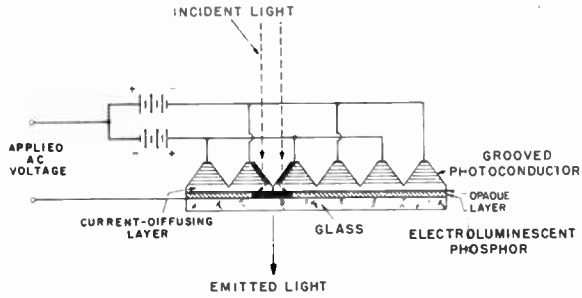

Fig. 6—Biased ac operation of light amplifier.

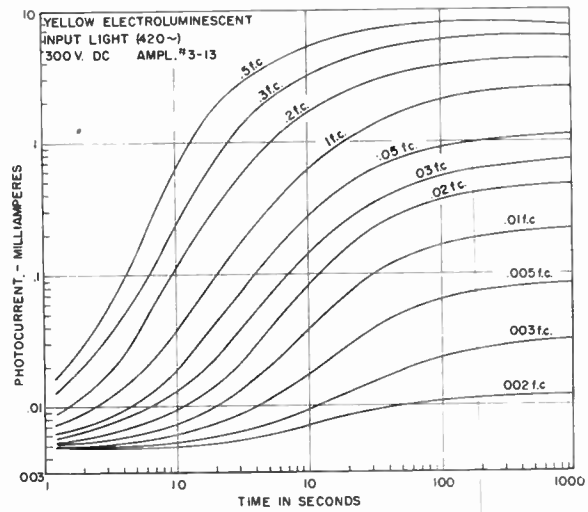

Fig. 7—DC photocurrent vs time for different input light levels.

recorded. Except for the very low light levels, a considerable portion of each curve is a straight line with a slope of about 2 indicating the photocurrent to rise as the square of the time. The time required for the individual curves to reach a specified fraction of their equilibrium levels depends on the input light level. This build-up time varies approximately inversely with the light level. At the higher voltage levels used in amplifier operation, the photoconductive layer has a sensitivity of about 40 amp/lumen (using low-level yellow electroluminescent input light peaked at about 550 millimicrons). Since more than 500 volts can be applied across the photoconductive layer (approximately 15 mils thick), it can control a power flow through it of $>10^4$ watt/lumen.

The effect of the photoconductor build-up on the amplifier operation is shown in the curves of Fig. 8 indicating output light vs time for different input light levels using biased ac operation. For a specific excitation time, the output light for different input light levels can be obtained from these curves. Such an input-output characteristic for a 10-second excitation time is shown in Fig. 9. For comparison, characteristics are also shown for the conventional ac and rectified ac methods of operation with a 10-second excitation time. The latter characteristics were obtained from sets of light output vs time curves similar to Fig. 8. In all of the measure-

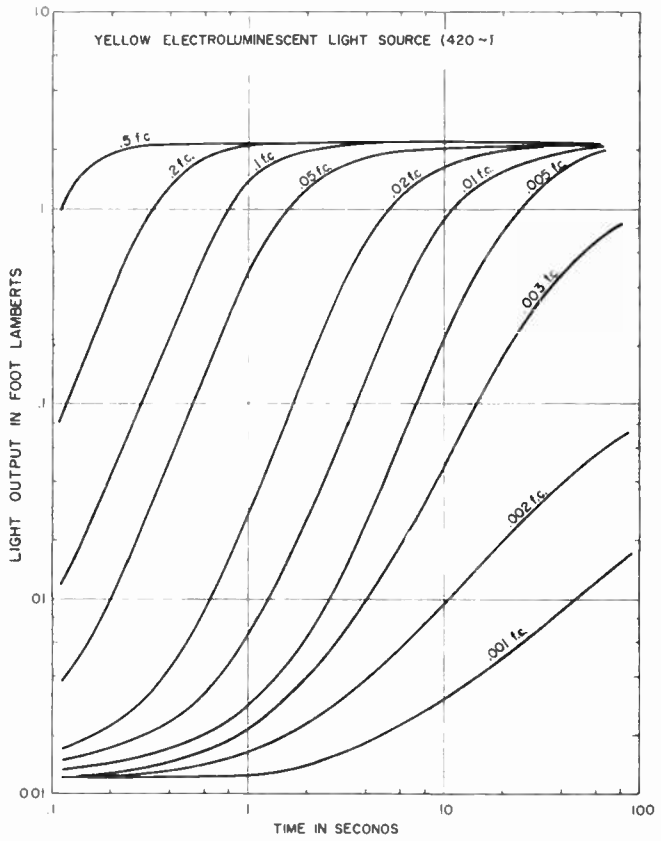

Fig. 8—Amplifier output vs time for different input light levels using biased ac.

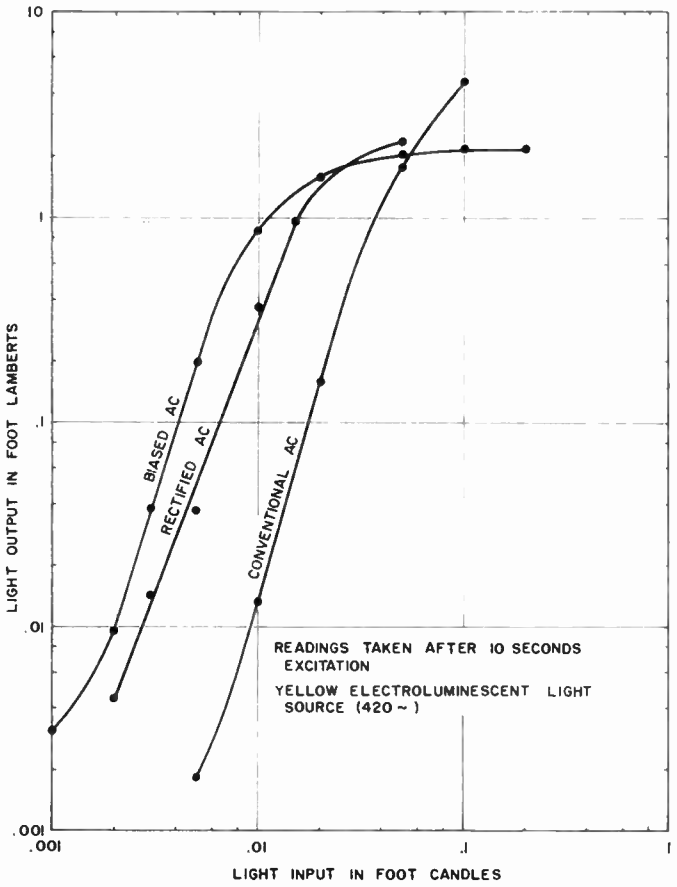

Fig. 9—Input-output characteristics for different methods of operation.

ments of light output vs time, irrespective of method of operation, the amplifier was initially pre-excited and allowed to fall to a specified output level of 0.0012 foot-lambert before recording the curves.

All of the curves have high slopes with a gamma of about 3. For low-level input light the rectified ac operation gives about 20 times as much output light as the conventional ac operation. Using biased ac operation, more than 50 times as much output light is obtained compared to the conventional ac operation. Alternatively, with biased ac, about 5 times less input light is required to produce a given output light compared to conventional ac, thus lowering threshold of operation.

At the higher output levels the ac characteristic begins to saturate slightly. The saturation is greater for the rectified ac characteristic while the biased ac characteristic becomes completely flat. The saturating effects of the rectified and biased ac are not due to a saturation of the photoconductor, but are caused by a leakage of charge through the photoconductive elements during the half cycle when they are assumed to be nonconducting. The clipping action of the biased ac is of practical advantage in protecting the phosphor layer from breakdown. If the amplifier is accidentally excited with high input lights this limits the voltage which can be applied to the phosphor.

For longer or shorter excitation times than the 10 seconds shown, sets of similar-shaped characteristics are obtained displaced to the left or right, respectively. With an excitation time of a minute, the curves of Fig. 8 show a maximum gain of about 400 times (0.005 foot-candle input). These curves were obtained with a yellow electroluminescent input light source of identical spectral distribution as the amplifier output. Since the photoconductor is peaked in the red at about 750 millimicrons it is not efficiently excited by the phosphor, peaked at 550 millimicrons.[1] Assuming an input light of about 750 millimicrons wavelength, the energy gain of the amplifier is about 800 times. Measurements with tungsten input light of about 2800°K indicate a gain in lumens of more than 1000 times with an excitation time of a minute.

Comparison of Operating Frequencies

The characteristics of Fig. 9 were obtained with 420-cycle ac. To determine the effects of operation at other frequencies, input-output characteristics were also obtained for 60 and 2000-cycle biased ac operation. Fig. 10 shows typical characteristics compared to a 420-cycle characteristic, all obtained with an equal excitation time. For comparative purposes the light output preceding excitation of the amplifier in all measurements was maintained constant (approximately 0.0012 foot-lambert). Except at high input levels, the 2000-cycle characteristic shows lower gain compared to the other

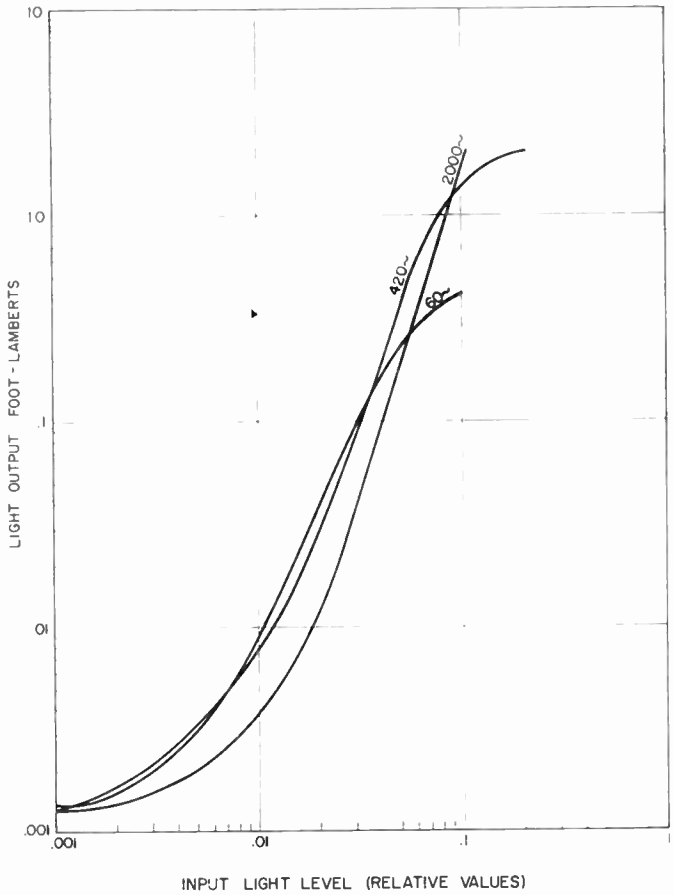

Fig. 10—Input-output characteristics comparing operating frequencies.

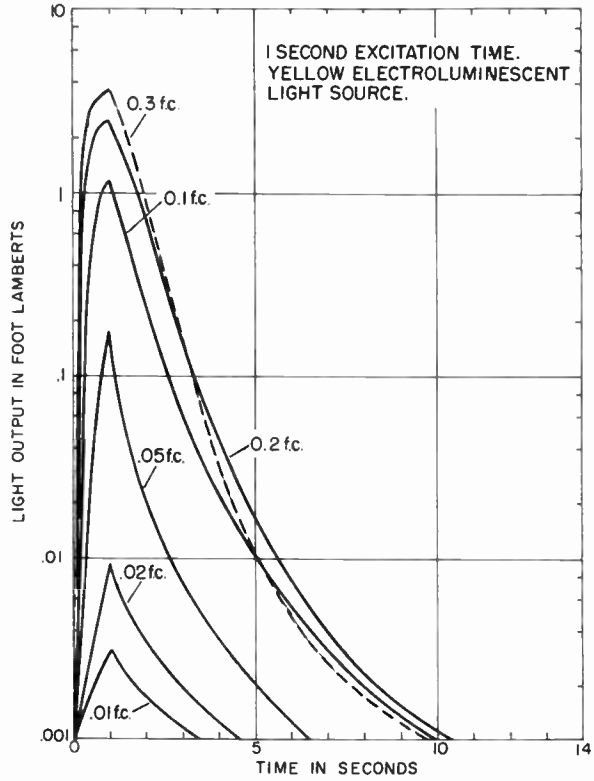

Fig. 11—Decay curves for ac operation.

curves. A comparison of the 60-cycle and 420-cycle characteristics shows approximately equal gain for both frequencies at low levels but with greater output light obtained from the 420-cycle operation before saturation. The lack of higher gain in 60-cycle operation is explained by the rapid drop in sensitivity of the photoconductor with reduction in current level. For a given threshold output light (as used in the frequency comparison), the current level at 60 cycles is considerably below the 420-cycle level. For many purposes, the 420-cycle operation is a useful compromise, enabling high gains at low levels and moderate output light levels of approximately 1 foot-lambert.

Decay Characteristics and Integrated Gain

In addition to its build-up properties, the present CdS photoconductor has a decay time of the order of seconds. Fig. 11 shows decay curves of the amplifier with ac operation for different levels of input excitation. Each curve was obtained by applying the input for one second and then allowing the amplifier to decay for the remaining time. About two to four seconds are required for the output to fall to one tenth its value, with the rate of decay greater for the higher input levels. At the highest input light level of 0.3-foot candle, the decay curve, shown as a dashed line, crosses below the lower curves. The increased rate of decay is caused by a temperature rise in the photoconductor due to power dissipated by the high photocurrents. Fig. 12 shows a similar set of build-up and decay curves for biased ac operation. The decay curves here are almost straight lines, indicating an exponential decay, with about eight seconds required for the output light to fall to one tenth its value. Here again, the curve for the highest input light level, shown as a dashed line, crosses the lower curves due to the temperature rise in the photoconductor.

From the curves of Fig. 12 the time-integrated output light can be obtained for each input light level. Fig. 13 shows the integrated output light corresponding to the different integrated input light values. This curve also has a high slope, indicating a gamma of about 2. The maximum integrated gain is about 100 times, using the yellow electroluminescent input light. With proper spectral match to the photoconductor, an integrated energy gain of about 200 is possible.

Picture Quality

Fig. 14 shows a photograph of the output picture produced on a 12-inch light amplifier with a low-level image projected from behind. In operation, biased ac was used. The photoconductive layer of this amplifier has horizontal grooves spaced 25 mils apart, allowing a picture resolution of about 500 lines. For a given number of photoconductor grooves, the resolution is the same for biased ac and conventional ac. In both cases each phos-

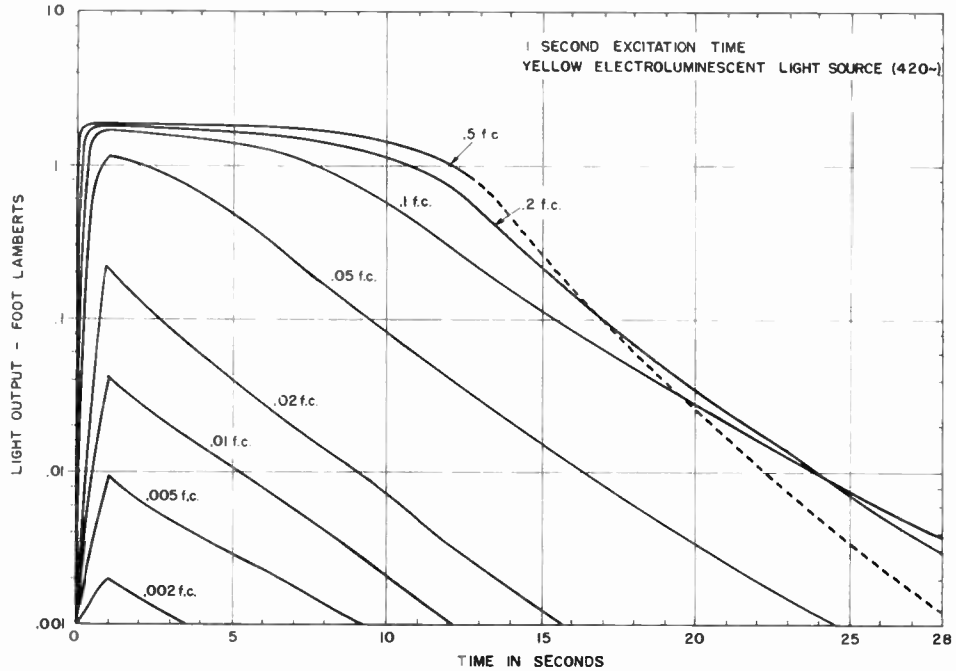

Fig. 12—Decay curves for biased ac operation.

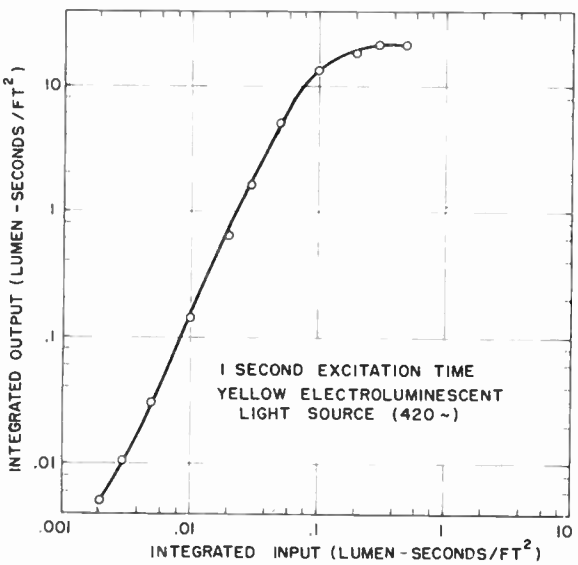

Fig. 13—Input-output characteristic for time-integrated light.

Fig. 14—Photograph of amplifier output.

phor element is supplied by photocurrent from the two adjacent photoconductor groove surfaces, which converge at the phosphor element.

Conclusion

The high light gains and long persistence of the present amplifier are potentially useful in slow tv and radar applications. In the case of slow tv it is desired to scan a single frame in a period as long as a minute, using low-frequency video information. For viewing the picture, storage is necessary for a frame period or longer. One relatively simple method is to use a cathode-ray tube with a long persistence phosphor. The available light during persistence, however, is very low and the image must be viewed in completely darkened surroundings. Utilizing the long decay and integrated energy gain of the amplifier, a much brighter picture can be obtained with long storage by projecting a cathode-ray tube image on the amplifier.

The problem of inadequate light level also occurs with the conventional P-7 radar screen where the decaying target traces require a darkened room for viewing. Here again the light amplifier is potentially useful for producing a bright, long-decay output picture from a projected cathode-ray tube image. Similar to the P-7

phosphor, the light amplifier has build-up properties, so that successive input pulses at short intervals cause an increase in the output light.

The present light amplifier is also sensitive to radiation in the near infrared, extending to about 900 millimicrons. For stationary scenes it can convert a low-level infrared image to a visible picture of much higher level. Alternatively, with a pulsed infrared source, an instantaneous image may be temporarily recorded for direct viewing.

The CdS photoconductor used in the amplifier is also highly sensitive to X rays. The panel can thus directly convert an X-ray image to a visible picture. Until now, the fluoroscope screen has been the primary means for the direct viewing of X-ray images in medical and industrial applications. As is well known, the image on the fluoroscope screen is frequently very dim, particularly in medical applications, requiring a darkened room for viewing and dark adaptation of the observer's eyes for many minutes. Because of the very low light levels and poor image contrast, details can be perceived with difficulty, or not at all. By comparison, the light amplifier with its high gain can convert an X-ray image into a visible picture 100 times brighter than the fluoroscope screen, using the same X-ray levels. The resultant intensified image can be viewed in moderate room light without dark adaptation. In addition, the high gamma of the amplifier greatly enhances the contrast of the output image so that details which might be overlooked on the fluoroscope screen can be easily observed on the amplifier.

With its long decay properties, the amplifier is expected to be of use in industrial applications involving stationary objects and in special medical applications where a temporary photograph or bright image is desired for viewing after the X rays have been cut off.

It is the object of further research effort to increase the gain and also the speed of response of the light amplifier with the ultimate aim of viewing motion. This involves the continuing research on the component materials and also the associated development of improved techniques for using these materials in new amplifier structures.

Acknowledgment

The author acknowledges the assistance of J. Berkeyheiser in making the many measurements involved. The support and encouragement of E. W. Herold in this work is appreciated, as are discussions with D. W. Epstein, F. H. Nicoll, and H. B. DeVore.

The Large-Signal Behavior of Crossed-Field Traveling-Wave Devices*

J. FEINSTEIN†, MEMBER, IRE, AND G. S. KINO†, ASSOCIATE, IRE

Summary—**A large-signal theory for the interaction between a slow wave and a beam of electrons traveling in crossed dc electric and magnetic fields is formulated. The adiabatic equations of motion are used, space-charge forces are neglected, but phase focusing by the rf field and loss of the beam at the anode and sole plate are taken into account. The limits of validity of the conventional small-signal theory are obtained, and an analog computer is employed to follow the interaction to power saturation. Results are presented for a forward-wave amplifier, backward-wave amplifier, and backward-wave oscillator. It is shown that for very short lengths the backward-wave amplifier may give superior results to the equivalent forward-wave amplifier but that otherwise greater gain and efficiency can be obtained with a forward-wave amplifier. However, it is shown that there is a mode of operation for a backward-wave tube equivalent to an oscillator started by and then locked to the input signal, a condition unlike anything obtained in the equivalent longitudinal twt. Also, it is shown that in a forward-wave or backward-wave tube, the gain is dependent on the input signal and may increase as the input signal level is increased. However, it is apparent that this type of device has inherently a low gain, especially when designed for high efficiency. Consequently, some suggestions which have been made for improving this deficiency are examined.**

* Original manuscript received by the IRE, May 3, 1957; revised manuscript received, July 23, 1957.

† Bell Telephone Labs., Inc., Murray Hill, N. J.

Introduction

THE HIGH POWER at high efficiency obtainable from the multicavity magnetron has always made the application of crossed-field electronics to other types of devices seem attractive. However, forward-wave-magnetron amplifiers have not been very successful owing to the low gains usually obtained. In the M-type Carcinotron,[1] on the other hand, the backward-wave oscillator has successfully been applied to crossed-field interaction, although certain experiments indicate that the optimum operating conditions for high efficiency are not usually achieved.

[1] R. R. Warnecke, "Some results obtained in the field of ultra high-frequency electron tubes," *Ann. Radioelect.*, vol. 9, pp. 107–136; April, 1954.

Up to the present time, only a small-signal theory of the operation of crossed-field tubes has been available. Since these devices have their main applicability in the large-signal regime, the analysis to be presented below has been developed as an attempt to clarify the situation.

Statement of the Problem

We shall consider the system of Fig. 1. A narrow sheet beam of electrons enters the rf field at $x=0$, $y=0$ and flows initially along the $y=0$ plane parallel to the direction of propagation of the rf field. It will be assumed that the beam would be under Brillouin flow conditions in the absence of rf field; *i.e.*, the beam would flow along the plane $y=0$ in the $+x$ direction under the influence of a uniform magnetic field, B, in the z direction, and a uniform electrostatic field, E_0, in the $-y$ direction. The initial dc velocity of the beam will therefore be U_0 where $U_0=E_0/B$.

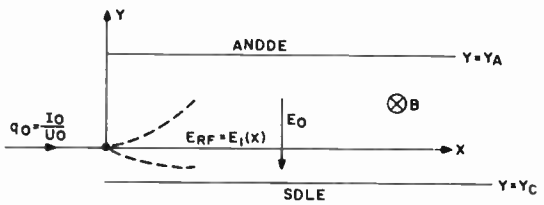

Fig. 1—Model of the magnetron amplifier considered in this paper.

It will be necessary to derive a trajectory equation for the beam under the combined action of rf and dc fields. In order to derive a reasonably simple expression, the following assumptions will be made:

1) The phase velocity of the rf field is U_0 and remains uniform along the direction of propagation even under large-signal conditions.
2) The influence of space charge on the rf and dc fields may be neglected.
3) The gain per wavelength along the propagating circuit is small.
4) The influence of the sole plate on the rf field distribution is negligible. However, collection of electrons at the sole plate will be taken into account.
5) The "adiabatic" equations of motion may be used, *i.e.*, the acceleration terms in the equations of motion may be neglected so as to obtain essentially an "average" trajectory for an electron.
6) For simplicity, the rf circuit loss will be assumed to be negligible. Such an assumption is not vital to the treatment.
7) Again for simplicity the phase velocity of the rf fields is taken to be small compared with the velocity of light.
8) The rf field strength at $y=0$ is much smaller in magnitude than the dc field.

Assumptions 3, 4, and 7 make it possible to express the rf fields in terms of a scalar potential of the form

$$V = V_1(x) \sin (\omega t - \beta x) e^{\beta y} \tag{1}$$

where $\beta=\omega/U_0$, ω is the angular frequency of the wave; $V_1(x)$ is a quantity proportional to the amplitude of the rf field at any point along the circuit, so that $|\partial V_1/\partial x| \ll |\beta V_1|$.

The rf fields may therefore be expressed in the form

$$E_x = E_1(x) \cos (\beta x - \omega t) e^{\beta y} \tag{2}$$

$$E_y = E_1(x) \sin (\beta x - \omega t) e^{\beta y} \tag{3}$$

where $E_1(x)=\beta V_1(x)$.

The equations of motion of an electron under the action of the combined rf and dc fields may then be written as follows

$$\frac{m}{e}\frac{d^2x}{dt_2} = E_1 \cos (\beta x - \omega t) e^{\beta y} - B\frac{dy}{dt} \tag{4}$$

$$\frac{m}{e}\frac{d^2y}{dt^2} = E_1 \sin (\beta x - \omega t) e^{\beta y} - E_0 + B\frac{dx}{dt} \tag{5}$$

where E_1 is written for $E_1(x)$, as it will be henceforth.

It is convenient as well as enlightening to a physical understanding of the electron motion to transform to a system of moving coordinates x', y' moving with a velocity $U_0=E_0/B$ in the x direction, and coincident with the stationary system at time $t=0$. In this case $x'=x-U_0t$, and $y'=y$, so that the equations of motion of an electron in the moving system become

$$\frac{m}{e}\frac{d^2x'}{dt^2} = E_1 \cos \beta x' e^{\beta y'} - B\frac{dy'}{dt} \tag{6}$$

$$\frac{m}{e}\frac{d^2y'}{dt^2} = E_1 \sin \beta x' e^{\beta y'} + B\frac{dx'}{dt}. \tag{7}$$

Finally, it is convenient to express the equations of motion in the moving system in terms of a set of normalized coordinates, $X=\beta x'$, $Y=\beta y'$, and $T=\omega t$, so that (6) and (7) become

$$\frac{\omega}{\omega_h}\dot{X} = \frac{E_1}{E_0}\cos X e^Y - \dot{Y} \tag{8}$$

and

$$\frac{\omega}{\omega_h}\dot{Y} = \frac{E_1}{E_0}\sin X e^Y + X \tag{9}$$

where $(\cdot)$ denotes differentiation with respect to T, and $\omega_h=eB/m$ is the cyclotron resonance frequency.

It can be seen that if $\omega/\omega_h \ll 1$, *i.e.*, if the magnetic field is large, the term on the left-hand side of (8) and (9) may be neglected. However, in most cases of interest ω_h/ω is not a large number but is of order unity. In accordance with assumption 5, we nevertheless neglect the left-hand side of (8) and (9).[2] Under this condition these equations take the very simple form

[2] A discussion of the error associated with this approximation is given in Appendix I.

$$\dot{Y} = \frac{E_1}{E_0} \cos X e^Y \tag{10}$$

$$\dot{X} = -\frac{E_1}{E_0} \sin X e^Y. \tag{11}$$

Eq. (10) may be divided by (11) to yield the following differential equation for the electron trajectories

$$\frac{dY}{dX} = -\cot X \tag{12}$$

with the trajectory solution

$$e^Y \sin X = \sin X_0 \tag{13}$$

for an electron entering the rf field at $Y=0$ with entrance phase, X_0.

Thus the shape of an electron trajectory in the moving system is independent of the strength of the rf field. However, the time which it takes an individual electron to traverse its path is, of course, dependent on the strength of the rf field. Also, it will be noted that an electron entering at phase, X_0, so that $-(\pi/2)<X_0<\pi/2$, will travel directly towards the anode. An electron entering the field at phase, X_0, so that $(\pi/2)<X_0<3\pi/2$, will initially move in the negative y direction, and ultimately strike the sole plate; or alternatively will reverse its y component of velocity before striking the sole plate, and then ultimately strike the anode.

It will be convenient to know not only the trajectory of an individual electron, but also its position and velocity with respect to normalized time, T, or distance along the circuit, x. These relations may be found by substitution of (13) in (10) and (11) to yield:

$$\dot{X} = -\frac{E_1}{E_0} \sin X_0. \tag{14}$$

However, if it is recalled that $T=\omega t$, $X=\beta x'$, and $x=x'+U_0 t$, then it is possible to write $\dot{X}$ in the form

$$\begin{aligned} \dot{X} &= \frac{dX}{dx}\frac{dx}{dt}\frac{dt}{dT} \\ &= \left(U_0 + \frac{dx'}{dt}\right)\frac{1}{\omega}\frac{dX}{dx} \\ &= \frac{1}{\beta}(1+\dot{X})\frac{dX}{dx}. \end{aligned} \tag{15}$$

It is therefore possible to express $\dot{X}$ directly in terms of dX/dx. However, in order to produce tractable integrals, it is convenient to neglect $\dot{X}$ compared with unity. This is reasonable, for it can be seen from (14) that only assumption 8, $(E_1/E_0)\ll 1$, is involved; this is certainly true for the types of slow wave circuits and beam perveances obtainable in practice. Thus (15) becomes

$$\frac{dX}{dx} = -\frac{\beta E_1}{E_0} \sin X_0$$

which may be integrated to give

$$X = X_0 - \frac{\beta \sin X_0}{E_0}\int_0^x E_1(x)dx. \tag{16}$$

It will be convenient to write

$$F = F(x) = \frac{\beta}{E_0}\int_0^x E_1(x)dx \tag{17}$$

so that (16) becomes

$$X = X_0 - F \sin X_0. \tag{18}$$

Substitution of (18) in (13) then yields the following expression for the Y coordinate of an electron starting at initial phase X_0:

$$e^Y = \frac{\sin X_0}{\sin (X_0 - F \sin X_0)}, \tag{19}$$

and it follows from (10) that

$$\dot{Y} = \frac{E_1}{E_0} \sin X_0 \cot (X_0 - F \sin X_0). \tag{20}$$

The position and velocity of an electron entering at arbitrary phase X_0 have now been expressed in terms of the fields existing in the system. It still remains to determine the expression for the field at any point of the circuit due to the motion of the beam. The combination of these two results will then yield the solution for F, and hence the field, E_1, as a function of distance along the circuit.

Consider the average power dP delivered to the circuit between x and $x+dx$. We may write

$$dP = \frac{dx}{2\pi}\int_{X_0=0}^{X_0=2\pi} q\bar{v}\cdot\bar{E}\, dX \tag{21}$$

where $\bar{E}$ is the rf field at any point distance x from where the beam enters the circuit, $q\,dX$ is the charge passing through dx, in the time required for a phase change dX, and the integration is taken over one cycle of rf, or a change in 2π of entrance phase.

Eq. (21) may be written in the form

$$dP = \frac{dx}{2\pi}\int_{X_0=0}^{X_0=2\pi} qU_0(E_x + \dot{X}E_x + \dot{Y}E_y)dX. \tag{22}$$

However, it may be seen by substitution of (10) and (11) in (22) that the second and third terms of the integrand add to zero, because in the moving system the trajectories are at right angles to the direction of the rf electric field, $\bar{E}$. It may also be seen from (2) and (10) that the first term of the integrand may be written in the form $qU_0\dot{Y}E_0$ to yield the following expression for dP

$$dP = \frac{dx}{2\pi}\int_{X_0=0}^{X_0=2\pi} qU_0\dot{Y}E_0 dX. \tag{23}$$

It may be seen that, as might be expected, (23) is just the expression for the dc power lost over the distance dx. Because of this, it is convenient to write

$$dP = I_{dc}E_0 dx \tag{24}$$

where

$$I_{dc} = \frac{1}{2\pi}\int_{X_0=0}^{X_0=2\pi} qU_0 \dot{Y} dX.$$

But if q is the charge per unit length at a distance x from the entry point of the beam into the circuit, then $q = q_0 dX_0/dX$, where q_0 is the charge per unit length entering the circuit, or $q_0 = I_0/U_0$. Hence

$$I_{dc} = \frac{I_0}{2\pi}\int_0^{2\pi} \dot{Y} dX_0. \tag{25}$$

The substitution of (20) in (25) yields the following expression for I_{dc}

$$I_{dc} = \frac{I_0 E_1}{2\pi E_0}\int_0^{2\pi} \sin X_0 \cot (X_0 - F \sin X_0) dX_0. \tag{26}$$

It will be convenient to write

$$G(F) = \frac{1}{2\pi}\int_0^{2\pi} \sin X_0 \cot (X_0 - F \sin X_0) dX_0, \tag{27}$$

so that (24) becomes

$$\frac{dP}{dx} = I_0 E_1 G(F). \tag{28}$$

Now, at a distance x along the system, the power flow, P, is directly proportional to the square of the amplitude of the rf field at $y=0$, E_1^2. Therefore, it is possible to write $P = E_1^2/2\beta^2 K$, where K is the impedance of the circuit at $y=0$. It is therefore possible to write (28) in the form

$$E_1 \frac{dE_1}{dx} = \pm K\beta^2 I_0 E_1 G(F)$$

where the + sign is taken for a forward wave, and the − sign for a backward wave. Therefore

$$\frac{dE_1}{dx} = \pm K\beta^2 I_0 G(F). \tag{29}$$

The substitution of (17) in (29) then yields the following differential equation for F from which may be determined the fields at any point of the system.

$$\frac{d^2F}{dx^2} = \pm \frac{K\beta^3 I_0}{E_0} G(F). \tag{30}$$

It is convenient to define a dimensionless gain parameter, D, given by the expression

$$D^2 = \frac{K\beta I_0}{E_0} = \frac{\omega}{\omega_h}\frac{KI_0}{2V_0} \tag{31}$$

where V_0 is the dc potential at which the beam enters the system. The differential equation for F then becomes

$$\frac{d^2F}{dx^2} = \pm D^2\beta^2 G(F). \tag{32}$$

Discussion of Results

Analytic Solution—Small Signal Treatment

Eq. (32) is not, in general, soluble analytically due to the nature of $G(F)$. Consequently, it is usually necessary to solve the equation numerically. As a first step, $G(F)$ is found as a function of F. This has been done on an analog computer, and the resultant function is plotted in Fig. 2.

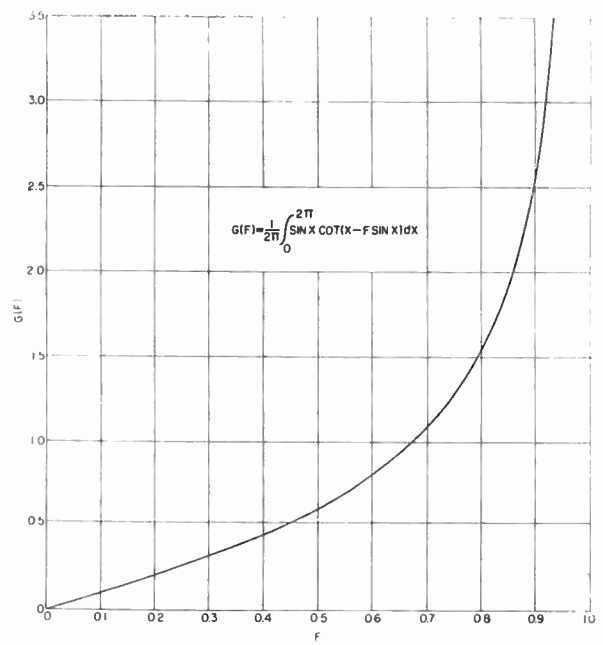

Fig. 2—The parameter $G(F) = (1/2\pi)\int_0^{2\pi} \sin X \cdot \cot (X - F \sin X) \cdot dX$. No beam interception is assumed.

However, for small signals, F is small so that it is possible to neglect second order terms in F in (27) and write $\cot (X_0 - F \sin X_0) \simeq \cot X_0 + F/\sin X_0$, thus yielding the simple form for $G(F)$, $G(F) \simeq F$. It may be seen from Fig. 2 that this expression for $G(F)$ is valid for values of F up to about 0.3, where the error in $G(F)$ is about 10 per cent.

Thus the small-signal approximation will yield (32) in the approximate form

$$\frac{d^2F}{dx^2} = \pm D^2\beta^2 F, \tag{33}$$

the sign being positive for a forward-wave system and negative for a backward-wave system.

In the case of a forward-wave amplifier, it will be seen from (17) that the boundary conditions at $x=0$ are

$$F(0) = 0$$
$$\left(\frac{dF}{dx}\right)_{x=0} = \frac{\beta E_1(0)}{E_0} \tag{34}$$

which yields the following solution for (33):

$$F(x) = \frac{E_1(0)}{E_0 D} \sinh \beta D x \tag{35}$$

and

$$E_1(x) = E_1(0) \cosh \beta D x. \tag{36}$$

This solution is identical to the small-signal solution given by Pierce[3] under the same conditions.

It is interesting, before proceeding further, to determine the range of validity of the small-signal solution. It has already been determined that the assumption $G(F) = F$ only gives reasonable accuracy for values of F up to about 0.3. Dividing (35) by (36) it will be seen that we may write

$$F(x) = \frac{E_1(x)}{E_0 D} \tanh \beta D x. \tag{37}$$

Hence the condition that $F(x) < 0.3$ yields the condition at the end of a tube of length, L:

$$\left[\frac{E_1(L)}{E_0 D}\right]^2 < 0.09 \coth^2 \beta D L. \tag{38}$$

By using (31) and the expression for the output power of the tube, $2P = E_1^2(L)/\beta^2 K$, we find that

$$P < 0.09 I_0 V_0 \omega_h (\coth \beta D L)^2 \omega. \tag{39}$$

However, for a tube of reasonable length, $\coth \beta D L \simeq 1$, so that the estimate for the output power for which the small-signal theory is valid becomes

$$P < 0.09 I_0 V_0 \omega_h / \omega \tag{40}$$

provided that the anode and sole plate are sufficiently far from the beam to preclude interception of electrons.

Consider now the solution for a backward-wave amplifier under small-signal conditions. It will be seen from (17) that the boundary conditions on (33) are

$$F(0) = 0$$
$$\left(\frac{dF}{dx}\right)_{x=L} = \frac{\beta E_1(L)}{E_0}$$

where L is the length of the amplifier.

Eq. (33) then yields the following solution

$$F(x) = \frac{E_1(L)}{E_0 D} \frac{\sin \beta D x}{\cos \beta D L}$$
$$E_1(x) = E_1(L) \frac{\cos \beta D x}{\cos \beta D L}. \tag{41}$$

For the usual oscillator case $E_1(L) = 0$, so that for oscillation there is the additional condition $\beta D L = (2n+1)\pi/2$. This solution and condition for oscillation agrees with the usual small-signal analysis, provided that it is assumed that the beam velocity on entry into the system is the same as the phase velocity of the rf along the circuit.[4]

Large Signal Solution

While it is possible to reduce (32) to quadratures even in the general case, the numerical form in which $G(F)$ is available for large F makes the differential analyzer an ideal tool for the solution of the equation.

However, before proceeding to obtain a solution of (32), it is necessary to modify the form of $G(F)$ to take account of the collection of electrons at the anode and the sole plate, as this effect is most important at large-signal levels. To make this modification, the limits of (27) must be changed so that Y can never exceed βy_a or be less than βy_c, where $y = y_a$ and $y = y_c$ are the positions of the anode and sole plate, respectively.

To find the correct limits on X_0 as a function of F, the anode and cathode positions are inserted in (19) to give

$$e^{\beta y_a} = \frac{\sin X_0}{\sin (X_0 - F \sin X_0)} \tag{42}$$

for one limit, and

$$e^{\beta y_c} = \frac{\sin X_0}{\sin (X_0 - F \sin X_0)} \tag{43}$$

for the other limit.

The parameters $\beta y_a = 3$, and $\beta y_c = -0.5$ have been chosen for the model to be discussed. In this case, (42) may be approximated by

$$\frac{X_0}{\sin X_0} \geq F + 0.05. \tag{44}$$

Thus the zero limit of integration is unaffected until F reaches 0.95 with this anode position; from (43) it can be seen that the first electron strikes the sole plate at $F = 0.65$. The new form of the $G(F)$ curve with these electrode spacings is shown in Fig. 3 and is the one that will be used henceforth. It will be seen that $G(F)$ does not now become infinite at $F = 1$, but reaches a maximum in the region of $F = 0.95$ where electrons bunched around the position of stable phase are collected by the anode. At $F = 4.6$, the upper and lower limits have coalesced signifying that all of the beam has been collected either at the anode or the cathode.

The complete solution for a forward-wave amplifier using the $G(F)$ of Fig. 3 has been carried out on an ana-

[3] J. R. Pierce, "Traveling Wave Tubes," D. Van Nostrand Co., Inc., New York, N. Y., ch. 15; 1950.

[4] R. Warnecke, P. Guenard, and O. Doehler, "Fundamental phenomena in traveling wave tubes," *Onde Elect.*, vol. 34, pp. 323–328; April, 1954.

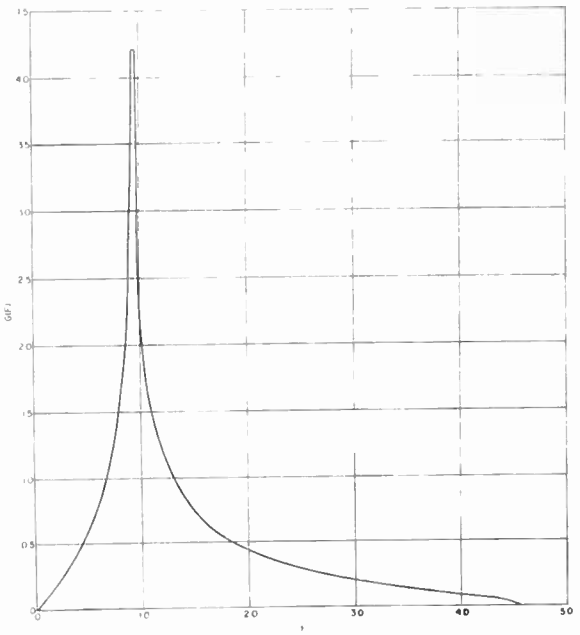

Fig. 3—$G(F)$ for integration limits corrected for finite electrode spacings: $\beta Y_a = 3$, $\beta Y_c = -\frac{1}{2}$.

log computer. The results of this computation are given in Fig. 4 and Fig. 5; F and E_1/E_0D are respectively plotted against DN, N being the number of wavelengths along the tube. It will be seen that the rate of growth of the signal along the tube is initially small, increasing as part of the beam approaches the anode and enters a strong rf field region. In the region where F approaches 0.95, the rate of growth of the signal approaches its maximum value, and then, as the beam is gradually collected at the anode, the rate of growth decreases until the output becomes constant when $F > 4.6$. At this point, the maximum possible output power which could be delivered to the load is the sum of the input rf power and the dc power expended in moving the beam from its original position to hit the anode. If the anode potential is V, the rf power supplied by the tube will be somewhat less than $(V - V_0)I_0$ due to the loss of a certain portion of the beam at the sole plate and of the rf energy dissipated by these electrons.

It should be noted that the theory indicates one decided difference in the operation of this type of tube and its equivalent longitudinal twt. This difference is that if operation is well below saturation level, the gain may increase as the input signal level is increased. Consider, for instance, the gain in a tube with $DN = 0.35$: it will be seen from Fig. 4 that for an input $E_1(0) = 0.04\, E_0D$, $E_1(L) = 0.13\, E_0D$, so that the power gain of the tube is $[(0.13)^2 - (0.04)^2]/(0.04)^2$ or a gain of 9.56. However, for an input $E_1(0) = 0.2\ E_0D$, the output $E_1(L) = 1.24\ E_0D$, so that the power gain is 31. Thus, with larger input the tube gives larger gain; the reason being, of course, that at large-signal levels the beam moves nearer the anode circuit and hence the effective circuit impedance at the beam is increased. But it will be apparent that this trend does not continue indefinitely, for when $E_1(0) = 0.8$ the power gain is only 7.27 and would decrease still further for larger input signals due to collection of a sizable portion of the beam at the anode within the length of the tube.

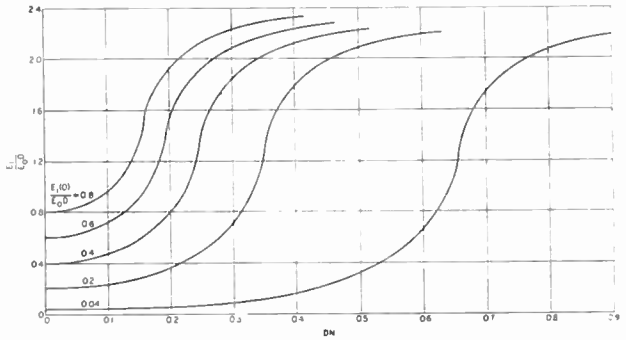

Fig. 4—The amplitude of the rf field, E_1, of a forward-wave amplifier as a function of position along the circuit measured in wavelengths, N, for the electrode spacings of Fig. 3. The parameter D is proportional to the square root of the ratio of circuit to beam impedance, as defined in the text.

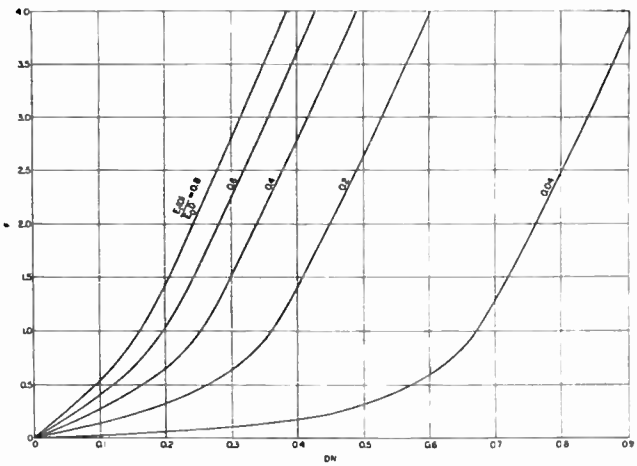

Fig. 5—The variation of F along the circuit for the case of Fig. 4.

Consider, now, the solutions obtained on the analog computer for the operation of a backward-wave oscillator, the $G(F)$ curve in Fig. 3 being used as before. The tube is assumed to be terminated at $x = L$ and the boundary condition $E_1(L) = 0$ has been taken as in the small-signal case. The resultant solutions for E_1/E_0D and F are plotted against DN in Fig. 6 and Fig. 7. For any particular curve of Fig. 6 the abscissa for $E_1 = 0$ corresponds to the length of the tube, and the ordinate at $DN = 0$ corresponds to the field at the output of a tube of this length, the square of the ordinate being proportional to the output power of the tube.

It will be remembered that (41) implies that small-signal oscillation takes place when $\beta DL = \pi/2$ or $DN = 0.25$, though it should always be possible to obtain oscillation for $DN > 0.25$. The large-signal theory, as can be seen from Fig. 6 shows that DN must be considerably greater than 0.25 to obtain the full saturated output power; for instance, when the tube length corresponds

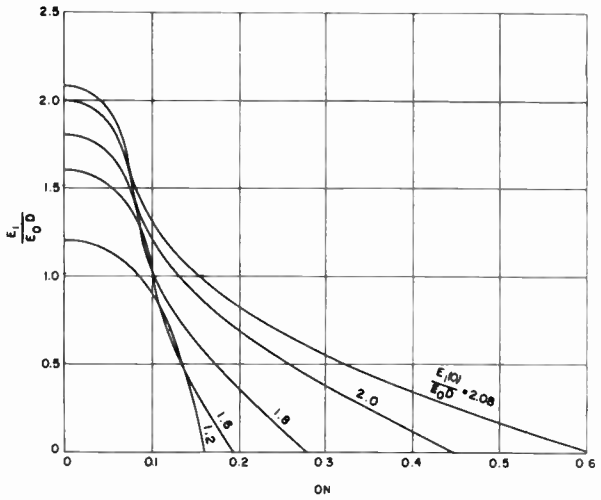

Fig. 6—The amplitude of the rf field, E_1, of a backward-wave oscillator as a function of position along the circuit for the electrode spacings of Fig. 3.

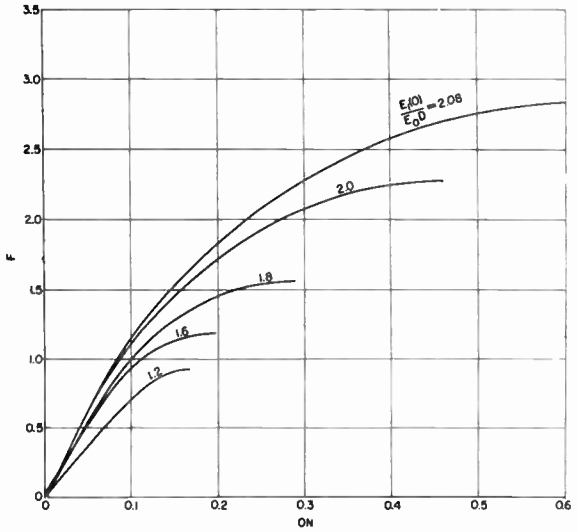

Fig. 7—The variation of F along the circuit for the case of Fig. 6.

to $DN=0.28$, the output power is $(1.8)^2$ units or 3.24 units, while when the tube length $DN=0.6$, the output power is $(2.08)^2$ units or 4.32 units.

One important implication of the theory which points out the difference between this type of tube and the corresponding O-type Carcinotron is that the curves of Fig. 6 for $DN<0.25$ imply that it is possible for oscillation to take place for a tube length $DN<0.25$, because at large-signal levels the beam moves closer to the anode over a portion of its length, and the corresponding rf impedance of the circuit at the beam is therefore higher than at the position $y=0$. However, it would not be expected that this type of oscillation would be self-starting, as the tube would not oscillate at small-signal levels, *i.e.*, with only noise input to start it for a tube length $DN<0.25$. Thus a type of hysteresis effect is implied: no initial oscillation but persistence of oscillation if a large enough input signal at $x=L$ is applied and then removed.

However, for full efficiency as an oscillator, it can be of help to apply an input signal at $x=L$. Fig. 8 and Fig. 9 show the difference in the situation, as obtained on the analog computer, when an input signal is applied at $x=L$. As in Fig. 6, the ordinate of Fig. 8 at $x=0$ gives the output power of the tube. Now consider a tube length $DN=0.28$. From Fig. 6 the output power with zero input signal is $(1.8)^2$ units or 3.24 units. But it may be seen from the lowest curve of Fig. 8 that if an input power of $(0.83)^2=0.69$ is applied to a tube of the same length the output power at $x=0$ will be $(2.2)^2$ or 4.84 units; thus the rf power contribution of the tube is 4.84 $-0.69=4.15$ units or almost a 30 per cent increase in output power. Thus if the tube is too short to obtain maximum saturated output power, the theory implies that substantially the full output power may be obtained by the application of an input signal. This effect arises again because the application of an input signal serves to bring the beam up to the anode quicker and thus makes the effective DN of the oscillator larger than for a self-excited oscillator.

The hysteresis effect that has already been noted is also apparent from the curves of Fig. 8. Consider, for instance, a tube of length $DN=0.192$: from the lowest curve of Fig. 8 an input of $(1.03)^2$ or 1.06 units would give an output of $(2.2)^2$ or 4.84 units, the contributed power of the tube being 3.78 units. If this input is removed, the tube will still remain oscillating with an output of $(1.6)^2$ or 2.56 units. Thus, in this case the rf output contributed by the tube is increased by over 50 per cent when an input signal is present, but the tube would not oscillate if the input signal had never been applied. However, if the original input signal applied had been small enough, this signal would have been amplified and the output of the tube would not have persisted after the input signal had been removed. This particular condition has not been plotted, but of course the possible gain in such a case could be determined from the theory.

Evaluation of Crossed-Field Devices

It will be seen from the curves of Fig. 4 that for a forward-wave amplifier there is no apparent limit to the possible gain obtainable for saturation output, provided that there is no restriction on the length of the tube. However, length is restricted not only by considerations of physical size but also by the difficulty encountered in practice of maintaining a focused electron beam over a great length in an M-type device. The backward-wave amplifier, on the other hand, will not yield large gain at optimum efficiency. Thus, in order to prevent persistence of oscillation after removal of the input signal with a tube of length $DN=0.192$ it would be necessary to use an input signal that would yield an output less than the output of the tube when oscillating, *i.e.*, $(1.6)^2$ or 2.56 units, the maximum possible output which the tube is capable of yielding being greater than $(2.08)^2$ or 4.28 units. Thus the backward-wave structure, when used as

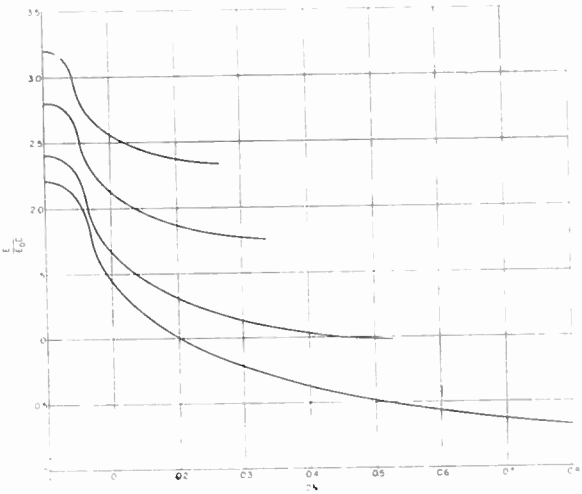

Fig. 8—The amplitude of the rf field of a backward wave amplifier as a function of position along the circuit for the electrode spacings of Fig. 3.

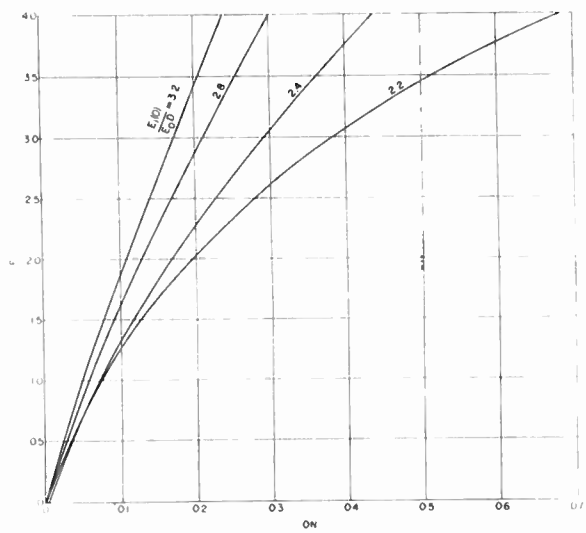

Fig. 9—The variation of F along the circuit for the case of Fig. 8.

an amplifier rather than a locked oscillator can only give very poor efficiency.

Now let us compare a backward-wave amplifier used as a locked oscillator of length $DN=0.25$ with the corresponding forward-wave amplifier of length $DN=0.25$. It will be seen from the lowest curve of Fig. 8 that an input of $E_1=0.88\ E_0D$ at the point $DN=0.25$ will give an output of $E_1=2.2\ E_0D$, so with an input power of $(0.88)^2=0.775$ units the output contributed by the tube is $(2.2)^2-0.775=4.07$ units, yielding a gain of 5.26 or 7.2 db. Likewise, it will be seen from the upper curve of Fig. 4 that for a forward-wave tube an input of $E_1=0.8\ E_0D$ or 0.64 units yields an output of $E_1=2.13\ E_0D$ at $DN=0.25$, or an output power of 4.54 units, the contributed power of the tube being 3.90 units, and the gain being $(3.90/.64)=6.1$ or 7.86 db. Thus the equivalent tubes give virtually the same gain and output for a length of $DN=0.25$, the difference being that the backward-wave tube would keep on oscillating after the input signal had been removed. The gain obtainable at good efficiencies from a backward-wave tube are likely to be less than this figure, unless possibly it could be made sufficiently long to be a free running oscillator, yet still be capable of being locked by a small input signal. However, it would seem that the only possible way of obtaining a true amplifier of large gain and good efficiency would be to use a forward-wave circuit and make the tube sufficiently long to fulfill the requirement of high gain.

An alternative method for obtaining higher gain without an increase in physical length might be to move a portion of the anode circuit closer to the beam at entrance, thereby obtaining higher impedance in this region. The dc potential of this portion of the anode would be lowered in accordance with its new position so as to leave the dc electric field unaltered. Electronic efficiency would not be sacrificed since the curves indicate that few electrons reach the anode during the initial interaction. Practical difficulties would arise here in keeping the dc field lines uniform in the transition region between the two anode heights.

Another suggestion calls for the introduction of an rf field at the cathode, or sole electrode in the entrance region. It is well-known[3] that such a field cannot yield gain since the unfavorably phased electrons, which acquire energy from the rf field, move into regions of stronger field (toward the cathode), while those in proper phase to deliver energy to the field move farther from the circuit. Nevertheless it was hoped that a strong premodulation could be effected by such an input circuit as a result of the proximity of the beam to the cathode. The analysis indicates, however, that to first order, no modulation is produced. Physically this result arises from the cancellation of the y scalloping effect by a density modulation which bunches electrons into the depressed portion of the scallops. For greater amounts of modulation a net effect does appear, but the magnitude of the ac produced in the beam under optimum conditions differs by only a factor of about two from its value for the same length of circuit placed at the anode. Thus it would appear that a cathode input circuit cannot contribute materially toward raising the gain of a magnetron amplifier. The calculations indicate that it may be of value in quickly removing the unfavorably phased electrons, reducing the anode circuit length required for good efficiency. In this connection it should be noted that the use of a reentrant beam would also make possible operation at high efficiency with anode lengths corresponding to $F=1.5$, rather than the $F=4.6$ found necessary for the collection of all electrons. The uncollected half of the beam would then simply be recirculated.

In the case of backward-wave interaction, the strong rf field present at the beam entrance position reduces the physical distance required to effect a given degree of beam modulation. However, as power saturation is ap-

proached, this effect becomes relatively unimportant. An additional advantage inherent to this mode of operation lies in the greater control over the beam achieved at entrance, possibly preventing space charge and cycloid effects, neglected in our idealized model, from exerting a deleterious effect. The weak rf field near the collector end for normal oscillator operation, however, makes a long circuit necessary if one wishes to obtain full saturated power from this device. The effect of a strong input signal at the collector end in overcoming this limitation has already been discussed. In the absence of such a signal, a reentrant beam would at least prevent a reduction in efficiency from accompanying the reduced power output.

Finally, the use of a continuously emitting cathode rather than the single beam dealt with here has been proposed as a means of increasing the perveance of these devices. Such a system would combine some features of the magnetron oscillator with the uniform beam, traveling-wave analysis given here. If such a device could indeed be controlled it might lead to greatly enhanced power outputs and efficiencies. Since the additional current is fed into the system in regions of strong rf fields, however, it would not necessarily ameliorate the low gain problem.

Appendix

Figs. 10–13 give a comparison of the electron trajectories obtained from (8) and (9) for various values of ω/ω_h and for two entrance conditions into the rf field. The dependence of E_1/E_0 on distance X has been taken from typical solutions for the forward and backward wave cases given respectively on Fig. 4 and Fig. 6. The parameter D has been chosen as 0.1, a case of rather rapid build-up, and therefore one which furnishes a severe test of the adiabatic approximation. The $\omega/\omega_h=0$ curves are of course those obtained with this approximation. The two sets of initial conditions specified for the nonzero values of ω/ω_h, $\dot{X}(0)=\dot{Y}(0)=0$, and $\dot{X}(0)=1$, $\dot{Y}(0)=0$, represent an adiabatic entrance into the rf field produced by fringing effects, and a sharp cut-off of rf field at $X=0$, respectively. In general, one would expect the curves for adiabatic entrance at the lowest value of ω/ω_h to agree best with the approximation used in this paper. While it does appear to be the case that the sharp cut-off type of entrance condition does give rise to more cycloidal looping, the mean trajectories agree about equally well with those for $\omega/\omega_h=0$. A qualitative assessment of the effect of the trajectory departures upon the curves of Figs. 4 and Fig. 6 may be obtained by noting that the energy delivered to the circuit by an electron depends only upon its Y displacement. Thus a lateral displacement of a trajectory from its true position results in a corresponding change in the X position along the circuit at which the induced energy appears. If the displacement for many trajectories are random about the assumed ($\omega/\omega_h=0$) position then the final curves for field strength (E_1/E_0) vs circuit distance would be expected to continue to hold. If, as appears more likely, there is a net displacement of the trajectories [see *e.g.*, 0° and 45° on Fig. 11(a)], then the shape of the circuit field curve would be affected within a lateral distance of the order of the trajectory displace-

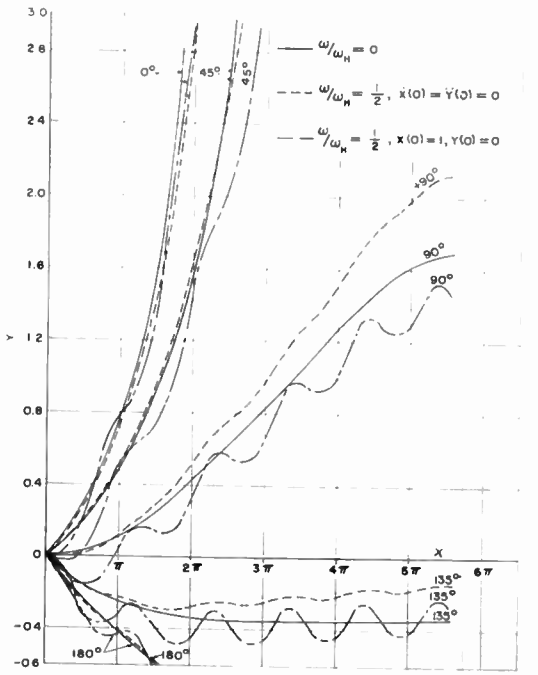

(a)

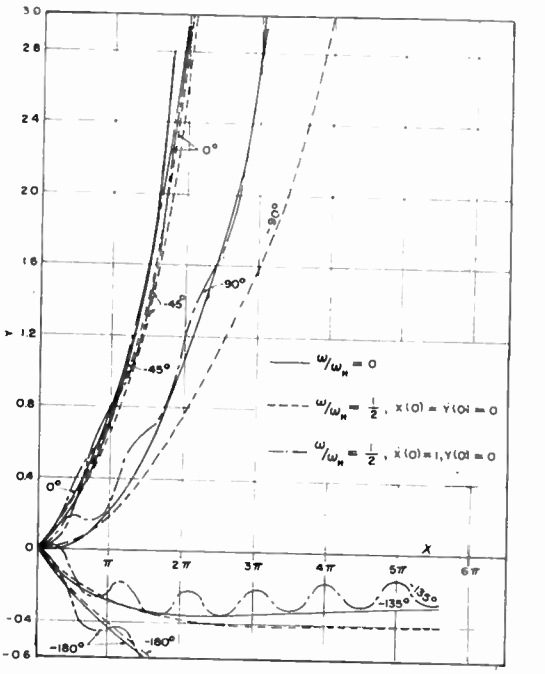

(b)

Fig. 10—Comparison of trajectories for the backward wave oscillator case. Trajectories shown are for an rf field variation specified by the curve $E_1(0)/E_0D=1.8$ on Fig. 6. The entrance phase, X_0, is specified on each trajectory.

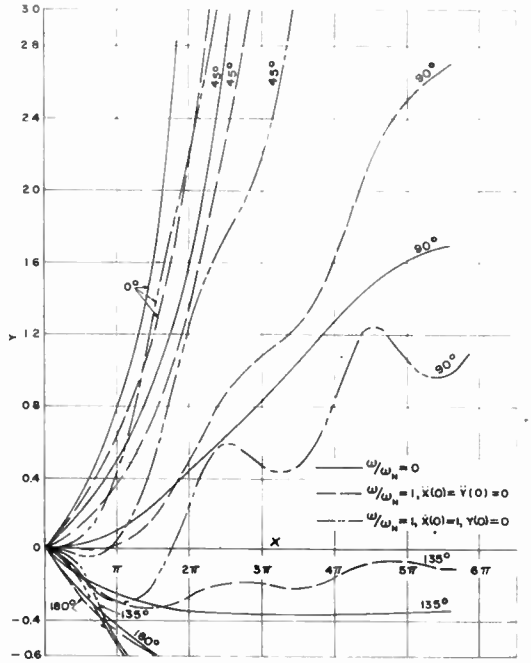

(a)

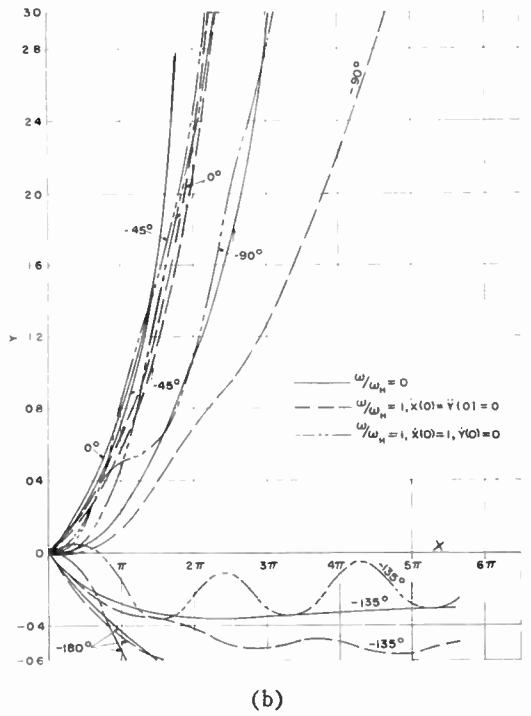

(b)

Fig. 11—Comparison of trajectories for the same case as Fig. 10, but with $\omega/\omega_h = 1$.

ment. For trajectories which do not reach the anode within the tube length [see, *e.g.*, 90° on Fig. 11(a)], there can be a serious error in the extracted energy. Note, however, that the assumed trajectory in this last case lies between those obtained with the two entrance conditions.

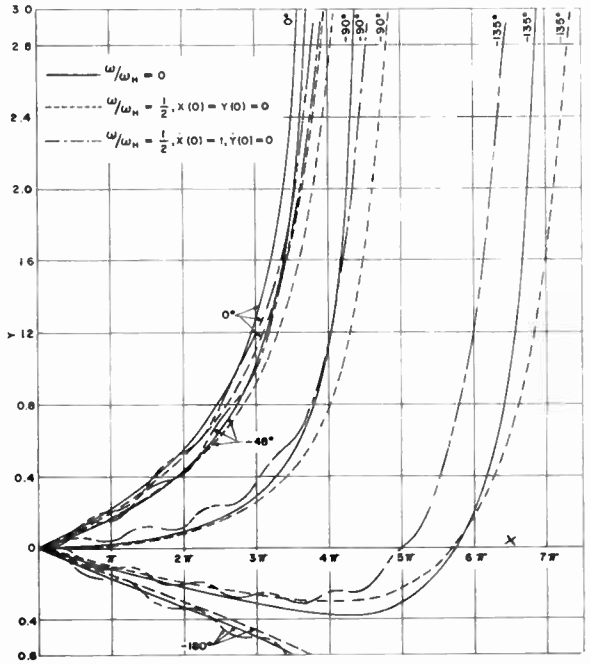

Fig. 12—Comparison of trajectories for the forward-wave amplifier case. Trajectories shown are for an rf field variation specified by the curve $E_1(0)/E_0D = 0.6$ on Fig. 4.

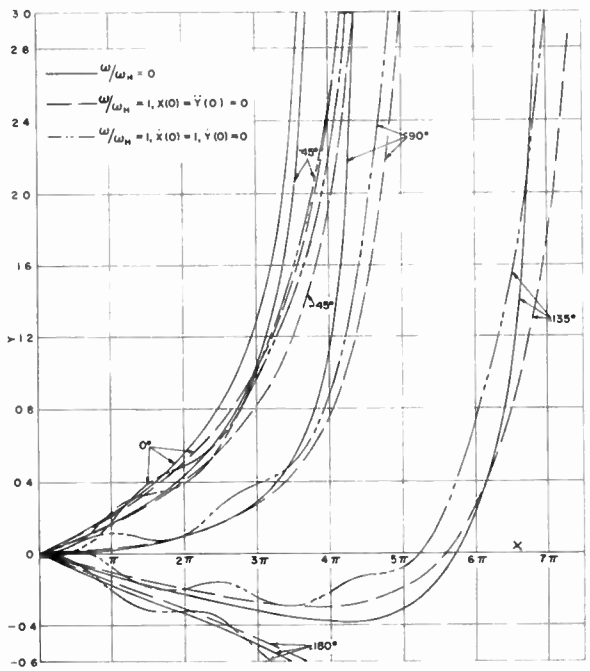

Fig. 13—Comparison of trajectories for the same case as Fig. 12, but with $\omega/\omega_h = 1$.

Acknowledgment

We wish to express our thanks to Mrs. L. R. Lee of the Mathematics Department, Bell Telephone Laboratories, for her work in computing the numerical solutions.

A Versatile Multiport Biconical Antenna*

R. C. HONEY†, ASSOCIATE, IRE, AND E. M. T. JONES†, SENIOR MEMBER, IRE

Summary—This paper describes a multiport, biconical antenna that can be used as a wide-band direction finder or multiplexer. When the antenna is used for reception, incident plane waves excite in the feeding coaxial line both the TEM mode and the orthogonal TE_{11} mode whose azimuthal orientation depends on the direction of arrival of the signal. Directional information can be obtained by measuring the sum of these two modes at four fixed detectors arranged at 90-degree intervals around the coaxial lines. Alternatively, the linearly-polarized TE_{11} mode can be resolved, with appropriate circuitry, into right- and left-hand circularly-polarized TE_{11} modes. Then directional information can be obtained by measuring the phase difference between either of the circularly-polarized modes and the TEM mode. This latter form of direction finder is well suited to multiplexing applications, because each of its three ports is well isolated from the others. Furthermore, this antenna has the unique property that a signal fed into any one of these three ports will cause the antenna to radiate omnidirectionally in azimuth. A waveguide version of this antenna has been built and tested and found to operate well over the frequency range of 8.2 to 12.4 kmc.

General Description

THE novel multiport antenna, described here, has interesting applications to wide-band direction finding and multiplexing. Basically, the antenna uses various orthogonal modes with differing azimuthal properties to yield directional information, and uses the decoupling among these various modes to yield the isolation required for multiplexing.[1–3]

As shown in Figs. 1 and 2, the antenna consists of a biconical radiator which tapers into a coaxial line at its center. A plane wave incident on the antenna excites a large number of propagating radial-line modes in the antenna, which are transformed into coaxial-line modes by the flared section between the biconical antenna and the uniform coaxial line. This coaxial line is only large enough to propagate the TEM and the TE_{11} modes, all others being cut off. Thus the TEM radial-line mode is transformed into the TEM coaxial line mode, and the TE_{10} radial-line mode is transformed into the TE_{11} coaxial-line mode.

The coaxial line is divided into four waveguide channels, located symmetrically about the axis of the coaxial line. A wide-band (at least 1.5 to 1 frequency range) instantaneous direction finder can be constructed by connecting four well-matched square-law detectors to these four waveguide channels. The direction of arrival of a received signal is inferred from the relative amplitudes of the sums of the TEM and the TE_{11} coaxial-line modes as measured by these four detectors.

It is possible, by replacing the four detectors with additional waveguide circuitry, to separate the linearly

Fig. 1—Instantaneous video direction-finding antenna.

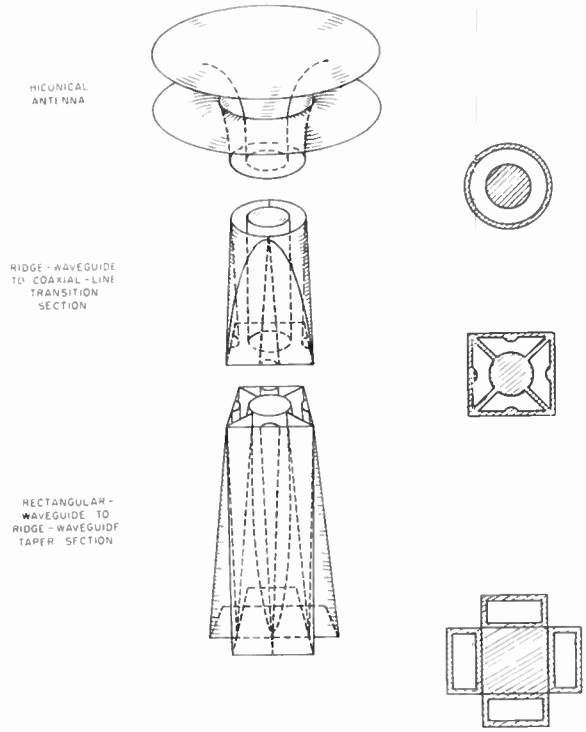

Fig. 2—Video direction-finder circuitry.

* Original manuscript received by the IRE, April 1, 1957; revised manuscript received, June 6, 1957. The work reported in this paper was supported by The Signal Corps under Contract No. DA 36-039 SC-63236.

† Stanford Res. Inst., Menlo Park, Calif.

[1] The Staff of the Radio Res. Lab., Harvard Univ., "Very High Frequency Techniques," McGraw-Hill Book Co., Inc., New York, N. Y., Vol. I, p. 236; 1947.

[2] Leonard Hatkin of SCEL has considered instantaneous direction-finders of this type in unpublished memoranda.

[3] O. M. Woodward, Jr. and J. J. Gibson, "The omniguide antenna—an omnidirectional waveguide array for uhf-television broadcasting," *RCA Rev.*, vol. 17, pp. 13–36; March, 1956.

polarized TE_{11} coaxial-line mode into two circularly-polarized components rotating in opposite directions. In this way, three orthogonal modes—right- and left-hand circularly-polarized TE_{11} coaxial-line modes and the TEM mode—can be brought out to three separate ports. The direction of arrival of a received signal may be determined with no ambiguity by measuring the phase difference between the TEM mode and either of the circularly-polarized modes. Furthermore, since the modes are orthogonal, and since each radiates essentially the same omnidirectional power pattern, this antenna can be used as a three-terminal-pair omnidirectional multiplexing antenna over at least a 1.5 to 1 frequency band.

The antenna systems described here operate with vertical polarization. There are various ways, however, by which the polarization may be modified. For example, metal vanes oriented at 45° from the axis and mounted around the circumference of the aperture will cause the radiated signal to be linearly polarized at approximately 45° if the vanes are less than a half-wavelength apart, and to be elliptically or circularly polarized if the vanes are over a half-wavelength apart. The accuracy of the various directing-finding systems or the isolation of the multiplexing system should not be impaired by this modification.

Application to Omnidirectional Wide-Band Video Direction-Finding

This antenna, described above and shown in Figs. 1 and 2, can instantaneously determine the direction of arrival of a received signal from any azimuth direction over a 1.5 to 1 frequency band. It requires four square-law detectors whose reflection coefficients and sensitivities are as nearly alike as possible over the frequency band. These detectors measure the sum of the TEM and the TE_{11} coaxial-line modes. By taking the difference in the signals from opposite pairs of detectors, two output signals are obtained:

$$E_v = C \sin \phi \cos \delta$$

and

$$E_h = C \cos \phi \cos \delta,$$

where ϕ is the angular bearing of the received signal and δ is the net phase difference between the TEM mode and the TE_{10} radial-line and TE_{11} coaxial-line modes due to the different phase velocities in the antenna and coaxial line. If these two signals are applied to the vertical and horizontal plates of an oscilloscope, the angular position of the radial trace is a direct measure of the bearing angle.

Since both E_v and E_h are proportional to $\cos \delta$, the video output of the difference signals goes to zero whenever $\cos \delta$ goes to zero. It is desirable, therefore, to maintain $|\cos \delta|$ as near unity as possible throughout the frequency band.

Because of the various lengths of nonuniform transmission line in the biconical antenna, in the flared coaxial feed, and in the transition section from coaxial-line to ridge-waveguide, it is difficult to estimate δ accurately. In the first version of this direction finder, which was built to operate from 8.2 to 12.4 kmc, $\delta = 270°$ at 9.33 kmc, and extrapolation of the measured values of δ showed that $\delta = 360°$ and 180° at 7.8 and 13.2 kmc, respectively. Thus, $\cos \delta$ was zero at 9.33 kmc, and output signals E_v and E_h dropped to zero at this frequency.

This direction finder was then modified by removing one inch of the uniform coaxial-line connecting the antenna to the ridge-waveguide transition section. This moved the point at which $\delta = 180°$ to 9.6 kmc, with $\delta = 220°$ and 147° at 8.2 and 12.4 kmc, respectively. Hence, with this change the output drops by only 2.3 and 1.5 db, respectively, at the two ends of the band. However, the concurrent reduction of the cutoff attenuation of the higher-order modes, particularly the TE_{21} coaxial-line modes, seriously increased the bearing errors at the high-frequency end of the band. A redesign of the ridge-guide to coaxial-line transition section should increase the attenuation of the TE_{21} mode and reduce the bearing errors.

The bearing errors for the direction finder were measured in the following manner. At each test frequency, opposite pairs of detectors were matched and their sensitivities equalized. The difference in the outputs from opposite pairs of detectors was recorded as a function of azimuth angle as the antenna was rotated on the antenna pattern range. Such a difference pattern is shown in Fig. 3. For a given true bearing, ϕ, the apparent bearing is given by

$$\phi' = \tan^{-1} \frac{A}{B}$$

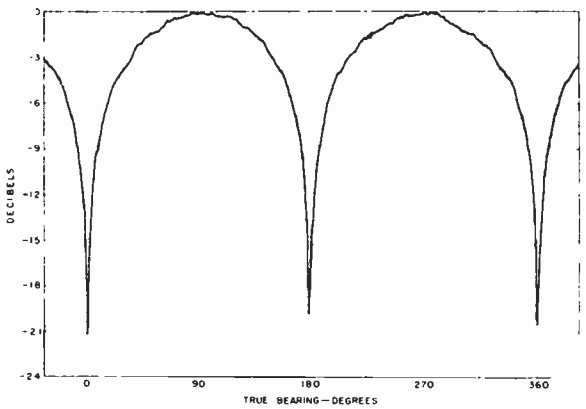

Fig. 3—Response of one pair of detectors on the video direction finder at 8.3 kmc.

where A is the amplitude of the sinusoidal curve from one pair of detectors at ϕ, and B is the amplitude of the cosinusoidal curve from the other pair at ϕ. The indicated bearing would be ϕ' if the two signals were applied to the horizontal and vertical plates of an oscilloscope that introduced no additional errors of its own. The difference between ϕ and ϕ' is the bearing error.

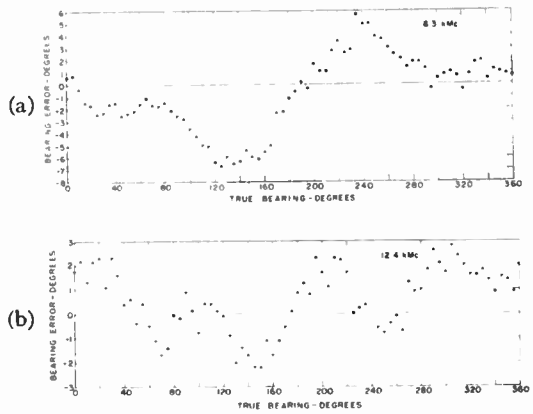

Fig. 4—Bearing errors for original video direction-finder.

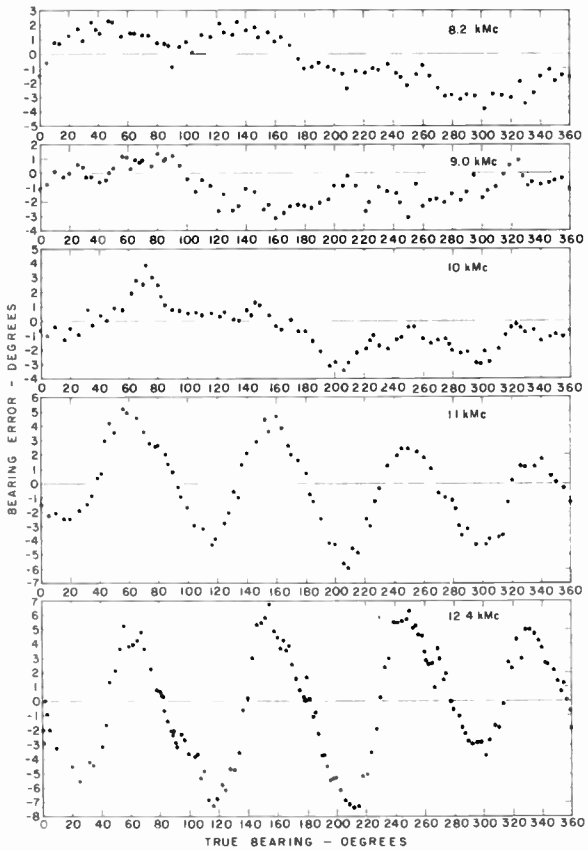

Fig. 5—Bearing errors for shortened video direction-finder.

The bearing errors for the first version of the direction finder at 8.3 and 12.4 kmc are shown in Fig. 4. At 8.3 kmc, the maximum bearing error is 6° from the mean, while at 12.4 kmc the maximum error is 2.2° from the mean. The bearing errors for the same direction finder with one inch less of coaxial line are shown in Fig. 5 for five frequencies in the band 8.2 to 12.4 kmc. It can be seen from the figure how the presence of the TE_{21} coaxial-line mode increases the errors as the frequency is increased. At 8.2 kmc, the maximum error is $\pm 3°$, while at 12.4 kmc it has increased to $\pm 7°$. The 90-degree period of the cycle variation of the bearing errors indicates the presence of the TE_{21} mode.

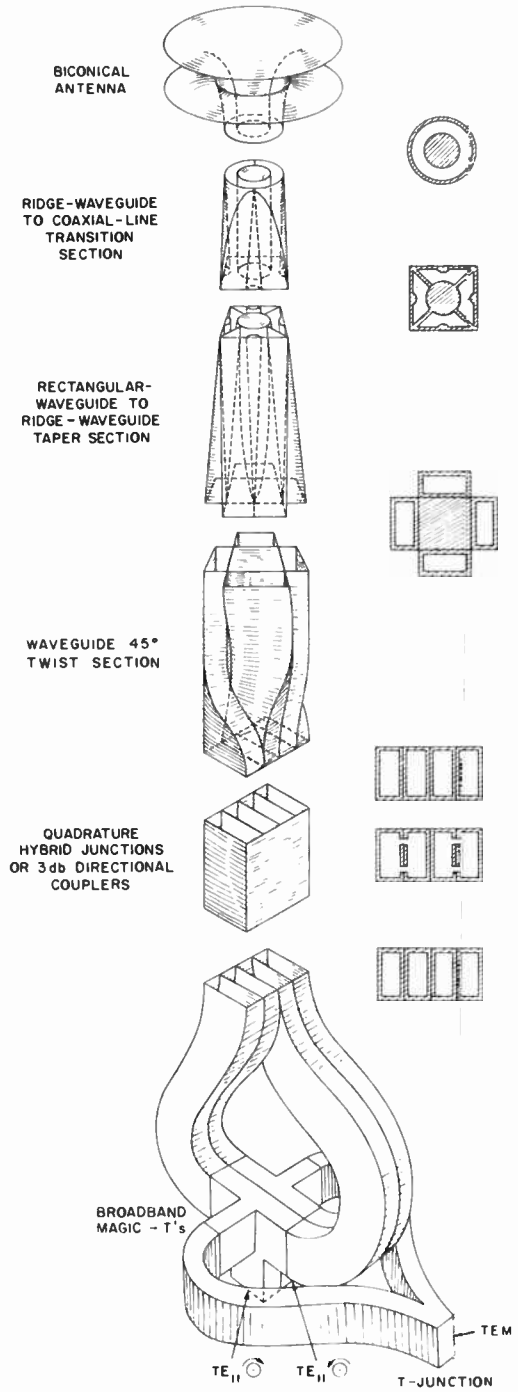

Fig. 6—Wide-band multiplexing and direction-finding antenna.

The bearing errors of a direction finder of this type can arise from five sources:

1) Mechanical asymmetries in the antenna, the antenna's environment, and the transition section;
2) Unequal current sensitivities among the four detectors;
3) Mismatched detectors;
4) Inadequate attenuation of the higher-order modes;
5) Deviation from square-law detector response.

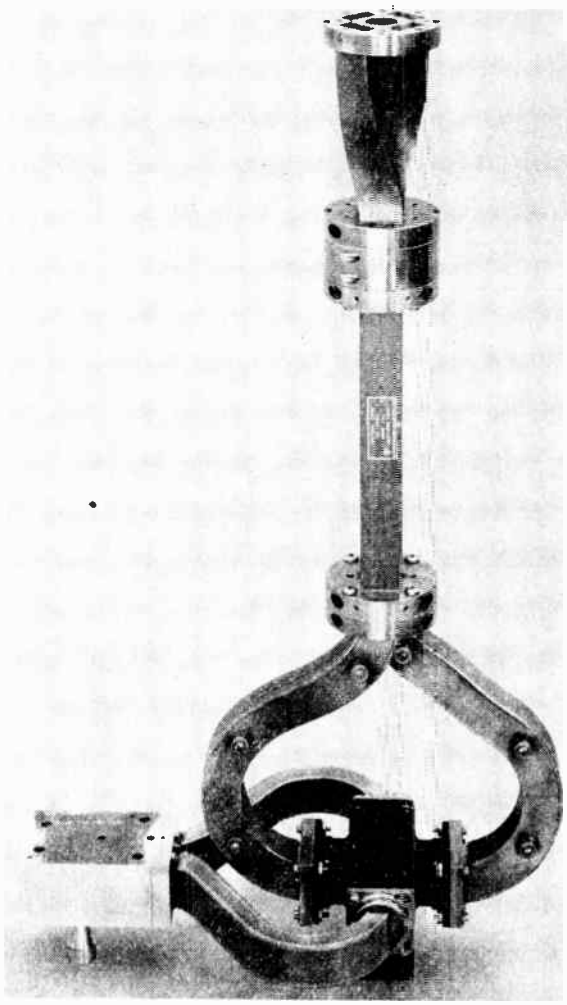

Fig. 7—Wide-band waveguide circuitry.

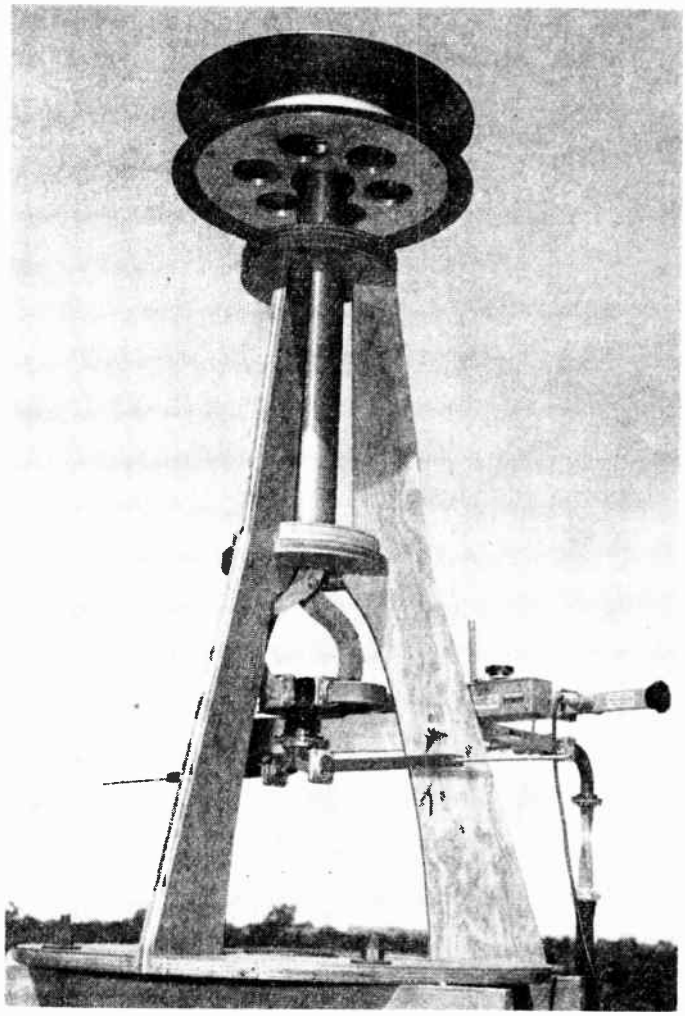

Fig. 8—Wide-band multiplexing antenna on pattern range.

The first source of error has been minimized by employing precision construction techniques which result in a high degree of symmetry among the four channels. It is felt that asymmetries contribute only slightly to the residual errors of the present system. The second source of errors, unequal current sensitivities among the four detectors, is treated in Appendix II-A, where it is shown that the errors will be less than $\pm 2°$ if the video output signals from the detectors are within $\pm \frac{1}{2}$ db of each other for equal rf input signals. The third source of errors, mismatched detectors, is treated in Appendix II-B, where it is shown that the errors will be less than $\pm 2°$ if a single detector has an input vswr less than 1.3. If all detectors have identical reflection coefficients, the errors cancel out. The fourth source of errors, inadequate attenuation of higher-order modes, is treated in Appendix II-C, where it is shown that the below cutoff attenuation of the TE_{21} mode must be greater than 30 db to keep the bearing errors below $\pm 2°$.

The measured bearing errors arose principally from the first and fourth sources, since the errors introduced by the remaining sources were made quite small.

Application to Omnidirectional Wide-Band Multiplexing and Direction-Finding

This antenna utilizes the same components as the video direction finder, except that the detectors are replaced by the additional waveguide circuitry shown in Fig. 6. A photograph of this additional circuitry is shown in Fig. 7, while the complete assembly mounted on the antenna pattern range for tests is shown in Fig. 8. This waveguide circuitry is designed to bring the TEM mode out one port, and to separate the linearly polarized TE_{11} coaxial-line mode into its two equal, orthogonal, circularly-polarized components and bring them out two additional ports. These two components rotate in opposite directions at the rf frequency and have amplitudes of one-half the amplitude of the linearly-polarized mode. Furthermore, since the power received by the linearly-polarized TE_{11} coaxial-line mode is twice that received by the TEM mode (see Appendix I), the power associated with each of the right- and left-hand circularly-polarized components is equal to that of the TEM mode.

A signal fed into one of the TE_{11} ports will excite a

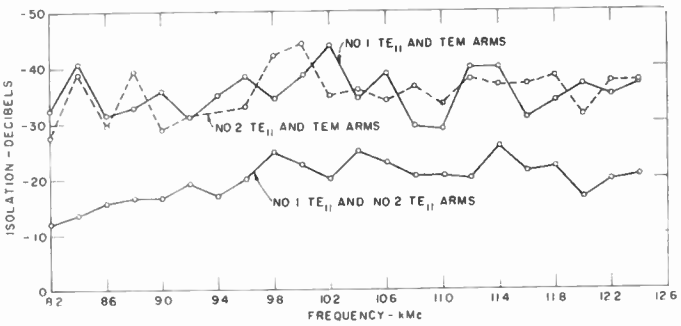

Fig. 9—Isolation between various pairs of ports of the multiplexing antenna.

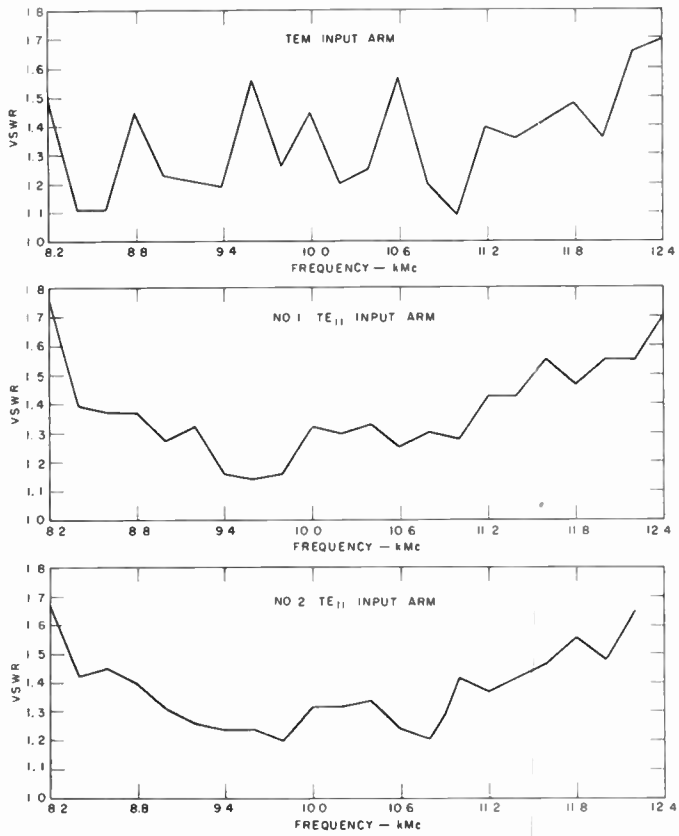

Fig. 10—VSWR vs frequency looking into the three ports of the multiplexing antenna.

circularly-polarized TE_{11} mode in the coaxial line, which is transformed to a spiral-phase TE_{10} radial-line mode in the biconical antenna. The radiation pattern of the TE_{10} radial-line mode is a figure-eight which rotates at the rf frequency. This rotating field distribution is termed a "spiral-phase" mode, since a line of constant phase in the far-field radiation pattern forms a spiral.

The manner in which the circuitry shown in Fig. 6 separates the three orthogonal modes in the coaxial line can be understood by considering the transmitting case. Fig. 6 shows three waveguide ports at the bottom of the figure, one coupling to the TEM mode, and two coupling to the two circularly-polarized modes. A signal fed into the TEM port will excite all four waveguides at the top of the figure in phase and hence excite only the TEM mode in the coaxial line. On the other hand, a signal fed into either TE_{11} port will also divide equally among the four waveguides; however, the 180-degree phase shifts introduced by the Magic-T's and the 90-degree phase shifts introduced by the 3-db directional couplers cause the four waveguides to have a progressive 90-degree phase difference around the periphery of the coaxial line. Therefore, a signal fed into either TE_{11} terminal excites a circularly-polarized TE_{11} mode in the coaxial line. Additional study has shown that all three terminals are isolated from each other.

An analysis of the cross-coupling between ports shows that it is not necessary that the 3-db couplers split the power exactly, only that they be identical. For 0.1-db difference between the two couplers, isolations of at least 45 to 50 db could be obtained if the remaining components were perfect. The best available broad-band Magic-T's provide minimum isolations of only 35 db over the waveguide band, hence they are the principal limiting factor. The isolation between the two TE_{11} ports is directly affected by any symmetrical mismatch in the coaxial line or antenna, since such a reflection returns directly out the opposite channel.

As the multiplexer, then, this antenna has the following characteristics.

1) Three isolated input channels producing essentially the same far-field power radiation patterns.
2) Coverage over at least a 1.5 to 1 frequency band—in this case, 8.2 to 12.4 kmc.
3) Fairly high isolation between the TEM port and either TE_{11} port—averaging between 30 and 40 db over the band with presently available components (see Fig. 9).
4) Somewhat less isolation between the two TE_{11} ports—averaging around 20 db, but dropping to 12 db at 8.2 kmc (see Fig. 9).
5) Reasonably good match looking into any of the ports—the vswr averaging around 1.35, but never above 1.70—again limited by the performance of presently available broad-band Magic-T's (see Fig. 10).

To use this same antenna as a direction finder, it is necessary to measure the phase difference between the TEM mode and either spiral-phase TE_{10} radial-line mode, since this phase difference is linearly related to the azimuth angle at a given frequency. Signals at different frequencies coming from the same direction appear to have different bearings because the electrical lengths of the antenna and associated coaxial line are shorter for the TE_{10} and TE_{11} modes than for the TEM mode. Because the undesired phase difference between these modes depends only on the frequency of the received signal, it is possible to compensate accurately for this difference by ganging an rf or IF phase-correcting element with the local-oscillator frequency control feeding the mixers on each output port. It is also possible to compensate for this difference by inserting a phase-

equalizing network in one of the waveguide channels after the various modes have been separated.

Some of the details involved in the construction and testing of the various components for these direction-finding and multiplexing antennas are given in Appendix III.

Appendix I

A. Analysis of Operation of Video Direction Finder

The video system measures the direction of arrival of a received signal by comparing the amplitudes of the signals received from each of the four waveguides connected to the coaxial line. Ideally, a signal of angular frequency, ω, incident on the biconical antenna from an azimuth direction, ϕ, will excite signals in the four waveguides having amplitudes proportional to the sum of the amplitudes of the radial-line TEM and TE_{10} modes. Specifically, the signals in the four waveguides will be

$$\begin{aligned} E_1 &= A \sin \omega t + B \sin \phi \sin (\omega t - \delta) \\ E_2 &= A \sin \omega t + B \cos \phi \sin (\omega t - \delta) \\ E_3 &= A \sin \omega t - B \sin \phi \sin (\omega t - \delta) \qquad (1) \end{aligned}$$

and

$$E_4 = A \sin \omega t - B \cos \phi \sin (\omega t - \delta),$$

where

A = E-field amplitude induced in one waveguide by the TEM mode;

B = E-field amplitude induced in one waveguide by the TE_{10} radial-line mode;

δ = the amount that the phase of the signal induced by the TEM mode leads that of the signal induced by the TE_{10} mode.

Separate detection of each of these signals by identical square-law detectors produces video signals of the following relative amplitudes:

$$\begin{aligned} E_{1d} &= A^2 + 2AB \sin \phi \cos \delta + B^2 \sin^2 \phi \\ E_{2d} &= A^2 + 2AB \cos \phi \cos \delta + B^2 \cos^2 \phi \\ E_{3d} &= A^2 - 2AB \sin \phi \cos \delta + B^2 \sin^2 \phi \\ E_{4d} &= A^2 - 2AB \cos \phi \cos \delta + B^2 \cos^2 \phi. \qquad (2) \end{aligned}$$

In Fig. 11 E_{1d} is plotted as a function of azimuth angle, ϕ, for several values of δ for $B = 2A$. By taking the difference between the detected signals from opposite pairs of detectors, video signals are obtained that are proportional to $\sin \phi \cos \delta$ and $\cos \phi \cos \delta$, respectively.

Although the operation of the video-direction-finding system is independent of the amplitudes of the two orthogonal modes, it will prove useful in determining bearing errors to find the relationship between them. The amount of available power in the orthogonal TEM and TE_{10} radial-line modes excited in the biconical antenna by an incident plane wave can be most easily determined by considering the directive gain of the biconical antenna when it is supporting each of these modes separately. Consider the case where the biconical antenna extends to infinity and assume that the antenna is transmitting. Then it is seen that at a constant radius the electric-field amplitude of the TEM mode is independent of azimuth angle, while that of the TE_{10} mode, which radiates a stationary figure-eight pattern, is proportional to the sine of the azimuth angle. By integrating the electric-field amplitude of each mode separately over all azimuth angles, it is readily shown that the maximum directive gain of the antenna when supporting the TE_{10} radial-line mode is twice that when the antenna is supporting the TEM mode. Therefore, when the antenna is used for reception, there is twice as much power available in the TE_{10} radial-line mode as there is in the TEM mode. From (1) the power available from the TE_{10} radial-line mode is proportional to $2B^2$, and the power available from the TEM mode is proportional to $4A^2$; therefore, $B = 2A$. It has been assumed that both modes are perfectly matched into the four waveguides.

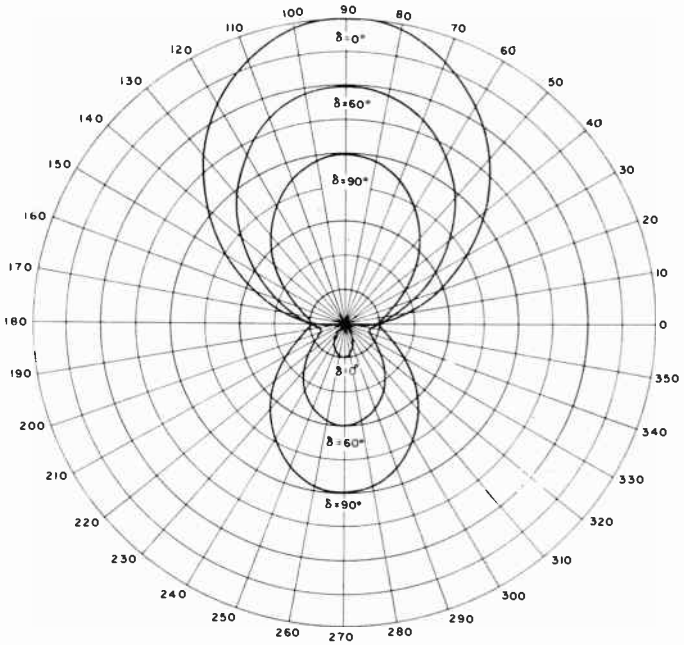

Fig. 11—Received power as a function of azimuth angle for a single detector in the video direction-finder.

The above discussion also assumes that the biconical antenna extends to infinity. In an actual antenna of finite extent but still many wavelengths in circumference, it is clear that relationships similar to those given above will apply, at least within a restricted range of elevation angles above and below horizontal, depending on the vertical directivity of the antenna.

Appendix II

A. Bearing Errors for Video Direction Finder

As mentioned in the text, bearing errors may result from a number of sources, several of which may be analyzed as follows.

Unequal Detector Sensitivities

It is shown in Appendix I that, $B=2A$, hence the video output signals given in (1) become:

It is shown in Appendix I, $B=2A$, hence the video output signals given in (1) become:

$$E_{1d} = C_1(1 + 4\sin\phi + 4\sin^2\phi)$$
$$E_{2d} = C_2(1 + 4\cos\phi + 4\cos^2\phi)$$
$$E_{3d} = C_3(1 - 4\sin\phi + 4\sin^2\phi)$$
$$E_{4d} = C_4(1 - 4\cos\phi + 4\cos^2\phi), \qquad (3)$$

where C_n is proportional to the current sensitivity of the *nth* detector and $\cos\delta = 1$.

Taking the difference between opposite channels and applying the resultant signals to the vertical and horizontal plates of an oscilloscope, as before, gives

$$\tan\phi' = \frac{4(C_1 + C_3)\sin\phi + (C_1 - C_3)(1 + 4\sin^2\phi)}{4(C_2 + C_4)\cos\phi + (C_2 - C_4)(1 + 4\cos^2\phi)}. \qquad (4)$$

The bearing error is then defined as

$$\Delta\phi = \phi' - \phi. \qquad (5)$$

This bearing error has been plotted as a function of true bearing, ϕ, for a number of values of detector output voltages in Fig. 12. A study of the various curves reveals that the minimum bearing errors are obtained (for a given maximum difference between two crystals) when the most sensitive and the least sensitive crystals are placed opposite each other, thus minimizing the difference in sensitivity between adjacent crystals.

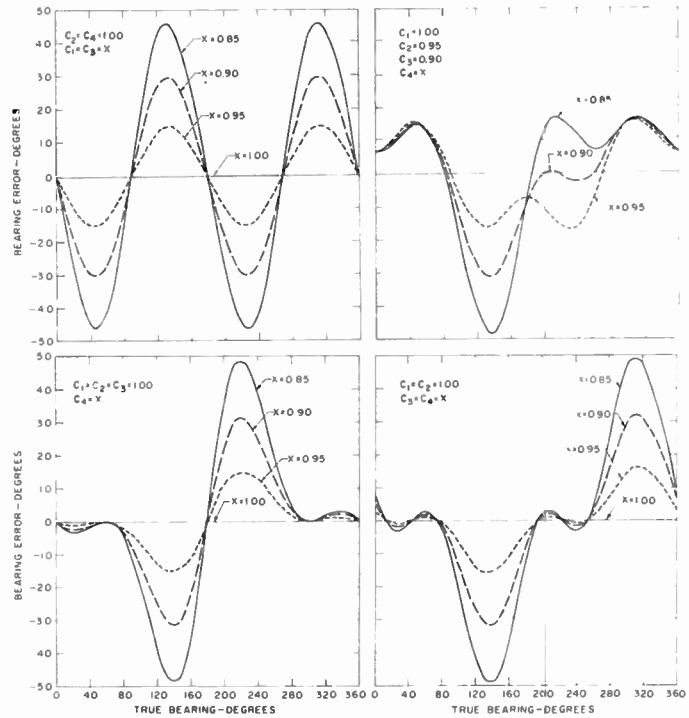

Fig. 12—Bearing error vs true bearing for several values of the sensitivities of the square-law detectors.

B. Mismatched Video Detectors

The effect of mismatched video detectors is most easily determined from the scattering matrix for the ridge-waveguide to the coaxial-line transition section. This transition section is actually a seven-port junction, consisting of four waveguide ports, one TEM mode port in the coaxial line, and two linearly polarized TE_{11} mode ports oriented at right angles to each other in the coaxial line. If one labels the four waveguide ports Nos. 1, 2, 3, and 4, respectively, the TEM port No. 5, and the two TE_{11} ports Nos. 6 and 7, the scattering matrix for the perfect lossless junction can be determined as follows:

1) If a signal is put in port 5, it will be divided equally among ports 1 to 4 with equal amplitudes and phases, and no signal will emerge from ports 6 and 7. Thus, in the scattering matrix $S_{55} = S_{65} = S_{75} = 0$ and $S_{15} = S_{25} = S_{35} = S_{45} = \frac{1}{2}$.
2) Conversely, if four signals of equal amplitudes and phases are put into ports 1 to 4, they will add and emerge from port 5 and none will emerge from ports 6 and 7. Thus, $S_{n1} + S_{n2} + S_{n3} + S_{n4} = 0$, where $n = 1, 2, 3$, and 4.
3) If a signal is put into port 6, and if the plane of polarization of this TE_{11} mode is in line with ports 1 and 3, the signal will divide equally between ports 1 and 3, but with opposite phases. Thus, $S_{26} = S_{46} = S_{56} = S_{66} = S_{76} = 0$, $S_{16} = 1/\sqrt{2}$, and $S_{36} = -1/\sqrt{2}$.
4) Conversely, if equal amplitude signals with opposite phases are put into ports 1 and 3, the signals will add and all emerge from port 6. Thus, $S_{n1} - S_{n3} = 0$, where $n = 1, 2, 3$, and 4.
5) Results similar to those obtained in steps 3 and 4 for port 6 can be derived for port 7.
6) By symmetry, $S_{11} = S_{22} = S_{33} = S_{44}$ and $S_{66} = S_{77}$.

By combining these results, and noting that the scattering matrix must be symmetrical, the following matrix is obtained:

$$S = \begin{bmatrix} \frac{1}{4} & -\frac{1}{4} & \frac{1}{4} & -\frac{1}{4} & \frac{1}{2} & 1/\sqrt{2} & 0 \\ -\frac{1}{4} & \frac{1}{4} & -\frac{1}{4} & \frac{1}{4} & \frac{1}{2} & 0 & 1/\sqrt{2} \\ \frac{1}{4} & -\frac{1}{4} & \frac{1}{4} & -\frac{1}{4} & \frac{1}{2} & -1/\sqrt{2} & 0 \\ -\frac{1}{4} & \frac{1}{4} & -\frac{1}{4} & \frac{1}{4} & \frac{1}{2} & 0 & -1/\sqrt{2} \\ \frac{1}{2} & \frac{1}{2} & \frac{1}{2} & \frac{1}{2} & 0 & 0 & 0 \\ 1/\sqrt{2} & 0 & -1/\sqrt{2} & 0 & 0 & 0 & 0 \\ 0 & 1/\sqrt{2} & 0 & -1/\sqrt{2} & 0 & 0 & 0 \end{bmatrix}. \qquad (6)$$

The use of this matrix makes it very simple to trace any waves which may be reflected back into the system from the detectors.

Let the signals incident on the four detectors be given by (1) for $A = 2B = 1$ and $\cos\delta = 1$. Then, if detector 1 is mismatched, a reflected wave enters port 1 and emerges from the various other ports in such a way that, for small reflections, the resultant field amplitudes are given by

$$E_1 = (1 - \Gamma^2)^{1/2}(1 + 2\sin\phi) + \frac{\Gamma}{4}(1 + 2\sin\phi)$$

$$E_2 = (1 + 2\cos\phi) - \frac{\Gamma}{4}(1 + 2\sin\phi)$$

$$E_3 = (1 - 2\sin\phi) + \frac{\Gamma}{4}(1 + 2\sin\phi)$$

$$E_4 = (1 - 2\cos\phi) - \frac{\Gamma}{4}(1 + 2\sin\phi). \quad (7)$$

For the sake of simplicity, assume that the reflection coefficient Γ of the mismatched detector is real at the reference planes chosen for the scattering matrix in (6).

The video output voltages for the four square-law detectors with current sensitivities given by C_1, C_2, C_3, and C_4, respectively, are

$$E_{1d} = C_1\left(\sqrt{1 - \Gamma^2} + \frac{\Gamma}{4}\right)^2(1 + 2\sin\phi)^2$$

$$E_{2d} = C_2\left[(1 + 2\cos\phi)^2 - \frac{\Gamma}{2}(1 + 2\cos\phi)(1 + 2\sin\phi) + \frac{\Gamma^2}{16}(1 + 2\sin\phi)^2\right]$$

$$E_{3d} = C_3\left[(1 - 2\sin\phi)^2 + \frac{\Gamma}{2}(1 - 4\sin^2\phi) + \frac{\Gamma^2}{16}(1 + 2\sin\phi)^2\right]$$

$$E_{4d} = C_4\left[(1 - 2\cos\phi)^2 - \frac{\Gamma}{2}(1 - 2\cos\phi)(1 + 2\sin\phi) + \frac{\Gamma^2}{16}(1 + 2\sin\phi)^2\right]. \quad (8)$$

In practice, the sensitivities of the four detectors will be equalized by rotating the antenna until the output from each detector is maximized when the antenna is receiving a signal from a distant source of constant amplitude. A radio frequency or a video attenuator can then be adjusted so that the maximum signal from each detector is the same. Thus, in (8), E_{1d} will have a maximum at $\phi = \pi/2$ of 9 $C_1(\sqrt{1-\Gamma^2}+\Gamma/4)^2$. Similarly, E_{2d} will have a maximum at $\phi = 0$ of $C_2(3-\Gamma/4)^2$.

The maxima for the output voltages E_{3d} and E_{4d} are the same as those for E_{2d}, with C_3 replacing C_2 in E_{3d} and C_4 replacing C_2 in E_{4d}. If these four signals are equalized, and if the following constants are arbitrarily set equal to unity

$$C_2 = C_3 = C_4 = 1,$$

then

$$C_1 = \frac{\left(1 - \frac{\Gamma}{12}\right)^2}{\left(\sqrt{1 - \Gamma^2} + \frac{\Gamma}{4}\right)^2}.$$

The four output signals as a function of bearing angle ϕ then become:

$$E_{1d}' = \left(1 - \frac{\Gamma}{12}\right)^2(1 + 2\sin\phi)^2$$

$$E_{2d}' = (1 + 2\cos\phi)^2 - \frac{\Gamma}{2}(1 + 2\cos\phi)(1 - 2\sin\phi) + \frac{\Gamma^2}{16}(1 + 2\sin\phi)^2$$

$$E_{3d}' = (1 - 2\sin\phi)^2 + \frac{\Gamma}{2}(1 - 4\sin^2\phi) + \frac{\Gamma^2}{16}(1 + 2\sin\phi)^2$$

$$E_{4d}' = (1 - 2\cos\phi)^2 - \frac{\Gamma}{2}(1 - 2\cos\phi)(1 + 2\sin\phi) + \frac{\Gamma^2}{16}(1 + 2\sin\phi)^2.$$

Taking the ratio of the difference between opposite channels, as before, gives for the indicated bearing angle ϕ':

$$\tan\phi' = \frac{E_v}{E_h} = \frac{\sin\phi - \frac{\Gamma}{12}(1 + 2\sin\phi)(1 - \sin\phi) - \frac{\Gamma^2}{144}(1 + 2\sin\phi)^2}{\cos\phi\left[1 - \frac{\Gamma}{4}(1 + 2\sin\phi)\right]}.$$

The bearing error, defined as

$$\Delta\phi = \phi' - \phi$$

is plotted in Fig. 13 as a function of the true bearing for several values of the reflection coefficient. The reflection coefficient is related to the input vswr of the detector in the usual way:

$$\text{vswr} = \frac{1 + |\Gamma|}{1 - |\Gamma|}$$

which for the values shown in Fig. 13 are

$\lvert\Gamma\rvert$	vswr
0.1	1.222
0.2	1.5
0.4	2.333.

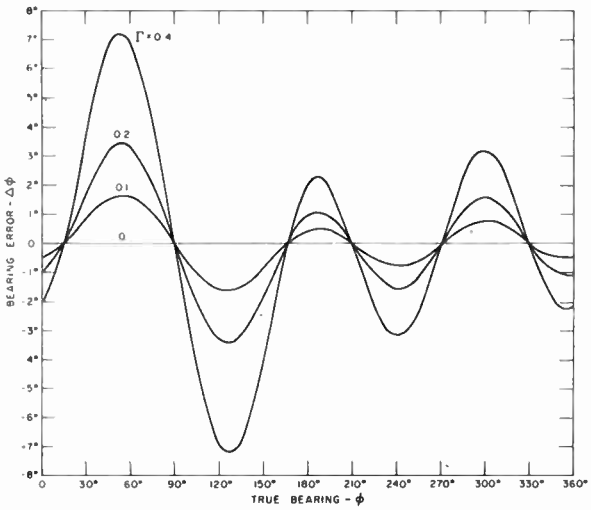

Fig. 13—Bearing errors as a function of true bearing for one mismatched detector with the reflection coefficient shown.

It can be seen that if the detector is matched to a vswr less than about 1.3, the maximum bearing errors will be less than 2°. It can be readily shown from the scattering matrix that if all of the detectors are mismatched such that $\Gamma_1=\Gamma_2=\Gamma_3=\Gamma_4$, then the bearing errors are zero everywhere. This is another case where symmetry is an aid, making it desirable to use four detectors and detector mounts that are identical to each other in as many respects as possible, in order to minimize the bearing errors resulting from any residual reflections.

C. Inadequate Attenuation of Higher-Order Modes

Since the experimental evidence indicates that the TE_{21} coaxial-line mode is the principal higher-order mode contributing to bearing errors, it will be treated here. If the TE_{21} mode is matched into the four waveguides, it excites a signal in them whose amplitude is the same as that excited by the TE_{11} mode, since the directive gains of the TE_{10} and the TE_{20} radial-line modes are equal. If α represents the cutoff attenuation of the TE_{21} mode in the coaxial line, as well as any mismatch loss, the resultant field amplitudes in the four waveguides become:

$$E_1 = 1 + 2\sin\phi - 2\alpha\cos 2\phi$$
$$E_2 = 1 + 2\cos\phi + 2\alpha\cos 2\phi$$
$$E_3 = 1 - 2\sin\phi - 2\alpha\cos 2\phi$$
$$E_4 = 1 - 2\cos\phi + 2\alpha\cos 2\phi$$

where δ has again been assumed equal to zero.

If these fields are incident on identical, matched, square-law detectors, the ratio of the differences between opposite detectors gives for the indicated bearing angle, ϕ',

$$\tan\phi' = \frac{E_v}{E_h} = \frac{1 - 2\alpha\cos 2\phi}{1 + 2\alpha\cos 2\phi}\tan\phi.$$

The bearing errors, given by $\phi'-\phi$, have a period of $\pi/2$ in ϕ and have the following typical amplitudes:

α	Attenuation	Bearing Error
0.05	26 db	±2.7°
0.025	32 db	±1.4°

Appendix III

A. Construction and Performance Data for the Components

Biconical Antenna

The biconical antenna, illustrated at the top of Fig. 6, was formed by drawing two round flat sheets over a suitably shaped die. The flared coaxial line feeding the antenna was machined. The antenna has a diameter of 17.5 inches and a vertical aperture of 4 inches. The vswr looking from the coaxial line into the antenna was less than 1.18 over the 8.2 to 12.4 kmc band for the TEM mode.

Ridge-Waveguide to Coaxial-Line Transition Section

This transition section, shown just beneath the antenna in Fig. 6, has a total length of 3 inches. The round inner conductor, machined from aluminum, tapers linearly from a diameter of 0.4 inch at the top to 0.7 inch at the bottom. The outer conductor, of electroformed copper, tapers from a round inside diameter of 0.75 inch at the top to a square with an inside dimension of 0.9 inch on a side. At the same time, four ridges taper along the centers of the flat sides from zero height at the top to a maximum height of 0.040 inch at the bottom. The division into four-ridge-waveguide channels is accomplished at the bottom with four thin fins whose knife edges are perpendicular to the axis and extend from the inner conductor to the corners of the square outer conductor. The vswr of the transition section is less than 1.3 for the TEM mode and less than 1.22 for the TE_{11} mode over the 8.2 to 12.4 kmc band.

Rectangular-Waveguide to Ridge-Waveguide Taper Section

The taper section, shown next in Fig. 6, has a total length of 5 inches and was electroformed on aluminum mandrels. The vswr for each of the four identical channels is less than 1.12 over the 8.2 to 12.4 kmc band.

Waveguide 45-Degree-Twist Section

This multiple-channel twist section was formed from stacks of thin shims strung together on wires and soldered. The electrical lengths of the four channels were adjusted to within ±0.7° of each other over the 8.2 to 12.4 kmc band. This section and the technique used to construct it are described by Jones and Honey.[4]

[4] E. M. T. Jones and R. C. Honey, "A novel technique for making precision waveguide twists," IRE Trans., vol. MTT-4, pp. 131–132; April, 1956.

Quadrature Hybrid Junctions or 3-DB Directional Couplers

Two Hewlett-Packard X-752A multihole directional couplers were selected whose couplings differed from each other by less than 0.1 db and varied from −2.7 db to −3.3 db over the 8.2 to 12.4 kmc band.

Waveguide Bends

These bends, shown at the bottom of Fig. 6, were all electroformed on precision-machined aluminum mandrels, which were subsequently dissolved out in boiling sodium hydroxide. The electrical lengths of the various paths were checked and adjusted, where necessary, until they were within a degree of each other over the 8.2 to 12.4 kmc band.

Broad-Band Magic-T's

A pair of Airtron's No. 44055 broad-band Magic-T's were obtained for this purpose, and were oriented in the manner illustrated in Fig. 6. They were tested and found to have minimum isolations of 35 db over the 8.2 to 12.4 kmc band and a maximum vswr of 1.7.

T Junction

This T junction, whose symmetrical arm forms the TEM input terminal for the multiplexing antenna, is simply a carefully constructed tapered waveguide bifurcation. It splits the power incident from the symmetrical arm into two equal components within at least ±0.1 db. The symmetrical arm is matched to a vswr less than 1.02 over most of the 8.2 to 12.4 kmc band, increasing to 1.05 at the low end of the band. The total length of the junction is $3\frac{1}{2}$ inches.

ACKNOWLEDGMENT

The authors wish to thank Seymour B. Cohn for his advice and assistance.

Radio Propagation Above 40 MC Over Irregular Terrain*

JOHN J. EGLI†

Summary—**Radio transmissions in the vhf and uhf frequency region over land areas always contend with the irregularities of the terrain and the presence thereon of dispersed quantities of trees, buildings, and other man-made structures, or wave propagation incumbrances. The determination of path attenuation is not easily satisfied by simple, curved, or plane earth calculations. However, quantitative wave propagation data are available in varying degrees which take into account conditions experienced by fixed-to-fixed and fixed-to-moving transmissions over irregular terrain. This available statistical wave propagation information on terrain effects vs frequency, antenna height, polarization, and distance is analyzed, expressed by empirical formulas, and presented in the form of nomographs and correction curves amenable for use by the systems engineer.**

INTRODUCTION

RADIO transmissions above 40 mc more often than not take place over irregular terrain so that the ordinary method of calculating propagation attenuation over plane earth, curved earth, and simple diffraction edges becomes unsatisfactory. As one moves about in irregular terrain in a vehicle, the received signal is characterized by a slow variation dependent on the major features of the terrain and on distance, and by a fast variation about the median in a small sector which is independent of the transmission distance but is dependent on the speed of the vehicle and on the frequency of the transmission.

In the practical sense, the systems engineer is interested in knowing how well his equipment will be able to service an area, or how well his equipment will cover many areas in a very large area. Some of these areas may typify curved earth while other areas may be highly mountainous; all others will be in between these areas in terms of surface irregularity.

This irregular terrain has dotted on it, trees, buildings, and other man-made wave propagation encumbrances. If one could run the entire gamut of terrain conditions in a statistical manner and arrive at the transmission loss which would have to be designed into a system at a given frequency to provide the desired coverage, it would appear that such information would be invaluable to the systems engineer.

Fortunately, such data have been collected and studied by the Federal Communications Commission for use in connection with their studies of the vhf and uhf television allocation problems, and by others in connection with mobile service.

* Original manuscript received by the IRE, February 5, 1957; revised manuscript received, June 7, 1957.
† U.S. Army Signal Eng. Labs., Fort Monmouth, N. J.

The majority of the terrain data,[1] on which the following material will be derived, are based on survey data taken by commercial organizations in various parts of the country including New York, N. Y.; Washington, D. C.; Cleveland, and Toledo, Ohio; Harrisburg, Easton, Reading, Pittsburgh, and Scranton, Pa.; Kansas City, Mo.; Cedar Rapids, Iowa; San Francisco, Calif.; Bridgeport, Conn.; Nashville, Tenn.; Fort Wayne, Ind.; Richmond and Norfolk, Va.; and Newark, N. J. In each of these locations, a number of radials were investigated. In all, over the uhf range, 288 to 910 mc, 804 miles on 63 radials are represented in the data. The method of measurement, while not the same at all locations, falls into three categories: continuous mobile recording sampling every 0.2 mile, spot measurements properly weighted so as to be considered unbiased, and clusters of measurements. In the vhf region, 50 to 250 mc, approximately 1400 measurements, consisting of continuous data analyzed over 1-mile and 2-mile sectors, are included in the data.

In discussing service area, we will be concerned with expressing the percentage of locations one could expect to cover statistically at a predescribed distance. Thus, if one arbitrarily divides a 10-mile circle into 100 equal parts with each division represented by a point (location) and superimposes this configuration on the statistically derived landscape represented by the data, then 10 per cent coverage would mean that 10 of the points (locations) would receive satisfactory or better transmissions, while at the balance of the points reception would not be possible. Likewise, when considering 90 per cent coverage, 90 of the 100 points would receive transmissions while the balance would have no reception.

Actually, in dividing the circle into 100 locations, it was assumed that these locations represented the median value of signals in the immediate vicinity of the location, since one finds that in the immediate vicinity of a given location, say a few hundred feet, there will be fine variations in received field strength.

Terrain-Frequency, Distance Dependence

The theoretical plane earth field strength expression is given by

$$E = \frac{h_t h_r f}{95 d^2} \sqrt{P_t}$$

where

E = field intensity in microvolts per meter
h_t = transmitting antenna height in feet
h_r = receiving antenna height in feet
f = transmission frequency in megacycles
d = distance from transmitter in miles
P_t = effective radiated power in watts.

Eq. (1) is limited to those geographical areas which are similar to plane earth, such as relatively short overwater and very flat barren land paths. Even in these areas man has erected bridges, Texas towers, billboards, and so forth, which alter considerably the propagation characteristics as expressed by the theoretical plane earth formula.

While the theoretical received field strength increases with frequency, all other constraints being the same, it is important to note that the voltage across the input to a receiver will be the same at all frequencies when the receiving antenna is a half-wave dipole. However, if the antenna at the higher frequency is constructed so that it presents an effective area equal to that of the half-wave dipole at the lower frequency, then this increased field strength at the higher frequency will be realized as increased voltage at the input to the receiver.

The measured field strength data[1] over irregular terrain were compared with what one could expect over plane earth rather than curved earth, since the best median field strength data fit for distances up to 30 to 40 miles shows that the inverse distance squared trend for plane earth is better than the curved earth field, at least for low antenna heights. Beyond 30 miles to 40 miles the data are sufficiently meager as to be unworthy of analysis as a representive quantity of data. Therefore, the median field at a given frequency can be described by the theoretical plane earth field intensity, less the median deviation therefrom. This median deviation data from the theoretical plane earth field, called terrain factor, is shown in Fig. 1. The straight line on this figure very nearly passes through all the FCC data, and it will be noted that the deviation from the plane earth field strength varies inversely with the frequency and is independent of distance. The intersection of this line with the theoretical plane earth field strength is at 40 mc, so that the variation with frequency is with respect to this frequency.

With this statistical information, (1) becomes empirically for the median field at the 50 percentile locations, E_{50}, independent of frequency

$$E_{50} = \frac{40 h_t h_r}{95 d^2} \sqrt{P_t} \tag{2}$$

This E_{50} field strength may be obtained quickly from the nomograph, Fig. 2.

The theoretical plane earth received power between half-wave dipoles (3) is independent of frequency.

$$P_r = 0.345 \left(\frac{h_t h_r}{d^2} \right)^2 P_t \times 10^{-14}. \tag{3}$$

Making use of the power law variation with frequency for the median deviation from the theoretical plane

[1] H. Fine, "UHF Propagation Within Line of Sight," FCC, TRR Rep. No. 2.4.12; June 1, 1951. Contains material taken from K. A. Norton, M. Schulkin, and R. S. Kirby, "Ground Wave Propagation Over Irregular Terrain at Frequencies Above 50 MC," Ref. C, Rep. of the Ad Hoc Committee of the FCC for the Evaluation of the Radio Propagation Factors Concerning the Television and Frequency Modulation Broadcasting Services in the Frequency Range Between 50 and 250 MC; June 6, 1949.

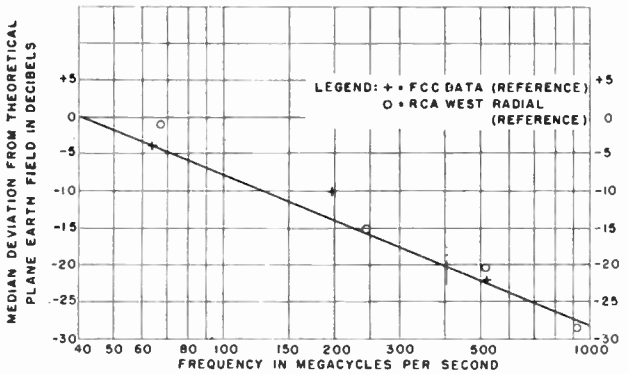

Fig. 1—Median terrain factor for fixed-to-vehicular or mobile service.

earth field, Fig. 1, (3) becomes empirically,

$$P_{50} = 0.345\left(\frac{h_t h_r}{d^2}\right)^2\left(\frac{40}{f}\right)^2 P_t \times 10^{-14}. \qquad (4)$$

Eqs. (2) and (4) show that nature, by interposing terrain features, has essentially placed in juxtaposition the frequency dependence of the field strength and received power above 40 mc over plane earth. Thus, while the theoretical received field strength over plane earth increases with frequency, the median received field intensity above 40 mc over irregular terrain is independent of frequency, and while the theoretical received power between half-wave dipole antennas is independent of frequency, over irregular terrain the median received power above 40 mc varies inversely as the frequency squared.

For the purpose of the systems engineer, in making irregular terrain calculations it is preferable to use the plane earth received power (3) shown in nomographic form in Fig. 2, in its theoretical form because field strength, median value statistically derived, and received power theoretically derived are, at this point of exploration of irregular terrain propagation, independent of frequency.

It is interesting to note that if one determines from diffraction theory the depth of hills[2] which will result in the median loss of Fig. 1, the statistical irregular terrain can be conceived as hills with a depth of about 500 feet. It is also interesting to note that the New York west radial terrain over which data are available[3] has an irregular depression of about 500 feet, 12 miles in extent and distance from the transmitter. Most of the data were accumulated in this portion of the radial, and the median values below plane earth theory are shown in Fig. 1 as the composite for the entire radial.

At this point in the paper it will be well to assume a rather simple problem and use it as a means of exemplifying the development of the material to be presented.

[2] K. Bullington, "Radio propagation variations at vhf and uhf," PROC. IRE, vol. 38, pp. 27–32; January, 1950.

[3] G. G. Brown, J. Epstein, and D. W. Peterson, "Comparative propagation measurements; television transmitters at 67.25, 288, 510 and 910 megacycles," *RCA Rev.*, vol. 9, pp. 171–201; June, 1948.

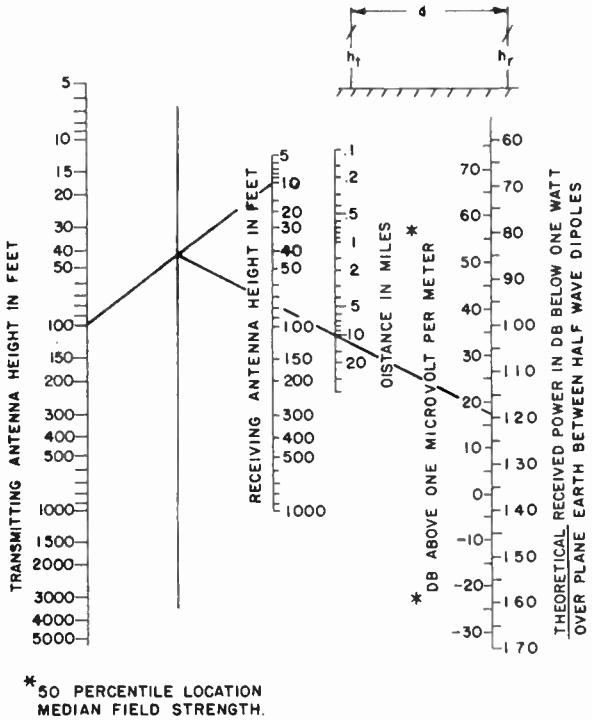

Fig. 2—Received power over plane earth and 50 per cent location median field strength—one watt radiated.

Assume:

Transmission frequency, 150 mc
Dipole antennas, half-wave
Transmitting antenna height, 100 feet
Receiving antenna height, 10 feet
Service range, 10 miles
Service to 90 per cent of locations at 10 miles
50 kc IF bandwidth
Suburban noise
No transmission line losses.

Required: Transmitter power output.

The theoretical received power in db below one watt will be from Fig. 2, 119 dbw. The field strength at 50 per cent of the locations, Fig. 2, will be 17.5 db above one microvolt per meter, one watt radiated.

Terrain-Frequency Dependence

If one explores the data[1] in terms of the distribution of received field strength over irregular terrain, one finds that the over-all terrain distribution when plotted in decibels above the theoretical plane earth attenuation, is log-normally distributed. Thus, on probability paper, the terrain distribution will appear linear and may be described by its median value and standard deviation, Fig. 3. The terrain distribution of field intensity in the vhf band, taken at a center frequency of 127.5 mc appears to have an over-all standard deviation of 8.3 db, while the terrain distribution of field intensity in the uhf region centered around 510 mc, appears to have an over-all standard deviation of 11.6 db. Of course, the median deviation from theoretical plane earth field is

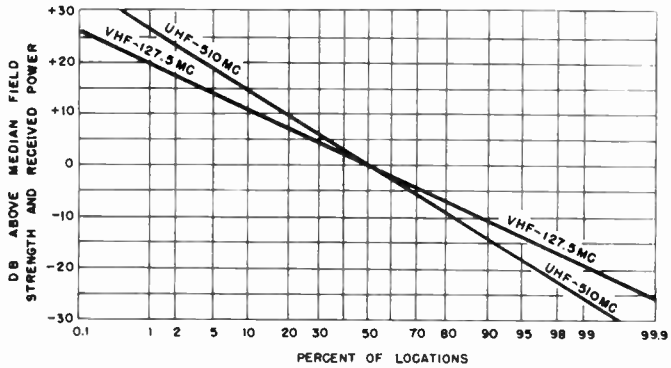

Fig. 3—VHF and uhf terrain distribution.

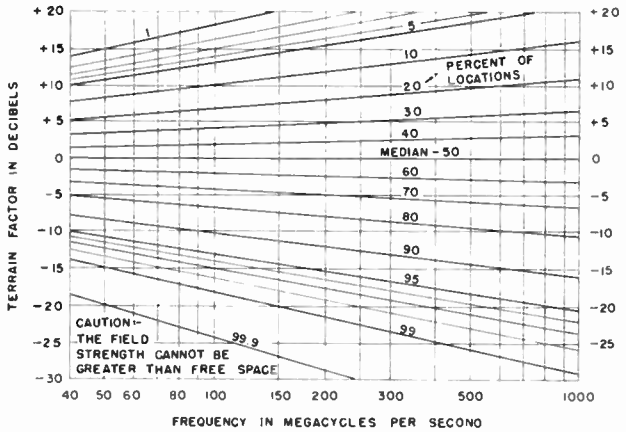

Fig. 4—Fixed-to-vehicular or mobile service field strength terrain factor.

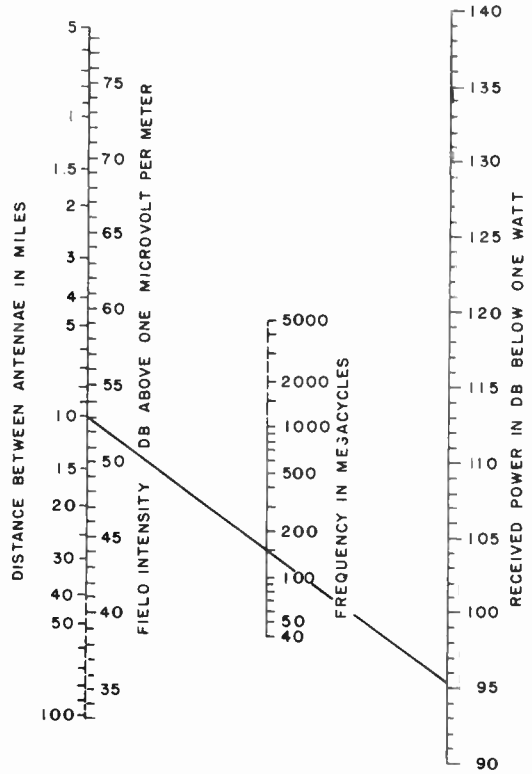

Fig. 5—Free space—one watt radiated between half-wave dipoles.

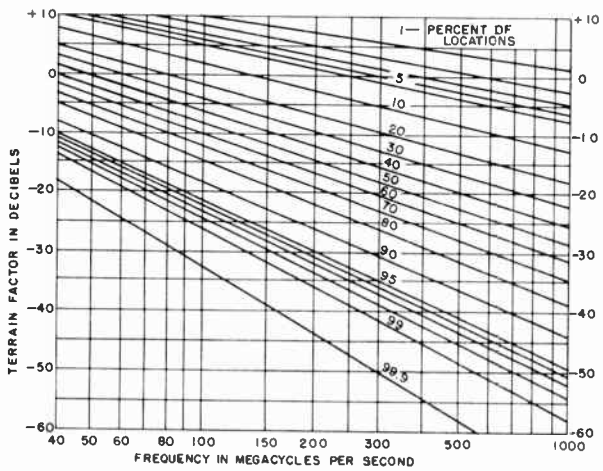

Fig. 6—Received power terrain factor for fixed-to-vehicular or mobile service.

displaced 12 db by the terrain factor for the two frequencies, Fig. 1. From this standard deviation data, Fig. 4 has been prepared which permits the determination of the correction factor to the E_{50} field strength when the received field strength to other than the 50 percentile location is desired. For example, as previously determined, E_{50} was 17.5 db above one microvolt per meter. Applying the terrain correction factor of -11.5 db for the 90 percentile location results in a median received field strength at the 90 percentile location of 6 db above one microvolt per meter, one watt radiated. This value of field strength does not exceed the free space value for 10 miles of 53 db above one microvolt per meter obtained from Fig. 5. Under conditions of greatly increased antenna heights and/or service to a small percentile of locations, the calculated field strength could exceed the free space field. If such is the case, the free space field should be used. It is interesting to note that while the median field strength (2) and terrain factor for 50 per cent of the locations (Fig. 4), are independent of frequency, for percentages of locations less than 50, the field strength increases with frequency, and for $E_{2.3}$ the field strength varies as $f^{1/2}$. Likewise for percentages of locations greater than 50, the field strength decreases with frequency and for $E_{97.7}$ varies inversely as $f^{1/2}$.

Likewise, Fig. 6 has been prepared to reflect the correction factor to the theoretical plane earth received power imposed by irregular terrain. The P_{50} value follows an inverse frequency squared relation as per (4), at $P_{97.7}$ an inverse frequency cubed relation, and at $P_{2.3}$ an inverse frequency relation. As previously determined, the theoretical received power is -119 dbw. The terrain correction factor for the 90 percentile location at 150 mc is -23 db, and the received power at this location will be -142 dbw, or the half-wave dipole-to-half-wave-dipole path attenuation for this degree of service is 142 db. The free space received power is -95.4 dbw from Fig. 3 which exceeds that for the 90 percentile location.

Terrain-Transmitting Antenna Height Dependence

The transmitting antenna height, used in conjunction with the data[1] is defined as the height above the median, 2–10 mile terrain level. This rule has not proven as reliable as one might expect, since it does not take into account the terrain within 2 miles or beyond 10 miles. For purposes of this report the effective height of the antenna will be the height of the antenna above plane earth. In actual practice the transmitting antenna heights could be taken as the effective height above local terrain. For all practical purposes, the data confirmed that the received field strength increased linearly with transmitting antenna height. Transmitter height-gain tests made around the New York area[4] seem to indicate that in poor service locations the effect of transmitting antenna height increase is somewhat less than one would theoretically predict. In median or 50 percentile locations the height gain would approximate the theoretical expected height gain, and for good service locations the height gain would be somewhat more than the theoretical. For purposes of this paper, the formulas and nomographs reflect a linear high gain for transmitting antenna height.

Terrain-Receiving Antenna Height Dependence

Receiving antenna height is the effective height above local terrain. The data do not appear to support any clear-cut variation of field strength with change in receiving antenna height. For receiving antennas which clear surrounding terrain features, the height gain appears to be linear. For receiving antennas which do not clear the surrounding terrain features, no orderly pattern is discernible. However, test results analyzed statistically,[1] show that in the 6 to 30 feet category, the field strength appears to support a square-root height gain variation. Above 30 feet, the height gain is linear. This variation is reflected in the nomograph of Fig. 2.

In practice, when using low antenna heights, as pointed out in the New York tests,[4] the dependence of field strength upon receiving antenna height is quite variable. When locating in a given area, within the confines of available antenna height, the maximum field strength should be found.

Terrain Fading

Both the vhf and uhf studies indicate that the time fading is much smaller for the distances involved than the terrain variation, and may be neglected as a power balance factor in equipment design. In the fear of being misunderstood, suppose equipment is designed for vehicular operation to cover 90 per cent of the locations, at 10 miles from the transmitter. Based on statistical terrain data, the variation in median signal throughout the terrain is far in excess of what the long-time fading would be between two fixed locations. However, fading becomes important for fixed service work. A subscriber land-based for an extended period of time in a poor location, marginal signal, might well compensate for the long-time fading which will ensue by moving to the optimum spot in the small area in which he is to be located, and also by having means for elevating his antenna, which can now be changed to a directional antenna, to the optimum height within the height-raising capability of his antenna system. These two expedients should compensate for time fading and be reflected in a highly reliable transmission circuit.

Terrain-Antenna Polarization

Theoretically, over plane earth at antenna heights greater than a wavelength and for small angles between the direct and reflected rays, as is the case for irregular terrain transmissions, polarization has negligible effect on the behavior of radio waves above 40 mc. Experimental evidence[5,6] over irregular terrain of the received characteristics of polarized waves appears in general to verify the above. While it appears that vertical polarization is somewhat better directly behind hills or deep in the shadow area, horizontally polarized waves afford better reception in back of, but away from, the deep shadows of hills. In wooded areas, the attenuation is less for horizontally polarized transmissions than for vertically polarized transmissions below 300 to 500 mc. In total, little difference can be detected in the average propagation characteristics.

There is one exception to the latter statement and it concerns propagation using antenna heights less than one wavelength. In this case the ground wave is dominant and theoretically vertical polarization provides an apparent height gain over horizontal polarization.[7] This effect is shown in Fig. 7 and pertains only to vertical polarization since for horizontal polarization the effective height is essentially the actual height at frequencies above 40 mc. As shown in Fig. 7, the effective height also depends on the conductivity of the soil over which the transmission will be effective. Unfortunately, as far as the author knows, terrain-statistical data are lacking on the propagation effects resulting from the use of very low vertically polarized antenna heights in the lower vhf region. Until such time as this theoretical information can be placed in dispute statistically by tests, it is

[4] J. Epstein and D. W. Peterson, "An experimental study of wave propagation at 850 mc," Proc. IRE, vol. 41, pp. 595–611; May, 1953.

[5] J. S. McPetrie and J. A. Saxton, "An experimental investigation of the propagation of radiation having wavelengths of 2 and 3 meters," *J. IEE*, vol. 87, pp. 146–153; August, 1940.

[6] J. A. Saxton and B. N. Harden, "Ground-wave field-strength surveys at 100 and 600 mc/s," *Proc. IEE*, vol. 101, part 3, pp. 215–221; July, 1954.

[7] K. Bullington, "Radio propagation at frequencies above 30 megacycles," Proc. IRE, vol. 35, pp. 1122–1136; October, 1947.

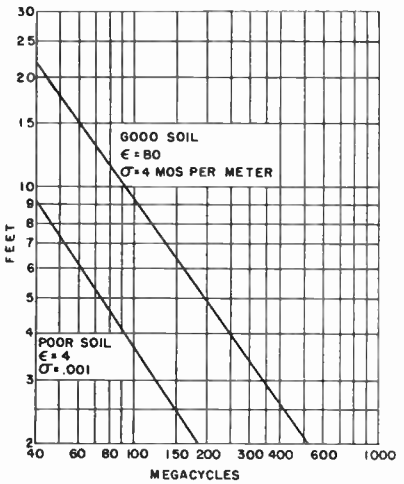

Fig. 7—Minimum effective antenna height for vertical polarization.

proposed that when vertically polarized transmissions are under consideration, Fig. 7 be used in finalizing the effective height of low antennas.

In our problem at 150 mc with an antenna height of 10 feet it can be seen from Fig. 7 that even with vertical polarization this height is also the effective height. If the problem had been one of transmission at 40 mc, then in using Fig. 2 the height would have remained the same for poor soil conditions, but would have to be taken as 23 feet over good soil conditions.

Terrain-Small Sector Field Strength Variation

As noted earlier, there is a fine amplitude variation about the median in a small distance or area which is independent of the distance from the radiation source. Some studies indicate that these fine variations of field strength have a normal distribution[1] which appears to be independent of frequency with a standard deviation of 5.5 db. Other studies,[8] indicate a Rayleigh distribution, Fig. 8. The latter appears more likely because the studies which indicate a normal distribution were taken over distances which perhaps exceeded the small sector variation. However the Rayleigh type fading may only occur and be applicable in areas replete with buildings, etc. In open areas the distribution may be log-normal over a small sector. Between the 10 and 90 per cent values of these distributions there is very little difference in the two distributions. The amplitude distribution is the same at all frequencies indicating that the range of constructive and destructive phase interference or standing wave effects is complete. However, the number of constructive and destructive interferences increases in a given distance or area with frequency.

Tests[9] conducted in the Phoenix, Ariz. area indicate that the average vehicle travel between these fine signal

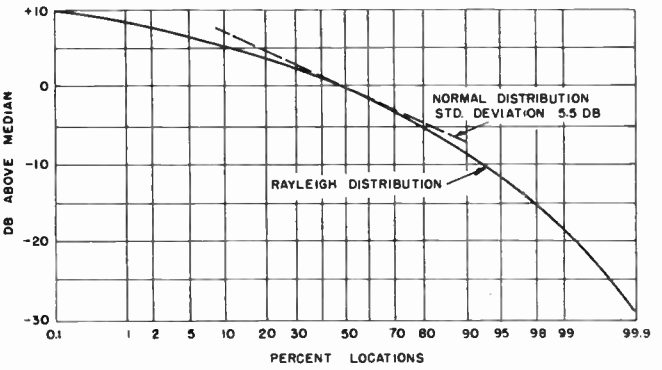

Fig. 8—Terrain-small sector variation.

minima is one wavelength in free space, while in the direction away from or toward the radiation, the distance between signal minima is the free space half-wave distance. With this information, in vehicular service the small sector amplitude fluctuations in received carrier level will increase in rapidity with frequency and the speed of the vehicle, or

$$A = \frac{v}{\lambda/2}, \text{ and in practical terms, } A = 0.003\,fv \quad (5)$$

where A is the average amplitude fluctuation rate in cps, f is the radio carrier frequency in mc, and v is the velocity of the vehicle in the direction of transmission in miles per hour. For ready use, (5) has been prepared in the form of a nomograph, Fig. 9. It shows, for example, that at 150 mc the received field in a vehicle traveling at 40 miles per hour in the direction of transmission would have an average fluctuation rate of 18 cps. For vehicular service, this is the rate which would have to be considered in the design of age circuitry with the audio or intelligence pass band designed above this frequency.

The small sector variations at 90 mc[10] appear to be small in open flat country and much greater in built-up areas as might be expected. The variations in built-up and treed areas appear greater for vertically polarized transmissions than for horizontally polarized transmissions.

Another characteristic of these variations which one would expect is that the higher the frequency, the steeper the fall and rise in field strength. In general, the variations appear to be deeper with the time between rise and fall smaller. Maximum envelopes occurring during a test[9] are shown in Fig. 10. At 15 db down, the "outage time" on 459 mc may be in the order of a few milliseconds at vehicle speeds of 40 miles per hour with perhaps no noticeable effect on speech transmissions, whereas at 156 mc the outage time at this level could cause the loss of voice information.

Unfortunately, data were not found which would permit an expression either quantitatively or qualitatively as to the useful distribution or design point criteria of

[8] W. R. Young, Jr., "Mobile radio transmission compared at 150 to 3700 mc," *Bell Sys. Tech. J.*, vol. 31, pp. 1068–1085; November, 1952.

[9] C. F. Meyer and D. Soule, "Field Strength Study," Motorola, Inc.; February, 1956. Work performed under Signal Corps Contract DA-36-039-sc-64737.

[10] H. L. Kirke, R. A. Rowden, and G. I. Ross, "A vhf field-strength survey on 90 mc/s," *Proc. IEE*, vol. 98, part 3, pp. 343–359; September, 1951.

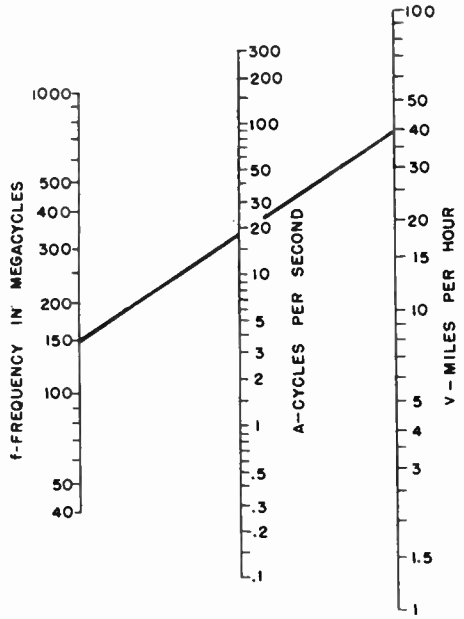

Fig. 9—Fluctuations in vehicles.

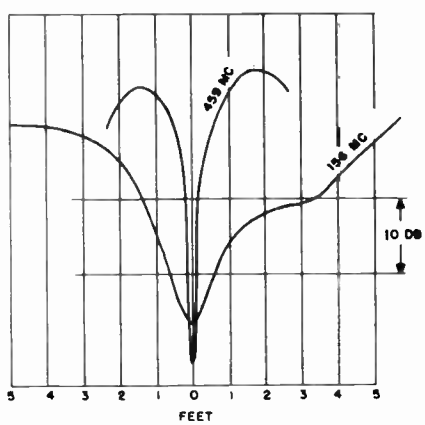

Fig. 10—Maximum small sector variation.

these small sector field strength variations. It may well be, at least for the present, that equipment should be designed to the median value of these find grain variations for the percentage of locations service desired.

Terrain-Wide Modulation Bandwidth Effects

The field strength variations discussed so far have been those taken over a very narrow bandwidth of the transmission frequency. On wide-band systems distortion effects may be introduced resulting from propagation via more than one path. These distortions may cause cross talk in multichannel voice systems, or shadows in television reception. This subject will be touched on lightly because not very much statistical data are available nor is literature available on the effects of multipath propagation on various types of modulation. The severity of multipath distortion[11] appears qualitatively to be independent of frequency and wave polarization, at least within the frequency range of 60 to 3300 mc. The consequences of multipath propagation are not serious for fixed transmission conditions, yet may be very serious in moving situations. For fixed service, movements of the receiving antenna either horizontally or vertically for a distance in the order of a few wavelengths ordinarily cleans up multipath distorted patterns in television reception. More multipath distortion appears in highly built-up and mountainous areas where large off-path reflecting surfaces are present. Directive antennas greatly reduce multipath effects,[11] which means that for equal antenna apertures, the use of the higher frequencies will result in less multipath distortion.

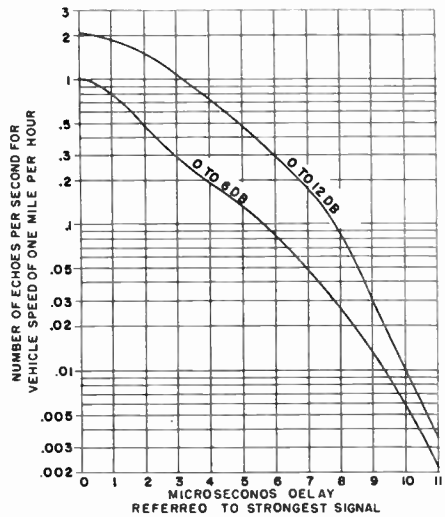

Fig. 11—Echoes in vehicles from a fixed transmission.

The only good statistical results, unfortunately unrelated to all of the terrain data made use of herein and therefore not representative of all the conditions on which this paper is based, are based on tests in the New York area,[12] where one encounters considerable, and perhaps the worst, multipath propagation conditions. In order to understand the difficulties one may encounter in engineering vehicular wide band systems, the New York data,[12] have been altered (Fig. 11) to reflect the number of echoes per second for a vehicle speed of one mile per hour vs delay of these echoes with amplitudes between 0 and 6 db less than the strongest received signal. Thus a remote television transmitter installed in a vehicle patroling New York at 30 miles per hour would present to the fixed television receiver a picture with thirty, 0- to 6-db echoes per second having $\frac{1}{4}$-μsec delay, 9 shadows per second having 3-μsec delay, and so forth. Besides this ghosting of the picture that is taking place, the synchronous circuit of the television receiver is in essence flip-flopping from the direct signal path amplitude to

[11] D. W. Peterson, "Army Television Problems Phase II Tasks 1 and 2 Final Report," January, 1956, RCA. Work performed under a Signal Corps Contract No. DA-36-039-sc-64438.

[12] W. R. Young, Jr. and L. Y. Lacy, "Echoes in transmission at 450 megacycles from land-to-car radio units," Proc. IRE, vol. 38, pp. 255–258; March, 1950.

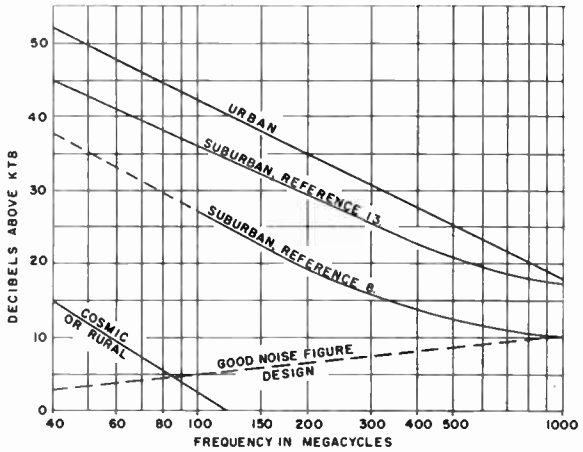

Fig. 12—Median indigenous noise.

the multipath signal amplitude when the ghost signal is the stronger of the two.

Indigenous Noise

While the relationship between received signal and frequency over irregular terrain has been covered pretty well, another important power balance factor in systems design is the establishment of the noise level of the receiver, or the signal required to assure satisfactory communication. Noise in the frequency range above 40 mc is mainly caused by man-made noise. The general classifications are rural, suburban or small town, and urban noise. Cosmic noise is still present up to 100 mc. Collectively this noise can be termed indigenous noise.

The extent to which this indigenous noise acts upon a receiver is shown in Fig. 12. Two curves have been drawn for suburban noise since the material for these curves have been drawn from two separate references.[8,12] The lower suburban noise curve is representative of the median indigenous noise experienced in areas suburban to New York, with extrapolated data shown by the dotted portion of the curve. The urban noise data taken from these same two references dovetailed into the same curve. The dotted curve represents the noise figure of a currently well-designed receiver and is shown only to give the figure perspective. The indigenous noise can be referenced with respect to the thermal noise, ktb, of a receiver and is shown in Fig. 12 as the correction factor which must be applied to ktb level, Fig. 13(b).

The difficulty in the use of these curves lies in just what level of noise should be applied in systems design work. Unfortunately indigenous noise data were not collected along with the field strength data. If this had been done a distribution of the magnitude of noise over the areas in which the field strength data were taken would have been available. It would appear that equipment designed for general use should at least consider the lower suburban curve of Fig. 11 with the thought that in urban areas advantage might be taken of the height-gain in these areas.

[13] Federal Telephone and Radio Corp., "Reference Data for Radio Engineers," 3rd ed., p. 442; 1949.

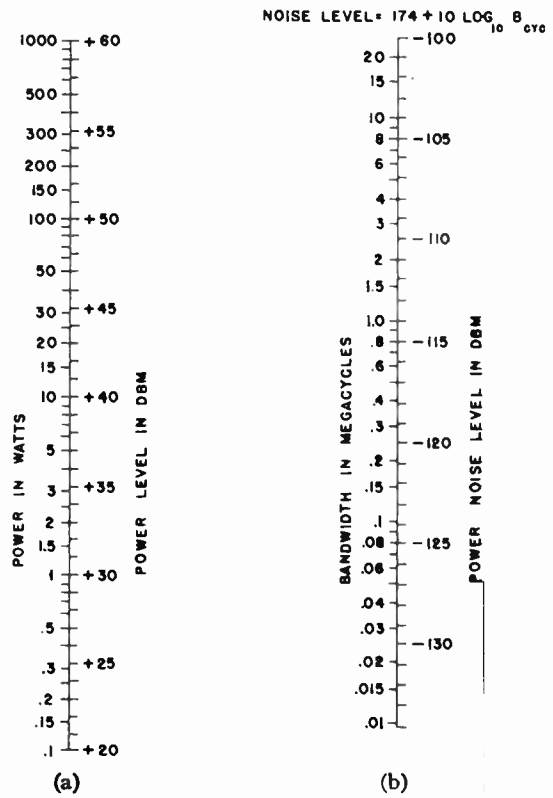

Fig. 13—(a) Conversion of power to dbm. (b) Conversion of bandwidth to thermal noise level.

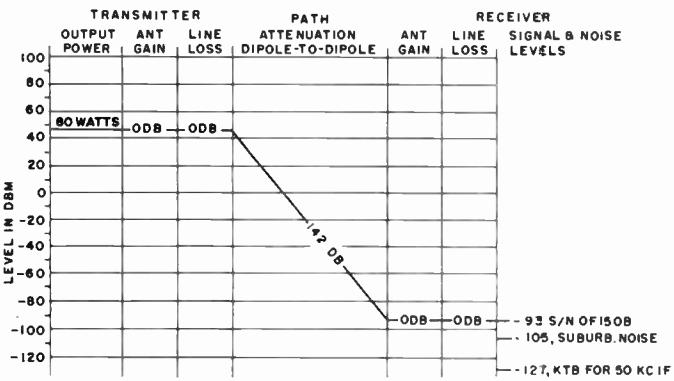

Fig. 14—Power level diagram.

Problem Solution

The entire problem is reviewed in Fig. 14 in the form of a power level diagram. Working the level diagram from the ktb level of −127 dbm obtained from Fig. 13(b), for a 50 kc IF, suburban noise and not noise figure plus approximately 12 db, establishes the lowest rf signal, −93 dbm, for an acceptable signal-to-noise ratio. Assuming no transmission line losses to the two dipole antennas and with the path attenuation loss over 10 miles of irregular terrain to the 90 percentile location of 142 db, one arrives at a required transmitter power of 49 dbm or 80 watts, Fig. 13(a).

Vehicular-to-Vehicular Transmissions

The entire discussion thus far has dealt with the subject of fixed-to-vehicular, or fixed-to-mobile transmissions over irregular terrain. It is in these subjects that data exist, while in the field of vehicular-to-vehicular transmission good statistical data are nonexistent, at least to the knowledge of the writer.

If one makes the reasonable assumption that the terrain factor will not change whether we deal with the moving-to-moving, fixed-to-fixed, or fixed-to-moving situations, then the median signal received by a vehicle in motion from another vehicle in motion is precisely that given in Fig. 4. However, by statistical theory,[14] it would appear that the standard deviation would be the square root of the sum of the variances of two fixed-to-moving distributions which in this type of transmission can be considered of the same magnitude. Thus the standard deviation for vehicular-to-vehicular transmission is the $\sqrt{2}$ times the standard deviation for the fixed-to-vehicular transmission. This is in essence the correction factor which must be applied to Fig. 6, in order to obtain the vehicular-to-vehicular received power terrain factor shown in Fig. 15. If the given problem were a vehicular-to-vehicular system, fictitiously assuming antenna heights were maintained for this service, the path attenuation at 10 miles to the 90 percentile location would be 119 db, from Fig. 2, plus 32.5 db, from Fig. 15, or 151.5 db compared to a path attenuation of 142 db derived earlier in this paper for the fixed-to-vehicular or mobile transmission. The transmitter power level of 49 dbm, on Fig. 14, must be raised to 58.5 dbm or 700 watts for vehicular-to-vehicular equivalent service.

Remarks

The statistical method of handling propagation over irregular terrain can be used in frequency assignment studies to determine the number of rf channels which should be designed into equipment for cochannel and adjacent channel field service. It has important usage in vulnerability studies of mutual interference, intentional and unintentional jamming, and countermeasures. It also appears to have application in spectrum allocation studies.

Of course the burning question of how well a particular piece of equipment will act in a given environment is difficult to answer. If the terrain is less irregular than the statistical irregular terrain, then better than predicted performance should result. On the other hand, in terrain more irregular than the statistical, a poorer performance should result. However, field operational procedures should be developed which permit a rapid evaluation of the service coverage from a given location. A possible technique for rapid evaluation is one based on a system utilizing the "ground clutter" pattern seen on the radar (PPI) scope.[15]

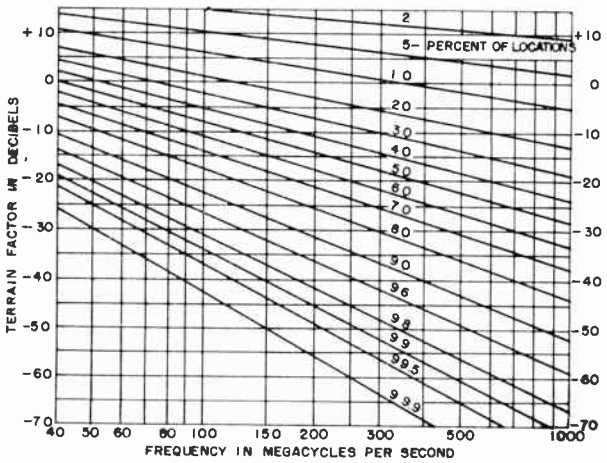

Fig. 15—Vehicular-to-vehicular received power terrain factor.

Conclusion

This paper is considered a modest start in the direction of supplying irregular terrain propagation information applicable to systems engineering. The author encourages constructive criticism or the supply of data which may be beneficial for deriving better statistical data. For example, much data are required on frequencies above 1000 mc; the nature of the fine variations and their effects upon types of modulation; propagation data on vehicular-to-vehicular transmissions; good statistical small sector variation data; and so forth.

Acknowledgment

The author wishes to express his gratitude to all those referenced authors who have made this paper possible by their efforts in collecting propagation data.

[14] A. Hald, "Statistical Theory with Engineering Applications," John Wiley and Sons, New York, N. Y.; 1952.

[15] R. E. Lacy and C. E. Sharp, "Radar-type propagation survey experiments for communication systems," 1956 IRE Convention Record, part 1, pp. 20–27.

Design Theory for Depletion Layer Transistors*

WOLFGANG W. GÄRTNER†, MEMBER, IRE

Summary—**A new class of high-frequency transistors, the Depletion Layer Transistors (DLT), utilizes maximum attainable carrier velocities in solids by injecting electrons or holes into the high electric fields that prevail in properly designed depletion layers of reverse-biased *p-n* junctions. The resulting short transit times should insure operation up to microwave frequencies.**

The design theory is presented for a particular example of a depletion layer transistor, discussing its low- and high-frequency, small-signal behavior, power gain, and stability. Other conceivable structures and modes of operation for DLT's are described and the potential importance of the depletion layer principle for solid-state microwave amplification is emphasized.

I. Introduction

CLASSICAL transistors are limited in their frequency response by either or both of two factors: the carrier transit time from the emitter to the collector junction, and the $r_b'C_c$ product. Various advances in technology during the past few years have greatly reduced these two quantities, resulting in correspondingly higher operating frequencies. Further improvements, however, have become increasingly difficult, which led to the search for new principles that would obviate some of the basic limitations inherent in classical transistors. In a high-frequency transistor, the carrier transit time through the structure must be short compared to the reciprocal operating frequency, and no appreciable debunching of carrier pulses must occur during the transport process. The first requirement asks for high carrier velocity; *i.e.*, high electric fields and, similarly, the second requirement may also be satisfied if the carriers travel in strong external fields compared to which the influence of diffusion and the carriers' own space charge is negligible. This concept forms the basic principle of a new class of high-frequency transistors known as Depletion Layer Transistors (DLT), which have recently been announced.[1–4] Proper design of these devices will also keep internal RC combinations at very low values and operating frequencies up to the microwave range have been predicted.

* Original manuscript received by the IRE, January 11, 1957; revised manuscript received July 1, 1957. A more detailed account of the design theory for depletion layer transistors is contained in USASEL Tech. Memo. No. M-1849; October, 1957.

† U. S. Army Signal Eng. Labs., Fort Monmouth, N. J.

[1] W. Gärtner, "A new uhf transistor structure," paper presented at WESCON Convention, Los Angeles, Calif.; August 21–24, 1956.

[2] W. Gärtner, F. A. Brand, and W. G. Matthei, "Design theory and exploratory development of the depletion layer transistor," paper presented at the PGED Second Annual Technical Meeting, Washington, D. C.; October, 1956.

[3] W. Gärtner, "Transistor physics," paper delivered before the Austrian Chem. and Phys. Soc., Vienna; January, 1957.

[4] W. Gärtner, "Transit time effects in depletion layer transistors," paper presented at the Symposium on the Role of Solid State Phenomena in Electric Circuits, Polytech. Inst., Brooklyn, Brooklyn, N. Y.; April, 1957.

II. Basic Principle of the DLT

Very high electric fields may be created in the depletion layer (DL) of a reverse biased p-n junction, and when carriers are injected directly into this region, their transit time from the emitter to the collector side of the DL is very short (see Fig. 1). In fact, in properly designed depletion layers, carriers will reach the maximum velocity they can attain in solids under any conditions. If a design around this basic principle can be found with small-signal parameters that will give power gain, a response up to very high frequencies, possibly microwave, should be insured.

In the following five sections the design theory for a typical example of a depletion layer transistor is worked out in detail. Other conceivable realizations are discussed in Section VIII.

III. Structural Models, Basic Equations, and Small-Signal Solutions

The derivation of the dc and ac current-voltage relationships will be carried out for the geometry and type of operation shown in Fig. 2. The analysis is one dimensional. It is expected to describe the essentials of operation although some of the proposed structures (see Fig. 3) may differ from this simple model. Emission into the depletion layer is assumed to occur from the "virtual emitter plane" indicated by a dashed line in Fig. 2; it may be realized physically by any kind of contact with the general characteristics described below. The current flow through the model structure is indicated in Fig. 4. The collector side has been assumed to be *n* type so that the active conduction current is carried by electrons which generally have a higher mobility and higher maximum velocity than holes. All of the following derivations are carried out for these doping conditions, and the results may be easily converted to the case of a *p*-type collector and holes as the active charge carriers.

The symbols in Fig. 4 have the following meanings: I_{1n} is the electron current flowing from emitter to collector, I_{1p} denotes the hole current flowing from emitter to base, I_{rev} is the current through the reverse biased *p-n* junction under zero emitter current conditions. In determining the dependence of these currents on the input and output voltages, V_1 and V_2, we assume that small ac voltages, v_1 and v_2, are superimposed on the dc voltages, V_{10} and V_{20}. The customary small-signal series expansion then yields for the emitter conduction current

$$I_{1,\text{cond}} = I_{1no} + i_{1n} + I_{1po} + i_{1p}$$
$$= I_{1no} + \eta_{n1}v_1 + \eta_{n2}v_2 + I_{1po} + \eta_{p1}v_1 + \eta_{2p\,2}v \quad (1)$$

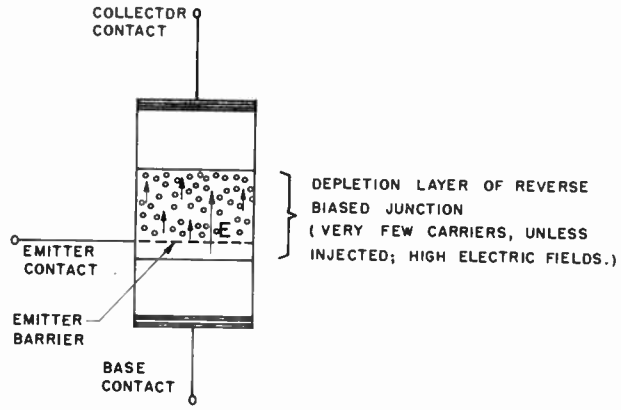

Fig. 1—Carriers injected directly into the depletion layer of a reverse biased p-n junction are swept towards the collector at high velocities.

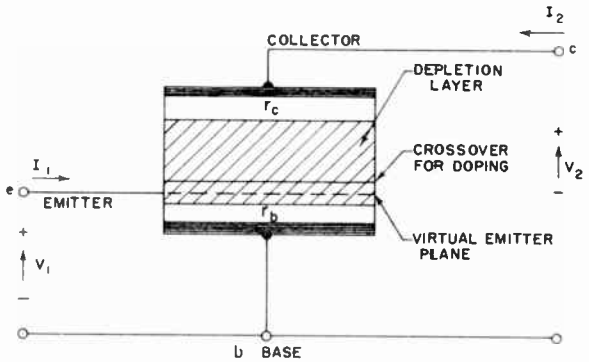

Fig. 2—One-dimensional model for geometrical structure of depletion layer transistor.

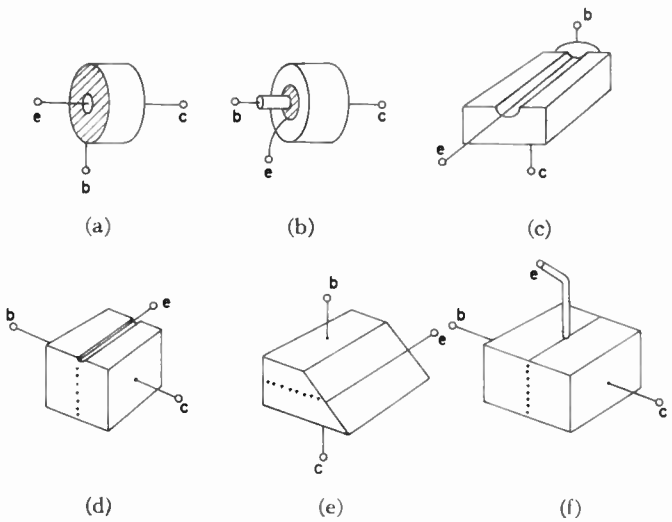

Fig. 3—Conceivable structures for depletion layer transistors (e, emitter; b, base; c, collector).

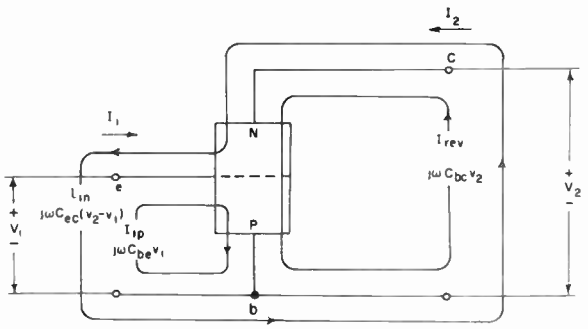

Fig. 4—Current flow through depletion layer transistor with p-type base and n-type collector.

where

$$\eta_{i1} = (\partial I_{1i}/\partial V_1)_{V_2=\text{const}}; \quad \eta_{i2} = (\partial I_{1i}/\partial V_2)_{V_1=\text{const}}$$

and the other symbols have the meanings indicated in the list of symbols at the end of this paper.

Under the assumption that the transit time from emitter to collector is negligible at the frequencies considered, and that no recombination takes place between emitter and collector,[5] the collector conduction current is the sum of the (voltage independent) junction reverse current, I_{co}, and the injected electron current, $I_{1no}+i_{1n}$,

$$-I_{2,\text{cond}} = I_{co} + I_{1no} + \eta_{n1}v_1 + \eta_{n2}v_2. \tag{2}$$

The input and output conduction currents are thus essentially determined by the dependence of the emitter injection current, $I_{1,\text{cond}}$, on the input and output voltages, V_1 and V_2. For a mathematical description of the injection process and an evaluation of the η, another more specific assumption about the mechanism of carrier emission into the depletion layer must be made.

The simplest possibility—supported by experimental evidence—is that a barrier (this loose term is used deliberately here because considerably more work is required to understand the physics of such contacts) exists between the emitter contact and the semiconductor material immediately underneath the contact, such that the emitter conduction current is given by

$$I_{1,\text{cond}} = I_{1n}(V_B) + I_{1p}(V_B) \simeq I_{1n}(V_{Bo}) + I_{1p}(V_{Bo}) + [(\partial I_{1n}/\partial V_B) + (\partial I_{1p}/\partial V_B)]v_B \tag{3}$$

where $V_{Bo} = V_{1o} - V_{so}$ and $v_B = v_1 - v_s$.

V_{so} and v_s are the dc and ac components, respectively, of the almost undisturbed[6] potential in the semiconductor underneath the emitter contact. This means that the magnitude of the injected emitter current depends solely on the potential difference, V_B, between the emitter contact and the point in the depletion region immediately underneath it. As an example, we may consider an exponential characteristic,[1] $I_{1n}(V_B) = A_0[\exp(\alpha V_B) - a]$ from which $(\partial I_{1n}/\partial V_B) = \alpha A_0 \exp(\alpha V_{Bo})$. The following derivations, however, do not depend on the specific nature of this emission function. The potential, $V_s = V_{so} + v_s$, underneath the emitter contact is a certain fraction of the output voltage,

[5] See in this connection C.-T. Sah, R. N. Noyce, and W. Shockley, "Carrier generation and recombination in p-n junctions and p-n junction characteristics," PROC. IRE, vol. 45, pp. 1228–1243, September, 1957.

[6] G. L. Pearson, W. T. Read, W. Shockley, "Probing the space charge layer in a p-n junction," *Phys. Rev.*, vol. 85, p. 1055; March 15, 1952.

$$V_{s0} = \kappa_0(x) \times V_{2e} \quad \text{and} \quad v_s = \kappa_1(x, V_{2e}) \times v_2, \tag{4}$$

the magnitude of which is determined by the impurity distribution across the junction, the position, x, of the emitter contact, and the applied dc bias.

In particular, the ac collector voltage feedback ratio, κ_1, is equal to $(\partial\psi/\partial V_2)_{V_{2e}}$, where $\psi(x)$ denotes the electrostatic potential across the depletion layer which may be calculated if the impurity distribution and applied dc voltage are known. Gain considerations, which will be discussed later, indicate that the voltage feedback ratio, κ_1, should be as small as possible and straightforward calculations on step junctions, graded junctions, $p\pi n$, $p\nu n$, and p-i-n junctions show that κ_1 becomes smaller the closer the emitter contact can be placed to the base end of the depletion layer (and still be inside).

If we now substitute back into the original (1) and (2), we obtain for the conduction currents

$$I_{1,\text{cond}} \simeq I_{1n0} + I_{1p0} + (\partial I_{1n}/\partial V_B)(v_1 - \kappa_1 v_2) + (\partial I_{1p}/\partial V_B)(v_1 - \kappa_1 v_2) \tag{5}$$

and

$$-I_{2,\text{cond}} \simeq I_{c0} + I_{1n0} + (\partial I_{1n}/\partial V_B)(v_1 - \kappa_1 v_2). \tag{6}$$

In addition to these conduction currents, displacement currents will flow through the structure. Between any two contacts there will exist a capacitance $C(V)$ which, in general, depends on the applied voltage, $V = V_0 + v$, but which may be assumed to be constant in a small-signal theory. The permissible values for the capacitances are determined by the desired gain and frequency response which will be discussed later. In view of the many conceivable geometries, the actual values of these capacitances shall not be calculated here, and we add a current $j\omega C_{ec}(v_1 - v_2) + j\omega C_{eb}v_1$ to the emitter conduction current and $j\omega C_{ec}(v_2 - v_1) + j\omega C_{bc}v_2$ to the collector conduction current where C_{ec}, C_{eb}, and C_{bc} are the (ac-voltage independent) capacitances between emitter and collector, emitter and base, and base and collector leads, respectively.

Thus with (5) and (6) we find for the small-signal, four-pole admittances

$$y_{11} = \partial I_1/\partial V_B + j\omega(C_{eb} + C_{ec}), \tag{7a}$$

$$y_{12} = -\kappa_1(\partial I_1/\partial V_B) - j\omega C_{ec}, \tag{7b}$$

$$y_{21} = -\partial I_{1n}/\partial V_B - j\omega C_{ec}, \tag{7c}$$

$$y_{22} = \kappa_1(\partial I_{1n}/\partial V_B) + j\omega(C_{cb} + C_{ec}). \tag{7d}$$

An equivalent circuit for the "intrinsic" device as characterized by (7) is shown in Fig. 5. The emitter and the collector branch each contain a current source as indicated.

The currents through the device will be somewhat modified by the impedances of the bulk material on both sides of the junction, r_b (base series impedance), and r_c (collector series impedance) and by the leakage conductance, g_s, across the junction. These, however,

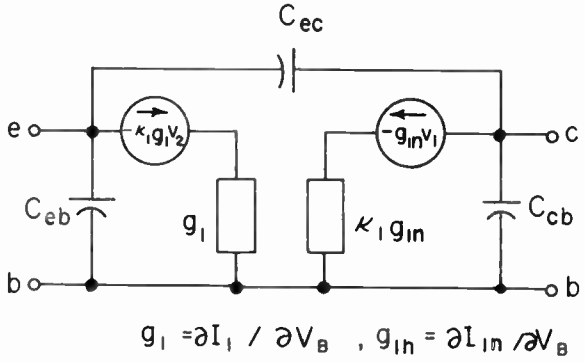

Fig. 5—Equivalent circuit for "intrinsic" DLT in common base configuration.

may easily be taken into account by simple four-pole transformations (a situation similar to the inclusion of the base spreading resistance in ordinary transistors). For optimum performance, all these quantities should be kept small.

Eq. (7) shows that the magnitude of the small-signal, four-pole admittance depends on the capacitances between the contacts, on the nature of the emission function (for which an exponential behavior was given above as an example), on the emitter efficiency; *i.e.*, on the fraction of total emitter current carried by electrons, and finally on the ac voltage feedback ratio, κ_1. In particular, the output admittance, y_{22} is by a factor κ_1 (for negligible capacitance effects) smaller than the input admittance (since $\kappa_1 \leq 1$ always), and the ratio between them is the source of ac power gain in this device which, without carrier multiplication, has a current gain of not more than unity.

The exact dependence of power gain on these various quantities is analyzed in Section VII.

IV. Calculation of Transit Time

To determine whether the assumption of negligible transit time, τ, from emitter to collector is justified at the frequency of operation or whether a more elaborate theory should be used, a calculation of the transit time

$$\tau = \int_{x_e}^{x_c} \frac{dx}{u} \tag{8}$$

must be carried out, where x_e and x_c are the coordinates of the emitter and collector, respectively, and $u(x)$ is the carrier velocity the field dependence of which has been investigated by Ryder, *et al.*[7] At low fields the velocity is proportional to the electric field, at higher fields it is proportional to only $E^{1/2}$, and finally it reaches

[7] E. J. Ryder and W. Shockley, "Mobilities of electrons in high electric fields," *Phys. Rev.*, vol. 81, p. 139; January, 1951.
W. Shockley, "Hot electrons in germanium and Ohm's law," *Bell Sys. Tech. J.*, vol. 30, p. 990; October, 1951.
E. J. Ryder, "Mobility of holes and electrons in high electric fields," *Phys. Rev.*, vol. 90, p. 766; June, 1953.
E. M. Conwell, "High field mobility in germanium with impurity scattering dominant," *Phys. Rev.*, vol. 90, p. 764; June, 1953, and "Mobility in high electric fields," *Phys. Rev.*, vol. 88, p. 1379; December, 1952.

ness. Emitter contacts with essentially unit efficiency can be made.[2,14] Thus for a depletion layer thickness of 3×10^{-3} cm in germanium and an optimum transit time (p-i-n junction) of 5×10^{-10} second, a κ_1 of 0.05 (location of effective emitter contact within 1.5×10^{-4} cm of base end of DL), an emitter-collector capacitance, C_{cc} of 0.1 $\mu\mu$f, and a value of g_1 of 10^{-2} mho, one finds from (14) a power gain of 10 db at 1000 mc/seconds. With the advent of more refined techniques which allow a closer control of small dimensions, an improvement in the maximum frequency of DLT's with negligible transit time may be expected. Similarly, if other semiconductors are found which have a higher maximum carrier velocity (this property has so far only been investigated in germanium and silicon) higher frequency cutoff will result.

If we consider the case of controlled carrier multiplication, we obtain with (10)

$$\frac{N_L}{N_i} = \frac{m^2 g_{1n}^2 + \omega^2 C_{cc}^2}{2\kappa_i m g_1 g_{1n} + 2\omega^2 C_{cc}^2 - 4g_1(I_{co} + I_{1no})(\partial m/\partial V_2)}. \quad (15)$$

Neglecting capacitances and the last term in the denominator, we find that the power gain will increase by a factor of m. In addition, because of the reduction in output impedance, the capacitances become less critical. Similarly, and maybe most important at the present time, κ_1; *i.e.*, the position of the emitter contact, is no longer the major gain-determining factor. In other words, the emitter contact may be anywhere in the depletion layer as long as only few carriers return to it (which must be avoided by proper structures or magnetic fields[10]) and a power gain of at least a value of m may be realized as long as capacitances and the ac modulation of the dc current through the junction are negligible. With these relaxed requirements on geometrical control in the structure, substantial power gains in the 10,000 mc range appear feasible because it is possible with existing techniques to locate a contact somewhere inside a 1μ depletion layer which possesses a transit time of the order of 2×10^{-11} seconds under optimized conditions (p-i-n junction). The upper limit on the permissible multiplication factor is imposed by the condition that the space charge of the mobile carriers must remain negligible in the depletion layer. Internal RC combinations which also limit the frequency response of classical transistors can be kept negligibly small by reducing the series resistance of the bulk material on either side of the depletion layer.

We have thus shown that on the basis of designs with negligible transit time, power gain up to the microwave region is possible. Other potential applications of the device include uhf and microwave oscillators and extremely fast switches. We now want to investigate the frequency dependence of power gain when the transit time becomes comparable to one period. Substituting (11) into (13), one obtains under the assumption of $\varphi\simeq1$ and $w_2\simeq w$

$$\frac{N_L}{N_i} = \frac{-g_{1n}^2\,|\,(e^{-j\omega\tau}-1)/(j\omega\tau)\,|^2}{(w_1/w)g_{1n}^2[4 - 2(\sin\omega\tau)/(\omega\tau)]}. \quad (16)$$

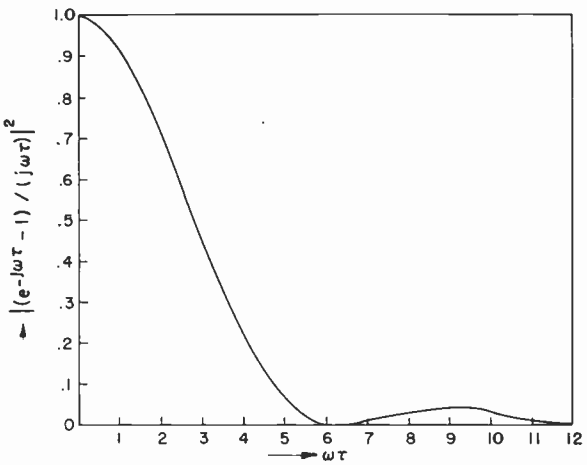

Fig. 8—The function $|(e^{-j\omega\tau}-1)/(j\omega\tau)|^2$ plotted vs $\omega\tau$.

Eq. (16) shows that even when the capacitances may be neglected, the power gain drops off with frequency as $|(e^{-j\omega\tau}-1)/(j\omega\tau)|^2$ which is shown in Fig. 8. It thus does not appear feasible to raise the frequency to much above twice the reciprocal transit time unless very high gain is available at lower frequencies which may be sacrificed in this cutoff tail and still give sufficient amplification at frequencies higher than the cutoff frequency.

The question of stability of a DLT may be analyzed with the help of Fig. 9. It shows the stable and unstable regions for the external admittances, Y_S and Y_L, of an active four-pole, and has been derived in Appendix II. If the external conductances are chosen to lie in the area where the two regions which are bounded by hyperbolas and straight lines, respectively, overlap, then oscillations without external feedback will result. Outside this area the device is stable. If the two regions do not overlap, which occurs for

$$|\,2\,\mathrm{Re}\,(y_{11})\,\mathrm{Re}\,(y_{22}) - \mathrm{Re}\,(y_{12}y_{21})\,| < |\,y_{12}y_{21}\,| \quad (17)$$

the device is unconditionally stable. If we now apply these considerations to the "intrinsic" DLT with negligible transit time, (7), we find that condition (17) is never satisfied; *i.e.*, that the two regions in Fig. 9 will always overlap. To determine the external admittances for which the DLT will oscillate at a certain frequency without external feedback, one thus draws a diagram like Fig. 9 for the particular frequency, and selects a pair of values for the real parts of the admittances from the doubly shaded region, and then calculates the corresponding imaginary parts from (35) and (36) in Appendix II. If stable amplifier operation is desired, one selects a pair of admittances outside the doubly shaded

[14] W. G. Matthei and F. A. Brand, "On the injection of carriers into a depletion layer," *J. Appl. Phys.*, vol. 28, p. 513; April, 1957.

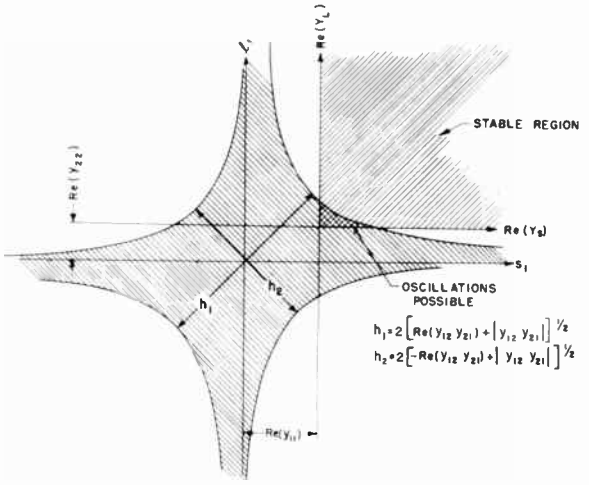

Fig. 9—Stable and unstable regions for external admittances between terminals of active four-pole.

region. To investigate the stability behavior over a frequency band, one would have to construct a three-dimensional scheme with the frequency as the third coordinate.

The same remarks essentially hold for the multiplication case, at least as long as the last term in (10d) is negligible. An investigation of the stability behavior based on the frequency dependent four-pole admittances of (11) leads to a complicated transcendental equation from which it is fairly easy to determine whether the device will oscillate at a given frequency. The calculation of the exact cutoff frequency, however, is difficult and would exceed the scope of this discussion.

With these remarks, we want to close the section on gain and stability because this paper deals mainly with the design theory of the device and not its circuitry. The main object of Section VII was to establish that the device described is indeed an active four-pole capable of power gain.

VIII. Other DLT Designs

In this section a number of DLT-type structures are mentioned, which appear feasible and illustrate the prediction that designs around the principle of carrier transport through high field depletion layers will play a similar role in very high-frequency solid-state amplification, as structures based on carrier diffusion do at lower frequencies. No mathematical analysis of these proposed devices shall be given in this paper.

It has been shown that for a regular DLT with no carrier multiplication the ac current amplification drops off rapidly when the transit time is comparable to one period. Higher frequency response thus requires narrower depletion layers. It has also been shown that the problem of properly locating the emitter contact in the narrow DL to keep the ac voltage feedback small may be circumvented by boosting the current amplification through controlled carrier multiplication.

A similar principle may be applied to a structure where the transit time is equal to several periods of the operating frequency. If, namely, a narrow region near the collector end of the depletion layer contains multiplying fields which offset the frequency-determined reduction in current amplification, then operation beyond the natural cutoff frequency appears feasible. The multiplied carriers of opposite sign must be prevented from returning to the emitter contact; this can be accomplished in several different ways: one may consider the amplification of pulses where the emitter is forward biased only during the duration of the pulse and reverse biased at all other times so that it will not collect carriers of the opposite sign. This device will show a certain delay between signal pulse and amplified pulse due to the transit time from the emitter contact to the multiplying region which, in itself, may find an application. When cw operation is desired, a magnetic field may be used to divert the returning carriers from the emitter contact. This type of operation resembles the "dissected amplifier" idea with the gyrating element built into the device close to the amplifying region.[15]

Another interesting modification of the basic DLT principle would be a device where the carriers are generated inside the DL by modulated light or microwave energy, or where the multiplication factor m is modulated by the microwave field parallel or perpendicular to the junction. In devices like this, the transition is found from amplification by principles at least vaguely related to transistor operation and amplification utilizing other solid-state phenomena.

It may also prove to be of great interest to investigate the properties of depletion layers at low temperatures where the maximum carrier velocities[7] and the mean free path of the carriers increase.

IX. Conclusion

The experimental phase of the development of the device is well underway and has been partially reported.[2,14] In particular, it has been shown that the injection into the depletion layer occurs as assumed in the theory and that the low-frequency gain depends on the voltage feedback ratio, κ_1, in the predicted manner. When more complete information is available, the design theory may be refined and generalized in many obvious ways. At that time also the noise problem may be attacked.

Appendix I

Calculation of the Four-pole Parameters of a DLT under Transit Time Conditions

In the first paper on the design theory of the proposed devices, the effects of transit time will be analyzed under the simplest assumptions. The many conceivable

[15] W. Shockley and W. P. Mason, "Dissected amplifiers using negative resistance," *J. Appl. Phys.*, vol. 25, p. 677; May, 1954.

generalizations shall be carried out when more experimental information is available. We thus assume: 1) All ac quantities, a, may be expressed by $a=a_0 \exp(j\omega t)$ where a_0 is complex; 2) only electrons are injected which carry the entire ac conduction current, $i_n(x, t)$; 3) the virtual emitter has no other electrical influence than the emission of carriers; 4) the carriers move with a high, field-independent, constant velocity, u, and no "debunching" of the carrier waveform occurs due to either diffusion or the electron space charge; 5) the analysis applies to a p-i-n structure with highly doped p and n regions. Such a junction is well simulated by a plane parallel capacitor. The width, w, of the depletion layer is then assumed independent of ac voltage.

The derivation is based on the geometry of Fig. 10. The injected electron current depends on the voltage $V_B = V_1 - V_s$, where V_s is the potential inside the DL underneath the emitter junction. V_s is given by

$$V_s = \int_{-w_1}^{0} E(x, t)dx = E(-w_1, t) \times w_1 \qquad (18)$$

or

$$V_s = V_2 - \int_{0}^{w_2} E(x, t)dx. \qquad (19)$$

In the region $-w_1 < x < 0$, E is independent of distance, $E=E(-w_1, t)$, because of the absence of any space charge, whereas in the range of $0<x<w_2$ it is equal to

$$E(x, t) = E(-w_1, t) + (1/\epsilon)\int_{0}^{x} \rho(x, t)dx. \qquad (20)$$

As we are mainly interested in the linearized ac parameters (the dc relationships are identical with those of Section III), we separate the small ac part from the dc part and find for (18) and (19)

$$v_s = E_{AC}(-w, t) \times w_1 \qquad (21)$$

and

$$v_s = V_2 - E_{AC}(-w_1, t) \times w_2 + \frac{i_{1n}u}{\epsilon A\omega^2}(e^{-j\omega w_2/u} - 1) + j\frac{i_{1n}w_2}{\epsilon A\omega} \qquad (22)$$

where $(Au)^{-1} \times i_n(x, t) = (Au)^{-1} \times i_{1n}(t - x/u)$ has been substituted for the ac variations of the space charge, ρ_{AC}. Substituting E_{AC} from (21) into (22) thus yields

$$v_s = [w_1/(w_1 + w_2)](v_2 + i_{1n}\phi) \qquad (23)$$

where

$$\phi = \frac{w_2^2}{\epsilon Au} \frac{e^{-j\omega w_2/u} - 1 + j\omega w_2/u}{(\omega w_2/u)^2}. \qquad (24)$$

With (23) and

$$i_{1n} = (\partial I_{1n}/\partial V_B)v_B = g_{1n}v_B \qquad (25)$$

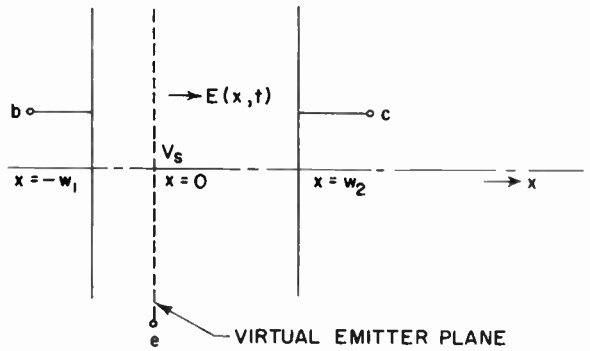

Fig. 10—Geometry for the analysis of transit time effects in the DLT.

one finds

$$i_{1n} = \frac{g_{1n}}{\varphi}v_1 - \frac{w_1}{w_1 + w_2}\frac{g_{1n}}{\varphi}v_2 \qquad (26)$$

with

$$\varphi = 1 + \frac{w_1}{w_1 + w_2}g_{1n}\phi. \qquad (27)$$

Since the conduction current is delayed by w_2/u on its way from emitter to collector, one obtains for the ac collector electron current

$$-i_{2n}(t) = i_{1n}(t - w_2/u) = \frac{g_{1n}}{\varphi}(e^{-j\omega w_2/u})v_1 - \frac{w_1}{w_1 + w_2}\frac{g_{1n}}{\varphi}(e^{-j\omega w_2/u})v_2. \qquad (28)$$

According to (20), i_{1n} is the total emitter current. The total collector current, however, is the sum of i_{2n} and the displacement current

$$-i_{2,\text{disp}} = \epsilon A\frac{\partial E(w_2, t)}{\partial t} = j\omega\frac{\epsilon A}{w_1 + w_2}\left[\frac{g_{1n}\phi}{\varphi}v_1 + \left(1 - \frac{w_1}{w_1 + w_2}\frac{g_{1n}\phi}{\varphi}v_2\right]\right. + i_{1n}(1 - e^{-j\omega w_2/u}). \qquad (29)$$

The first term in (29) is the capacitive current between base and collector, the second compensates for the phase shift in conduction current.

From (26), (28), and (29) it is thus possible to calculate the small-signal, four-pole admittances y_{ik}:

$$y_{11} = g_{1n}/\varphi \qquad (30a)$$

$$y_{12} = -\frac{w_1}{w_1 + w_2}\frac{g_{1n}}{\varphi} \qquad (30b)$$

$$y_{21} = -\frac{g_{1n}}{\varphi} - j\omega\frac{\epsilon A}{w_1 + w_2}\frac{g_{1n}\phi}{\varphi} \qquad (30c)$$

$$y_{22} = \frac{w_1}{w_1 + w_2}\frac{g_{1n}}{\varphi} - j\omega\frac{\epsilon A}{w_1 + w_2}\frac{1}{\varphi}. \qquad (30d)$$

Appendix II

Calculation of the Conditions for Unconditional Stability or Self-Excitation of an Active Four-pole

An active four-pole, the input of which is passively terminated by the admittance, Y_S, and the output of which is passively terminated by an admittance, Y_L, will oscillate if the condition[16]

$$\Delta = \begin{vmatrix} y_{11} + Y_s & y_{12} \\ y_{21} & y_{22} + Y_L \end{vmatrix} \tag{31}$$

is satisfied. Eq. (31) is equivalent to the following relationships:

$$s_1 l_1 - s_2 l_2 = a \tag{32}$$

and

$$s_1 l_2 + s_2 l_1 = b \tag{33}$$

where

$$\begin{aligned} s_1 &= \text{Re}\,(y_{11} + Y_S), \quad & s_2 &= \text{Im}\,(y_{11} + Y_S) \\ l_1 &= \text{Re}\,(y_{22} + Y_L), \quad & l_2 &= \text{Im}\,(y_{22} + Y_L) \\ a &= \text{Re}\,(y_{12}y_{21}), & b &= \text{Im}\,(y_{12}y_{21}). \end{aligned} \tag{34}$$

Eqs. (32) and (33) permit us to determine the values of Y_S, Y_L for which the four-pole will oscillate at a given frequency. For this purpose, we derive a solution of (32) and (33) for which s_1, s_2, l_1, l_2 are all real and Re $(Y_S)>0$, Re $(Y_L)>0$. We find

$$s_2 = \{b \pm [b^2 - 4(s_1^2 l_1^2 - a s_1 l_1)]^{1/2}\}/(2l_1) \tag{35}$$

and

$$l_2 = \{b \mp [b^2 - 4(s_1^2 l_1^2 - a s_1 l_1)]^{1/2}\}/(2s_1) \tag{36}$$

s_2 and l_2 may be positive or negative, but must be real which leads to the condition

$$s_1^2 l_1^2 - a s_1 l_1 - b^2/4 \leq 0. \tag{37}$$

Eq. (37) states that the permissible values on the $s_1 - l_1$ plane lie within the area bounded by the two hyperbolas

$$\begin{aligned} 2s_1 l_1 &= a + (a^2 + b^2)^{1/2} \\ &= \text{Re}\,(y_{12}y_{21}) + |\,y_{12}y_{21}\,| \end{aligned} \tag{38}$$

and

$$\begin{aligned} 2s_1 l_1 &= a - (a^2 + b^2)^{1/2} \\ &= \text{Re}\,(y_{12}y_{21}) - |\,y_{12}y_{21}\,| \end{aligned} \tag{39}$$

which is shown in Fig. 9. We now transform back according to (34)

$$\text{Re}\,(Y_S) = s_1 - \text{Re}\,(y_{11}) \tag{40}$$

$$\text{Re}\,(Y_L) = l_1 - \text{Re}\,(y_{22}) \tag{41}$$

which shifts the coordinate axes as indicated in Fig. 9. Since Re (Y_S) and Re (Y_L) must be positive, only those values of Re (Y_L) and Re (Y_S) will give oscillations which lie in the region where the positive quadrant of the Re (Y_S) – Re (Y_L) plane overlaps the area bounded by the hyperbolas (see Fig. 9). Outside this region, the four-pole is stable. If the positive quadrant does not intersect the hyperbolas at all, which occurs for

$$|\,2\,\text{Re}\,(y_{11})\,\text{Re}\,(y_{22}) - \text{Re}\,(y_{12}y_{21})\,| < |\,y_{12}y_{21}\,|, \tag{42}$$

the device is unconditionally stable.

[16] See, *e.g.*, H. W. König, "Laufzeittheorie der Elektronenröhren," Springer Verlag, Vienna; 1948. The discussion in the present paper is an adaptation of the methods developed by König which also contain stability criterion of Linvill (*op. cit.*) in implicit form.

List of Symbols Other Than Defined in the Text

A = conducting cross section of transistor.
E_{AC} = ac part of electric field strength.
I_{com} = dc reverse current under multiplication conditions.
I_{1no} = dc emitter electron current.
I_{1po} = dc emitter hole current.
i_{1n} = ac emitter electron current.
i_{1p} = ac emitter hole current.
$j = \sqrt{-1}$.
N_a = acceptor concentration.
N_d = donor concentration.
q = electron charge.
$w = w_1 + w_2$ = total width of depletion layer.
ϵ = dielectric constant.
ρ = electric charge density.
ρ_{ac} = ac part of electric charge density.
τ = transit time from emitter to collector.
ω = circular frequency.

Acknowledgment

The author wishes to thank F. A. Brand and W. G. Matthei of the U. S. Army Signal Engineering Laboratories for many discussions in connection with their experimental work on the device.

A Note on Numerical Transform Calculus*

RUBIN BOXER†, MEMBER, IRE

Summary—**Many of the numerical transform methods, developed for the solution of integrodifferential equations, exhibit difficulties when discontinuities occur at the origin. In this paper a procedure for including initial conditions is derived which effectively takes origin discontinuities into account.**

Although shown to be applicable to a number of transform methods, the derivation emphasizes application to the *z*-form integration operators because of their relatively greater accuracy.

Numerical examples illustrating the solution of a constant coefficient and a time-varying problem are given. The technique is equally applicable to the solution of nonlinear problems.

Introduction

During recent years a number of numerical techniques have been developed in operational form which systematize the obtaining of solutions to linear and nonlinear integrodifferential equations.[1–8]

Tustin,[1] operating in the time domain completely, developed a set of integration operators. He showed that given a function $y(t)$, defined at the points $y(0)$, $y(T)$, $y(2T)$, $\cdots$, the difference equation representation for the first integral of $y(t)$

$$\frac{T}{2}\,i_1(t+T) - \frac{T}{2}\,i_1(t) = \frac{T}{2}\,y(t+T) + \frac{T}{2}\,y(t) \qquad (1)$$

could be put into operational form. A convenient notation, which will be used in this paper, is the z transform. Using this notation, the transfer function for (1) is:

$$\frac{I_1(z)}{Y(z)} = \frac{T}{2}\,\frac{z+1}{z-1} \cong \frac{1}{p}\,. \qquad (2)$$

Here $1/p$ represents the integration operator and $z = \epsilon^{pT}$. Eq. (2) is equivalent to the transfer function for trapezoidal integration originally derived in z-transform notation by Salzer.[9]

Tustin further proposed that higher order integrating operators could be given by:

$$\frac{1}{p^k} \cong \left(\frac{T}{2}\,\frac{z+1}{z-1}\right)^k. \qquad (3)$$

Tustin's procedure works well, but has difficulty when the time functions operated on, or their derivatives, are not zero at the zero instant of time.

Madwed[2] improved upon the method of Tustin by developing integrating operators of greater accuracy in addition to introducing a fairly complex procedure for operating upon discontinuous functions. The first order integration operator of Madwed is identical to that of (2), but the higher order operators differ, and as stated above, are more accurate. For example, the second-order integrating operator of Madwed is

$$\frac{1}{p^2} \cong \frac{T^2}{6}\,\frac{z^2+4z+1}{(z-1)^2}\,. \qquad (4)$$

The simplification of Madwed's notation to that of the z transform was included in a paper by Truxal.[3]

Thaler and this author[4–5] used the frequency domain to demonstrate that it is possible to substitute integration operators, considered from a Laplace transform viewpoint, into the Laplace transforms of linear and nonlinear equations. The derived operators were termed z forms. For example, the z-form operator for $1/s^2$ is

$$\frac{1}{s^2} \cong \frac{T^2}{12}\,\frac{z^2+10z+1}{(z-1)^2}\,. \qquad (5)$$

In a recent report[10] the greater accuracy of the z forms was demonstrated and a method for calculating error was supplied. Table I lists the z forms for $1/s^k$, together with corresponding z transforms. The z transforms are shown in Table I to illustrate their relationship to the z forms. Table II illustrates the relative accuracies of the various integrating operators. Note that when the z transform is to be used as an integrating operator, it is multiplied by T.

The z-form method had a disadvantage. In order to obtain the full accuracy inherent in the operators, the time functions and their derivatives had to be of zero value at the time origin. To accomplish this in certain problems required a change of variable which, at times,

* Original manuscript received by the IRE, February 27, 1957; revised manuscript received June 17, 1957.

† Servomechanisms, Inc., Westbury, N. Y.; formerly with Rome Air Dev. Ctr., Rome, N.Y.

[1] A. Tustin, "A method analyzing the behavior of linear systems in terms of time series," and "A method of analyzing the effects of certain kinds of non-linearity in closed-cycle control systems," *J. IEE* (Proceedings of the Convention on Automatic Regulators and Servomechanisms) vol. 94, Part II-A, p. 130 ff.; May, 1947.

[2] A. Madwed, "Number Series Method of Solving Linear and Nonlinear Differential Equations," M.I.T. Instr. Lab. Rep. No. 6445-T-26; April, 1950.

[3] J. G. Truxal, "Numerical analysis for network design," IRE Trans., vol. CT-1, pp. 49–60; September, 1954.

[4] R. Boxer and S. Thaler, "A simplified method of solving linear and nonlinear systems," Proc. IRE, vol. 44, pp. 89–101; January, 1956.

[5] S. Thaler and R. Boxer, "An operational calculus for numerical analysis," 1956 IRE Convention Record, part 2, pp. 100–105.

[6] S. Amarel, L. Lambert, and J. Millman, "A Transformation Calculus for Obtaining Approximate Solutions to Linear Integro-Differential Equations with Constant Coefficients," Columbia Univ. Electronics Res. Labs. Tech. Rep. T-7/C; August, 1954.

[7] S. Amarel, "A Computational Method for Treating Networks Containing Nonlinear Elements," Columbia Univ. Electronics Res. Labs., Tech. Rep. T-3/C; August, 1954.

[8] S. Amarel, "An Operational Method for the Treatment of Transients in Waveform Circuits (Linear and Nonlinear)," Columbia Univ. Electronics Res. Labs., Tech. Rep. T-5/C; April, 1955.

[9] J. M. Salzer, "Frequency analysis of digital computers operating in real time," Proc. IRE , vol. 42, pp. 457–466; February, 1954.

[10] R. Boxer and S. Thaler, "Extensions of Numerical Transform Theory," Rome Air Dev. Ctr. Tech. Rep. 56–115, November, 1956.

TABLE I

Z TRANSFORMS AND Z FORMS

$\frac{1}{S^k}$	z transform $\bar{F}_k(z) = \frac{N_k(z)}{D_k(z)}$	z form $F_k(z)$
$\frac{1}{S}$	$\frac{z}{z-1}$	$\frac{Tz}{z-1} - \frac{T}{2} = \frac{T}{2}\frac{z+1}{z-1}$
$\frac{1}{S^2}$	$\frac{Tz}{(z-1)^2}$	$\frac{T^2z}{(z-1)^2} + \frac{T^2}{12} = \frac{T^2}{12}\frac{z^2+10z+1}{(z-1)^2}$
$\frac{1}{S^3}$	$\frac{T^2}{2}\frac{z(z+1)}{(z-1)^3}$	$\frac{T^3}{2}\frac{z(z+1)}{(z-1)^3}$
$\frac{1}{S^4}$	$\frac{T^3}{6}\frac{z(z^2+4z+1)}{(z-1)^4}$	$\frac{T^4}{6}\frac{z(z^2+4z+1)}{(z-1)^4} - \frac{T^4}{720}$
$\frac{1}{S^5}$	$\frac{T^4}{24}\frac{z(z^3+11z^2+11z+1)}{(z-1)^5}$	$\frac{T^5}{24}\frac{z(z^3+11z^2+11z+1)}{(z-1)^5}$
$\frac{1}{S^k}$	$\frac{Tz}{k-1}\frac{(k-1)N_{k-1}(z) - (z-1)N'_{k-1}(z)}{(z-1)^k}$	$T\bar{F}_k(z) + T^kA_k(-1)^{k/2+1}$ where A_k is the Bernoulli Coefficient*

Legend:
1) The $N_k(z)$ terms include the constant multiplier.
2) The term $N_k'(z)$ represents $dN_k(z)/d(z)$.
3) The general formula for $F_k(z)$ holds for $k>1$.

* C. H. Richardson, "An Introduction to the Calculus of Finite Differences," D. Van Nostrand Co. Inc., New York, N. Y., pp. 45–46; 1954.

increased the amount of labor necessary to obtain a solution. Furthermore, the method had the inconvenience of the solution being in error at the origin. This was of small consequence, however, as this initial value was always known.

A group at Columbia University, under the direction of Millman, developed an operational method in which initial conditions are included in integrating and differentiating operators.[6] The basic operators are those of Tustin, but the usefulness of the operators was considerably extended in that the origin problems were eliminated.

In this paper, a different approach to the problem of initial conditions is given. Although the procedure will be shown to be applicable to any of the methods indicated by Table II the basic derivations will be directed toward the z forms, because of their relatively greater accuracy. When applied to the operators of Tustin, the results obtained are similar to those derived at Columbia, except that additional terms are obtained which lead to greater accuracy in problems above the first order.

THEORY

The integrating operators shown in column 3 of Table I, can be derived by the procedure illustrated below for the second order case.[5,10] Given a function $y(t)$, it is desired that $i_2(t)$ be obtained where

$$i_2(t) = \int\int y(t)dt. \tag{6}$$

If (6) is to be approximated by a second-order difference equation, then

$$Ai_2(t+2T) + Bi_2(t+T) + Ci_2(t) = Dy(t+2T) + Ey(t+T) + Fy(t). \tag{7}$$

In operational form

$$f(t+nT) = \epsilon^{pnT}f(t) \tag{8}$$

and

$$i_2(t) = \frac{1}{p^2}\,y(t).$$

Thus (7) can be expressed

$$\frac{A}{p^2}\epsilon^{2pT}y(t) + \frac{B}{p^2}\epsilon^{pT}y(t) + \frac{C}{p^2}\,y(t) = D\epsilon^{2pT}y(t) + E\epsilon^{pT}y(t) + Fy(t). \tag{9}$$

If the exponential operators are expanded in a Taylor Series, the coefficients A, B, C, D, E, and F can be determined by equating the maximum number of like powers of p on both sides of (9), consistent with the number of unknown coefficients. If this is done and the values of the coefficients are substituted into (7), the difference equation for second-order integration obtained is:

TABLE II
COMPARISON OF INTEGRATING OPERATORS

$1/S^k$	Method	Operator	Series Expansion of Operator
$\frac{1}{S}$	Tustin	$\frac{T}{2}\frac{z+1}{z-1}$	$\frac{1}{S} + \frac{ST^2}{12} - \frac{S^3T^4}{720} + \frac{S^5T^6}{30240} + \cdots$
	Madwed-Truxal	$\frac{T}{2}\frac{z+1}{z-1}$	$\frac{1}{S} + \frac{ST^2}{12} - \frac{S^3T^4}{720} + \frac{S^5T^6}{30240} + \cdots$
	Exact z Transform	$\frac{Tz}{z-1}$	$\frac{1}{S} + \frac{T}{2} + \frac{ST^2}{12} - \frac{S^3T^4}{720} + \frac{S^5T^6}{30240} + \cdots$
	z Form	$\frac{T}{2}\frac{z+1}{z-1}$	$\frac{1}{S} + \frac{ST^2}{12} - \frac{S^3T^4}{720} + \frac{S^5T^6}{30240} + \cdots$
$\frac{1}{S^2}$	Tustin	$\frac{T^2}{4}\frac{z^2+2z+1}{(z-1)^2}$	$\frac{1}{S^2} + \frac{T^2}{6} + \frac{S^2T^4}{240} - \frac{S^4T^6}{6048} + \cdots$
	Madwed-Truxal	$\frac{T^2}{6}\frac{z^2+4z+1}{(z-1)^2}$	$\frac{1}{S^2} + \frac{T^2}{12} + \frac{S^2T^4}{240} - \frac{S^4T^6}{6048} + \cdots$
	Exact z Transform	$\frac{T^2z}{(z-1)^2}$	$\frac{1}{S^2} - \frac{T^2}{12} + \frac{S^2T^4}{240} - \frac{S^4T^6}{6048} + \cdots$
	z Form	$\frac{T^2}{12}\frac{z^2+10z+1}{(z-1)^2}$	$\frac{1}{S^2} + \frac{S^2T^4}{240} - \frac{S^4T^6}{6048} + \cdots$
$\frac{1}{S^3}$	Tustin	$\frac{T^3}{8}\frac{z^3+3z^2+3z+1}{(z-1)^3}$	$\frac{1}{S^3} + \frac{T^2}{4}\frac{1}{S} + \frac{ST^4}{60} - \frac{S^3T^6}{60480} + \cdots$
	Madwed-Truxal	$\frac{T^3}{24}\frac{z^3+11z^2+11z+1}{(z-1)^3}$	$\frac{1}{S^3} + \frac{T^2}{12}\frac{1}{S} + \frac{ST^4}{360} + \frac{13S^3T^6}{60480} + \cdots$
	Exact z Transform	$\frac{T^3}{2}\frac{z(z+1)}{(z-1)^3}$	$\frac{1}{S^3} - \frac{ST^4}{240} + \frac{S^3T^6}{3024} + \cdots$
	z Form	$\frac{T^3}{2}\frac{z(z+1)}{(z-1)^3}$	$\frac{1}{S^3} - \frac{ST^4}{240} + \frac{S^3T^6}{3024} + \cdots$
$\frac{1}{S^4}$	Tustin	$\frac{T^4}{16}\frac{z^4+4z^3+6z^2+4z+1}{(z-1)^4}$	$\frac{1}{S^4} + \frac{T^2}{3}\frac{1}{S^2} + \frac{13T^4}{360} + \frac{S^2T^6}{945} + \cdots$
	Madwed-Truxal	$\frac{T^4}{120}\frac{z^4+26z^3+66z^2+26z+1}{(z-1)^4}$	$\frac{1}{S^4} + \frac{T^2}{12}\frac{1}{S^2} + \frac{T^4}{360} + \frac{S^2T^6}{60480} + \cdots$
	Exact z Transform	$\frac{T^4}{6}\frac{z(z^2+4z+1)}{(z-1)^4}$	$\frac{1}{S^4} + \frac{T^4}{720} - \frac{S^2T^6}{3024} + \cdots$
	z Form	$\frac{T^4}{6}\frac{z(z^2+4z+1)}{(z-1)^4} - \frac{T^4}{720}$	$\frac{1}{S^4} - \frac{S^2T^6}{3024} + \cdots$

$$i_2(t+2T) - 2i_2(t+T) + i_2(t) = \frac{T^2}{12}y(t+2T) + \frac{10T^2}{12}y(t+T) + \frac{T^2}{12}y(t). \quad (10)$$

Eq. (10) has been derived neglecting initial conditions, and if Laplace transformed, the result is

$$\frac{I_2(s)}{Y(s)} = \frac{T^2}{12}\frac{\epsilon^{2sT} + 10\epsilon^{sT} + 1}{\epsilon^{2sT} - 2\epsilon^{sT} + 1} \quad (11)$$

or in z-transform notation

$$\frac{I_2(z)}{Y(z)} = \frac{T^2}{12}\frac{z^2+10z+1}{(z-1)^2}. \quad (12)$$

The remainder of the z forms shown in Table I can be derived in the same manner and represent difference equation approximations for integration that are optimum in the sense indicated.

If the initial conditions are not zero, the z transform of (10) yields terms in addition to those shown in (12). It can be shown[11] that the z transform of $f(t+mT)$ is given by

$$\mathcal{Z}[f(t+mT)] = z^m\left[F(z) - \sum_{n=0}^{m-1} f(nT)z^{-n}\right]. \quad (13)$$

Using (13), the z transform of (10) is

$$\frac{T^2}{12}[z^2Y(z)-z^2y(0)-zy(T)]+)\frac{10T^2}{12}[zY(z)-zy(0)]+\frac{T^2}{12}Y(z)$$
$$= z^2I_2(z)-z^2i_2(0)-zi_2(T)-2[zI_2(z)-zi_2(0)]+I_2(z). \quad (14)$$

However, $y(T)$, $i_2(T)$, and $i_2(0)$ can be expressed:

$$y(T) = y(0) + Ty'(0) + \frac{T^2}{2!}y''(0) + \cdots = \sum_{n=0}^{\infty}\frac{T^n}{n!}y^n(0)$$

$$i_2(T) = y^{-2}(0) + Ty^{-1}(0) + \frac{T^2}{2}y(0) + \cdots = \sum_{n=0}^{\infty}\frac{T^n}{n!}y^{n-2}(0)$$

$$i_2(0) = y^{-2}(0). \quad (15)$$

Substituting (15) into (14), the result after algebraic manipulation is:

$$I_2(z) = \frac{T^2}{12}\frac{z^2+10z+1}{(z-1)^2}Y(z) - \frac{T^2}{12}\frac{z(z+10)}{(z-1)^2}y(0) - \sum_{n=0}^{\infty}\frac{T^{n+2}}{12n!}\frac{z}{(z-1)^2}\left(\frac{n^2+3n-10}{n^2+3n+2}\right)y^n(0) + \sum_{q=1}^{2}\overline{F_{3-q}(z)}y^{-q}(0), \quad (16)$$

where $\overline{F_k(z)}$ is the exact z transform for $1/s^k$ given in Table I. Expanding (16) by performing the indicated summations yields:

$$I_2(z) = \frac{T^2}{12}\frac{z^2+10z+1}{(z-1)^2}Y(z) - \frac{T^2}{12}\frac{z(z+5)}{(z-1)^2}y(0) + \frac{T^3}{12}\frac{z}{(z-1)^2}y'(0) - \frac{T^5}{180}\frac{z}{(z-1)^2}y'''(0) + \cdots + \frac{Tz}{(z-1)^2}y^{-1}(0) + \frac{z}{z-1}y^{-2}(0), \quad (17)$$

[11] R. Boxer, "Analysis of sampled data systems and digital computers in the frequency domain," 1955 IRE Convention Record, part 10, pp. 78–85.

where it should be noted that the second derivative term is absent. The result of a similar procedure for the first-order integrating operator would be:

$$I_1(z) = \frac{T}{2}\frac{z+1}{z-1}Y(z) - \frac{Tz}{2(z-1)}y(0) + \frac{z}{z-1}y^{-1}(0). \quad (18)$$

Examples

To illustrate the use of the z forms, including initial conditions, two problems will be carried out in some detail. The first is a constant coefficient problem, while the second is time varying.

Example 1

A typical second-order differential equation with constant coefficients is

$$\frac{d^2y}{dt^2} + 3\frac{dy}{dt} + 2y = 0 \quad y(0) = +3; \quad y'(0) = -4. \quad (19)$$

The Laplace transform of (19) is

$$Y(s) + \frac{3}{s}Y(s) + \frac{2}{s^2}Y(s) = \frac{3}{s} + \frac{5}{s^2}. \quad (20)$$

To obtain a difference equation approximation, (20) is z transformed, using (18) and the first three terms of (17) in the left side of the equation and the z transforms of Table I in the right side.

$$Y(z) + \frac{3T}{2}\frac{z+1}{z-1}Y(z) - \frac{9Tz}{2(z-1)} + \frac{T^2}{6}\frac{z^2+10z+1}{(z-1)^2} - \frac{T^2}{2}\frac{z(z+5)}{(z-1)^2} - \frac{2T^3z}{3(z-1)^2} = \frac{3z}{z-1} + \frac{5Tz}{(z-1)^2}. \quad (21)$$

Solving for $Y(z)$,

$$Y(z) = \frac{(18+27T+3T^2)z^2-(18-3T-15T^2-4T^3)z}{(6+9T+T^2)z^2-(12-10T^2)z+(6-9T+T^2)}. \quad (22)$$

If T is chosen as 0.1,

$$Y(z) = \frac{3.0z^2 - 2.539219z}{1.0z^2 - 1.722142z + 0.739508}. \quad (23)$$

The solution for $y(t)$ is obtained by carrying out the indicated synthetic division. The results are shown in Table III, together with the exact solution.

Example 2

A time-varying problem, suggested to the author by Millman, is

$$\frac{d^2}{dt^2}[(t^2-1)y] - \frac{d}{dt}[2ty] - 6y = 0$$
$$y(0) = -0.5; \quad y'(0) = 0 \quad (24)$$

TABLE III
SOLUTION OF CONSTANT COEFFICIENT PROBLEM

t	$y(t)$—Exact	$y(t)$—Calculated
0	3.000000	3.000000
0.1	2.628405	2.627207
0.2	2.307782	2.305900
0.3	2.030448	2.028246
0.4	1.789969	1.787697
0.5	1.580941	1.578764
0.6	1.398818	1.396840
0.7	1.239767	1.238048
0.8	1.100555	1.099120
0.9	0.978439	0.977295
1.0	0.871093	0.870233

TABLE IV
SOLUTION OF TIME-VARYING PROBLEM

t	$y(t)$—Exact	$y(t)$—Calculated
0	−0.500000	−0.500000
0.1	−0.485000	−0.485075
0.2	−0.440000	−0.440299
0.3	−0.365000	−0.365672
0.4	−0.260000	−0.261194
0.5	−0.125000	−0.126865
0.6	+0.040000	+0.037321
0.7	+0.235000	+0.231355
0.8	+0.460000	+0.455240
0.9	+0.715000	+0.708975
1.0	+1.000000	+0.992555

which has the analytic solution

$$y(t) = 0.5(3t^2 - 1) \qquad 0 \leq t \leq 1.0. \tag{25}$$

Transforming (24) yields

$$\mathcal{L}[(t^2 - 1)y] - \frac{1}{s}\mathcal{L}[(2t)y] - \frac{6}{s^2}y = \frac{1}{2s}. \tag{26}$$

Taking the z transform using (17) and (18):

$$c_2 Y(z) - \frac{c_1 T}{2}\frac{z+1}{z-1}Y(z) - \frac{T^2}{2}\frac{z^2+10z+1}{(z-1)^2}Y(z) = \frac{z}{2(z-1)} + \frac{T^2}{4}\frac{z(z+5)}{(z-1)^2} \tag{27}$$

where

$$c_1 = 2t$$
$$c_2 = t^2 - 1 \tag{28}$$

Solving for $Y(z)$

$$Y(z) = \frac{(12 + T^2)z^2 - (2 - 5T^2)z}{(4c_2 - 2c_1T - 2T^2)z^2 - (8c_2 + 20T^2)z + (4c_2 + 2c_1T - 2T^2)}. \tag{29}$$

With $T = 0.1$

$$Y(z) = \frac{2.01z^2 - 1.95z}{(4c_2 - 0.2c_1 - 0.02)z^2 - (8c_2 + 0.20)z + (4c_2 + 0.2c_1 - 0.02)}. \tag{30}$$

Carrying out the indicated division, using (28) for the values of c_1 and c_2 at each step of the division process, yields the results shown in Table IV.

The procedure for solving a nonlinear problem is identical to that for time-varying problems, with the exception that the values obtained for the dependent variable are used to evaluate the denominator constants during the division process. The justification for treating the varying coefficients as constants was presented in a previous paper.[4]

DISCUSSION

In standard numerical analysis practice, differential equations are solved by difference equation approximations. Special care is required to start the solution correctly for a given set of initial conditions. One of the procedures is to obtain the first few values of the solution very accurately through the use of a Taylor series expansion and then to continue the solution using the difference equation. The operational procedure described in this paper is analogous to such a technique. The z-form integrating operators lead to an accurate difference equation approximation to the differential equation with initial conditions equal to zero. The addition of the initial condition terms such as those in (17) and (18) adjust the numerator of the z-transform transfer function approximation in order that the solution may be started accurately. A first-order system requires only the initial condition in order to continue the solution. Thus, the first-order integrating operator given by (18) only need contain a term that is dependent upon the initial condition and, of course, initial integral values.

Higher order problems, utilizing integrating relations such as (17), lead to higher order difference equations. A number of solution values equal to the order of the difference equation are required to start and continue the solution. Thus, the integrating operators for $1/s^k$ for $k > 1$ contain an infinite number of terms that are functions of the higher derivatives of the solution. The greater the number of these terms used, the greater the accuracy of the initial values of the solution. This permits fuller utilization of the accuracy inherent in the characteristic difference equation.

This paper has illustrated the use of the z forms and initial condition terms as integrating approximations. One might desire to know whether the reciprocals of the z-form operators with suitable initial conditions could be used as differentiating operators. The same procedures for obtaining the integrating operators would yield for first- and second-order differentiation

$$D_1(z) = \frac{2}{T}\frac{z-1}{z+1}Y(z) - \frac{2}{T}\frac{z}{z+1}y(0) + \frac{z}{z+1}y'(0) \quad (31)$$

$$D_2(z) = \frac{12}{T_2}\frac{(z-1)^2}{z^2+10z+1}Y(z) - \frac{12}{T^2}\frac{z(z-1)}{z^2+10z+1}y(0) - \frac{12}{T}\frac{z}{z^2+10z+1}y'(0) + \frac{z(z+5)}{z^2+10z+1}y''(0) + \sum_{n=1}^{\infty}\frac{T^n}{n!}\frac{z}{z^2+10z+1}\frac{n^2+3n-10}{n^2+3n+2}y^{n+2}(0). \quad (32)$$

As differentiating operators, the use of (31) and (32) leads to difficulty in some problems. Terms such as $(z^2+10z+1)$ in (32) do not contain the factor $(z+1)$ as in (31). In certain applications this will cause the required difference equation to be of higher order than necessary, and introduces extraneous roots in the characteristic equation. These extraneous roots cause incorrect transient phonomena to appear. In fact, as the magnitude of the roots place them outside the unit circle in the z plane, the solution obtained is unstable. One should note, however, that the amount of labor required to solve a problem by derivative operators would be about the same as the amount of labor performed in using the integrating operators, even if the undesirable effects were not present. In practice, therefore, it is recommended that the integrating operators be used.

The method for introducing initial conditions shown here can be applied to the various available operators such as those of Table II in addition to the z-form operators. The required relations for integration of any order can be obtained by using the following equation:

$$I_k(z) = F_k(z)Y(z) + \sum_{m=0}^{\infty}\sum_{p=1}^{k}\sum_{n=p}^{k}\left[b_n\frac{(pT-T)^{k+m}}{(k+m)!} - a_n\frac{(pT-T)^m}{m!}\right]\cdot\left[y^m(0)\frac{z^{n-p+1}}{(z-1)^k}\right] + \sum_{q=1}^{k}\overline{F_{k-q+1}}(z)y^{-q}(0) \quad (33)$$

where

$$F_k(z) = \frac{a_kz^k + a_{k-1}z^{k-1} + \cdots + a_0}{b_kz^k + b_{k-1}z^{k-1} + \cdots + b_0} \quad (34)$$

is any of the operators and

$$y^0(0) = y(0)$$
$$y^n(0) = \left.\frac{d^ny}{dt^n}\right|_{t=0}$$
$$y^{-q}(0) = \int_q\cdots\int_{-\infty}^{\prime} y(t)dt \quad (35)$$
$$\overline{F_k}(z) = z \text{ transform for } 1/s^k.$$

When the initial condition terms are obtained for the Tustin operators, no difficulty is encountered in their use as differentiating operators. The first-order differentiating equation for Tustin's operator would be identical to (31), while that for second-order differentiation is

$$D_2(z) = \frac{4}{T^2}\frac{(z-1)^2}{(z+1)^2}Y(z) - \frac{4}{T^2}\frac{z(z+1)}{(z+1)^2}y(0) - \frac{4z}{T(z+1)^2}y'(0) + \frac{z}{z+1}y''(0) + \sum_{n=1}^{\infty}\frac{T^n}{n!}\frac{z}{(z+1)^2}\left(\frac{n^2+3n+2}{n^2+3n+2}\right)y^{n+2}(0). \quad (36)$$

It is to be emphasized that a method for extending the Tustin operators for initial conditions was first accomplished by the Millman group at Columbia. They have also made extensive use of the flexibility, due to the ability to use the operators in either the integrating or differentiating sense. The procedure of this paper, however, when applied to the Tustin forms yields additional corrective terms, such as represented by the series

$$\sum_{n=1}^{\infty}\frac{T^n}{n!}\frac{z}{(z+1)^2}\left(\frac{n^2+3n-2}{n^2+3n+2}\right)y^{n+2}(0) \quad (37)$$

in (36).

A final comment may be appropriate. The method for obtaining a numerical solution is equally valid from the time and frequency domain points of view. The differential equations used in the illustrative examples could have been integrated directly, yielding in operational form

$$y(t) + \frac{3}{p}y(t) + \frac{2}{p^2}y(t) = 3 + \frac{5}{p} \quad (38)$$

for the constant coefficient case and

$$(t^2-1)y(t) - \frac{1}{p}(2t)y(t) - \frac{6}{p^2}y(t) = 0.5 \quad (39)$$

for the time-varying problem. Upon z transforming these equations, substituting the z-form operators for the indicated integration operators, the solution proceeds as before.

Acknowledgment

The author desires to express his thanks to his friend and associate, S. Thaler, at present with the Hughes Aircraft Corporation. During our association at the Rome Air Development Center, Mr. Thaler provided tutelage and guidance which have implicitly contributed to this paper.

Thanks are also due J. Millman of Columbia University for many interesting and stimulating discussions relating to the numerical transform field.

Correspondence

Transverse Impedance Transformation for Ferromagnetic Media*

This letter describes a transverse impedance transformation for ferromagnetic media magnetized in a transverse direction. It is valid for TE_{m0} modes when the magnetization is in the direction of the E field.

Fig. 1 indicates the basic geometry.

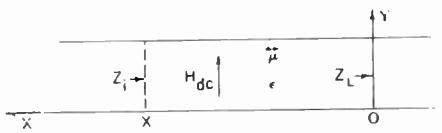

Fig. 1.

The propagation is in the $+Z$ direction and $e^{j\omega t-\gamma z}$ variation is assumed for all three field components E_y, H_x, and H_z. It is well known that the solutions of the tensor wave equation

$$\nabla\times\nabla\times\vec{H}=\omega^2\overleftrightarrow{\epsilon\mu}\cdot\vec{H} \text{ are}$$

$$E_y = A\sin K_m\chi + B\cos K_m\chi$$

$$H_z = \frac{j}{\omega\mu_{\text{eff}}}\left[\left(K_mA + j\frac{K}{\mu}\gamma B\right)\cos K_m\chi + \left(-K_mB + j\frac{K}{\mu}\gamma A\right)\sin K_m\chi\right]$$

for the transverse components, where

$$\overleftrightarrow{\mu}_{xyz} = \begin{bmatrix} \mu & 0 & jK \\ 0 & \mu_0 & 0 \\ -jK & 0 & \mu \end{bmatrix}$$

$$K_m^2 = \omega^2\mu_{\text{eff}}\epsilon + \gamma^2 \quad \text{and} \quad \mu_{\text{eff}} = \frac{\mu^2 - K^2}{\mu}.$$

Since tangential E and H are matched at all transverse boundaries a transverse impedance $Z_t = E_y/H_z$ is defined (1).

At $x=0$

$$Z_t(0) = \frac{-j\omega\mu_{\text{eff}}B}{K_mA + j\dfrac{K}{\mu}\gamma B} = Z_L.$$

Solving for B and substituting in the expression for Z_t gives after simplification (2).

But

$$\frac{-\omega\mu_{\text{eff}}}{K_m}\sqrt{\frac{\dfrac{\mu_{\text{eff}}}{\epsilon}}{1+\left(\dfrac{\lambda_{0m}\gamma}{2\pi}\right)^2}} = \sqrt{\frac{\dfrac{\mu_{\text{eff}}}{\epsilon}}{1-\left(\dfrac{\lambda_{0m}}{\lambda_g}\right)^2}}_{\gamma=j\beta} \equiv Z_{0m}.$$

Therefore, it is readily seen (3), especially from the second form, that Z_t reduces to the familiar impedance transformation when the ferromagnetic is demagnetized and $K=0$, $\mu=\mu_0$. If $\gamma=j\beta$, for the lossless case, (4).

$$Z_t = \frac{-j\omega\mu_{\text{eff}}(A\sin K_m\chi + B\cos K_m\chi)}{\left(K_mA + j\dfrac{K}{\mu}\gamma B\right)\cos K_m\chi + \left(j\dfrac{K}{\mu}\gamma A - K_mB\right)\sin K_m\chi}. \tag{1}$$

$$Z_t = \frac{\dfrac{\omega\mu_{\text{eff}}}{K_m}\left[\dfrac{K_mZ_L}{\omega\mu_{\text{eff}}}\cos K_m\chi - j\left(\dfrac{K}{\mu}\gamma\dfrac{Z_L}{\omega\mu_{\text{eff}}}+1\right)\sin K_m\chi\right]}{\cos K_m\chi + j\left[\left(\dfrac{K}{\mu}\gamma\right)^2\dfrac{Z_L}{K_m\omega\mu_{\text{eff}}} + \dfrac{K}{\mu}\dfrac{\gamma}{K_m} - \dfrac{K_mZ_L}{\omega\mu_{\text{eff}}}\right]\sin K_m\chi}. \tag{2}$$

$$\frac{Z_t}{Z_{0m}} = \frac{\dfrac{Z_L}{Z_{0m}}\cos K_m\chi + j\left(1 - \dfrac{K}{\mu}\dfrac{\gamma}{K_m}\dfrac{Z_L}{Z_{0m}}\right)\sin K_m\chi}{\cos K_m\chi + j\left[\dfrac{Z_L}{Z_{0m}}\left\{1-\left(\dfrac{K}{\mu}\dfrac{\gamma}{K_m}\right)^2\right\} + \dfrac{K}{\mu}\dfrac{\gamma}{K_m}\right]\sin K_m\chi}$$

$$= \frac{\left(\dfrac{\dfrac{Z_L}{Z_{0m}}\cot K_m\chi + j}{\cot K_m\chi + j\dfrac{Z_L}{Z_{0m}}}\right) - \left(\dfrac{j\dfrac{K}{\mu}\dfrac{\gamma}{K_m}\dfrac{Z_L}{Z_{0m}}}{\cot K_m\chi + j\dfrac{Z_L}{Z_{0m}}}\right)}{1 + \dfrac{j\dfrac{K}{\mu}\dfrac{\gamma}{K_m}\left[1-\left(\dfrac{K}{\mu}\dfrac{\gamma}{K_m}\right)\dfrac{Z_L}{Z_{0m}}\right]}{\cot K_m\chi + j\dfrac{Z_L}{Z_{0m}}}}. \tag{3}$$

$$\frac{Z_t}{Z_{0m}} = \frac{\dfrac{Z_L}{Z_{0m}}\left(\cot K_m\chi + \dfrac{K}{\mu}\dfrac{\beta}{K_m}\right) + \left(\cot K_m\chi - \dfrac{K}{\mu}\dfrac{\beta}{K_m}\right) + j\dfrac{Z_L}{Z_{0m}}\left[1+\left(\dfrac{K}{\mu}\dfrac{\beta}{K_m}\right)^2\right]}. \tag{4}$$

Example

Any geometry (such as Fig. 2) where transverse boundary conditions must be matched may now be solved using standard transverse resonance techniques.

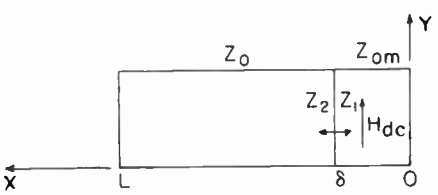

Fig. 2.

Waveguide equations hold in each region:

$K_a^2 = \omega^2\mu_0\epsilon_0 + \gamma^2$ (in the air-filled section)

$K_m^2 = \omega^2\mu_{\text{eff}}\epsilon + \gamma^2$ (in the ferromagnetic section)

$$\mu_{\text{eff}} = \frac{\mu^2 - K^2}{\mu}.$$

The sum of transverse impedances must equal 0 at any x, but pick $x=\delta$ for convenience.

$$\frac{Z_2}{Z_0} = j\tan K_a(L-\delta)$$

from normal Z transformation ($Z_L = 0$)

$$\frac{Z_1}{Z_{0m}} = \frac{j}{j\dfrac{K}{\mu}\dfrac{\gamma}{K_m} + \cot K_m\delta}$$

from Z transformation just derived for ferrite section ($Z_L = 0$)

$$\frac{Z_0}{Z_{0m}} = \frac{K_m}{K_a}\frac{\mu_0}{\mu_{\text{eff}}}$$

$$Z_1 + Z_2 = 0.$$

Therefore

$$\tan K_a(L-\delta) = \frac{-K_a\dfrac{\mu_{\text{eff}}}{\mu_0}}{j\dfrac{K}{\mu}\gamma + K_m\cot K_m\delta}$$

as is well known from Button and Lax's work.[1]

FREDERIC R. MORGENTHALER
AF Cambridge Res. Ctr.
Bedford, Mass.

* Received by the IRE, April 29, 1957.

[1] K. J. Button and B. Lax, "Theory of ferrites in rectangular waveguide," IRE TRANS., vol. AP-4, pp. 531–537; July, 1956.

Doppler Shift of the Received Frequency from the Standard Station Reflected by the Ionosphere*

While comparing the frequency from the standard station JJY of Japan with that of the Stark modulation atomic clock[1] here, we experienced that the received frequency shifted, which could be attributed to the movement of the ionosphere.[1,2] Then we expected it should be possible to investigate the ionosphere by measuring Doppler shift.

As a preliminary experiment for this investigation, we made a continuous recording of the beat frequency between the received frequency of a standard wave (4 mc) from JJY and that of the quartz chronometer (100 kc) in our laboratory. The stability of the quartz chronometer was better than 2×10^{-8} per day, and was considered sufficient for our purpose.

The block diagram of the apparatus is shown in Fig. 1.

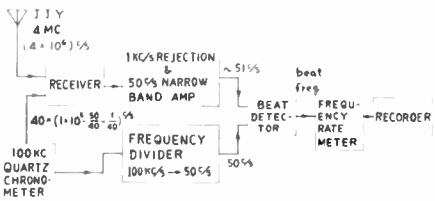

Fig. 1—Block diagram of the apparatus.

In Fig. 2 is shown the schematic diagram of the beat detector, which was used to improve signal-to-noise ratio and consisted of a phase sensitive detector modified for our purpose. The frequency rate meter was of a common type.[3,4] The whole apparatus was able to be operated continuously without changing recording paper for about 12 days.

As a typical example, Fig. 3 shows the observations from November 10–13, 1956. Our laboratory in Kyoto (E 139°29.3′, N 35°42.4′) is about 400 km away from the standard frequency station JJY in Tokyo (E 135°47.5′, N 35°01.7′). During the day (0700–1600), a radio wave of 4 mc is reflected by the E layer and the received frequency was very stable as shown by the flat curve in Fig. 3, though the field intensity was rather weak. Therefore, the virtual height of the E layer at which the radio wave was reflected was concluded to be almost constant. This is consistent with the constancy of the virtual height of the maximum electron density of the E layer, which is widely known. At night, the electric field intensity was strong but was accompanied

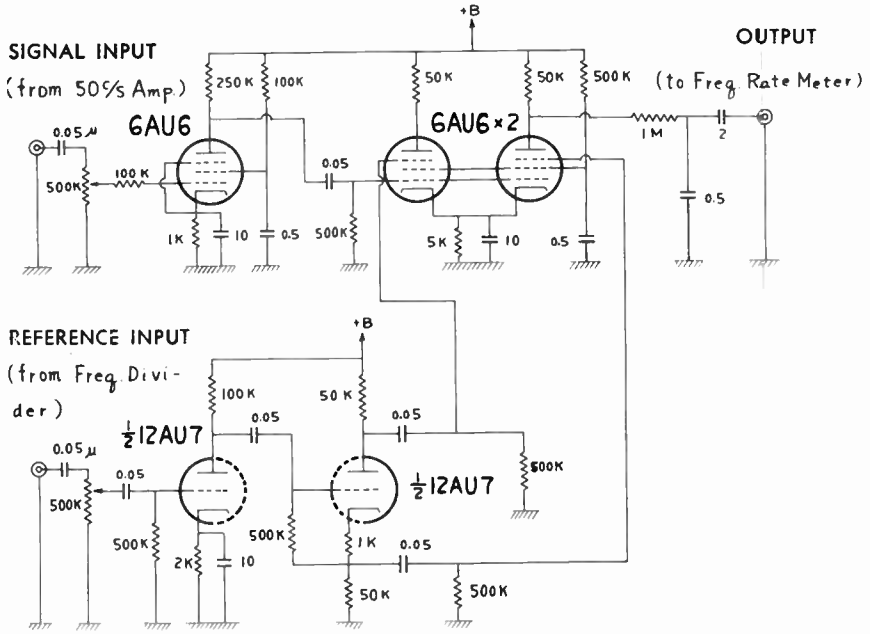

Fig. 2—Schematic diagram of the beat detector.

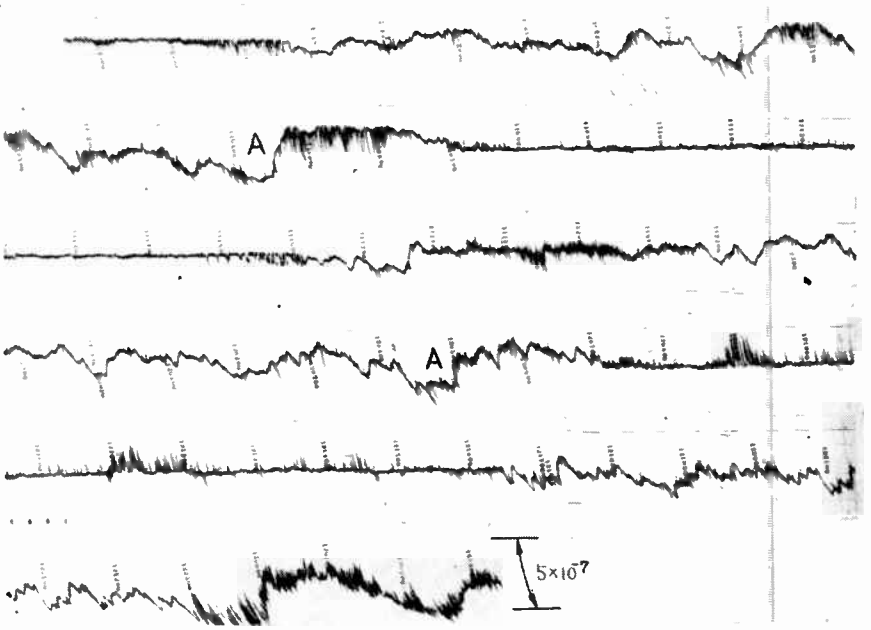

Fig. 3—A typical example of observations: continuous recording of the beat between the received frequency of 4 mc from JJY and that of the quartz chronometer (100 kc). Deflection downwards corresponds to the increase of the received frequency. Time (JST) is represented in figures, in such a way that the first two denote the date of November, 1956; the second, the hour of the day; and the last, the minutes. *e.g.*, 101500 stands for 1500, November 10, 1956.

by deep fadings, and the received frequency fluctuated in the magnitude of the order of 10^{-7} as seen in Fig. 3. In this case, the radio wave was reflected by the F layer. The peak denoted by point A in Fig. 3 appeared just before 0500 every day, so from this time, the E layer seemed to become rapidly appreciable and the radio wave became reflected by the E layer again. This method could be developed so that more detailed information about the ionosphere might be obtained, for example, dynamic behavior and small fluctuation in short time. Since an inverted-L-type antenna 20 meters long was used, the radio waves coming by different paths were received. For further precise observations, a directional receiving antenna would be necessary.

The authors appreciate the conveniences given by S. Kurachi and T. Nagatake of the standard station JJY.

I. Takahashi, T. Ogawa,
M. Yamano, A. Hirai,
and M. Takiuchi
Department of Physics and
Abuyama Seismological Observatory
Kyoto University
Kyoto, Japan

* Received by the IRE, May 13, 1957.

[1] I. Takahashi, T. Ogawa, M. Yamano, A. Hirai, nd M. Takeyama, "Stark modulation atomic clock," *ev. Sci. Instr.*, vol. 27, pp. 739–745; September, 1956.

[2] See, *e.g.*, J. M. Steele, "The standard frequency monitor at the National Physical Laboratory," *Proc. IEE*, vol. 102, part B, pp. 155–165; March, 1955.

[3] W. C. Elmore and M. Sands, "Electronic Experimental Techniques," McGraw-Hill Book Co., Inc., New York, N. Y., p. 202; 1949.

[4] R. M. Kloepper and F. E. Hoecker, "A double-channel, direct reading, low frequency counting rate meter and counting rate comparator," *Rev. Sci. Instr.*, vol. 20, pp. 17–22; January, 1949.

On the Statistics of Individual Variations in Productivity in Research Laboratories*

Unfortunately, Mr. Shockley's observations in the above paper,[1] include no mention of creative productivity resulting from incentives other than an annual salary.

That approximately half of the annual patent output goes to independent inventors, with no salary consideration whatsoever, is indicated by patent statistics. Here, creativity is defined by the patent statutes, as contrasted with published material of other types—creative, analytical, or merely reportorial—which form so large a part of Shockley's case histories, wherein the annual salary appears to constitute the chief incentive.

It is generally recognized that special incentives, such as financial rewards over and above a salary, produce greater invention productivity than mere elevation of professional stature as measured by paper publication rate or salary alone. For this reason, unsalariedindependent inventorsand salaried inventors with extra incentives produce much more creative output than the "salary-only" researchers.

However, the project team concept, so widely practiced in the larger industrial laboratories, is not very amenable to the extra compensation plan, although some of these laboratories do use it to some not very remunerative degree. But with the independent inventor, financial incentive is almost always the prime incentive. But, his creative activities are not confined by company policies into narrow channels.

Since promotion of scientific and engineering creativity is now so much in the forefront of our public's concern, especially in view of Russia's strenuous efforts to achieve this creativity, it appears that the key to the preservation of the wellsprings of our very way of life itself, is the restoration of the stimuli which have worked so well in the past. These fruitful incentives have all but disappeared in the workings of our large industrial laboratories, which are so frantically outbidding one another for our young scientists and engineers.

It has been proven many times that creativity lies in the individual mind and not in the project team. The latter, with many specialized-training members, can effectively and quickly whip the raw creation into commercially usable shape, but it can never invent anything; nor has it any real incentive to do so. This applies almost as well to the individual members of these teams simply because the catalytic stimuli are lacking.

"Our species is the only creative species, and it has only one creative instrument, the individual mind and spirit of man. There are no good collaborations, whether in music, in art, in poetry, in mathematics, in philosophy. Once the miracle of creation has taken place, the group can build and extend it, but the group never invents anything. The preciousness lies in the lonely mind of man."[2]

When those who set policies in our large industrial enterprises realize these fundamental facts, and act on them wisely, the tradition of Yankee ingenuity will again come into full flower, and we need never fear Russia or any other nation. But if we continue to allow our former system of adequate incentives for invention creativity to retrogress, as it has been during the past 30 years, we will be as insecure industrially as we would be biologically, if we reduced, to a tenuous thread, the stimuli and rewards for reproduction of our species. We are now well along that road, for the patent output has already dropped to almost half of that of a quarter century ago.

As a constructive and informative suggestion, may I add that for several years now our Congress has been holding hearings and receiving reports on the workings of our Patent System, and in my opinion, a study of these workings and the various bills for improvement of this system would be very worthwhile.

BENJAMIN F. MIESSNER
Miessner Inventions, Inc.
Morristown, N. J.
(Also Pres., Patent Equity Assn.)

[2] Quoted from J. Steinbeck, "East of Eden," by *Reader's Digest*, p. 20; August, 1957. See also, C. Fadiman (ed.), "American Treasury." Harper and Brothers, New York, N.Y.

Author's Comment[3]

Mr. Miessner's thoughtful comments evidently represent an experienced and sincere evaluation of the relative importance of various incentives in provoking invention. His professional experience is quite different from mine and this may explain why his views are not ones I can wholly accept.

Actually, in his discussion of incentives, he starts a new subject and one which I did not attempt to treat in my paper. I think it would be much more difficult to deduce quantitative conclusions about incentives than about productivity.

I disagree with Miessner's main conclusion. I am not an advocate of a system which gives specific monetary rewards to a member of an industrial laboratory for the filing of a patent application or the issuance of a patent. I think the disadvantages of such a system far outweigh the advantages. The chief disadvantages, in order of increasing importance, are:

1) Individuals are motivated to get inventions processed regardless of worth. This clutters up the company's patent department, leads to patent emphasis for the most aggressive rather than the most brilliant inventor, and compounds confusion in the patent literature.

2) The emphasis of the work of the development engineer is shifted towards claiming originality rather than creating.

3) Cooperation between individuals and the free flow of ideas is inhibited.

An inventor in a conference will hold back ideas which might lead to inventions until he has had an opportunity to work them up to the point where his rights are preserved. More ill will results from circumstances surrounding the determination of who invented what when the winners get a specific financial reward. While at Bell Telephone Laboratories, where I was one of the most active inventors over a period of several years, I was often glad that no patent incentive system existed. I am sure it would have made my relationship with the members of my group much more difficult if I had been getting extra money for making inventions stimulated by their activities.

Furthermore, there are grave difficulties in trying to assess the work of an application or patent. To give a fixed reward for each application is unjust. To give a reward determined by executive judgment is much better. In fact, this is essentially what is done now and by using executive judgment, patents, publications, and other factors are weighed in a subjective way[4] and used to determine salary.

I disagree with Miessner's paragraph on the project team. I believe that the environment of a project team can be highly stimulating to the individual. In my own case, I recall that the basic thinking preceding the invention of the junction transistor was stimulated by an active experimentation program on semiconductor surfaces.

Fortunately, we live in a time and country where many patterns of activity are possible. Here, Miessner and I agree in personally seeking more challenge and stimulation outside of a large organization. Depending on his tastes, the outstanding young engineer can find or make his opportunity today either as a member of a very large and secure team with less personal incentives, or as an independent inventor or consultant with maximum incentives, or in the middle ground of smaller enterprises like my own.

WILLIAM SHOCKLEY
Shockley Semiconductor Lab.
of Beckman Instr. Inc.
Mountain View, Calif.

[4] Shockley, *op. cit.*, p. 287.

Letter from Mr. Miessner[5]

I agree with Mr. Shockley's three objections to specific monetary awards for creative work in industrial laboratories, but individual awards are made nevertheless in inventive credit for patent applications, authorship of papers, or promotion in rank, not to mention monetary awards in the form of salary increases. Therefore, these objections, as well as his others, are applicable in either case, to project teams in the large laboratories.

* Received by the IRE, March 18, 1957.
[1] W. Shockley, PROC. IRE, vol. 45, pp. 279–290; March, 1957.

[3] Received by the IRE, April 25, 1957.

[5] Received by the IRE, June 14, 1957.

As to the project team environment, I can think of no better argument against it than H. L. Mencken's "The Cosmic Secretariat," reprinted in his more recent "Crestomothy." Additionally I may mention that, when an outstanding ability develops in such teams, that individual, more often than not, leaves it for the more rewarding climate of individual effort, as evidenced by Mr. Shockley's own experience. Mr. Mueller[6] has also strongly supported my own convictions anent project team creativity.

I still maintain that the most favorable climate for most productive creativity does not exist in the project teams of our large laboratories and that some satisfactory solution must be found if we, as a nation, are to match the reported incentives now prevalent in our chief competitor, Russia.

B. F. MIESSNER

[6] R. E. Mueller, "A note on the limits of brainstorming," PROC. IRE, vol. 45, p. 874; June, 1957.

A General Circuit Theorem on Rectification*

The prospect of achieving rectification using nonlinear capacitors and nonlinear inductors with dc bias would appear to be promising from the point of view of avoiding losses inherent in the nonlinear resistors in present circuits. No nonlinear resistors (diodes, switches, etc.) are perfect, and hence energy is always lost in the rectification process.

The circuit of Fig. 1 illustrates an elementary application of this idea. A sinusoidal voltage source feeds the linear resistance R, representing the load, through a

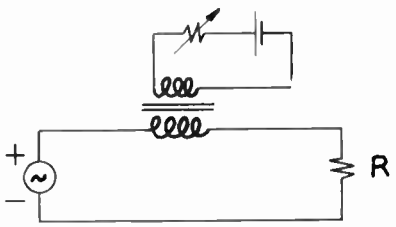

Fig. 1.

nonlinear inductance biased to the knee of the saturation curve by a dc current in a second winding. However, analysis of this circuit gives zero average current through the load, regardless of the shape of the magnetization curve or the bias point.

Unless one is easily discouraged, he may not be convinced that this one example disproves the possibility of obtaining rectification by some other combination of nonlinear reactive elements. One must also consider the possibility of using more than one source in the circuit. Speculation on these possibilities may be ended once and for all by the following theorem.

> Theorem: It is impossible to obtain a rectified dc power output from an ac source or sources unless nonlinear resistance is present in the circuit.

To prove this theorem, consider a general network containing any number of sinusoidal voltage and current sources, nonlinear capacitors, nonlinear inductors, and *linear* resistors. The inductors may be permanently magnetized and may be coupled to other parts of the circuit. The reactive elements may have hysteresis loss, but other losses, such as eddy current loss, must be represented by equivalent linear resistance.

The most general branch of this network is as shown in Fig. 2, where only the resistance need be linear. $\tilde{L}_k$ includes all series elements whose voltage drop depends on a rate of change of flux linkages, and $\tilde{C}_k$ includes all elements whose voltage drop depends on the amount of stored charge.

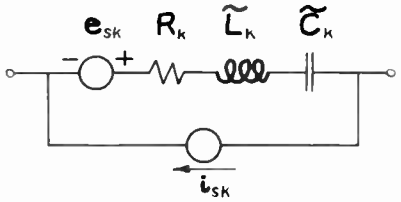

Fig. 2.

All branches containing series capacitance may be eliminated from further consideration, since any dc currents must flow around closed loops without capacitance. Thus, the problem reduces to a consideration of the subgraph obtained by eliminating these branches.

Next, Kirchhoff loop equations for the average voltages across the elements are written for this subgraph. The average voltage across an inductance is shown to be zero as follows:

$$\frac{1}{T}\int_0^T N\frac{d\phi}{dt}\,dt = \frac{N}{T}\int_0^T d\phi = \frac{N}{T}\left[\phi(T) - \phi(0)\right] = 0,$$

where T is the period if all sources have the same frequency. ϕ is the total equivalent flux, including mutual flux. If the frequencies are different, T may be some common period. If the frequencies are arbitrary irrational numbers, T may be made to approach infinity; that is, the average must be taken over a long time. Note that the above is still true even if hysteresis loss is present.

The average voltages or currents of the ac sources are, of course, zero. Thus, the equations reduce to sums over the dc voltage drops across the resistors alone. Since the resistors are all linear, the dc voltage drop for any resistor is given by the product of the resistance and the average value of the current.

The problem is, therefore, equivalent to that of a resistive network in which all sources are zero. The voltage across any resistor is zero. Thus, the average voltage across any resistor in the general nonlinear network with linear resistors is also zero.

Finally, a few words may be said concerning the general nonlinear network, wherein nonlinear resistors are included. Here, the currents from the capacitance branches again have an average value of zero. However, the voltage drop across the nonlinear resistors due to these currents is not necessarily zero. One may, therefore, utilize these currents to decrease the average power loss in the nonlinear resistors for a given average voltage and average current. By the same reasoning as in the case with linear resistors, one sees that the amount of rectified power output depends directly on the average voltage and average current in the nonlinear resistors. For example, for the case of a circuit with one linear and one nonlinear resistor, the product of the average voltage drop and average current for the nonlinear resistor is the negative of the dc power for the linear resistor.

Thus, in the general case one may utilize nonlinear (or linear) reactive elements to optimize the efficiency of rectification for a given dc power output when using imperfect nonlinear resistors.

JAMES W. GEWARTOWSKI
Electronic Labs.
Stanford University
Stanford, Calif.

A Calibration Procedure for Microwave Radiometers*

One of the persistent problems of microwave radiometry is the calibration of the radiometer in terms of the absolute temperature of a thermal source. The usual method is to substitute a noise source, either a hot load or a gas tube, for the antenna, and to calibrate the radiometer with this source. A difficulty with this procedure is the fact that the entire antenna system, with all its losses and multiple lobes, is interposed between the source to be measured and the point at which the calibrating signal is introduced. Determination of the unknown temperature thus requires a knowledge of the complete antenna pattern, including side and back lobes, as well as the absolute gain in the forward direction. This information is not easy to obtain. In addition, matching problems are introduced by the interchange of noise source and antenna.

A calibration procedure[1] developed in this laboratory eliminates some of these difficulties, and also corrects for atmospheric absorption. Consider the idealized antenna shown in Fig. 1. A is the fractional energy radiated into (or received from) the for-

* Received by the IRE, May 6, 1957; revised manuscript received, June 10, 1957.

* Received by the IRE, June 3, 1957.

[1] R. N. Whitehurst, J. Copeland, and F. H. Mitchell, "Solar radiation and atmospheric attenuation at 6-millimeter wavelength," *J. Appl. Phys.*, vol. 28, pp. 295–298; March, 1957.

ward lobes; B, the fractional energy radiated into the side lobes; and C, the fractional energy radiated into the back lobes. Ω is the effective solid angle subtended by the for-

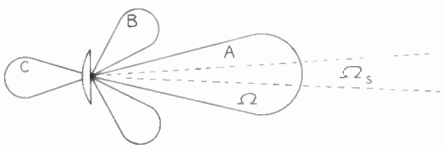

Fig. 1—Idealized antenna pattern.

ward lobes as weighted by the antenna gain, and Ω_s is the weighted solid angle subtended by the source to be measured.

Let the antenna be directed toward a point in the sky to the west of the source to be measured and be fixed in position. Assume that thermal radiation is received from the atmosphere in the forward lobes and from the ground and surroundings in the side and back lobes. If the atmosphere is assumed isothermal at ambient temperature, T_0, and the average temperatures "seen" by the side and back lobes are T_B and T_C, respectively, the antenna temperature is

$$T_1 = AT_0(1 - e^{-TVA \sec \theta}) + BT_B + CT_C$$

where TVA is the total attenuation in a vertical path through the atmosphere, and θ is the angle between the direction of observation and the zenith.

When the source in its westward motion moves into the center of the beam, the antenna temperature becomes

$$T_2 = T_1 + \frac{\Omega_s}{\Omega} AT_s e^{-TVA \sec \theta}$$

where T_s is the weighted mean source temperature.

Finally, let a piece of microwave absorber at ambient temperature be placed so that it intercepts only the forward lobes. The antenna temperature becomes

$$T_3 = AT_0 + BT_B + CT_C.$$

Suppose that the radiometer output scale deflections corresponding to temperatures T_1, T_2, and T_3 are d_1, d_2, and d_3, respectively. Then

$$d_2 - d_1 = k(T_2 - T_1) = k \frac{\Omega_s}{\Omega} AT_s e^{-TVA \sec \theta}$$

and

$$d_3 - d_1 = k(T_3 - T_1) = KAT_0 e^{-TVA \sec \theta}$$

where k is the radiometer sensitivity. Solution of these equations yields, for the weighted mean source temperature,

$$T_s = \frac{\Omega}{\Omega_s} \frac{d_2 - d_1}{d_3 - d_1} T_0.$$

Therefore, the three deflections plus knowledge of the shape of only the forward lobes of the antenna pattern are sufficient to determine the average source temperature in terms of ambient temperature. The ratio Ω/Ω_s is easily determined graphically.[1]

The primary advantage of this procedure is that the antenna losses and the radiation in the side and back lobes are included as part of the radiometer. They raise the noise figure but do not affect the calibration.

The assumption that the atmosphere is isothermal at T_0 needs examination. Actually, of course, it is not. However, except at large zenith angles, it may be assumed isothermal at some temperature, which must be near ambient since most of the contribution is from the lower layers of the atmosphere. Analysis shows that if the attenuation is reasonably small a large error in the assumed atmospheric temperature would be required to cause a significant error in the source temperature measurement. A verification of the validity of this assumption has been made experimentally. If it were significantly in error, the measured temperatures would depend on zenith angle. No such dependence has been found, either at 6 or 7.5 mm wavelength.

R. N. Whitehurst
F. H. Mitchell
University of Alabama
University, Ala.
J. Copeland
North American Aviation
Downey, Calif.
Formerly University of Alabama
University, Ala.

The Effective Electrical Constants of Soil at Low Frequencies*

The anomalous electrical properties of soils at low radio frequencies can have a profound influence on the propagation of the ground wave.[1] This factor is generally overlooked. It may seem rather unusual that relative dielectric constants of the order of 10^3 prevail in many soils at frequencies of the order of 15 kc. In fact, in this frequency range Smith-Rose[2] has found that the apparent dielectric constant varies almost inversely with frequency. The apparent conductivity also varies with frequency. Usually the conductivity increases with increasing frequency becoming more or less constant at 1 mc.

It is the purpose of this note to present a simple phenomenological theory for the measured behavior of alternating current conduction in soils and rocks and low radio frequencies. It is supposed that the medium is a heterogeneous one consisting of small, highly-conducting particles each covered with a thin gaseous film. Such films occur in many instances on conduction of current from an electrolytic solution to a metallic electrode. It is quite possible that a similar condition exists in soils at rocks in situ where the pores are filled or partially filled with an electrolytic fluid. At higher radio frequencies the reactance of thin film surrounding the particle is negligible and the effective conductivity and dielectric constant would not be expected to be frequency dependent. At the lower frequencies, however, the reactance of the encasing film becomes significant and imparts an appreciable phase shift between the macroscopic current density and the applied electric field. In the analysis that follows, the particles are assumed to be spherical in shape, each with a concentric dielectric film.

A single spherical particle of conductivity σ_p, radius a, has an insulating film of thickness t_m and dielectric constant ϵ_m. The suspending medium has a conductivity σ. A conventional spherical coordinate system (r, θ, ϕ) is chosen with the origin at the center of a single particle. The applied electric field $E_0 e^{i\omega t}$ is in the polar $(\theta = 0)$ direction. The resulting potentials ϕ_p and ϕ inside and outside the particle, respectively, are solutions of Laplace's equation since the significant dimensions in the problem are small compared to the wavelength. The boundary conditions at the film are that the normal current density is continuous and that the potentials are discontinuous by an amount equal to the voltage across the film. These two conditions lead to the following equations:

$$\sigma \frac{\partial \phi}{\partial r}\Big]_{r=a+t_m} = \sigma_p \frac{\partial \phi_p}{\partial r}\Big]_{r=a} \quad (1)$$

and

$$\phi - \frac{t_m \sigma}{i\epsilon_m \omega} \frac{\partial \phi}{\partial r}\Big]_{r=a+t_m} = \phi_p\Big]_{r=a} \quad (2)$$

where it is assumed that $t_m \ll a$. The exterior potential function is then found to be

$$\phi = -E_0 r \cos\theta + \frac{E_0 a^3}{r^2}\left[\frac{1-\delta}{1+2\delta}\right]\cos\theta \quad (3)$$

where

$$\delta = \frac{\sigma}{\sigma_p} + \frac{t_m \sigma}{i\epsilon_m \omega a}.$$

Now if there are N such particles per unit volume arranged in a regular lattice, the dipole moment A per unit volume per unit applied field is

$$A = 3v \frac{1-\delta}{1+2\delta} \quad (4)$$

where $v = 4\pi a^3 N/3$ is the volume of particles per unit volume. The Clausius-Mosotti relation of dielectric theory[3] can now be employed to obtain an expression for the effective conductivity σ_e and dielectric constant ϵ_e of the array of spherical particles, so that

$$\sigma_e + i\omega\epsilon_e = \sigma\left(1 + \frac{A}{1 - A/3}\right). \quad (5)$$

To illustrate this result it is assumed that the volume loading of the particles is small (*i.e.*, $v \ll 1$) and that the conductivity of the particles is large (*i.e.*, $\sigma_p \gg \sigma$). It then follows that

$$\frac{\sigma_e + i\omega\epsilon_e}{\sigma} \cong 1 + 3v\left(\frac{1-\delta}{1+2\delta}\right). \quad (6)$$

* Received by the IRE, July 25, 1957.

[1] J. R. Wait and L. L. Campbell, "Effect of a large dielectric constant on ground wave propagation," *Can. J. Phys.*, vol. 31, pp. 456–457; April, 1953.

[2] R. L. Smith-Rose, "Measured electrical properties of soils for alternating current," *J. IEE*, vol. 75, pp. 231–237; March, 1934.

[3] H. Frohlich, "Theory of Dielectrics," Oxford University Press, London, England, p. 169; 1949.

Consequently,

$$\frac{\sigma_e}{\sigma} \cong 1 + 3v\frac{1-2X^2}{1+4X^2} \tag{7}$$

and

$$\frac{\epsilon_e\omega}{\sigma} \cong \frac{9vX}{1+4X^2} \tag{8}$$

where

$$X = \frac{l_m\sigma}{\omega\epsilon_m a}.$$

If $X \gg 1$, the particle behaves essentially as an insulator and

$$\frac{\sigma_e}{\sigma} \cong 1 - 3v/2 \text{ and } \epsilon_e\omega/\sigma \cong 9v/4X. \tag{9}$$

If the admittance of the film is very large such that $X \ll 1$,

$$\frac{\sigma_e}{\sigma} \cong 1 + 3v \text{ and } \frac{\epsilon_e\omega}{\sigma} \cong 9vX. \tag{10}$$

In both these cases the dielectric constant expressed as a parameter $\epsilon_e\omega/\sigma$ is very small compared to unity. However, if the film has an admittance of an intermediate value, the effective dielectric constant can be relatively much larger. In fact, its maximum value can be seen to occur when $X=2$ and is given by

$$\left.\frac{\epsilon_e\omega}{\sigma}\right]_{\max} \cong 18v/17. \tag{11}$$

That is, in the macroscopic sense, the phase angle between the electric field and current density can be of the order of v radians for a suspension of film-covered conducting spherical particles if $X \cong 2$.

This mechanism is a possible explanation for the large dielectric constants that have been observed in soils at low radio frequencies.[1,4]

James R. Wait
Natl. Bureau of Standards
Boulder, Colo.
Formerly at Univ. of Toronto
Toronto, Ontario, Canada

[4] D. G. Frood, Radio Physics Lab., Ottawa, Ont., Can., unpublished work.

The Gyrator in Dual Circuits*

Dual circuits are planar circuits in which every mesh of one circuit can be paired off with an intersecting mesh of the other circuit, as illustrated by Fig. 1, and in which the voltages and currents in both meshes are related by:

$$(v_i - v_j) = \delta R_0(I_i - I_j) \tag{1}$$

$$V_k - V_l = \delta R_0(i_k - i_l) \tag{2}$$

$$v_i - v_j = Z(i_k - i_l) \tag{3}$$

$$Z(V_k - V_l) = R_0^2(I_i - I_l) \tag{4}$$

where $\delta = \pm 1$.

* Received by the IRE, June 27, 1957.

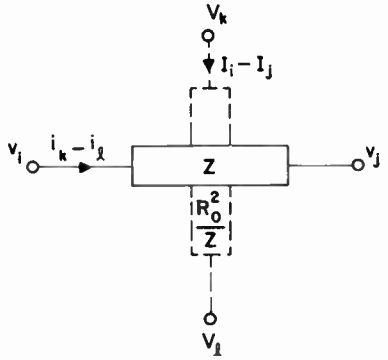

Fig. 1—Intersection meshes of dual circuits.

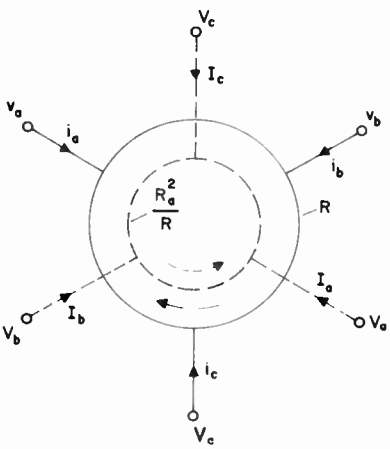

Fig. 2—Intersecting gyrators of dual circuits.

The purpose of this note is to indicate that the concept of dual circuits can be extended to circuits containing gyrators.

Consider the gyrator of Fig. 2, in which the voltages and currents are related by:

$$\begin{aligned} v_a - v_b &= Ri_c \\ v_b - v_c &= Ri_a \\ v_c - v_a &= Ri_b. \end{aligned} \tag{5}$$

Assume the existence of a dual gyrator, indicated by dotted lines in Fig. 2. The application of relations (1) and (2) to this assumed dual gyrator yields

$$(v_a - v_b) = \delta R_0 I_c, \text{ etc.} \tag{6}$$

and

$$V_a - V_b = -\delta R_0 i_c, \text{ etc.} \tag{7}$$

Combining (5), (6), and (7) we obtain

$$V_a - V_b = -\frac{R_0^2}{R} I_c, \text{ etc.} \tag{8}$$

This last relation indicates that the impedance of the assumed dual gyrator is related to that of the original one by the same relations as for paired meshes in dual circuits, except that the handedness of a gyrator is opposite that of its dual. It follows that repeating the process of obtaining the dual gyrator reproduces the original gyrator, and that no contradiction will result from the assumption of the dual gyrator specified by (8).

Marcel J. E. Golay
Philco Corp.
Philadelphia, Pa.

Noisy and Noise-Free Two-Port Networks Treated by the Isometric Circle Method*

The isometric circle method is a graphical method of transforming a complex variable by the linear fractional transformation.[1] If the variable is a complex impedance Z, then the linear fractional tranformation

$$Z' = \frac{aZ+b}{cZ+d}, \qquad ad - bc = 1 \tag{1}$$

can be interpreted as an impedance transformation through a bilateral, two-port network which, for a fixed frequency, is characterized by the four complex constants, a, b, c, and d.

The isometric circle is defined as the circle which is the complete locus of points in the neighborhood of which lengths are unaltered in magnitude by (1). The isometric circle of the direct transformation, C_d, has its center at $O_d = -d/c$ and a radius $R_c = 1/|c|$; the isometric circle of the inverse transformation, C_i, has its center at $O_i = a/c$ and the same radius.

Mathematically, transformation (1) is divided into two classes of transformations: the loxodromic transformation, characterized by $a+d$=complex, and the nonloxodromic transformation, characterized by $a+d$=real. The latter transformation is further divided into the hyperbolic, parabolic, and elliptic transformations specified by $|a+d| \gtrless 2$.

If the two isometric circles are drawn in the complex Z plane, $Z = R + jX$, the following graphical constructions yield a graphical method for transforming Z into Z' in the loxodromic case (see Fig. 1):

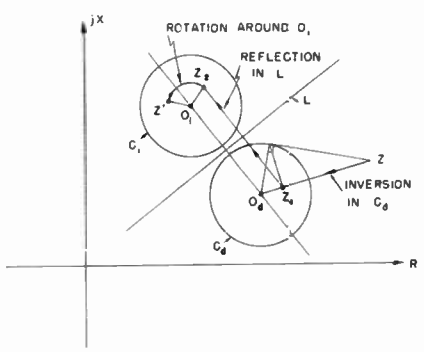

Fig. 1—The isometric circle method.

1) an inversion in the isometric circle of the direct transformation C_d, $Z \rightarrow Z_1$; 2) a reflection in the symmetry line L to the two circles, $Z_1 \rightarrow Z_2$; and 3) a rotation around the center O_i of the isometric circle of the inverse transformation through an angle $-2 \arg (a+d)$, $Z_2 \rightarrow Z'$.

The different steps for performing the graphical constructions can be expressed in analytical form.[2] Indicating a complex conjugate quantity by a star, we obtain

* Received by the IRE, June 17, 1957. This work was supported in part by the U. S. Army (Signal Corps), the U. S. Air Force (Office of Scientific Res., Air Res. and Dev. Command), and the U. S. Navy (Office of Naval Res.).

[1] L. R. Ford, "Automorphic Functions," 2nd ed., Chelsea Publishing Co., New York, N. Y.; 1951.

[2] E. F. Bolinder, "The Isometric Circle Method in Analytical Form," Res. Lab. of Electronics, M.I.T., Quart. Prog. Rep., pp. 149–152, January 15, 1957.

$$\left.\begin{aligned} Z_1^* &= \frac{\frac{d^*}{c^*}Z + \frac{|d|^2-1}{|c|^2}}{Z+\frac{d}{c}} \\ &\equiv \text{nversion in } C_d \\ Z_2 &= \frac{-\frac{a+d}{c}Z_1^* + \frac{|a|^2-|d|^2}{c|^2}}{\frac{a^*+d^*}{c^*}} \\ &\equiv \text{reflection in } L \\ Z'-\frac{a}{c} &= \left(Z_2-\frac{a}{c}\right)e^{-j2\arg(a+d)} \\ &\equiv \text{rotation around } O_i \end{aligned}\right\} \quad (2)$$

If the bilateral, two-port network is lossless, (1) takes the form

$$Z' = \frac{a'Z+jb''}{jc''Z+d'}, \qquad a'd'+b''c''=1 \quad (3)$$

where $a=a'+ja''$, etc. Eq. (3) is a nonloxodromic transformation, and in this case the third operation given above is eliminated. We obtain

$$\left.\begin{aligned} Z_1^* &= \frac{d'Z - j\frac{d'^2-1}{c''}}{jc''Z+d'} \equiv \text{inversion in } C_d \\ Z' &= Z_1^* - j\frac{a'-d'}{c''} \equiv \text{reflection in } L \end{aligned}\right\} \quad (4)$$

A plotting of the isometric circles immediately specifies the nonloxodromic transformation. If the two circles intersect, the elliptic (above-cutoff) case exists; if the circles are tangent, the parabolic (cutoff) case exists; and, finally, if the two circles are external the hyperbolic (below-cutoff) case exists.

The isometric circle method has recently been applied to impedance transformations through both lossy and lossless bilateral, two-port networks.[3-6] Often, especially when the radii of the isometric circles are large, it is convenient to use non-Euclidean hyperbolic geometry. It has been shown that for impedance transformations through lossless, bilateral, two-port networks the isometric circle method converts into two non-Euclidean reflections in two straight lines in the Cayley-Klein model of the two-dimensional hyperbolic space.[7] Similarly, for impedance transformations through lossy, bilateral, two-port networks the isometric circle method converts into two non-Euclidean reflections in two straight lines in the Cayley-Klein model of the three-dimensional hyperbolic space.[8] Finally, noisy two-port networks can be treated by extending the isometric circle method to three dimensions, so that a circle is extended to a hemisphere[9] —a method that will be discussed later.

E. Folke Bolinder
Res. Lab. of Electronics
Mass. Inst. Tech.
Cambridge, Mass.

[3] E. F. Bolinder, "Impedance Transformations by the Isometric Circle Method," Res. Lab. of Electronics, M.I.T., Quart. Prog. Rep., pp. 123–126; April 15, 1956.
[4] E. F. Bolinder, "Impedance and polarization-ratio transformations by a graphical method using the isometric circles," IRE Trans., vol. MTT-4, pp. 176–180; July, 1956.
[5] E. F. Bolinder, "Some applications of the isometric circle method to impedance transformations through lossless two-port networks," Paper presented at the URSI-USA meeting, Washington, D. C., May 22–25, 1957.
[6] E. F. Bolinder, "Study of the Exponential Line by the Isometric Circle Method and Hyperbolic Geometry," *Acta Polytech.*, No. 214, *Elec. Eng. Ser.*, vol. 7, 1957.
[7] E. F. Bolinder, "Graphical Methods for Transforming Impedances Through Lossless Networks by the Cayley-Klein Diagrams," *Acta Polytech.*, No. 202, *Elec. Eng. Ser.*, vol. 7, 1956.
[8] E. F. Bolinder, "Impedance transformations by extension of the isometric circle method to the three-dimensional hyperbolic space," *J. Math. Phys.*, vol. 36, April 1957.
[9] E. F. Bolinder, "Geometric-Analytic Theory of Noisy Two-Ports," Res. Lab. of Electronics, M.I.T., Quart. Prog. Rep., July 15, 1957.

Signal-Flow Graphs and Random Signals*

In his interesting and important paper on signal-flow graphs and random signals,[1] Huggins derives, among other results, a general expression for the correlation function of a train of pulses having a given form.

By considering separately the positive and negative ranges of the argument of the correlation function, Huggins is seemingly able to avoid the use of backward expectations and probability density functions in his analysis. However, upon a careful examination of the underlying assumptions, it appears that backward probabilities and expectations must be considered even when the argument τ is restricted to positive values, and that the general expression given by Huggins is in need of some modification. The following analysis clarifies this point and, incidentally, provides an alternative and somewhat simpler method of obtaining a general expression for the correlation function of a train of pulses.

Consider the random signal generator shown in Fig. 1, in which, for simplicity,

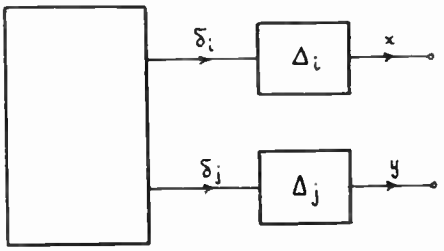

Fig. 1—Generation of the pulse trains x and y impulse trains δ_i and δ_j.

there are just two component function generators, Δ_i and Δ_j, with impulsive responses $\Delta_i(t)$ and $\Delta_j(t)$, respectively. We shall not assume, as is done by Huggins, that $\Delta_i(t)$ and $\Delta_j(t)$ have a finite duration and vanish for negative t.

The component function generators Δ_i and Δ_j are "triggered" by events ϵ_i and ϵ_j, in the sense that at each occurrence of ϵ_i an impulse is applied to Δ_i, and at each occurrence of ϵ_j an impulse is applied to Δ_j. Thus, the inputs to Δ_i and Δ_j have the form of trains of *impulses* which will be denoted by δ_i and δ_j, respectively. Correspondingly, the *pulse* trains at the outputs of Δ_i and Δ_j will be denoted by $x(t)$ and $y(t)$.

Now the cross-spectral density of $x(t)$ and $y(t)$ is related to that of δ_i and δ_j by the well-known relation

$$\Phi_{x_iy_j}(s) = \Delta_i(-s)\Delta_j(s)\Phi_{\delta_i\delta_j}(s), \quad (1)$$

where $\Delta_i(s)$ and $\Delta_j(s)$ denote the bilateral Laplace transforms of $\Delta_i(t)$ and $\Delta_j(t)$, and $\Phi_{\delta_i\delta_j}(s)$ denotes the cross-spectral density of the impulse trains δ_i and δ_j. Thus, the determination of $\Phi_{x_iy_j}(s)$ is reduced to the calculation of $\Phi_{\delta_i\delta_j}(s)$.

To calculate $\Phi_{\delta_i\delta_j}(s)$, it is expedient to replace the impulses in δ_i and δ_j by narrow pulses of width dt and amplitude $1/dt$, and then let dt approach zero. With reference to Fig. 2, it is seen that, for positive τ, the

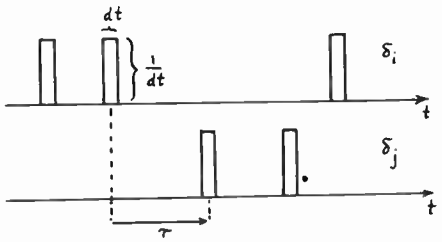

Fig. 2—Pulse train approximations to δ_i and δ_j.

correlation function of δ_i and δ_j is given by

$$\phi_{\delta_i\delta}(\tau) = \langle \delta_i(t)\delta_j(t+\tau)\rangle_{Av} = \frac{1}{dt^2}p_{ij}(\tau)dt^2 \quad (2)$$

where $p_{ij}(\tau)dt^2$ is the probability of joint occurrence of ϵ_i in the interval $(t, t+dt)$ and ϵ_j in the interval $(t+\tau, t+\tau+dt)$.

Now $p_{ij}(\tau)$ is given by

$$p_{ij}(\tau) = p_i u_{ij}(\tau) \quad (3)$$

where p_i is the steady-state probability of occurrence of ϵ_i, and $u_{ij}(\tau)$ is the expectation density of the occurrence of ϵ_j τ seconds after the occurrence of ϵ_i. Consequently,

$$\phi_{\delta_i\delta_j}(\tau) = p_i u_{ij}(\tau) \text{ for } \tau > 0 \quad (4)$$

and similarly

$$\phi_{\delta_i\delta}(\tau) = p_j u_{ji}(-\tau) \text{ for } \tau < 0. \quad (5)$$

Eqs. (4) and (5) can be combined into the single equation

$$\phi_{\delta_i\delta}(\tau) = p_i u_{ij}(\tau) + p_j u_{ji}(-\tau) \quad (6)$$

on the understanding that $u_{ij}(\tau)$ and $u_{ji}(\tau)$ are zero for negative τ. Thus, the cross-spectral density, which is the bilateral La place transform of $\phi_{\delta_i\delta_j}(\tau)$, is given by

$$\Phi_{\delta_i\delta}(s) = p_i U_{ij}(s) + p_j U_{ji}(-s), \quad (7)$$

where $U_{ij}(s)$, the Laplace transform of $u_{ij}(\tau)$, is the transmission (in signal-flow graph sense) from node i to node j.

The desired expression for $\Phi_{x_iy_j}(s)$ can now be obtained by substituting $\Phi_{\delta_i\delta_j}(s)$ in (1):

$$\Phi_{x_iy_j}(s) = \Delta_i(-s)\Delta_j(s)\left[p_i U_{ij}(s) + p_j U_{ji}(-s)\right]. \quad (8)$$

* Received by the IRE, June 25, 1957.
[1] W. H. Huggins, Proc. IRE, vol. 45, pp. 74–86; January, 1957.

More generally, when the signals $x(t)$ and $y(t)$ consist of additive combinations of the outputs of two or more component function generators, the expression for the cross-spectral density of x and y becomes

$$\Phi_{xy}(s) = \sum_i \sum_j \Delta_i(-s)\Delta_j(s)\left[p_i U_{ij}(s) + p_j U_{ji}(-s)\right], \quad (9)$$

where i and j range over the indices of the component function generators of x and y, respectively.

In piecing together the two parts of $\phi_{\delta_i\delta_j}(\tau)$, it should be noted that a delta function occurring in $u_{ij}(\tau)$ at $\tau=0$, will also occur in $u_{ji}(-\tau)$. Hence, to avoid duplication it is necessary to split the delta function in two halves and associate one half with $u_{ij}(\tau)$ and the other with $u_{ji}(-\tau)$. This is equivalent to replacing $U_{ij}(s)$ in (9) with $U_{ij}(s)-\frac{1}{2}$ whenever the corresponding $u_{ij}(\tau)$ has a delta function at $\tau=0$.

The result expressed by (9) can be put into a different though equivalent form involving backward expectations. Thus, let $v_{ij}(\tau)d\tau$ denote the conditional probability that ϵ_i occurred in the interval $(-\tau, -\tau-d\tau)$ given that ϵ_j occurred at $\tau=0$. Then $v_{ij}(\tau)$ is the backward expectation density, which is related to the forward expectation density $u_{ij}(\tau)$ by the equation

$$p_i u_{ij}(\tau) = p_j v_{ij}(\tau) \quad (10)$$

or, in terms of transmission functions,

$$p_i U_{ij}(s) = p_j V_{ij}(s), \quad (11)$$

where $V_{ij}(s)$, the Laplace transform of $v_{ij}(\tau)$, is the backward transmission function from i to j.

Thus, in terms of both forward and backward expectation densities, (9) can be written as

$$\Phi_{xy}(s) = \sum_i \sum_j \Delta_i(-s)\Delta_j(s)p_i\left[U_{ij}(s) + V_{ji}(-s)\right]. \quad (12)$$

In the foregoing analysis, we have not made use of the average message $\bar{Y}_j(s)$ which plays a central role in the method employed by Huggins. Had we done so, we would have found the following expression for $\bar{Y}_j(s)$:

$$\bar{Y}_j(s) = \sum_k \Delta_k(s)\left[U_{jk}(s) + V_{kj}(-s)\right] \quad (13)$$

which differs from that given by Huggins in the presence of the backward expectation term $V_{kj}(-s)$. Intuitively, this means that even when τ is restricted to positive values, one cannot disregard the contributions to $y(\tau)$ due to events which occurred prior to $\tau=0$.

It should also be noted that $\Phi_{xy}(s)$ as given by (9) yields both the continuous and the discrete (line) components of the power spectrum. However, some care must be exercised in the use of (9) in order to obtain the discrete component. Specifically, $\Phi_{\delta_i\delta_j}(\omega)$ [as given by (7)] should be regarded as the bilateral Fourier transform of $p_i u_{ij}(\tau) + p_j u_{ji}(-\tau)$, rather than as the sum of unilateral Laplace transforms of $p_i u_{ij}(\tau)$ and $p_j u_{ji}(-\tau)$. For example, in the case of the Poisson process considered by Huggins, $p_i=p_j=\lambda$, $u_{ij}(\tau)=\delta(\tau)+\lambda$ for $\tau>0$, and hence $\phi_{\delta_i\delta_j}(\tau)=\delta(\tau)+\lambda$ for all τ. Consequently, $\Phi_{\delta_i\delta_j}(\omega)=1+\lambda\delta(\omega)$ and the spectral density function is given by $\Phi_{xy}(\omega)=\lambda+\lambda^2\delta(\omega)$, which exhibits a line of magnitude λ^2 at $\omega=0$.

L. A. Zadeh
Dept. of Elec. Eng.
Columbia University
New York 27, N. Y.

Author's Comment[2]

The general expression (9) for the correlation function given by Zadeh is an important improvement upon the results of my paper in that it avoids the piecing together of partial solutions and thus eliminates a dangerous pitfall for the unwary. In particular, if in (20) of my paper, one uses the expected signal $\bar{Y}_j(s)$ valid for all τ by including the backward expectation given by Zadeh, there results

$$\bar{Y}_j(s) = \sum_k \Delta_k(s)\left[U_{jk}(s) + \frac{p_k}{p_j}U_{kj}(-s)\right]. \quad (23a)$$

and

$$\Phi_{xy}(s) = \sum_j p_j\Delta_j(-s)\bar{Y}_j(s) \quad (20)$$

where the index j ranges over all symbols of the x signal. This expression is a correct representation of the correlation function for all τ and the inconsistencies that I handled as the "negative-τ artifact" are avoided. In addition to making these changes in my paper, the interested reader should also replace (23b) by

$$\bar{X}_k(s) = \sum_j \Delta_j(s)\left[U_{kj}(s) + \frac{p_j}{p_k}U_{jk}(-s)\right]. \quad (23b)$$

With these changes suggested by Zadeh, the four paragraphs of my paper leading to (26) are unnecessary and should likewise be deleted. Fortunately, the artifact corrections led to the correct final results in each of the specific examples given in my original paper. I am indebted to Zadeh for showing how these difficulties can be avoided in an elegant and systematic way.

W. H. Huggins
Johns Hopkins University
Baltimore 18, Md.

[2] Received by the IRE, June 25, 1957.

How to Prepare a Talk*

Several times, prior to speaking at IRE meetings, I have been thoughtfully supplied with a reprint of a generally admirable article, "How to Address the American Physical Society," by K. K. Darrow.

I agree with most of Dr. Darrow's remarks. I am sure that his advice "2) Write out your speech in advance and commit it to memory," and "3) If you cannot memorize your manuscript read it aloud," has led to many fine presentations; his own incomparable talks may serve as an example. I believe, however, that this is not the only way to deliver an acceptable talk, and indeed I doubt that it is the best way for most people.

My advice would be something as follows: First, think over what you have to say and make notes in the form of headings; second, go into a room, shut the door, note the time, and try to give the talk; third, think over points at which you have had difficulty, revise your notes, and rehearse difficult portions; fourth, repeat this process until you can give the talk smoothly and in the time allotted. This should not result in a fixed set of words.

I believe that following my prescription will result in a good talk, that it will help the speaker to answer questions, and that it will make it increasingly easy for him to speak.

I realize that this matter may be controversial. After having received a reprint of Dr. Darrow's estimable remarks on several occasions, I feel like starting a controversy.

John R. Pierce
Bell Telephone Labs.
Murray Hill, N. J.

* Received by the IRE, June 24, 1957.

An Extension of the Kelly Betting System to Binary Decision Feedback*

A recent paper by Kelly[1] considers the transmission of the results of a chance situation over a one-way noisy communication channel, permitting a gambler to place bets at the original odds. The paper studies the exponential rate of growth of capital that results therefrom, and demonstrates that the maximum growth occurs at a rate equal to the capacity of the channel.

The following discussion extends the application of Kelly's approach to a two-way communication link involving binary decision feedback. In this system, the receiver has the option of rejecting the received signal as ambiguous and of requesting a repeat from the transmitter over an error-free feedback path. The decision process considered here uses two thresholds to define the region of ambiguity.

In showing the application of the Kelly method to the two-way case, the information rate of the binary decision feedback system is derived first. Let n be the average number of transmissions per message and let q_A be the probability that the finally accepted message is correct. In N transmissions there will be N/n accepted messages, each containing the information $[1+q_A \log q_A + (1-q_A)\log(1-q_A)]$. Therefore, the information per transmitted symbol, I, is

* Received by the IRE, July 9, 1957. Supported by the Air Force Cambridge Res. Ctr, Air Res. and Dev. Comm., under Contract No. AF 19(604)1964.

[1] J. L. Kelly, Jr., "A new interpretation of information rate," *Bell Sys. Tech. J.*, Vol. 35, pp. 917–926; July, 1956.

$$I=\frac{1}{N}\binom{N}{n}[1+q_A \log q_A+(1-q_A)\log(1-q_A)]$$

$$=\frac{1}{n}[1+q_A \log q_A+(1-q_A)\log(1-q_A)]. \quad (1)$$

Having derived the expression for information rate, we now obtain the expression for maximum rate of increase of capital in a betting situation a la Kelly. Assume that a noisy channel is reporting one of two outcomes to a gambler. If the received signal is ambiguous, the gambler asks for repetition. If the gambler rejects entirely the message on which repetition is requested (noncumulative case), there is no gain from the gambler's point of view as a result of using feedback. In this case, it is just as profitable for him not to bet at all on the uncertain event, but to wait instead for new information. If, on the other hand, he integrates the repeated digits until a certain probability threshold is reached (cumulative case), an advantage is gained. Let V_0 be the initial capital, V_N the capital after N transmissions, and l the fraction of capital invested each time. Then,

$$V_N = (1+l)^{Nq_A/m}\cdot(1-l)^{N(1-q_A)/m}\cdot V_0$$

and

$$G_{\max} = \max \lim_{N\to\infty} \frac{1}{N}\log\frac{V_N}{V_0}$$

$$= \frac{1}{n}[1+q_A \log q_A+(1-q_A)\log(1-q_A)].$$

the expression for the information rate of the binary decision feedback system.

Thus, it is seen that for the binary decision feedback system, as well as for the unidirectional system treated by Kelly, the maximum exponential rate of growth of capital is equal to the capacity of the channel.

J. J. Metzner
and L. S. Schwartz
College of Engineering
New York University
New York, N. Y

The Limits of Brainstorming*

Having had some experience with brainstorming sessions, the writer wishes to compliment Mueller for his viewpoints.[1] True enough, there is no great discovery or fabulous invention made by a body of brainstormers; however, without that body many theories and devices would still be uninvented, notwithstanding the fact that in the end there is generally only one solitary mind behind the result.

One of the greatest and most severe limitations to the mind of the trained scientist is *routine thinking*, a limitation unknown to the inventor of yesterday who scarcely went through high school. There are numerous known cases of a mind struggling with a difficult problem for a ten-year period or so, and then, *through the impetus of another mind*, the concept of the missing link appears, and in a flash of unequalled excellence of mind the great discovery is made.

The true fact behind the resultant success of any brainstorming session, and particularly a brainstorming session in network theory, perhaps in network synthesis, appears to the writer to lie in the deep thinking ability of the individual in solitary confinement, assisted in his thinking by the routine-channel-breaking power of frequent brainstorming sessions. The individual thinker, trying to penetrate the unknown, is like a blind person, trying to find his way up to the top of the jungle gym. He can lift himself to higher and higher levels, but only if he becomes conscious of the existence of additional points of support. The brainstorming session has one function, in addition to the often overlooked psychological one, and that is to give the "blind climber" enough "inner light" to see new and perhaps unexpected "points of support," upon which all the mental forces of the keen mind can be concentrated.

Expanding on the psychological factor, not mentioned by Mueller, this writer feels that it is the intellectual competition, the *game factor*, which is responsible for the stimulance of the mind, making brainstorming sessions beneficial to mankind.

As is probably implied by Mueller, one million years of one million brainstormers cannot equal one flickering second's activity of the superior mind.

Harry Stockman
Neutronics Research Co.
Waltham, Mass

* Received by the IRE, June 20, 1957.
[1] R. E. Mueller, Proc. IRE, vol. 45, p. 874; June, 1957.

An Improved Operational Amplifier*

There are two operational errors to be considered in reference to Nitzberg's comment.[1] The first, called computational error by Nitzberg arises from the fact that the internal amplifier gain or more exactly the loop gain is less than infinite. The proposed solution is to introduce an inner regenerative loop which might be adjusted to eliminate all computational error before each computation. For the case where the operational function is algebraic addition, the adjustment can more simply be made in the R_1 and R_2 components (*i.e.*, the mixing or "beta" network). In this way the computational error can be eliminated without any need for adding an internal regenerative loop.

The second error, which might be called drift error, is caused by change in values of the components due to aging and environmental influences. It is this error which frequently makes high amplifier gain a necessity. Over-all drift error can be stated as

$$E_d = \frac{A_d}{1-(KB)_n(1+A_d)}$$

where A_d is the fractional drift error in the internal amplifier gain and $(KB)_n$ is the nominal loop gain. It cannot be said that, in general, the addition of an internal regenerative loop will reduce this error. True, $(KB)_n$ will be increased but because of the characteristic nature of many regenerative circuits, A_d will also be increased and the result can be a new over-all error E_d which is larger than it was before the addition of the regenerative circuit.

There is a step which can be taken to reduce drift error where the internal errors A_d are expected to be distributed normally around zero (plus and minus). Note in the equation that for two fairly large equal values of A_d, one positive and one negative, the negative A_d will produce much the larger drift error E_d. The mixing network R_1, and R_2 can be designed or adjusted in manufacture to introduce a small positive error in the over-all gain of such size that the ensuing positive and negative A_d will each produce the same size error with respect to the over-all nominal gain. This technique can be combined with that suggested in the first paragraph (see Fig. 1). Standard value mix-

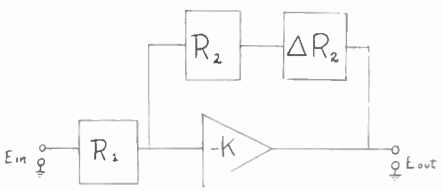

Fig. 1.

ing network components are used, computational error is eliminated and the maximum probable drift error has been minimized.

A. Bossinger
Senior Elec. Engr.
Sperry Gyroscope Co.
Division of Sperry-Rand Inc.
Great Neck, N. Y.

* Received by the IRE, June 27, 1957.
[1] R. Nitzberg, Proc. IRE, vol. 45, p. 880; June, 1957.

Letter from Mr. Staudhammer[2]

In Nitzberg's article,[2] the approximate transfer functions of two analog computer diagrams are shown. Both computer connections are designed to result in a transfer function of $-Z_2/Z_1$. However, the transfer functions, excluding grid currents and loading effects for the two configurations, are, given erroneously. The computer diagrams and their transfer functions are repeated below (Figs. 1 and 2):

$$G=\frac{e_{out}}{e_{in}}=-\frac{Z_2}{Z_1}\frac{1}{1+\dfrac{1+\dfrac{Z_2}{Z_1}}{K}} \quad (1)$$

or

$$G=-\frac{Z_2}{Z_1}\left[1-\frac{1+\dfrac{Z_2}{Z_1}}{K}+\cdots\right] \quad (2)$$

[2] Received by the IRE, July 12, 1957.

$$G' = -\frac{Z_2}{Z_1}\,\frac{1}{1+\dfrac{\left(1+\dfrac{Z_2}{Z_1}\right)}{K_1}\left|\dfrac{1+\dfrac{Z_a}{Z_b}}{K_2}-\dfrac{Z_a}{Z_b}\right|} \quad (3)$$

or

$$G' = -\frac{Z_2}{Z_1}\left\{1-\frac{1+\dfrac{Z_2}{Z_1}}{K_1}\left|\frac{\dfrac{Z_a}{Z_b}+1}{K_2}-\frac{Z_a}{Z_b}\right| + \cdots\right\}. \quad (4)$$

Since the desired transfer function is $G_d = -Z_2/Z_1$, the error in implementing G_d is as a first approximation

$$dG = \frac{Z_2}{Z_1}\left(1+\frac{Z_2}{Z_1}\right)\left(\frac{1}{K}\right)$$

for Fig. 1.

Nitzberg correctly deduces the condition for $G_d = G^1$, namely the expression in the second brackets of (3) must vanish. This is met when

$$\frac{Z_a}{Z_b} = \frac{1}{K_2 - 1} \quad (5)$$

where evidently $K_2 > 1$.

However, it is not always possible to meet exactly the condition imposed by (5). Let us assume that a mismatch of the amount P is present. Then we must find the discrepancy in G^1, dG^1 which then will be a function of the mismatch P.

For this amount of impedance mismatch we have

$$\frac{Z_a}{Z_b} = \frac{1-P}{K_2 - 1} \quad (6$$

and

$$dG^1(P) = \frac{Z_2}{Z_1}\left(1+\frac{Z_2}{Z_1}\right)\left(\frac{1}{K_1}\right)\left(\frac{+P}{K_2}\right). \quad (7)$$

The object in going from a simple circuit of Fig. 1 to a more complicated circuit like Fig. 2 is either to reduce the error dG or to permit a dG^1 as high (almost) as dG but by reducing the required gain K to some lower value K_1. Let us find the improvement possible with the circuit of Fig. 2. This improvement can be given as

$$\frac{|dG'|}{|dG|} = \frac{\left|\dfrac{Z_2}{Z_1}\left(1+\dfrac{Z_2}{Z_1}\right)\left(\dfrac{1}{K_1}\right)\left(\dfrac{+P}{K_2}\right)\right|}{\left|\dfrac{Z_2}{Z_1}\left(1+\dfrac{Z_2}{Z_1}\right)\left(\dfrac{1}{K}\right)\right|}$$

$$= \frac{KP}{K_1K_2}. \quad (8)$$

For a true improvement

$$\frac{|dG'|}{|dG|} = \frac{KP}{K_1K_2} \ll 1 \quad (9)$$

where we must not forget that K is (most usually) a very high number, and P should stand for the uncertainty in matching components [including drift of K_2 as obtainable from (6)]. Since P can normally be small, (9) is satisfied if both K_1 and K_2 are high-gain amplifiers. For example, let us find the necessary K_2 for a 99 per cent reduction in

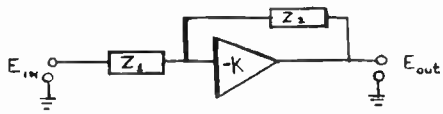

Fig. 1—G.

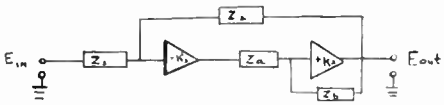

Fig. 2—G'.

error of a system with $K = 50{,}000$ if $P = 5$ per cent and $K_1 = 1000$. Eq. (8) yields

$$0.01 = \frac{50{,}000 \times .05}{1000 \times K_2} \quad \text{or} \quad K_2 = 250.$$

Thus it is obvious that a very large improvement can be made in going from circuit of Fig. 1 to circuit of Fig. 2. However, the price paid is one additional amplifier of positive gain, which in most computers is not available or can be obtained only by cascading two operational amplifiers, making three the total number of operational amplifiers used in Fig. 2.

JOHN STAUDHAMMER
Dept. of Eng.
University of California
Los Angeles 24, Calif.

Calculation of Inductance of Toroids with Rectangular Cross Section and Few Turns*

INTRODUCTION

The measurement of magnetic permeability of ferrite ring samples at radio frequencies demands that the inductance of a toroid with the sample as a core be compared to the inductance of an identical toroid with an air core. It was found, in talking with various ferrite manufacturers, that at least one of them used for the latter value, the inductance *calculated* from the known dimensions, by application of a widely used, universally accepted formula.[1] Another manufacturer's testing department used for the value of the air-cored toroid, the value *measured*, when the coil was wound on a polystyrene core. Investigation showed that these two approaches led to different results.

CIRCUMFERENTIAL INDUCTANCE

The accepted formula for the inductance of a toroid with rectangular cross section $L = 0.0117 \times$ thickness (inches) $\times n^2 \times \log_{10} r_2/r_1) \mu H$ is based upon a "current sheet" approach. It assumes that there are sufficient turns to represent the current as a "sheet" whose value is $n \times i$. A correction can be made for the fact that there is winding space between turns. This correction leads to a *reduction* of the calculated inductance.[2] Careful experiments have shown, however, that the measured inductance was always *greater* than that calculated. Table I shows this divergence. Although it is admitted that the measurements had many sources of error (*e.g.*, lead inductance), it was found on careful examination that these errors could not account for the total error. It was suspected, particularly at low number of turns, that the contribution of the circumferential component of current to inductance might be significant. Measurements showed this to be so. We shall term this correction the "circumferential component" of toroid inductance.

TABLE I

RATIO OF MEASURED INDUCTANCE TO CALCULATED INDUCTANCE FOR VARIOUS TOROIDAL CORES

No.	Description	$\frac{L \text{ measured}}{L \text{ calculated}}$
	All samples wound on 1.878 inches od $\times$1.404 inches id $\times$0.246 inch thick plexiglass cores.	
1)	194 turns no. 24 wire	1.37
2)	119 turns no. 20 wire	1.46
3)	56 turns, $\frac{1}{16}$-inch copper braid	3.96
4)	10 turns, $\frac{5}{16}$-inch copper strap	3.36
5)	10 turns, electro deposited on form with nearly constant $\frac{3}{32}$-inch spacing between turns	2.88
6)	4 turns, electro deposited on form with nearly constant $\frac{1}{4}$-inch spacing between turns	12.20
7)	2 turns electro deposited on form with nearly constant $\frac{1}{4}$-inch spacing between turns	43.00

DESCRIPTION OF EXPERIMENTS

A number of rectangular cross section lucite rings were made whose dimensions were the same as those of a ferrite sample to be tested (1.878 inches od $\times$ 1.404 inches id $\times$ 0.246 inch thick). In the first experiments these were wound with various numbers of turns of either wire or strap, but it was soon realized that with such methods it was impossible to hold the winding to the dimensions of the core, giving the effect of a larger core cross section and, most certainly, lack of agreement with theory (see Appendix).

The next technique used was to paint the turns on the plastic form with Du Pont Number 4817 Silver Paint, then to copper plate on top of this to ensure good conductivity and a solderable surface for connections.

By this means, toroids were made with 10, 4, 2, and 1 turn having a nearly constant turn spacing of $\frac{1}{16}$ to $\frac{1}{8}$ inch between turns. Two varieties of a 1-turn toroid were made, one with two circumferential turns and the other with zero circumferential turns (*i.e.*, a split ring). It might be argued that the latter is not a toroid, and the writer would not greatly dispute it except that it represents

* Received by the IRE, May 16, 1956.

[1] "Radio Instruments and Measurements," Circular C74, U. S. Dept. of Commerce, Natl. Bur. of Standards, p. 251, 1924.

[2] F. W. Grover, "Inductance Calculations," D. Van Nostrand Co., Inc., New York, N. Y., p. 170; 1946.

a limiting case. In addition to these, a 1-turn ring was made.

Measurements were carried out on a Boonton 160-A Q-meter over a range of frequencies and tuning capacitances, in order that the effects of stray capacitance could be evaluated by the well-known method of plotting wavelength squared vs tuning capacitance. The result is a straight line plot, although it was found that the experimental points did not always lie precisely on such a line, but showed considerable scattering. Rather than depend upon a graphical "guess" at the supposed plot, the average slope was computed from the experimental data and from this slope the inductance was calculated as follows:

$$Lo = \frac{\text{slope in meters}^2/\mu\mu\text{f}}{3.542}\ \mu\text{ henries.}$$

For each of the toroids tested the inductance value was also calculated. Finally the inductance of a single circumferential turn was measured, and that of the leads used was measured.

Results

The results of these tests are shown in Table II. The true toroid coil measurements are given, but the split ring results showed too much scattering to be of any use.

Columns A, B, and C of Table II give the various contributions due to toroidal, circumferential, and lead components. Column D gives the sum of these components. The last two columns give the value of L as determined by measurement. Lo is the dc value calculated from the slope of the λ^2-C plot, while the last column is the average value measured. It is noted that fair agreement exists between column D and the last two columns except in the last case. The reason supposed for the disagreement in that case is that a high leakage inductance may exist due to the unusual configuration. We may conclude, therefore, that for toroids of small numbers of turns the circumferential contribution is a large portion of the measured value. Consequently, for measurements of permeability of core materials, comparison must be made to the value of inductance calculated by the accepted formula quoted above.

TABLE II

Comparison of Measured Inductance and that Calculated by the Addition of Contributing Components

Sample No.	No. of turns	A Calculated toroidal L (μh)	B Circumferential inductance (μh)	C Estimated lead inductance (μh)	D Sum of A, B, and C (μh)	Value of Lo calculated from slope of λ^2-C plot (μh)	Average value of measured L in frequency range of measurement (μh)
5	10	0.0362	0.0620	0.0112	0.1094	0.1041	0.1056
6	4	0.00580	0.0620	0.0067	0.0745	0.0707	0.0769
7	2	0.00145	0.0620	0.0020	0.0655	0.0622	0.0631
8	1	0.0003622	0.1240	0.0067	0.1311	0.2085	0.2152

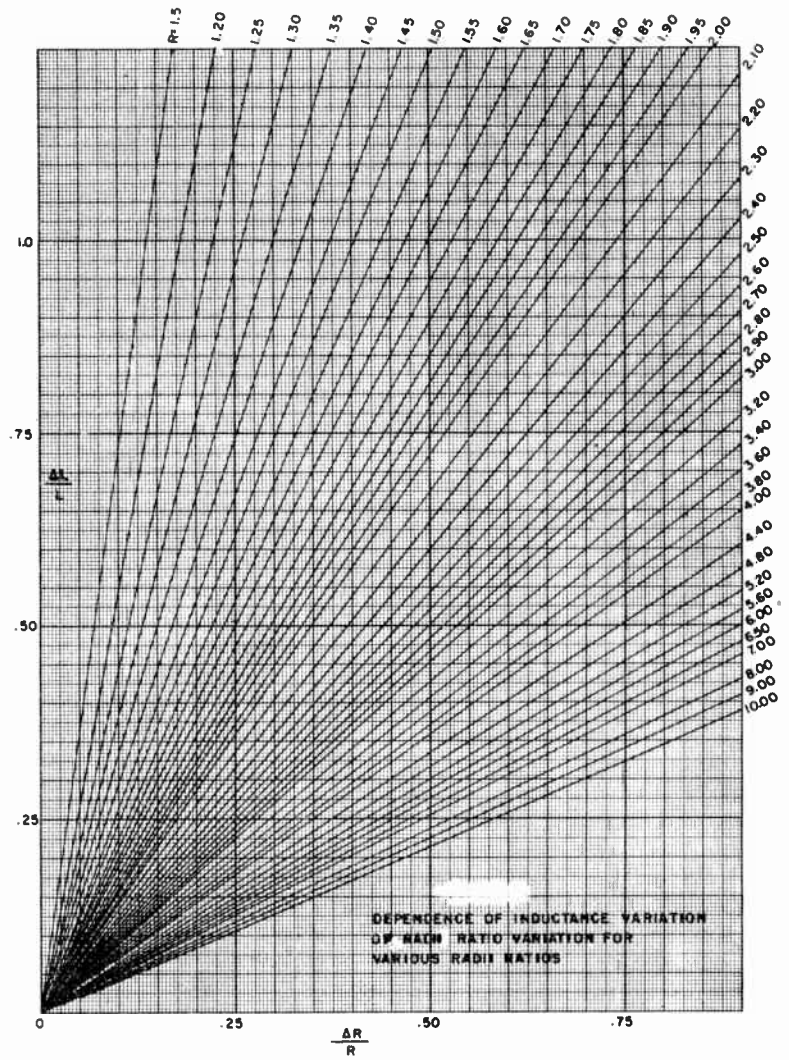

Fig. 1.

Appendix

Effect of Variations in Core Cross Section on Inductance

If we have

$$L = 0.0117 \times t \times n^2 \times \log_{10}\frac{r_2}{r_1}\ \mu\text{h}$$

where t is the thickness in inches, n is the number of turns, and $\log_{10} r_2/r_1$ is the ten-base logarithm of the radius ratio, or

$$L = 0.2 \times t \times n^2 \times \ln\frac{r_2}{r_1}\ \mu\text{h}$$

with t the thickness in meters, n the number of turns, and $\ln r_2/r_1$ natural logarithm of the radius ratio, we may investigate the effect of variations in r_2/r_1 on inductance by taking the derivative. Denoting r_2/r_1 by R we have:

$$\Delta L = 0.2 \times t \times n^2 \times \frac{1}{R}\Delta R$$

and the decimal variation is

$$\frac{\Delta L}{L} = \frac{\Delta R}{R \ln R}.$$

In other words, since $\ln R$ is always less than 1, the percentage variation in L is considerably greater than the variation in R. This effect is shown in Fig. 1.

In the core samples tested, R was 1.338, hence the error caused by either mismeasuring the core diameter or by variations in diameter (*i.e.*, eccentricity) can be great. A 5 per cent error or variation in R will cause, in this case, a 17 per cent error in L.

In the case of thickness the situation is not so bad since L varies directly with t, and a certain per cent error in t will give the same per cent error in L. But this error is additive, and a 5 per cent variation in both t and R may yield an inductance error of 22 per cent.

Richard F. Schwartz
Moore School of Elec. Eng.
University of Pennsylvania
Philadelphia 4, Pa.

Distribution Theory and the Strip Beam*

The following example may awaken some interest in the controversy for a full use and understanding of the remarkable theoretical help one can get from Schwartz's distribution theory.[1]

In many problems arising from the interaction of electromagnetic waves with an electron beam, one linearizes the solution by assuming that the physical quantities appearing in quadratic expressions are equal to the sum of a large dc and a small ac term. There is no difficulty when the ac forces on the electrons result in actions tangential to the dc trajectories (ordinary axial traveling-wave tube, for instance). There is a slight difficulty, however, when the actions are normal to the dc trajectories (transverse traveling-wave tube, carcinotron). In this case, the ac actions displace the beam from its equilibrium, creating, at times, an accumulation of space charge where none existed at equilibrium and, possibly, removing, at times, the space charge completely from where it was at equilibrium.

The Schwartzian distribution theory permits obtaining the linear solution to this problem with simple rigor. In the more common case, the beam at equilibrium is coplanar ($y=0$) and the trajectories are colinear (parallel to the z axis). The dc space-charge density is given by

$$\rho_0 = Q_0\delta_0(y) \tag{1}$$

in which $\delta_0(y)$ is Dirac's Delta function of the variable y placed at y equals zero. When the ac actions displace the beam to y equals d, the space charge density becomes:

$$\rho = Q_0\delta_d(y). \tag{2}$$

One wishes to write

$$\rho = \rho_0 + \rho_1 \tag{3}$$

or

$$Q_0\delta_d(y) = Q_0\delta_0(y) + \rho_1. \tag{4}$$

Let one project (4) on the Φ space (space of the class D of functions). Using the formula:

$$f(y) = \int_{-\infty}^{+\infty} f(y)\phi(y)dy \tag{5}$$

one obtains

$$\rho_1(\phi) = Q_0[\phi(d) - \phi_{(0)}]. \tag{6}$$

But d is small and $\phi(y)$ is a well-behaved indefinitely continuous function which can be expended in Taylor series. The first term of the expansion yields:

$$\rho_1(\phi) = Q_0 d\phi^I{}_{(0)} \tag{7}$$

in which the Latin numeral is for order of differentiation.

However,

$$\phi^I{}_{(0)} = \int_{-\infty}^{+\infty} \phi^I(y)\delta_0(y)dy$$

$$= -\int_{-\infty}^{+\infty} \delta_0{}^I(y)\phi(y)dy = -\delta_0{}^I(\phi) \tag{8}$$

hence:

$$\rho = Q_0\delta_0(y) - Q_0 d\delta_0{}^I(y). \tag{9}$$

Eq. (9) is the rigorous linear expansion of ρ. The minus sign in (9) may surprise; the formalism used is, however, the only correct one and, of course, yields the usual Taylor series expansion when such expansion exists in common algebra.

In general, one can find that

$$\delta_d(y) = \sum_0^\infty \frac{d^n}{n!}(-1)^n\delta_0{}^N(y) \tag{10}$$

(N for order of differentiation).

In the same manner,

$$Y_d(y) = Y_0(y) - \sum_0^\infty \frac{d^{n+1}}{n+1!}(-1)^n\delta_0{}^N(y) \tag{11}$$

in which $Y_d(y)$ is Heaviside's step function of the variable y starting at y equals d.

The rest of the problem is usual. Basically, one integrates the complete inhomogeneous set of Maxwell's equations to which one has added Lorentz's force equation. There are a few remarks of interest. First, in the ballistic equations, the discontinuities in the fields, due to the infinite space charge density within the beam, do not appear because charges are not affected by their own fields. Second, in the case of dc-focusing fields which are functions of the normal coordinate y, the ac displacement of the beam creates an ac variation of the force on the electrons due to the focusing fields which adds to the ac variation of this same force due to the ac velocities. Third, when solving the inhomogeneous set of Maxwell's equations, one must not forget the ac variations of the Coulomb and magnetostatic fields produced by the beam itself due to the fact that the beam has been displaced. For instance, the dc-Coulomb field (in Gaussian units) is given by

$$Ey = -2\pi Q_0 + 4\pi Q_0 Y_0(y). \tag{12}$$

When the beam is displaced by d it becomes

$$Ey = -2\pi Q_0 + 4\pi Q_0 Y_d(y). \tag{13}$$

Using the Taylor series for Y_d, one obtains an ac contribution:

$$Ey = -4\pi Q_0 d\delta_0(y). \tag{14}$$

More trivial is the fact that the normal velocity of the electron is related to the normal excursion by

$$Vy = \frac{dd}{dt}. \tag{15}$$

Finally, when all the different field contributions and the different current contributions are replaced in the inhomogeneous set of Maxwell's equations, one uses the property that the Dirac Delta function, its derivative, and ordinary functions cannot be of the same order of infinitude, so that each equation must be satisfied independently by the terms in which the Delta function appears, by the terms in which its derivative appears, and by the terms in which only ordinary functions appear.

PHILIPPE A. CLAVIER
Zenith Radio Corp.
Chicago 39, Ill.

* Received by the IRE, July 12, 1957.
[1] P. A. Clavier, "The dirac delta function," PROC. IRE, vol. 44, p. 1877; December, 1956. (See Bibliography.)

On the Use of Ferrites for Microwave Single-Sideband Modulators*

With reference to the note by Kemanis[1] on the use of a rotating quarter-wave differential phase-shift section in the form of a suitably magnetized ferrite to produce single-sideband modulation with a loss of 3 db, it is not necessary to limit the argument to a differential phase shift of $\pi/2$ radians in the section. In fact, a rotating section with any differential phase shift, when suitably used, could produce single-sideband modulation. The minimum loss attainable is dependent on the differential phase shift of the rotating section.

A simple equation deduced from circular polarization considerations gives the loss as

$$-20\log_{10}\left|\sin\frac{\theta}{2}\right| \text{ db}$$

where θ is the differential phase shift of the rotating section in radians. The losses of π and $\pi/2$ sections are 0 and 3 db, respectively.

K. I. KHOURY
Decca Radar Ltd.
London, England

* Received by the IRE, July 15, 1957.
[1] G. Kemanis, "On the cotton-mouton effect in ferrites," PROC. IRE, vol. 45, p. 687; May, 1957.

Figure of Merit of Resonance-Type Isolator*

This note studies the figure of merit of a resonance-type isolator, shown by Lax.[1] Some further results are reported, which are: 1) The optimum front-to-back ratio is derived as a function of the ferrite geometry, and 2) Lax's optimum ratio is also derived when the optimum geometry of ferrite and small microwave power are assumed.

As is well known, microwave behavior of ferrite is described in the following differential equations.

$$\frac{d\vec{M}}{dt} = \gamma(\vec{M}\times\vec{H}) - \lambda\frac{\vec{M}\times(\vec{M}\times\vec{H})}{(\vec{M}\cdot\vec{M})} \tag{1}$$

$$\frac{d\vec{M}}{dt} = \gamma(\vec{M}\times\vec{H}) - \frac{\vec{M}-\vec{M}_0}{\tau} + \frac{|M|}{|H|}\frac{\vec{H}}{\tau}. \tag{2}$$

Eq. (1) is called a Landau-Lifshitz type and (2), a Bloch-Bloembergen type.

In the resonance-type isolator in rectangular waveguide, effective tensor permeabilities χ_{xx}, χ_{yy}, and χ_{xy} are introduced as

$$\begin{aligned} m_x &= \chi_{xx}h_{0x} - j\chi_{xy}h_{0y} \\ m_y &= j\chi_{xy}h_{0x} + \chi_{yy}h_{0y} \end{aligned} \tag{3}$$

where m_x, m_y, and h_{0x} h_{0y} are magnetizations

* Received by the IRE, July 15, 1957.
[1] B. Lax, "Frequency and loss characteristics of microwave ferrite devices," PROC. IRE, vol. 44, pp. 1368–1386; October, 1956.

and external magnetic components in x and y direction, respectively.

χ_{xx}, χ_{yy}, and χ_{xy} are calculated as follows if L-L type equation is employed:

$$\chi_{xx} = \frac{\gamma^2 M(H_a + N_y - N_z M) + \lambda(j\omega + \lambda/\chi_0 + N_y)}{(j\omega + \lambda/\chi_0 + N_x)(j\omega + \lambda/\chi_0 + N_y) + \omega_r^2}$$

$$\chi_{yy} = \frac{\gamma^2 M(H_a + N_x - N_z M) + \lambda(j\omega + \lambda/\chi_0 + N_x)}{(j\omega + \lambda/\chi_0 + N_x)(j\omega + \lambda/\chi_0 + N_y) + \omega_r^2} \quad (4)$$

$$\chi_{xy} = \frac{\gamma M\omega}{(j\omega + \lambda/\chi_0 + N_x)(j\omega + \lambda/\chi_0 + N_y) + \omega_r^2}$$

where

H_a = static magnetic field applied in z direction
H = internal static magnetic field
M = magnetization due to static field
$\chi_0 = M/H$ = static magnetic susceptibility
N_x = demagnetizing factor in x direction
N_y = demagnetizing factor in y direction
N_z = demagnetizing factor in z direction
ω = operating frequency
$\omega_r = \gamma\sqrt{(H_a + N_x - N_z M)(H_a + N_y - N_z M)}$ = magnetic resonance frequency.

As Lax has derived by using perturbation theory, the optimum front to back ratio as a function of ferrite position, is given as

$$R = \frac{\sqrt{\chi_{xx}''\chi_{yy}''} + \chi_{xy}''}{\sqrt{\chi_{xx}''\chi_{yy}''} - \chi_{xy}''} \quad (5)$$

where χ_{xx}'', χ_{yy}'', and χ_{xy}'' are imaginary parts of the effective susceptibilities.

The ratio R is calculated as the following, when the incoming wave is on resonance.

$$R = \left(\frac{2\omega_r}{\lambda}\right)^2 \frac{1}{(1/\chi_0 + N_x)(1/\chi_0 + N_y)}. \quad (6)$$

The optimum ratio as a function of slab geometry, is obtained as

$$R_{max} = \left(\frac{2\omega_r\chi_0}{\lambda}\right)^2 \quad (7)$$

when demagnetizing factors N_x and N_y equal zero. As the static magnetic field is applied transversally, *i.e.*, in z direction, the optimum condition is achieved when a thin ferrite slab is so placed on the broad face of the rectangular waveguide that the flat plane of the slab is on the (x, y) plane.

As Bloembergen[2] has pointed out, two differential equations, *i.e.*, L-L and B-B types, become equivalent, provided one takes

$$\lambda/\chi_0 = 1/\tau \quad (8)$$

where τ means the same relaxation time as in the B-B type and this condition is achieved when the phenomenon is assumed in small-signal region. If this equation is introduced to (7), we have

$$R_{max} = (2\omega_r\tau)^2. \quad (9)$$

Though the result obtained in (6) seems a little bit different from the value Lax obtained, we now have the same expression.

The criterion we have for the optimum condition of the front-to-back ratio has been experimentally established by Fox, Miller, and Weiss, but the author would like to add one more experimental result.[3]

Three slabs of magnesium manganese ferrite were tested at 2800 mc. The ferrite positions were all 18 mm from the narrow wall. The width and the length were ground to 10.8 mm and 111 mm in all cases. The thicknesses of the three slabs were 7.2, 4.8, and 2.4 mm. The attenuations in two ways are shown in Fig. 1. From this experiment,

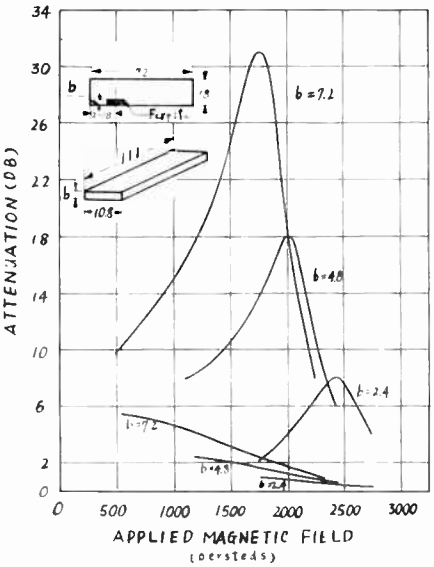

Fig. 1.

the front-to-back ratios were measured as 13, 15, and 20 for the slabs whose thicknesses were 7.2, 4.8, and 2.4 mm, respectively.

Syuiti Hayasi
Matsuda Res. Lab.
Tokyo-Shibaura Electric Co.
Kawasaki, Japan

[2] N. Bloembergen, "Magnetic resonance in ferrites," Proc. IRE, vol. 44, pp. 1259–1269; October, 1956.

[3] S. Hayasi, S. Yoshida, T. Nagai, and K. Kurihara, to be published in *Toshiba Rev.*, Japan, 1957.

The Elements of Nonreciprocal Microwave Devices*

In the above article,[1] Hogan describes the development of various types of load isolators and other nonreciprocal components.

In the discussion of resonance absorption isolators, Hogan shows, in Figs. 23 and 27, bad and good ferrite configurations, and mentions that the one in Fig. 27, is especially suited for high powers and/or low frequencies.

In this connection, it should be noted that the first practical resonance absorption isolator was described by Chait.[2] Further, the important and, at first, surprising fact that the configuration of Fig. 27 has significant advantages over that of Fig. 23, was found through experiments in our organization in the spring and summer of 1954. The configurations of Hogan's Figs. 23 and 27 were first discussed as Figs. 4 and 6 in my paper.[3]

Jorgen P. Vinding
Cascade Research Corp.
Los Gatos, Calif.

[2] H. N. Chait, "Non-reciprocal microwave components," 1954 IRE Convention Record, part 8, pp. 82–87.

[3] J. P. Vinding, "Microwave devices using ferrite and transverse magnetic field," 1955 IRE Convention Record, part 8, pp. 105–108.

* Received by the IRE, May 17, 1957; revised manuscript received, July 25, 1957.

[1] C. L. Hogan, Proc. IRE, vol. 44, pp. 1345–1368; October, 1956.

A New High-Power Frequency Multiplier*

The delicacy of electrode construction and the necessity for high current density are the two most difficult problems to be dealt with in extending the frequency of coherent oscillators into the submillimeter wave region. At this laboratory we have a great interest in the use of incoherent oscillations as a means of coping with the difficulties encountered in the coherent oscillator.

It is a well-known fact that high-frequency energy can be radiated from a dc discharge. We have found that in a microwave discharge, the frequencies of the output signals are integral multiples of the applied field frequency. Therefore, we will present the experimental results of this new phenomenon together with the possibility of developing a high-power and high-efficiency frequency multiplier in the submillimeter wave region.

Margenau and Hartman[1] have shown that the distribution function in the microwave discharge assumes the form

$$f(a, v, t) = \sum_{l=0}^{\infty} P_l(a) \Big\{ f_0^l(v) + \sum_{m=1}^{\infty} [f_m^l(v) \cos m\omega t + g_m^l(v) \sin m\omega t] \Big\} \quad (1)$$

where $P_l(a)$ is the Legendre polynomial, degree l; t is time; v is electron velocity; ω is the angular frequency of the applied field, and $a = v_z/v$. If (1) is true and if the phase of the vibrating electrons can be adjusted as desired, then a strong power at a particular frequency should be detected. We have tried to detect the harmonic components of

* Received by the IRE, July 18, 1957.

[1] H. Margenau and L. M. Hartman, "Theory of high frequency gas discharges. II," *Phys. Rev.*, vol. 73, p. 309; February 15, 1948.

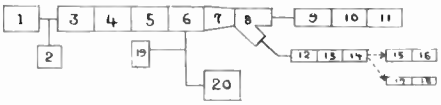

1) Magnetron M312A
2) 3000-mc wavemeter
3) Attenuator
4) Unidirectional circuit
5) Standing-wave detector
6) Discharge cavity
7) Tapered waveguide (from 3000 mc to 6000 mc)
8) Switch
9) High-pass filter
10) Standing-wave detector
11) Crystal mount or power meter
12) High-pass filter
13) Standing-wave detector
14) 10,000-mc wavemeter
15) Variable attenuator
16) Crystal mount or power meter
17) High-pass filter
18) Crystal mount
19) Vacuum gauge
20) Vacuum pump

Fig. 1—Block diagram of experimental apparatus.

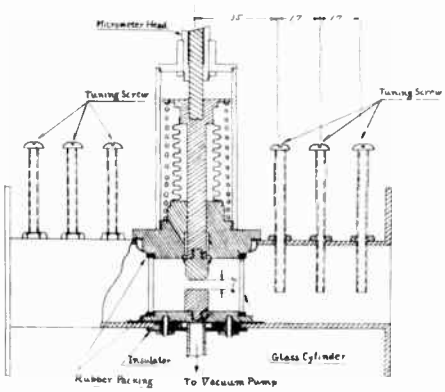

Fig. 2—Discharge cavity.

the applied field from the microwave discharge by utilizing an apparatus which was originally designed to measure the microwave breakdown voltage as shown in Fig. 1. A discharge cavity used in this experiment is shown in Fig. 2. A discharge gap composed of two cylindrical posts of 7-mm diameter is exposed in the low-pressure atmosphere, between 0.4–4 mm Hg. About 1000 volts at 50 cps is applied across the discharge gap to help initiate the microwave discharge. The output of a 3000-mc continuous-wave magnetron passes through the discharge cavity with about 3-mm gap length. The circuit impedance is controlled by six tuning screws so that a gap voltage equal to the breakdown voltage can be reached. After the discharge is started, the ac voltage is removed and the tuning screws and the gap length are readjusted to provide the best matching that can be obtained at the input circuit; at the same time, the maximum output of the particular harmonic component can be obtained. The output power is picked up through the high-pass filter. The incident wave itself includes the harmonic components, but their levels are very low. The vswr in the magnetron output is kept smaller than 1.07 throughout the experiment.

The frequency of the output signal was measured, and it was found that the very strong signals, for which the frequencies were integral multiples of the applied field frequency, were the only possible ones to be detected by our apparatus whatever the pressure and the circuit conditions of the discharge cavity might be. The harmonic components measured were the second, third and fourth. The frequency of each harmonic was as follows:

Applied field frequency	3033 mc.
Second harmonic	6070 mc.
Third harmonic	9099 mc.
Fourth harmonic	12,130 mc.

The errors of the frequencies of the second and fourth harmonics are within the error of the frequency meter used. The output frequency was constant over a wide change of pressure, although the output power changed considerably. From these facts, it is reasonable to conclude that the output frequency is exactly a harmonic of the driving field frequency. The output power of each harmonic component was a function of the circuit condition, the discharge gap length, and the pressure.

The output power of each harmonic component is compared with the maximum output power from the generator itself in Table I.

TABLE I

	Magnetron	Microwave Discharge
Fundamental	12.4 watts	—
Second harmonic	1 mw	60 mw
Third harmonic	0.3 mw	21 mw
Fourth harmonic	a few mw	0.6 mw

The output power was increased if the gap length was increased. After all conditions were adjusted to optimum, if the pressure was increased, the output was decreased. For a fixed gap length, power output decreases with increasing pressure. If power output-pressure characteristics are measured for different gap lengths, the maximum output powers are not obtained at the same pressures, but occur at lower pressures for larger gap lengths. According to our experimental results, the maximum output was obtained with a gap length of 4 mm, although this was the maximum possible length obtainable in our apparatus. Why the output power is increased as the gap length is increased is not clear, but it might be due to the loss of electrons resulting from decreased diffusion, while at the same time, the total number of electrons is increased. This fact is very important from the standpoint of electrode dimensions. It seems that effective harmonic radiation happens to occur around a special pressure-gap length condition that corresponds to the breakdown voltage minimum in the PL–V_s curve, where P is the pressure, L is the gap length, and V_s is the breakdown voltage. In general, the output power changed in proportion to the input power. The modulated waveforms of the incident wave and third harmonic were observed by the oscilloscope. Around the maximum output condition, the third harmonic waveform was almost exactly reproduced from the incident wave. However, when the output power was decreased due to the misadjustment of the circuit values and the pressure, the waveform was distorted and noise components appeared. By adjusting the tuning screws, the discharge domain could be moved from the discharge gap to the outside of it. In this case, no harmonic output was observed.

From the above mentioned experimental results, we know that a microwave discharge in the particular gas works as a high-power frequency multiplier. This frequency multiplier has the following features:

1) A large power input can be used.
2) The electrode construction is very simple and dimensions are much larger than those of the conventional type of microwave generator.
3) The efficiency of frequency conversion is better than that of the crystal frequency multiplier.

It is clear that the harmonic signal radiation is not due to plasma oscillations. The amplitude of electron vibration should be much smaller than the gap length. Thus it is expected that the harmonic current flowing through the electrode surface is smaller than that in the middle part of the discharge gap. If this is true, the minimum current density necessary to extract appreciable power would be considerably smaller than that of the conventional type of generator. It is believed that this mechanism provides a great possibility for extending the generation of microwave power into the millimeter and submillimeter wavelength range.

The authors wish to express their appreciation to Professor E. M. Boone, Director of the Electron Device Laboratory, The Ohio State University, and to Dr. E. D. Reed, Bell Telephone Laboratories, for their suggestions and for reading and revising the manuscript.

MICHIZO UENOHARA, MICHIYUKI UENOHARA, T. MASUTANI, AND K. INADA
Faculty of Engineering
Nihon University
Tokyo, Japan

Comparison of Subtraction-Type and Multiplier-Type Radiometers*

The operation of the Dicke radiometer and the two-receiver radiometer has been recently discussed by Goldstein, Tucker, and Graham.[1,2] These two multiplier-type radiometers are superior in their stability to subtraction-type radiometers used in early work of detecting noise signals.[3–6] The accuracy of a subtraction-type radiometer is dependent on the constancy of receiver gain in the time interval between the zero adjustment and the output observation. Gain changes or drift make periodic zero adjustments mandatory. However, this disadvantage of subtraction-type radiometers may be partially offset in some applications by the

* Received by the IRE, July 25, 1957. This work was supported by the U. S. Air Force, Rome Air Development Center.

[1] S. J. Goldstein, Jr., "A comparison of two radiometer circuits," PROC. IRE, vol. 43, pp. 1663–1666; November, 1955.

[2] D. G. Tucker, M. H. Graham, and S. J. Goldstein, Jr., "A comparison of two radiometer circuits," PROC. IRE, vol. 45, pp. 365–366; March, 1957.

[3] K. G. Jansky, "Directional studies of atmospherics at high frequencies," PROC. IRE, vol. 20, pp. 1920–1932; December, 1932.

[4] G. Reber, "Cosmic static," PROC. IRE, vol. 30, pp. 367–378; August, 1942.

[5] G. C. Southworth, "Microwave radiation from sun," *J. Franklin Inst.*, vol. 239, pp. 285–297; April, 1945.

[6] R. H. Dicke, "The measurement of thermal radiation at microwave frequencies," *Rev. Sci. Instr.*, vol. 17, pp. 268–275; July, 1946.

higher sensitivity and by the simplicity of design.

It is the purpose of this letter to compare the thresholds of subtraction-type and multiplier-type radiometers and to establish rates of amplifier gain variations that result in nonessential, *i.e.*, 3 db or less, threshold degradation of the subtraction-type radiometer.

The first subtraction-type radiometer considered consists of a receiver with a square-law second detector, followed by a dc balancing or subtraction device, a low-pass filter, and an indicator, as shown in Fig. 1. The power spectrum $G_1(f)$ of the detector output V_1 is obtained from the relation listed by Lawson and Uhlenbeck[7], assuming that both signal and noise have uncorrelated Gaussian amplitude distributions with zero mean and a flat input power spectrum of bandwidth α cps. Thus

$$G_1(f) = 2(\sigma_s^2 + \sigma_n^2)^2[\delta(f) + (\alpha - f)/\alpha^2]$$

where σ_s and σ_n are the rms values of signal and noise, respectively. The dc voltage component of the above spectrum is

$$(V_1)dc = \sigma_s^2 + \sigma_n^2.$$

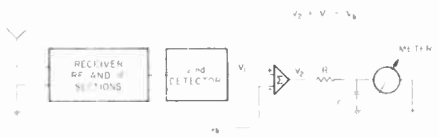

Fig. 1—Subtraction-type radiometer.

The reference voltage V_b is assumed to differ slightly from the part of $(V_1)_{dc}$ that is due to system noise. In practice, this difference may be caused by gain variations or drift of the amplifier. V_b is defined by

$$V_b = \sigma_n^2(1 - \epsilon)$$

where $|\epsilon| < 1$. The dc part of the output of the substraction circuit V_2 is

$$(V_2)dc = \sigma_s^2 + \epsilon\sigma_n^2.$$

The power spectrum of V_2 is

$$G_2(f) = 2(\sigma_s^2 + \epsilon\sigma_n^2)^2\delta(f) + 2(\sigma_s^2 + \sigma_n^2)^2(\alpha - f)/\alpha^2.$$

The dc part of the output of the low-pass filter is considered as the signal, the ac part as the noise. Designating the half-power bandwidth of the low-pass filter by γ, *i.e.*, $\gamma = 1/(2\pi RC)$ and restricting the consideration to cases where $\gamma \ll \alpha$, the indicated output signal power-to-noise power ratio is

$$\left(\frac{s}{n}\right)_0 = \frac{(\sigma_s^2 + \epsilon\sigma_n^2)^2}{(\sigma_s^2 + \sigma_n^2)^2}\,\frac{\alpha}{\pi\gamma}.$$

For small signal-to-noise ratios, *i.e.*,

$$\sigma_s^2 \ll \sigma_n^2$$

the above ratio reduces to

$$\left(\frac{s}{n}\right)_0 \approx \frac{(\sigma_s^2 + \epsilon\sigma_n^2)^2}{\sigma_n^4}\left(\frac{\alpha}{\pi\gamma}\right).$$

Matching the reference voltage V_b to the dc output caused by noise, $\epsilon = 0$ and

$$\left(\frac{s}{n}\right) \approx \frac{\sigma_s^4}{\sigma_n^4}\,\frac{\alpha}{\pi\gamma}.$$

Following Goldstein,[1] the least detectable input signal is considered to produce a unity output signal-to-noise ratio.

This least detectable signal power is

$$\sigma_{ld}^2 = \sigma_n^2\sqrt{\pi\gamma/\alpha}.$$

Inaccurate reference voltage V_b will result in erroneous signal indications, if $\epsilon\sigma_n^2$ is a sizeable fraction of σ_s^2. The lower are the signal levels to be detected, the closer are the tolerances imposed on the reference voltage V_b, or the smaller are the permissible fluctuations of gain ϵ. Considering an error of the radiometer output equal to σ_{ld}^2 to be tolerable, ϵ has to satisfy $|\epsilon|\sigma_n^2 \leq \sigma_{ld}^2$.

This error in V_b may occur between the time the system is adjusted for zero balance and the time when the signal observation is made. The minimum time interval required for determining the signal presence depends on the low-pass filter bandwidth γ. Finite observation time degrades the output signal-to-noise ratio. The equation relating the signal-to-noise output ratio of the receiver for infinite observation time may be modified to take into account the finite time available between the balancing operation and the signal observation. The low-frequency noise output of the radiometer is not affected by the balancing operation. Noise can be assumed to be applied for an infinite time to the output meter, while the signal is applied only after the dc balance is established at time $t = 0$. The observation of the radiometer output is made at time $t = T$. The output peak signal power-to-average-noise power ratio is computed following the method given by Davenport.[8] For small input signal-to-noise ratios

$$\left(\frac{s}{n}\right)_0 = \frac{\sigma_s^4}{\sigma_n^4}\,\frac{\alpha}{\pi\gamma}\,(1 - e^{-2\pi\gamma T})^2.$$

For small input signal-to-noise ratios, the cross terms of noise and signal are negligible as compared with the noise constituting the low-frequency radiometer output fluctuations. These fluctuations are independent of observation time. The signal output has the same time dependency as the output of an RC low-pass filter with a step of voltage applied at $t = 0$. For a given observation time T, the signal-to-noise ratio, is maximized if γ satisfies the relation[9] $\gamma = 0.2/T$.

This can also be seen from a plot of the output signal-to-noise ratio for T constant shown in Fig. 2. The maximum signal-to-noise ratio is obtained as

$$\left[\left(\frac{s}{n}\right)_0\right]_{\max} = 0.81\alpha T\sigma_s^4/\sigma_n^4.$$

The least detectable signal gives unity output signal-to-noise ratio according to the convention established earlier. The least detectable signal for a given observation time T is, therefore

$$\sigma_{ld}^2 = 1.11(\alpha T)^{-0.5}\sigma_n^2.$$

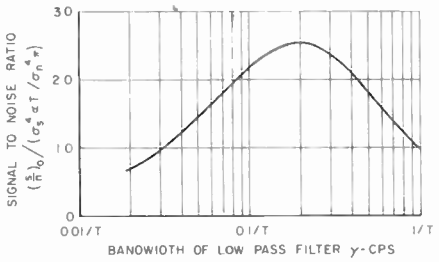

Fig. 2—The output signal-to-noise ratio as a function of the low-pass filter bandwidth for constant observation time.

Using the above expression for σ_{ld}^2 ϵ is related to T as

$$\frac{|\epsilon|}{T} \leq 1.11(\alpha T^3)^{-0.5}.$$

The least detectable signal in time interval T for a zero drift system σ_{ld}^2 and the drift rate that gives a maximum error equal to σ_{ld}^2 in the detector output are shown in Fig. 3. Drift of the above magnitude may degrade the radiometer threshold by no more than 3 *db*. The maximum deterioration of the detection threshold occurs if the gain variation ϵ is not uniformly distributed over the observation time T, but occurs as a step after the balancing has been performed. The step variation of the gain will give the 3-*db* threshold deterioration indicated above. Gradual gain changes have less effect on the radiometer threshold.

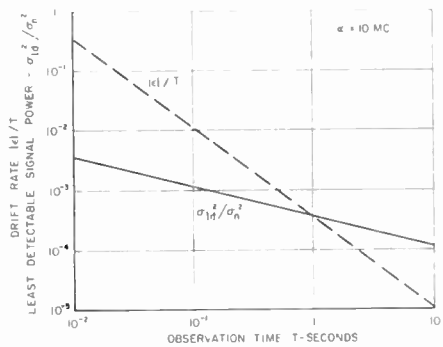

Fig. 3—The least detectable signal power and the permissible output drift rate as functions of observation time for a square-law detector radiometer.

The analysis of the radiometer using a linear detector follows the pattern of the preceding analysis. For zero drift ($\epsilon = 0$) and for small input signal-to-noise ratios, the linear detector gives the same signal-to-noise ratio as the square-law detector and hence the same least detectable signal power σ_{ld}^2. However, the drift rate that gives an error equal to σ_{ld}^2 in the radiometer output using a linear second detector is one-half of the drift rate in a square-law detector radiometer. The amplifier gain variation or drift of the linear detector radiometer can be only one-half of the drift of the square-law detector radiometer for the same degradation in the reception thresholds.[10]

The least detectable signal powers of the Dicke, two-receiver, and subtraction-type

[7] J. L. Lawson and G. E. Uhlenbeck, "Threshold Signals," M.I.T. Series, McGraw-Hill Book Co., Inc., New York, N. Y., vol. 24, p. 62; 1950.

[8] W. B. Davenport, Jr., "Correlator Errors Due to Finite Observation Intervals," M.I.T. Res. Lab. of Electronics Tech. Rep. No. 191; March 8, 1951.

[9] The same relation applies to Dicke and two-receiver radiometers assuming γ is much less than the input bandwidth α or the pass band of the postdetection filter β.

[10] Cf., W. H. Huggins and D. Middleton, "A comparison of the phase and amplitude principles in signal detection, *Proc. Natl. Electronics Conf.*, vol. 11, pp. 304–317; 1955; See p. 316, Fig. 5.

radiometers are all of the form

$$\sigma_{in}^2 = \sigma_n^2 k \sqrt{\gamma/\alpha}.$$

The constants k have the following values

Dicke radiometer with sinusoidal modulation,[11]

$$k = 2\sqrt{2\pi}.$$

Dicke radiometer with square-wave modulation,[11]

$$k = \pi\sqrt{\pi/2}.$$

Two-receiver radiometer considering total signal power received,[11]

$$k = \sqrt{2\pi}.$$

[11] The constants k given here differ from the corresponding constants listed by Goldstein (footnote 2) by a factor of $\sqrt{\pi/2}$. Goldstein considers an idealized flat low-pass filter. The above thresholds apply to a single-section RC low-pass filter.

Subtraction-type radiometer with driftless amplifiers,

$$k = \sqrt{\pi}.$$

The thresholds of the radiometers considered differ by no more than 4.5 db. The subtraction-type radiometer exhibits the lowest signal threshold. If the output drift rate does not exceed the limit specified in Fig. 3, the subtraction-type radiometer is comparable in sensitivity with the other radiometers.

The equivalence of the sensitivites of the two types of radiometers has been checked experimentally.[12] The operation of the subtraction-type radiometers requires frequent checks of zero level of the output meter or recorder which can be done by periodically disconnecting the antenna. This superimposes a square or trapezoidal wave over the output, that is easily distinguished from the gradual output changes caused by drift. The above radiometer operation resembles the operation of the Dicke radiometer, if the human operator is considered a substitute for the input modulator and the post detection band-pass filter.

The subtraction-type radiometers appear to merit consideration if the integration time is in the order of seconds or less. For longer integration times the stability requirements of the subtraction-type radiometers may make them more complex than the multiplier-type radiometers.

JANIS GALEJS
Appl. Res. Lab.
Sylvania Electric Products Inc.
Waltham, Mass.
Formerly at Cook Research Labs.
Chicago, Ill.

[12] Tests conducted by F. Splitt in Cook Research Labs., Chicago, Ill.

Contributors

Rubin Boxer (S'49–A'49–M'55) was born in New York, N. Y., on August 6, 1927. He received the B.E.E. degree in 1949 from Cooper Union and the M.E.E. degree from Syracuse University, Syracuse, N. Y., in 1955.

R. BOXER

From 1949 to 1950, Mr. Boxer was a project engineer at the Wright Air Development Center, Dayton, Ohio. He was employed by the Rome Air Development Center, Rome, N. Y., from 1950 to 1955, where he was engaged in the development of control systems involving aircraft and guided missiles.

Since 1956, Mr. Boxer has been a staff engineer with Servomechanisms, Inc., Westbury, N. Y., concerned with the development of air data computers. He is the author of several publications in the fields of air traffic control., sampled data systems, and numerical methods.

He is an associate member of Sigma Xi.

❖

John J. Egli (A'47–SM'56) was born on October 22, 1911, in Teaneck, N. J. He received the B.S. degree in electrical engineering from Cooper Union in 1933, the E.E. degree from New York University in 1940, and graduate credit from Rutgers University in 1948. From 1929 to 1936, Mr. Egli was in the engineering department of the Mackay Radio and Telegraph Company, concerned with radiotelegraph equipment design and installation. From 1936 to 1941, with the Commercial Products Department, of the Bell Telephone Laboratories, he participated in the design of radio-broadcast equipment, magnetic tape records, and voder equipment.

J. J. EGLI

Since 1941, Mr. Egli has been associated with the United States Army Signal Engineering Laboratories at Fort Monmouth, N. J. as chief of the Deisgn and Construction Section of the Communications Engineering Branch; chief of the Radio-Relay and Microwave Section of the Radio Communication Branch; and at present is a specialist on matters pertaining to wave propagation and radio-systems engineering for the Spectrum Utilization Branch, Office of Technical Plans.

Mr. Egli is a member of Eta Kappa Nu.

❖

Joseph Feinstein (S'41–A'46–M'51) was born on July 8, 1925 in Brooklyn, N. Y. He received the B.E.E. degree from Cooper Union in 1944, the M.A. degree in physics from Columbia University in 1947, and the Ph.D. degree in physics from New York University in 1951.

J. FEINSTEIN

He was employed by the Federal Telecommunications Laboratories from 1944 to 1946. From 1947 to 1949, he was an instructor at Brooklyn College. In 1949 he joined the National Bureau of Standards where he was engaged in work on radio propagation. Since 1954, he has been with Bell Telephone Laboratories, working on microwave tubes.

Dr. Feinstein is a member of Tau Beta Pi and the American Physical Society.

❖

For a biography and photograph of Wolfgang W. Gärtner, see page 699 of the May 1957 issue of PROCEEDINGS.

❖

Ross Gunn (A'35–SM'47–F'49) was born in Cleveland, Ohio, in May, 1897. He received the B.S.E.E. and M.S. degrees in electrical engineering at the University of Michigan, Ann Arbor, Mich., in 1920 and 1921, respectively, and the Ph.D. degree in physics from Yale University, New Haven Conn., in 1926.

R. GUNN

Dr. Gunn was an instructor in engineering physics at the University of Michigan from 1920 to 1922. In 1922 and 1923, he was radio research engineer for the U. S. Air Service. From 1923 to 1927, he was an instructor in the Physics Department of Yale University and in charge of the high-frequency laboratory during 1926 and 1927.

In 1927, Dr. Gunn joined the Naval Research Laboratory where he was super-

intendent of both the Mechanics and Electricity Division and the Aircraft Electrical Research Division, technical adviser to the Naval Administration, and technical director of the Army-Navy Precipitation Static Project. In 1946 he became Superintendent of the Physics Division and Technical Director of the Army-Navy Atmospheric Electricity Research Project.

In 1947 Dr. Gunn transferred to the U. S. Weather Bureau as the Director of the Physical Research Division and has since been made the Director of their Office of Physical Research. In 1955 he became the Assistant Chief of Bureau for Technical Services.

Dr. Gunn has invented a number of basic electrical instruments; he holds more than 40 U. S. patents. He initiated the Navy's isotope separation and nuclear submarine program. He was cited by the Secretary of the Navy in September, 1945, for Exceptionally Distinguished Service. In 1951, Dr. Gunn was given the Distinguished Service Award of the Flight Safety Foundation. He received the 1956 Robert M. Losey award of the Institute of Aeronautical Sciences and the Department of Commerce Gold Medal for Exceptional Service.

Dr. Gunn is a member of the National Academy of Sciences and a Fellow of the American Physical Society.

❖

R. C. Honey (S'48–A'53) was born in Portland, Ore., on March 9, 1924. He received the B.S. degree in physics from the California Institute of Technology in 1945, and the E.E. and Ph.D. degrees in electrical engineering from Stanford University in 1950 and 1953 respectively.

R. C. Honey

He served as a radio technician in the U. S. Navy until 1946 and was a member of the local oscillator microwave project at Stanford University Electronics Research Laboratory from 1948 to 1952. Since 1952, he has been with the Microwave Group of Stanford Research Institute.

❖

E. M. T. Jones (S'46–A'50–SM'56) was born in Topeka, Kans., in 1924. He received the B.S. degree in electrical engineering from Swarthmore College in 1944 and the M.S. and Ph.D. degrees in electrical engineering from Stanford University in 1948 and 1950, respectively. Dr. Jones was a radar maintenance officer in the U. S. Navy from 1944 to 1946. From 1948 to 1950 he was a research associate at Stanford University, working on the microwave local oscillator project. Dr. Jones joined the staff of Stanford Research Institute in 1950 where he is assistant head of the microwave group of the Antenna Systems Laboratory.

E. M. T. Jones

He is a member of Sigma Tau and RESA.

❖

B. Kazan was born in New York, N. Y. on May 8, 1917. He received the B.S. degree in physics from the California Institute of Technology in 1938 and the M.A. degree in physics from Columbia University in 1940.

B. Kazan

He joined the Signal Corps Engineering Laboratories in 1940 and was engaged in early experimental work with radar equipment. From 1944 to 1950, he was chief of the Special Purpose Tube Section at the Evans Signal Laboratory, where he was responsible for development and application engineering of traveling-wave tubes, klystrons, display tubes, and transistor devices. Since 1951, Mr. Kazan has been engaged in research on television tubes and display devices at the RCA Laboratories, Princeton, N. J.

Mr. Kazan is a member of the American Physical Society, Sigma Xi, and Tau Beta Pi.

❖

Gordon S. Kino (S'52–A'54) was born on June 15, 1928, in Melbourne, Australia. He received the B.Sc. degree in mathematics in 1948 and the M.Sc. degree in mathematics in 1950 from London University. In 1955, he received the Ph.D. degree in electrical engineering from Stanford University.

G. S. Kino

He joined the Mullard Radio Valve Co., Salfords, Surrey, England, in 1947 as a managerial apprentice. In 1948, he became a member of the Mullard Vacuum Physics Laboratory, where he was engaged in research on microwave triodes, traveling-wave tubes, and klystrons.

From 1951 to 1955, he was employed as a research assistant at the Electronics Research Laboratory of Stanford University, Stanford, Calif., where he carried out research on traveling-wave tubes and electromagnetic theory. He then worked as a research associate of the Microwave Laboratory at Stanford on electromagnetic theory.

He was a member of the technical staff of the Bell Telephone Laboratories, Murray Hill, N. J., where he was associated with the Electron Tube Development Department and carried out research on magnetrons. Dr. Kino returned to Stanford in February, 1957.

Dr. Kino is a member of Sigma Xi.

IRE News and Radio Notes

PGME Begins Testing Program

The Buffalo-Niagara Chapter of the IRE Professional Group on Medical Electronics has launched a local program to make some modern electronic techniques available to Niagara Frontier medical research institutions. Under the plan, local electronic instrument manufacturers develop new instrument prototypes at their own expense. The medical research institutions then use the instruments in their laboratories for a trial period and perform gratis any necessary tests. If the instrument proves useful to the medical men, the instrument company then builds a final model of the tested prototype which the medical research institution can purchase at a nominal price if it wishes.

This plan for cooperation between electronic companies and medical research groups was the idea of Wilson Greatbatch, former Chairman of Buffalo-Niagara PGME, now of Taber Instrument Corporation; the present co-chairmen of the Buffalo-Niagara PGME, Robert Cohn, of the Chronic Disease Research Institute; and Godfrey Buranich of Bell Aircraft Corp.

Medical institutions which benefit from this program are the Chronic Disease Research Institute, the University of Buffalo Medical School and Children's Hospital.

Some of the instruments developed as a result of the cooperative effort include the first fully transistorized electrocardiograph, a transistorized decade amplifier for amplifying nerve currents and a complete medical electronic telemetering system for multichannel data recording on a single channel.

RETMA Changes Name to EIA

The Radio-Electronics-Television Manufacturers' Association has changed its name to the Electronic Industries Association. The new name was selected as being more representative of the expanding industry which the association serves.

The change in name will become effective upon approval of a charter revision by the state of Illinois.

EJC Conference Set for Dec.

The 1957 Eastern Joint Computer Conference will be held at the Sheraton Park Hotel, Washington, D. C., December 9–13. The conference will be devoted to the problems which arise in the design and application of computers which are required to perform their job within a specified time cycle. Advance registrations may be obtained from R. T. Burroughs, IBM Corp., 1220 19 St., N.W., Washington, D. C. for $4.00. After November 25, the registration fee, paid either by mail or at the conference, will be $5.00.

Among the topics to be discussed at the conference will be industrial control computers and instrumentation, traffic control, navigation and surveillance, simulation in real-time, synthesis of real-time systems, on-line business systems, digital communications techniques, document reading, pattern recognition and output devices. Exhibits will also be on display. The IRE, the Association for Computing Machinery, and the AIEE are sponsors; the National Simulation Council is also participating.

Call for Papers

November 1 Is Deadline for 1958 IRE National Convention Papers

The 1958 IRE National Convention will be held at the Waldorf-Astoria Hotel and New York Coliseum, New York City, March 24–27, 1958.

Prospective authors are requested to submit all of the following by November 1, 1957.

(1) 100-word abstract *in triplicate*, title of paper, name and address;
(2) 500-word summary *in triplicate*, title of paper, name and address; and an indication of the technical field in which the paper falls.

The technical fields which may be covered are:

Aeronautical & Navigational Electronics
Antennas and Propagation
Audio
Automatic Control
Broadcast & Television Receivers
Broadcast Transmission Systems
Circuit Theory
Communications Systems
Component Parts
Education
Electron Devices
Electronic Computers
Engineering Management
Engineering Writing and Speech
Industrial Electronics
Information Theory
Instrumentation
Medical Electronics
Microwave Theory & Techniques
Military Electronics
Nuclear Science
Production Techniques
Reliability & Quality Control
Telemetry & Remote Control
Ultrasonics Engineering
Vehicular Communications

Address all material to: G. L. Haller, Chairman
1958 Technical Program Committee,
The Institute of Radio Engineers,
1 East 79 St., New York 21, N.Y.

Calendar of Coming Events and Authors' Deadlines

Nat'l Electronics Conference, Hotel Sherman, Chicago, Ill., Oct. 7–9
1957 Convention of Audio Eng. Soc., Trade Show Bldg., New York City, Oct. 8–12
Computers in Control Symp., Chalfonte-Haddon Hall Hotel, Atlantic City, N. J., Oct. 16–18
IRE Canadian Convention Exhibition Park, Toronto, Can., Oct. 16–18
Conf. on Eng. Writ. Speech, Sheraton-McAlpin Hotel, New York City, Oct. 21–22
International Conf. on UHF Circuits, Paris, France, Oct. 21–26
Computer Applications Symp., Hotel Sherman, Chicago, Ill., Oct. 24–25
East Coast Aero. & Nav. Conf., Lord Baltimore Hotel & 5th Reg. Armory, Balt., Md., Oct. 28–30
PGED Meeting, Shoreham Hotel, Wash., D. C., Oct. 31–Nov. 1
PGNS Annual Meeting, Henry Hudson Hotel, New York City, Oct. 31–Nov. 1
Annual Symp. on Aero Commun., Hotel Utica, Utica, N. Y., Nov. 6–8
Radio Fall Meeting, King Edward Hotel, Toronto, Can., Nov. 11–13
PGI Conference, Atlanta-Biltmore Hotel, Atlanta, Ga., Nov. 11–13
Mid-America Electronics Convention, Kan. City Mun. Audit., Kan. City, Mo., Nov. 13–14
New England Radio Eng. Mtg., Mechanics Bldg, Boston, Mass., Nov. 15–16
Conf. on Magnetism, Sheraton-Park Hotel, Wash., D. C., Nov. 18–21
Elec. Computer Exhibition, Olympia, London, England, Nov. 28–Dec. 4
PGVS Conf., Hotel Statler, Wash., D. C., Dec. 4–5
Eastern Joint Computer Conf, Park-Sheraton Hotel, Wash., D. C., Dec. 8–11
Nat'l Symp. on Reliability & Quality Control, Statler Hotel, Wash., D. C., Jan 6–8, 1958
Transistor-Solid State Circuits Conf., Phil., Pa., Feb. 20–21
Nuclear Eng. and Science Congress, Palmer House, Chicago, Ill., Mar. 16–21
IRE Nat'l Convention, N. Y. Coliseum and Waldorf-Astoria Hotel, New York City, Mar. 24–27 (DL*: Nov. 1 G. L. Haller, IRE Headquarters, New York City)
Instruments & Regulators Conf., Univ. of Del., Newark, Del., March 31–Apr. 2
SW Regional Conf. & Show, Mun. Audit., San Antonio, Tex., Apr. 10–12
Conf. on Automatic Techniques, Statler Hotel, Detroit, Mich., Apr. 14–16
Elec. Components Symp., Los Angeles, Calif., Apr. 22–24
Seventh Region Conf. & Show, Sacramento, Calif., Apr. 30–May 2
Western Joint Computer Conf., Ambassador Hotel, Los Angeles, Calif., May 6–8 (DL* Jan. 15, P.O. Box 213, Claremont, Calif.)

* DL = Deadline for submitting abstracts

ACTIVITIES OF THE IRE SECTIONS AND PROFESSIONAL GROUPS

1957 Aeronautical and Navigational Electronics Pioneer Awards were conferred on Dr. Lawrence A. Hyland (left) and posthumously on Dr. Alessandro Artom, whose award is accepted by his sons, Barone Dr. Guido Artom (second from left) and Barone Dr. Emilio Artom (right). Brig. Gen. Pete Sandretto (second from right), Chairman of PGANE Awards Committee announced the awards at the Banquet of the Ninth Annual National Conference on Airborne Electronics at Dayton, Ohio on May 14, 1957.

G. H. Knight (left) presents John Ryder, 1955 IRE President, and J. J. Gershon with their commissions as Admirals in the Great Navy of Nebraska as J. C. Jensen (right) looks on. Dr. Jensen, teacher and department head at Nebraska Weslevan University for 50 years, was a 1957 IRE Fellow Award winner.

The Albuquerque-Los Alamos IRE Section recently held a competition in conjunction with the New Mexico Science Fair and awarded a $200 scholarship to Royce Fletcher (right). S. C. Hight (left), R. K. Moore, and W. W. Granneman served on the Section's Scholastic Awards committee.

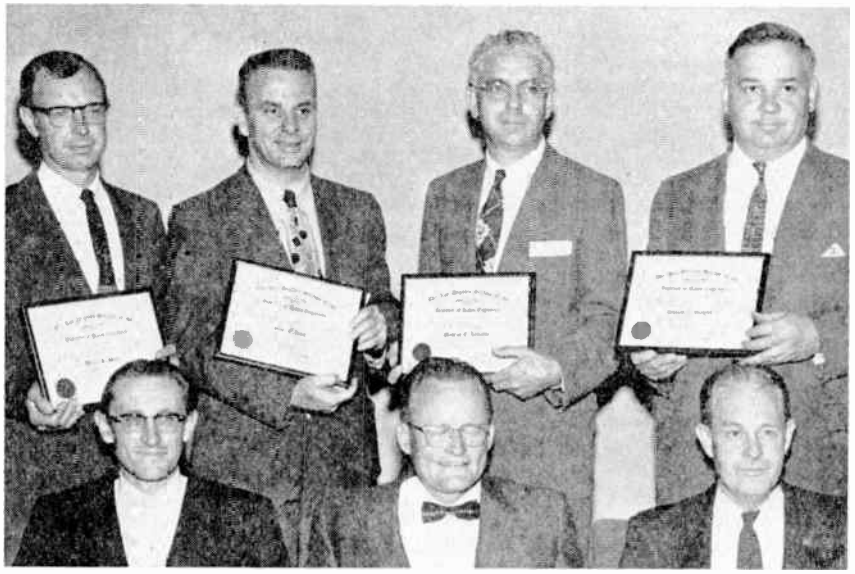

Recipients of Los Angeles IRE Section Awards at the annual meeting are shown above (left to right, standing): Willis Ware, Ellis King, Maurice Kennedy and E. C. Bertolet. Seated—Willard Fenn, W. E. Peterson, and M. L. Swan.

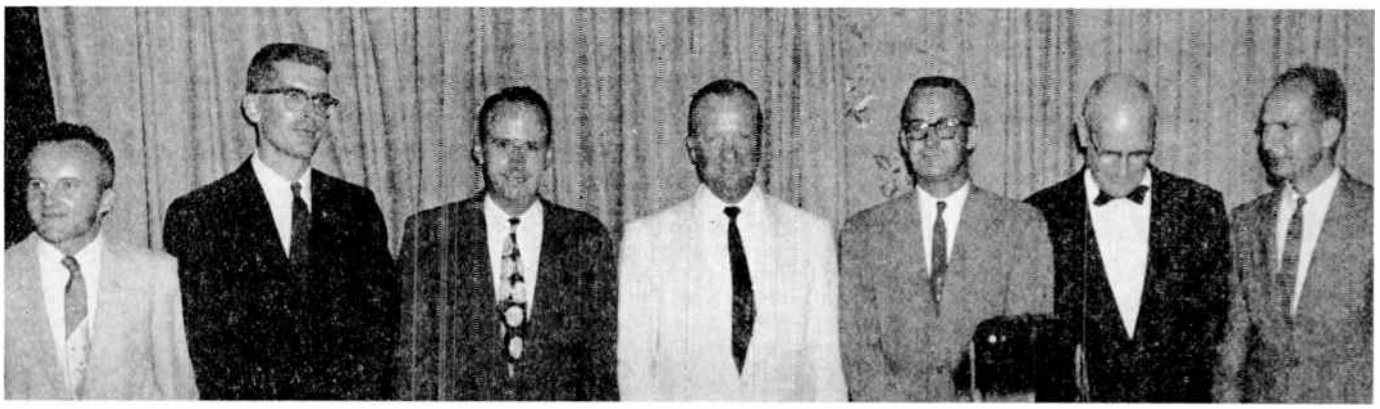

New and retiring officers of the IRE Northwest Florida Section and the new Fort Walton Chapter of the IRE Professional Group on Military Electronics surround honorary Chapter Chairman E. P. Mechling, Maj. Gen., USAF, Commander, Air Force Armament Center. Left to right: W. W. Garnel, Canoga Corp., past Section Secretary-Treasurer and incoming Vice-Chairman; J. J. Niedrauer, Bell Aircraft, Chapter Organizer and first Chapter Chairman; First Lieut. W. F. Kirlin, USAF, AF Armament Center, Section and Chapter Secretary-Treasurer; General Mechling; E. F. Sapp Jr., Vitro Corp., Chapter Vice-Chairman; G. C. Fleming, Eglin Proving Ground, past Vice-Chairman and incoming Chairman of the Section; and F. E. Howard Jr., AF Armament Center, retiring Section Chairman.

MARS Radio Announces its October Schedule and Topics

The Air Force MARS Eastern Technical Net, which broadcasts over the air every Sunday afternoon at 2 p.m. (EDT) on 3295 and 7540 kc, announces its guest speakers for October: October 6—E. H. Shively, Dielectric Products Engineering Co. Topic: Antennas for vhf and uhf. October 13—G. W. Bailey, IRE Executive Secretary. Topic: Services of the IRE. October 20—Leonard Kahn, Kahn Research Lab. Topic: Compatible side band. October 27—Edward Tilton, ARRL. Topic: The world above 50 megacycles.

Conference on Magnetism Adds Another Day to its Program

The 1957 Conference on Magnetism and Magnetic Materials will be held at the Hotel Sheraton-Park, Washington, D. C., November 18–21. Because of the general interest shown in the conference as evidenced by the large number of contributed papers, its duration has been extended from three days to four.

The program of the conference is designed to emphasize topics of current interest in magnetism. A number of invited papers will survey past developments as well as give the latest progress in such fields as maser devices, garnets and other new magnetic materials, ferromagnetic resonance effects, magnetic properties of thin films, and magnetic annealing. Contributed papers cover a wide variety of topics related to magnetism and magnetic materials.

MISCELLANEOUS IRE PUBLICATIONS

The following issues of miscellaneous publications are available from the Institute of Radio Engineers, Inc., 1 East 79th Street, New York 21, New York, at the prices listed below:

Publications	Price per Copy
Component Symposiums	
Proceedings of the 1954 Electronic Components Symposium, May 4–6, 1954, Washington, D. C.	$4.50
Proceedings of the 1957 Electronic Components Symposium, May 1–3, 1957, Chicago, Ill.	5.00
Electronic Computer Conferences	
Proceedings of the Joint AIEE-IRE-ACM Western Computer Conference, February 11–12, 1954, Los Angeles, Calif.	3.00
Proceedings of the Joint AIEE-IRE-ACM Western Computer Conference, March 1–3, 1955, Los Angeles, Calif.	3.00
Proceedings of the Joint AIEE-IRE-ACM Western Computer Conference, February 7–9, 1956, San Francisco, Calif.	3.00
Proceedings of the Joint AIEE-IRE-ACM Western Computer Conference, February 26–28, 1957, Los Angeles, Calif.	4.00
Review of Electronic Digital Computers, Joint AIEE-IRE Computer Conferences, December 10–12, 1951, Philadelphia, Pa.	3.50
Proceedings of the Joint AIEE-IRE-ACM Eastern Computer Conference, December 8–10, 1954, Philadelphia, Pa.	3.00
Proceedings of the Joint AIEE-IRE-ACM Eastern Computer Conference, November 7–9, 1955, Boston, Mass.	3.00
Proceedings of the Joint AIEE-IRE-ACM Eastern Computer Conference, December 10–12, 1956, New York, N. Y.	3.00
Magnetic Amplifiers Conference	
Proceedings of the Conference on Magnetic Amplifiers, April 5–6, 1956, Syracuse, N. Y.	4.00
Reliability & Quality Control Symposiums	
Proceedings of the National Symposium on Quality & Reliability in Electronics, November 12–13, 1954, New York, N. Y.	5.00
Proceedings of the Second National Symposium on Quality & Reliability in Electronics, January 9–10, 1956, Washington, D. C.	5.00*
Proceedings of the Third National Symposium on Quality Control & Reliability in Electronics, January 14–16, 1957, Washington, D. C.	5.00
Telemetering Conference	
1953 National Telemetering Conference, May 20–22, 1953, Chicago, Ill.	2.00

* IRE member rate—$3.00.

Obituaries

William B. Cowilich, former Assistant Secretary of the IRE, died on August 3rd as a result of injuries sustained in an automobile accident two days before.

Mr. Cowilich, who was born April 10, 1906, served as IRE Assistant Secretary during the period 1942–1944. In this capacity he was in charge of IRE headquarters operations in New York City. For the past 12 years he was sales representative for the Cleworth Publishing Co., a publisher of trade magazines, in Cos Cob, Conn.

John F. Farrington (A'19–M'29–F'31) died suddenly July 5 at his summer place at Centre Harbor, N.H. at the age of 62.

J. F. Farrington

Mr. Farrington, after graduating from Bliss Electrical School in 1916, had entered the employ of the Western Electric Co. in New York in the radio research department. He took an active part in the development of radiotelephone equipment for the Army, Navy, and Air Force in World War I. He participated in much of the radio research and development work of the Western Electric Co. and Bell Telephone Laboratories up to 1929, including work on transoceanic radiotelephone circuits, short-wave transmission, and ship-shore radio. In 1929 he joined the IT&T Co. in charge of radio development. From 1934 to 1939 he was associated with the Hazeltine Corporation, and from 1941 until his death he worked for the Raytheon Company where he served as manager of the circuit development department at the Bedford Laboratory.

His experience covered all phases of radiotelephony since its practical beginning, and included transmitters, receivers, radio transmission, and military equipment. He was one of the authorities on electronic receiver circuits, and he had secured over fifty U.S. patents.

He had served on the IRE Admissions Committee, and New York Program Committee during part of his New York residence.

James Leslie Finch (A'19–M'28–SM'43–F'54), assistant chief engineer for RCA Communications, Inc., died recently after a long illness.

A graduate of the University of Washington, Mr. Finch joined the General Electric Co. in 1915 and worked with E. F. W. Alexanderson, inventor of the longwave alternator. In World War I he served as the executive officer of the United States Naval radio station at New Brunswick, N. J., in charge of maintenance and technical operation of the first Alexanderson alternator.

Mr. Finch joined RCA in 1920. He received many honors, including the Gold Cross for Meritorious Service from Poland for his work in establishing that country's first transmitting station in 1924.

Mr. Finch designed the mountaintop radio transmitting antenna at Haiku, Hawaii, for the Navy and the antenna system for the Navy's giant radio station at Jim Creek, Wash. At the time of his death, Mr. Finch held sixty-four United States patents on communications and electronics inventions, all assigned to RCA.

He had specialized in Alexanderson radio equipment and transmitter design.

Books

Electrical Measurements and Their Applications by W. C. Michels

Published (1957) by D. Van Nostrand Co., Inc., 257 Fourth Ave., N. Y. 10, N. Y. 320 pages+2 appendix pages+9 index pages+viii pages. Illus. 9¼×6¼. $6.75.

This book is a successor to *Advanced Electrical Measurements* by W. R. Smythe and W. C. Michels. It is a textbook for college students and contains instructions for experiments as part of the text. In some places, important points regarding a measurement are discussed only in these experiment instructions, so these should not be skipped by the nonstudent reader.

The first part of the book, covering basic measurements, comprises nine chapters and about 72 per cent of the text. The second part covers applications to magnetic measurements, electrical thermometry, electrical measurements in mechanics and acoustics, and electrical measurements in nuclear physics. It comprises four chapters and about 28 per cent of the text. Chapters five through nine cover null measurements at low frequencies, amplifiers, oscillators, measurements at radio frequencies, and measurements at high frequencies, and comprise about 40 per cent of the book. This is the area of primary interest to radio engineers.

Much of the treatment of measurements circuits at radio frequencies is qualitative, and some of the rather fundamental instruments are only briefly mentioned. For example, the Q-meter receives one page and no analysis of the circuit is given, the susceptance variation method is not mentioned, nor are bridged-T and double-T circuits mentioned. In some places, the analytical work is good, as in the early part of the chapter on amplifiers, but at other places the book must be read with extreme caution. Some examples of statements which must be carefully examined are " . . . current generator, with zero internal impedance" (p. 118); " . . . the phase angle between the current and the voltage at resonance is 45°" (p. 178); and "These half-wave rectifying meters are identical in principle with the peak value meters . . . " (p. 180).

The second part of the book is quite valuable, because it shows a variety of uses of electrical measurements in the measurement of nonelectrical quantities. It is stimulating to the student to see this wide diversity of applications.

On the whole, the book is a good one for students beginning their work in electrical measurements. It emphasizes the utility and value of electronic equipment in electrical measurement, without sacrificing the ground work in basic dc measurements.

G. B. Hoadley
North Carolina State College
Raleigh, N. C.

Technical Aspects of Sound, Vol. Two, ed. by E. G. Richardson

Published (1957) by D. Van Nostrand Co., Inc., 257 Fourth Ave., N. Y. 10, N. Y. 406 pages+6 index pages+xii pages. 206 figures. 9¼×6¼. $11.75.

In this second volume of *Technical Aspects of Sound*, Professor Richardson, as editor, has maintained the high standards set in the first volume. The glittering list of contributors includes such names as Dean Erwin Meyer of Goettingen, Germany, and Harvey Hubbard of Langley Field, Virginia.

The book's four hundred pages are about equally divided between the three subjects: underwater sound, ultrasonics, and aircraft noise. Of particular interest is the section on underwater acoustics, since it includes a report on very recent work on air bubbles at Goettingen and a fairly complete discussion of the work on underwater absorbers which was carried on the U. S. and in Germany during the war. The sections on aircraft noise and underwater noise, though short, should also prove useful, since little has appeared on these subjects except in the classified literature.

The section on propagation of sound in the sea is unfortunately rather short, as is the list of references. However, the discussion of long distance propagation of sound in the atmosphere includes material that is new and interesting.

Ultrasonic transducers are treated rather thoroughly as are the applications of ultrasonics, particularly the biological applications, a field which is much more active in Europe than in America. Chapter 5 brings to the English literature a discussion of the extensive work of the past six or seven years on air bubbles by Dean Meyer and his several co-workers (Miss Exner and Messrs. Tamm, Skudrzyk, and Esche).

All in all, the book is easy to read and forms a valuable reference work for researchers in the physical acoustics field.

W. E. Kock
Bendix Aviation Corp.
Ann Arbor, Mich.

Statistical Methods in Quality Control by D. J. Cowden

Published (1957) by Prentice-Hall, Inc., 70 Fifth Ave., N. Y. 11, N. Y. 633 pages+15 index pages+74 pages of appendix+xxiv pages. Illus. 9¼×6¼. $12.00.

Manufacturers of electronic equipment are realizing the need of quality control procedures for attaining predictable product, since predictability is a necessary ingredient of reliability.[1] This book describes and illustrates many statistical techniques that may be used as aids in controlling the quality characteristics of a product as well as statistical sampling plans that may be used for judging whether the quality of a lot is acceptable or not.

The book is divided into three parts. The first ten chapters deal mainly with statistical methods that are applicable in general, such as certain types of distributions, estimators of the parameters of distributions, various tests of hypotheses concerning the values of parameters together with operating characteristics of the tests and an introduction to analysis of variance. Chapters 11 and 12 cover "tests of control," including the control chart.

Chapters 13–14, 16–17, 21–24, 26 and 28 in the second part, describe the use of tests of control for controlling production processes. Operating characteristic curves for several types of control charts for variables are constructed in Chapter 18 and used to evaluate different sampling frequencies in Chapter 19. The economics of control charts, Chapter 29, may be of particular interest to process control supervisors. Chapter 15 gives methods for setting specification limits by statistical methods and Chapter 27 outlines the procedure for fitting a straight line by least squares, which is used for sloping control lines.

The reviewer feels that more warning should be given about the increase in the risk of looking for trouble that does not exist when multiple tests of control are used on the same data as in Chapter 12. It is true that the effect of the multiplicity of tests is mentioned on page 173, but no allowance is made for it in the examples. Again, on pages 230–232, several "warning signals" are suggested for use with control charts, but the increased risk of looking for trouble that does not exist is not evaluated for the combination of tests.

The third part of the book, Chapters 30–40, is concerned mainly with "product control," or acceptance sampling plans. A few popular misconceptions are included in this part of the book, for example:

(1) The idea that a sampling plan has only one type of operating characteristic curve relating to lot quality and properly computed by means of the hypergeometric distribution. Actually there are two types of curves,[2] one relating to "lot" quality, and the other relating to "product" quality assuming that the lot qualities are binomially distributed about the value of product quality. Most published operating characteristic curves, which are computed by means of the Poisson or binomial distributions, give the probability of acceptance for "product" of a given quality.

(2) The idea that the Army Service Forces Inspection Tables and later military tables, including Military Standard 105A, "minimize inspections before detailing" (pages 494 and 526).

(3) The idea that military acceptance sampling plans provide that "substantially all lots be satisfactory" (page 586). The specification of an AQL value in military plans does not describe protection to the consumer. The per cent defective in a substantial proportion of accepted lots may exceed the AQL value, since the AQL is the average level of lot quality that will be accepted most of the time by the sampling plan. The average level of per cent defective in submitted lots must be significantly larger than the AQL value before tightened inspection is called for.

This book was not written for the novice in either statistics or quality control. It is

[1] M. N. Torrey, "Quality control in electronics," Proc. IRE, vol. 44, pp. 1521–1530; November, 1956.

[2] W. E. Deming, "Some Theory of Sampling," John Wiley and Sons, Inc., New York, N. Y.; 1950, Chapter 8.

a good reference book for one who has had statistical training and experience in the use of quality control techniques, since it includes many statistical techniques that could be useful in the quality control operation. The nearest competitor to this book is probably *Quality Control and Industrial Statistics* by Duncan.[3] Professor Cowden's book includes more tests for control, or lack of it, while Professor Duncan's book includes more material on analysis of variance, regression and experimental design. The latter techniques can be useful in finding the assignable causes of lack of control.

On the whole, this is an above-average compilation of statistical techniques and tables. The quality control viewpoint is lacking as evidenced by the statement on page 155:

> "When testing whether or not control exists, the control chart should perhaps be considered mainly a diagnostic device, with final judgment based on other techniques."

The standard criteria for judging when control exists are based on the standard control chart.[4,5]

M. N. Torrey
Bell Tel. Labs.
New York, N. Y.

[3] A. J. Duncan, "Quality Control and Industrial Statistics," Richard D. Irwin, Inc., Homewood, Ill. 1955.
[4] W. A. Shewhart, "Statistical Method from the Viewpoint of Quality Control," Graduate School, Dept. of Agriculture, Washington, D. C., ed. by W. E. Deming; 1939.
[5] "American War Standard Control Chart Method of Controlling Quality During Production," Amer. Standards Assn., Inc., New York, N. Y., Z1.3-1942.

Recent Books

Alger, P. L., *Mathematics for Science and Engineering*. The trade edition based on *Engineering Mathematics* by C. P. Steinmetz. McGraw-Hill Book Co., 330 W. 42 St., N. Y. 36, N. Y. $6.95.

American Institute of Physics Handbook. McGraw-Hill Book Co., 330 W. 42 St., N. Y. 36, N. Y. $15.00.

Arguimbau, L. B., and Stuart, R. D., *Frequency Modulation*. John Wiley & Sons, Inc., 440 Fourth Ave., N. Y. 16, N. Y. $2.00.

Automatic Coding, Monograph No. 3. Proceedings of the symposium held Jan. 24–25, 1957 at The Franklin Institute, Philadelphia, Pa. Journal of The Franklin Institute, Philadelphia 3, Pa. $3.00.

Burris-Meyer, Harold, and Goodfriend, Lewis, *Acoustics for the Architect*. Reinhold Publishing Corp., 430 Park Ave., N. Y. 22, N. Y. $10.00.

Douglas, Alan, *The Electrical Production of Music*. Philosophical Library, Inc., 15 E. 40 St., N. Y. 16, N. Y. $12.00.

FM Stations Up-to-Date. Compiled by B. G. Cramer. Audiocraft Magazine, The Publishing House, Great Barrington, Mass. $0.50.

Glozsary of Terms in Nuclear Science and Technology (ASA American Standard N 1.1—1957). American Society of Mechanical Engineers, 29 W. 39 St., N. Y., N. Y. $5.00.

Hausmann, Erich, and Slack, E. P., *Physics*, 4th ed. D. Van Nostrand Co., Inc., 257 Fourth Ave., N. Y. 10, N. Y. $8.00.

Industrial Applications of Analog Computers: Proceedings of a Symposium for Management. April 10–11, 1956. Midwest Research Institute, 425 Volker Blvd., Kansas City 10, Mo. $5.00.

Industrial Rectifying Tubes, Vol. XIII. Philips Technical Library book obtainable from Elsevier Press, Inc., 2330 Holcombe Blvd., Houston 25, Tex. $2.15.

Kaufman, Milton, *Radio Operator's License Q&A Manual*, 6th ed. John F. Rider Publishers, Inc., 116 W. 14th St., N. Y. 11, N. Y. $6.60.

Murray, R. L., *Nuclear Reactor Physics*. Prentice-Hall, Inc., 70 Fifth Ave., N. Y. 11, N. Y. $10.00.

Nye, J. F., *Physical Properties of Crystals*. Oxford Univ. Press, 114 Fifth Ave., N. Y. 11, N. Y. $8.00.

Proceedings of the Second RETMA Conference on Reliable Electrical Connections. Engineering Publishers, GPO Box 1151, N. Y. 1, N. Y. $5.00.

Proceedings of the Second RETMA Symposium on Applied Reliability, Engineering Publishers, GPO Box 1151, N. Y. 1, N. Y. $5.00.

Semiconductor Abstracts, Vol. III—1955 issue. Abstracts of literature on semiconducting and luminescent materials and their applications, compiled by Battelle Memorial Institute. John Wiley & Sons, Inc., 440 Fourth Ave., N. Y. 16, N. Y. $10.00.

Varner, W. W., *Computing with Desk Calculators*. Reinhart & Co., Inc., 232 Madison Ave., N. Y. 16, N. Y. $2.00.

First National Symposium on Engineering Writing & Speech

Sheraton-McAlpin Hotel, New York City, October 21–22

The IRE Professional Group on Engineering Writing and Speech will sponsor its first national symposium at the Sheraton-McAlpin Hotel in New York City, Oct. 21–22, 1957. The registration fee at the hotel is $5.00. Members of the symposium committee include: D. J. McNamara, chairman; P. J. Lahey, program; H. B. Michaelson, finance; H. S. Renne, arrangements; T. E. Mount, registration; Lewis Winner, publicity; and E. M. McElwee, Group secretary.

Monday, October 21

Registration

Speech of welcome, D. J. McNamara, and symposium chairman.

Session I

Engineering Writing is Different, Lennox Grey, Teachers' College, Columbia Univ.

Tricks of the Trade, J. D. Chapline, Technical Reports Dept., Philco Corp.

When You Write for the Air Force, Brig. Gen. H. A. Boushey, Office of Deputy Chief of Staff, Development, Dept. of the Air Force.

Luncheon

Keynote address, J. R. Pierce, Bell Tel. Labs.

Session II

More Senses Make More Sense, C. N. Hoyler, RCA, Labs.

Panel discussion on "Should a Talk be Read from a Prepared Manuscript?" Participants: A. V. Loughren, Airborne Instruments Lab., and H. B. Michaelson, IBM Journal of Research and Development (*pro*); G. V. Eltgroth, Patent Council, Indus. Elec. Div., General Electric Co., and G. I. Robertson, Bell Tel. Labs. (*con*).

Reception and cocktail party

Session III

Scientific Staging, Lewis Winner, Bryan Davis Publishing Co.

Tuesday, October 22

Registration

Session IV

A Formula for Platform Poise, Rudy Norko, RCA.

Does It Have to be Slides?, Charles Tiene, Field Training Dept., Sperry Gyroscope Co.

Technical Films—A Luxury or a Necessity?, R. M. Murray, Engineering Services Dept., Hughes Aircraft Co.

Luncheon

A report of the formation, progress and plans of the PGEWS will be given.

Session V

Panel discussion on "What Magazine are You Writing for?" Moderator: Keith Henney, McGraw-Hill Publishing Co. Participants: Editorial staff members of Proceedings of the IRE, *Electronics*, *Electronic Design*, and *Electrical Manufacture*.

Fourth Annual East Coast Conference on Aeronautical & Navigational Electronics

FIFTH REGIMENT ARMORY AND LORD BALTIMORE HOTEL, BALTIMORE, MD.

OCTOBER 28–30, 1957

The IRE Baltimore Section and the IRE Professional Group on Aeronautical and Navigational Electronics will again hold their annual East Coast Conference. Exhibits and an array of 42 technical papers, presented at the Fifth Regiment Armory, will elaborate on the theme, "Electronics in the Jet Air Age." A banquet and dance will be held at the Lord Baltimore Hotel on the evening of October 29. Capt. H. T. Orville will be the speaker and J. A. Hutcheson, toastmaster. Registration is $1.00 for IRE members; $3.00 for non-members.

Members of the conference steering committee are: A. A. Nims, chairman; J. A. Houston, vice-chairman; T. T. Eaton, finance; K. F. Molz, local arrangements; C. R. Maynard, exhibits; Harald Schutz, technical program; Joseph General, printing; and C. J. Knight, publicity.

Monday, October 28

NAVIGATION SYSTEMS

The Navigational Computer, P. J. McKeown, Ford Instrument Co.

The Effects of Terrain Via Error on Doppler Navigator Accuracies, D. McColl and G. Burton, Raytheon Mfg. Co.

Air Route Surveillance Radar Facilities, B. McCaffrey, Raytheon Mfg. Co.

Transosonde System, H. Cubbage, U. S. Naval Research Lab.

Frontier Airline's Airways System, C. Longhart, Frontier Airlines.

Performance Analyis of Doppler Navigation Systems, W. R. Fried, WADC, USAF.

EQUIPMENT ANALYSIS

An Analytical Approach to the Vibration Design of Airborne Electronic Equipment, M. Gurtin, General Electric Co.

New Electronic and Metallurgical Ideas, Materials and Techniques, S. Freedman, Chemalloy Electronics Corp.

A Ram Air Cooling Study, R. Gammerman, Sylvania.

A Research Flight Simulator, J. Stoops and D. Entler, Jr., Westinghouse.

Procedures for Preliminary Analysis of Infra-Red Detection Systems, R. Laprade, R. Timm, and A. Schwartz, Westinghouse.

Factors Affecting Tracking Performance When Using the Moving Aircraft Display, M. Mazina and A. Kahn, Westinghouse.

Tuesday, October 29

MILITARY NAVIGATION TECHNIQUES

Sidelobe Suppression for ATC Beacon, C. Yule, NAS, Patuxent River.

A Hypothesis on the Use of Time, A. Knight, WADC, USAF.

A Proposal for an Automatic Position Correction of a Dead Reckoning Navigational Computer Using Astrotracker Derived Celestial Data, C. Smykowski, Ford Instrument Co.

Automatic Thrust Control for Turbojet Aircraft, P. Story, Sperry Gyroscope Co.

Radar Ground Mapping Resolution, R. Timm and R. Laprade, Westinghouse.

Air/Ground Communication Problems, W. Vincent, A. Peterson and R. Leadabrand, Stanford Research Inst.

EQUIPMENT DESIGN

Liaison Engineering, J. Berkley, General Electric Co.

Automatology, A. Maynard, General Electric Co.

Prediction of Temperatures in Forced Convection-Cooled Equipment, L. Fried, General Electric Co.

A Forced Air Cooling System in Present Aircraft, T. Ellison, United Airlines.

Progress in Transistorized Audio Systems for Modern Airlines, J. Tewksbury, Bendix.

An Electronic System for Protecting Aircraft Fuel Tanks from Fire and Explosion, W. Bordewieck, Electronics Corp. of America.

STUDENT CONFERENCE

CIVIL NAVIGATION TECHNIQUES

An Automatic Guidance Computer Using Magnetic Amplifiers, J. Rector, Collins Radio Co.

Radio Compass Testing with Small Shielded Enclosures, A. Markham, Bendix Radio.

A New Navigation Package for the VHF Omni-Range System of Aircraft Navigation, A. Hemphill, Bendix Radio.

New Design Philosophies for Lightweight Civil Airborne Weather Radars, B. L. Cordry, Bendix Radio.

Interference Blanker Development, M. Newman, J. Stahmann and J. D. Robb, Lightning and Transients Research Inst.

Wednesday, October 30

MICROWAVE COMPONENTS

Multiplex Ferrite Type Antenna Switch, H. C. Hanks, Jr., The Martin Co.

Ferrite Antenna Systems, H. Hanks, Jr. and J. Bruckert, The Martin Co.

Status in Systems Application of Available 8–9 Millimeter Wave Length Components, Magnetrons, TR and ATR Tubes, Crystal Mixers and Detectors, F. McCarthy, Sylvania.

A Novel Antenna Feed which Provides for any Remotely Selectable Polarization, Vertical, Horizontal Right or Left Hand, Circular Polarization without Moving Parts, T. Anderson, R. Hautzik, and E. Wantuch, Airtron, Inc.

A Packaged Medium-Power Traveling-Wave Amplifier Tube for Airborne Service, C. Novak and H. Wolkstein, RCA.

High-Power, Wide-Tuning-Range, X-Band Magnetrors Extremely Stable at Rates of Rise Above 200 KV/USEC, M. Ungar and J. Jacobs, RCA.

ELECTRONIC COMPONENTS

Ceramic Stacked-Mount Receiving Tubes, C. F. Douglass, Sylvania.

A Transistorized Pulse Generator, W. Donnell and J. Moffitt, Texas Instruments, Inc.

Applications of Direct View Storage Tubes to Air Traffic Control and Navigation, H. Gates, Farnsworth Electronics Co.

Improvement in Radar Presentation, K. Curtis and T. Kelly, Raytheon Mfg. Co.

Operating Time Indicator, W. Erickson, Raytheon Mfg. Co.

Floated Rate-Integrating Gyro Performance—Criteria Optimization, J. W. Lower, Minneapolis-Honeywell Regulator Co.

Third Aeronautical Communications Symposium

UTICA, N. Y., NOVEMBER 6, 7, 8, 1957

Wednesday, November 6

Registration at Hotel Utica.

SPECTRUM UTILIZATION

A Time Compressed Single Sideband System, John Mattern and M. I. Jacob, Westinghouse Electric Corp.

Comparison of Modulation Systems for Digital Transmission, R. Filipowsky and E. Scherer, Westinghouse Electric Corp.

Synchronous SSB for Aeronautical Communications, W. L. Firestone and Angus Macdonald, Motorola.

A Continuous Analysis Speech Bandwidth Compression System, T. E. Bayston and S. J. Campanella, Melpar, Inc.

An Experimental Realization of Spectrum Conservation, H. E. Haynes and D. T. Hoger, RCA.

Luncheon

COMPONENTS AND EQUIPMENT

Uniform Design Criteria for Airborne CN&I Equipment, H. Wamboldt, Wright Air Development Ctr., and R. Trachtenberg, RCA.

An Airborne Receiver Technique for Obtaining Information from the Beam of a Ground Based Tracking Radar, R. J. McNair, Bell Aircraft Co.

Aircraft Electrical Systems for Transistor Electronic Equipment, J. A. Doremus, Aircraft Radio Corp.

Public Air-Ground Telephone Service Trial, L. M. Augustus, Michigan Bell Telephone Co.

Improved Utilization of Technical Man Hours, A. S. Brown, Stanford Research Inst.

Thursday, November 7

ANTENNAS AND PROPAGATION

Recent Advances in Pattern and Gain Measurement Techniques as Applied to Aircraft and Missile Antennas, K. C. Collins, Airborne Instrument Lab.

Tropospheric Scatter System Design Chart, L. P. Yeh, Westinghouse Electric Corp.

Space Diversification for Receiving Antennas in Scatter Communication Systems, G. B. Parrent, Jr., and M. J. Beran, AF Cambridge Research Ctr.

Effects of Selective Fading on AM Signals, W. D. Nupp, U. S. Naval Air Development Ctr.

A Long Range VHF Meteor Burst Communications System, W. R. Vincent and A. M. Peterson, Stanford Research Inst.

TECHNIQUES AND SYSTEMS

Quaternary Data Transmission System with Swinging Waveforms, R. Filipowsky, Westinghouse Electric Corp.

Choosing the Optimum Type of Modulation: A Comparison of Several Systems of Communication, G. J. Kelley, General Electric Co.

ABC—Air Block Control, H. K. Morgan, Bendix Aviation Corp.

Communication in Air Traffic Control, Robert Stuckelman, Wright Air Development Ctr.

Air Force Communications Equipment Looks into the Future, J. H. Vogelman, Rome Air Dev. Ctr.

Third IRE Instrumentation Conference and Exhibit

BILTMORE HOTEL, ATLANTA, GEORGIA, NOVEMBER 11–13

Monday, November 11
2:30 p.m.

DATA HANDLING SYSTEMS

Instrumentation for Static Test of C-130A Hercules, W. W. Hartsfield, Georgia Division, Lockheed Aircraft Corp.

In-Flight Recording for System Malfunction Detection, John Jamgochian and T. K. Speer, Georgia Division, Lockheed Aircraft Corp.

Dynamic Data System, B. J. Fister and C. A. Woodcock, General Electric Co., Aircraft Gas Turbine Div.

A Semi-Digital Process Simulator, M. Terao and K. Tamura, Electrotechnical Lab., Tokyo, Japan.

Tuesday, November 12
9:30 a.m.

ANALOG-DIGITAL CONVERSION

Transistorized Digital to Analog Converter, W. D. Rowe, Motor and Control Division, Westinghouse Electric Corp.

A Novel Voltage Digitizer, Bernard Lippel, U.S. Army Signal Engineering Labs.

The Coding of Analog Lines for Transmission by Standard Teletype to Remote Displays, John Brown, Engineering Research Inst., Univ. of Mich.

Multi-Channel Digital Data Logging System, Joseph Luongo, Federal Telecommunication Labs.

2:30 p.m.

DATA REDUCTION AND PROCESSING

Economical On-Line Data-Reduction System for Wind-Tunnel Force and Pressure Tests, M. Bain and M. Seamons, Jet Propulsion Lab., California Inst. of Technology.

An Automatic System for Handling Telemetered Data, C. B. McGuire, Boeing Airplane Co.

Automatic Recording and Reduction Facility for Project Vanguard, D. H. Gridley and W. B. Poland, Jr., Naval Research Lab., and C. E. Keith and R. S. Bowers, Radiation, Inc.

Data Handling for a Reliability Test Program, V. W. Walter and F. I. Bien, Inland Testing Labs.

Evening

Reception and buffet supper.

Wednesday, November 13
9:30 a.m.

RECORDING DEVICES AND TECHNIQUES

A New Six Channel X-Y Recorder and Point Plotter, H. C. Craddock, Scientific-Atlanta, Incorporated.

A High Speed Direct Writing Recorder, W. E. Harrison, Midwestern Instruments.

Design of Oscillographic Recorders for Efficient Use, V. E. Payne, U.S. Naval Ordnance Unit, Key West, Fla.

Techniques in Evaluating Instrumentation Type Magnetic Recording Tape, T. O. Moore, Orradio Industries, Inc.

Electronic Techniques in Liquid Level Measurement, T. L. Greenwood, Redstone Arsenal.

2:30 p.m.

INSTRUMENTATION METHODS AND PRINCIPLES

Some Fundamental Topics in Analog-Digital Interconversion, Bernard Lippel, U.S. Army Signal Engineering Labs.

General Design Considerations for Man-Machine Systems, J. C. Groce, Federal Telecommunication Labs.

System Study Through Frequency Contour Mapping, J. H. Fisher and R. S. Gaylord, The Ramo-Wooldridge Corp.

Definition and Synthesis of Optimum Smoothing Processes in Filter Terms, E. M. Boughton, 1st Lt., USAF, Holloman AFB.

The Uncertainty of Ideal Measurement Systems, J. B. Chatterton, Sperry Gyroscope Co.

Radio Fall Meeting

NOVEMBER 11, 12, 13, 1957, KING EDWARD HOTEL, TORONTO, CANADA

The meeting is sponsored by the Engineering Department of the Electronic Industries Association with the active participation of the IRE Professional Groups. Advance registration will be available at $4.00 upon request to the EIA Engineering Department, Rm. 650, 11 W. 42 St., New York 36, N. Y. All checks should be made out to EIA Engineering Department. Registration at the door will be $5.00. All tickets for the Radio Fall Meeting dinner will be available for sale at the door only.

Monday, November 11

EIA ENGINEERING DEPARTMENT

M. A. Acheson, presiding.

Television in Ten Languages, C. J. Hirsch, Hazeltine Corp.

International Component Standardization, Leon Podolsky, Sprague Electric Co.

EIA Activities in Automation, J. J. Harrington, Arthur D. Little, Inc.

QUALITY IMPROVEMENT AND RELIABILITY

J. R. Steen, presiding.

Progress in TV Receiver Reliability, E. H. Boden, Sylvania Electric Products, Inc.

Reliability Control Based on Multiple Sequential Feedback, C. M. Ryerson, RCA.

Purchasing Reliability, E. J. Breiding, IBM Corp.

Establishing a Practical Routine for Measuring TV and Radio Tube Quality in the Customer's Plant, D. M. Palamountain, Raytheon Manufacturing Co.

Stag Party

Tuesday, November 12

RADIO AND TELEVISION

J. F. McAllister, presiding.

Development of the 12-Volt Plate-Voltage Hybrid Automobile Radio Receivers—AM, Signal-Seeker and FM, C. C. Hsu, Bendix Radio Div.

Local Oscillator Radiation from Television and FM Sets, W. G. Peterson, Warwick Manufacturing Corp.

Techniques Involved in Meeting FCC Radiation Requirements at UHF, John Bell, Zenith Radio Corp.

Design Consideration of a Development UHF Tuner Using an RF Amplifier, J. B. Quirk, General Electric Co.

All-Transistor FM Radio Receiver, H. V. Stewart, Texas Instrument Co.

RADIO AND TELEVISION

Preben Gomard, presiding.

Minimizing the Effect of Cut-Off in TV Vertical Oscillators, S. F. Love, Radio Valve Co., Ltd.

Automatic Fine Tuning Circuitry in TV Receivers, K. W. Farr and L. J. Sienkiewicz, Westinghouse Electric Corp.

Vacuum Tube Requirements in Vertical-Deflection Circuits, K. W. Angel, RCA.

The Property of TV Sync Separator Without and With Interference Pulses in the Composite Signal, Eduaid Luedicke, RCA Victor Co., Ltd.

Analysis and Synthesis of Magnetic Field-in Yokes Using Rotating Probes, H. S. Vasilevskis, Philco Corp.

Cocktail Party

Radio Fall Meeting Dinner

Toastmaster: J. T. Henderson, President, IRE.

Speaker: To be announced.

Wednesday, November 13

ELECTRON DEVICES I

J. T. Cimorelli, presiding.

Design and Development of the RCA-21CYP22 21 Glass Color Picture Tube, C. P. Smith, A. M. Morrell, R. C. Demmy, RCA.

Application of the RCA 21CYP22 Round Glass Color Picture Tube, H. N. Hillegass, R. W. Hagmann, D. J. Ransom, RCA.

Earth's Field Effects in Shadowmask Color Tubes, G. A. Burdick, Sr., Sylvania Electric Products, Inc.

Tetrode Driver Tube for Hybrid Auto Sets, Joseph Gaziano, Raytheon Manufacturing Co.

Typical Germanium Power Transistor Data and Typical Circuit Applications, W. C. Caldwell and L. L. Lehner, Bendix Aviation Corp.

ELECTRON DEVICES

H. L. Owens, presiding.

Present Status of Transistor Receiver Design Procedures, W. H. Ryer and W. E. Sheehan, Raytheon Manufacturing Co.

Design Considerations for Tfansistor Portable Reflex Receivers, R. V. Fournier, RCA.

A Broadcast Receiver Using Diffused Meltback Transistors, Erich Gottlieb, General Electric Co.

Silicon TV Rectifiers, H. W. Henkels and Victor Sils, Westinghouse Electric Corp.

Effect of Transient Voltage on Junction Transistors, H. C. Lin and W. F. Jordan, Jr., CBS-Hytron.

Parameter Variation Results Affecting Multi-Stable Circuits, W. J. Maloney, General Electric Co.

Abstracts of IRE TRANSACTIONS

The following issues of TRANSACTIONS have recently been published, and are now available from the Institute of Radio Engineers, Inc., 1 East 79th Street, New York 21, N. Y. at the following prices. The contents of each issue and, where available, abstracts of technical papers are given below.

Sponsoring Group	Publication	Group Members	IRE Members	Non-Members*
Circuit Theory	Vol. CT-4, No. 2	$0.70	$1.05	$2.10
Reliability & Quality Control	PGRQC-11	1.35	2.00	4.05

*** Public libraries and colleges may purchase copies at IRE Member rates.**

Circuit Theory

VOL. CT-4, NO. 2, JUNE, 1957

Design of Unsymmetrical Band-Pass Filters—R. F. Baum

The paper presents a new approach to the synthesis of band-pass filters, in particular of filters with electrical characteristics which are not symmetrical with respect to their center frequency when plotted on an arithmetic frequency scale.

The synthesis proceeds in three steps: approximation, representation by means of fic-

titious network elements in the low-pass domain, and subsequent low-pass, band-pass transformation.

The approximation process leads to network functions defined by polynomials containing complex coefficients. It is shown that these functions can be handled with available synthesis procedures, if suitable modifications are made. This technique is based upon the properties of quasi-Hurwitz polynomials, treated in the appendix. These procedures then lead to a network representation in the low-pass domain, which includes two fictitious network elements, namely, constant positive or negative imaginary quantities. After a low-pass, band-pass transformation has been applied the network becomes physically realizable.

It is shown that unsymmetrical lossless networks can be developed into canonic forms in the low-pass domain.

A practical example is given.

Analysis and Synthesis of Delay Line Periodic Filters—H. Urkowitz (p. 41)

A periodic filter has a frequency characteristic which is periodic. Such filters can be constructed using delay lines where the delay of each line is the reciprocal of the basic frequency period. The network function of the periodic filter is characterized by the presence of the factors of the form e^{npT}, where n is a positive or negative integer, T is the delay of each delay line, and p is the complex frequency variable. Analysis and synthesis are simplified by use of the z transform which has been used with much success in the study of sampled data systems. A transformation of the filter network function is made by substituting z for e^{pT}. This substitution transforms the imaginary axis of the p plane into the central unit circle in the z plane.

The properties of the periodic filter are now characterized by the poles and zeros of the z-plane transform. A rational method is presented for synthesizing any z-plane transform expressed as a rational fraction. Finally, the z-transform concept is used to analyze the behavior of periodic filters with pulsed inputs.

Reviews of Current Literature—Abstracts of Articles on Circuit Theory—Outline of Generalized Filter Theory—E. Henze (in German). (p. 54)

Neutralization of the Selective Transistor Amplifier—G. Meyer-Brotz (in German). (p. 54)

Admittance Matrix of Active and Passive Networks—H. Pecher (in German). (p. 54)

Gyrators and Non-Reciprocal Systems—M. Prudhon (in French). (p. 54)

A Low-Pass/Band-Pass Frequency Transformation—K. Irani (in English). (p. 54)

On the Coupling Between Two Cavities—R. N. Gould and A. Cunliffe (in English). (p. 54)

Nonlinear Oscillators with Constant Time Delay—W. J. Cunningham (in English). (p. 55)

Evaluation and Design of Dissipative Composite Wave Filters—J. Scholten (in English). (p. 55)

Frequency Conversion with Positive Nonlinear Resistors—C. H. Page (in English). (p. 55)

Some Theorems on the Decomposition of the Operational Impedance of a Two-Terminal Electric Network—L. Lunelli (in Italian). (p. 55)

Correspondence (p. 55)

PGCT News (p. 56)

Reliability & Quality Control

PGRQC-11, August, 1957

(Papers Presented at the Third National Symposium, Washington, D. C., Jan. 14-15, 1957)

Progress in Reliability of Military Electronic Equipment During 1956—J. M. Bridges (p. 1)

The Military Reliable Tube Program—K. C. Harding (p. 8)

Evaluation of Transistor Life Data—J. D. Johnson and B. VanSwearingen (p. 15)

The purpose of evaluating transistor life data is to make possible proper application, specification and design of transistors. There are many methods of testing and analyzing life characteristics. These methods are reviewed and discussed here from the standpoint of the user, with emphasis on a particular statistical approach.

Components are initially evaluated at different temperatures to determine such general characteristics as current gain and leakage currents in the collector and emittor cutoff region. Samples are also submitted to mechanical and environmental tests. Life tests are conducted at various temperature and power levels. As a control feature, shelf life tests are usually performed simultaneously. Data collected from life tests are recorded on punched cards. Each card contains all the data for a given transistor at a particular time during the life test. This information is used as the input for an electronic calculator by means of which statistical summaries can be computed. The use of calculators accelerates the evaluation period and therefore allows more data to be analyzed efficiently. This method permits either individual or group evaluation procedures. Results are presented on curves and charts.

On the Measurement of Component Reliability—I. K. Munson (p. 27)

In-Process Controls to Maximize Capacitor Reliability—H. S. Herrick (p. 34)

Military Weapon Systems Complex and the Professor Factor—D. E. Noble (p. 54)

Method for the Determination of Reliability—K. E. Portz and H. R. Smith (p. 65)

IRE COMMITTEES—1957

Executive

J. T. Henderson, *Chairman*
W. R. G. Baker, *Vice-Chairman*
Haraden Pratt, *Secretary*

D. G. Fink — J. D. Ryder
A. V. Loughren — Ernest Weber

Admissions

J. L. Sheldon, *Chairman*

H. S. Bennett — A. V. Loughren
T. M. Bloomer — F. S. Mabry
L. A. Byman, Jr. — H. G. Miller
E. T. Dickey — W. L. Rehm
A. D. Emurian — N. B. Ritchey
L. O. Goldstone — L. M. Rodgers
J. A. Hansen — G. M. Rose, Jr.

Appointments

J. D. Ryder, *Chairman*

J. T. Henderson — K. V. Newton
E. W. Herold — D. E. Noble
A. V. Loughren — J. R. Whinnery
C. F. Wolcott

Awards

L. R. Fink, *Chairman*

Robert Adler — J. E. Keto
F. J. Bingley — C. N. Kimball
Cledo Brunetti — Urner Liddel
H. Busignies — K. A. Norton
R. M. Fano — J. C. R. Punchard
E. B. Ferrell — George Sinclair
D. E. Foster — A. W. Straiton
A. V. Haeff — Irven Travis
C. J. Hirsch — W. L. Webb
D. R. Hull — H. W. Wells
J. F. Jordan — E. M. Williams
H. A. Zahl

Awards Coordination

A. V. Loughren, *Chairman*

F. B. Llewellyn — Ernest Weber

Constitution and Laws

A. W. Graf, *Chairman*

S. L. Bailey — R. A. Heising
I. S. Coggeshall — W. R. Hewlett

Editorial Board

D. G. Fink, *Chairman*
E. W. Herold, *Vice-Chairman*
E. K. Gannett, *Managing Editor*

Ferdinand Hamburger, Jr. — T. A. Hunter
A. V. Loughren
W. Norris Tuttle

Editorial Reviewers

W. R. Abbott — J. M. Barstow
M. Acheson — B. L. Basore
R. B. Adler — B. B. Bauer
Robert Adler — W. R. Beam
H. A. Affel — L. L. Beranek
H. A. Affel, Jr. — P. P. Beroza
W. J. Albersheim — F. J. Bingley
B. H. Alexander — H. S. Black
J. A. Aseltine — J. T. Bolljahn
W. S. Bachman — H. G. Booker
H. G. Baerwald — J. L. Bower
E. M. Baldwin — W. E. Bradley
J. T. Bangert — J. G. Brainerd
W. L. Barrow — J. H. Bryant

Kenneth Bullington
J. H. Burnett
R. P. Burr
C. R. Burrows
W. E. Caldes
H. J. Carlin
T. J. Carroll
J. A. Chambers
H. A. Chinn
Marvin Chodorow
J. W. Christensen
L. J. Chu
J. K. Clapp
E. L. Clarke
L. E. Closson
J. D. Cobine
R. E. Colander
J. W. Coltman
P. W. Crapuchettes
M. G. Crosby
C. C. Cutler
Sidney Darlington
B. J. Dasher
W. B. Davenport, Jr.
A. R. D'Heedene
A. C. Dickieson
Milton Dishal
Wellesley Dodds
Melvin Doelz
R. B. Dome
H. D. Doolittle
J. J. Ebers
J. O. Edson
W. A. Edson
D. W. Epstein
Jess Epstein
W. L. Everitt
E. M. Fano
L. M. Field
J. W. Forrester
W. H. Forester
G. A. Fowler
R. W. Frank
F. L. Fredendall
H. B. Frost
E. G. Fubini
I. A. Getting
L. J. Giacoletto
E. N. Gilbert
Bernard Gold
W. M. Goodall
A. W. Graf
J. V. N. Granger
V. H. Grinich
A. J. Grossman
R. A. Gudmundsen
E. A. Guillemin
A. V. Haeff
N. I. Hall
W. W. Harman
D. B. Harris
A. E. Harrison
L. B. Headrick
P. J. Herbst
J. C. Hilliard
C. J. Hirsch
Gunnar Hok
J. L. Hollis
W. H. Huggins
J. F. Hull
R. G. E. Hutter
D. D. Israel
E. T. Jaynes
A. G. Jensen
R. L. Jepsen
Harwick Johnson
E. C. Jordan
Robert Kahal
Martin Katzin
W. H. Kautz
R. D. Kell
C. R. Knight
W. E. Kock
Rudolph Kompfner
J. B. H. Kuper
A. E. Laemmel
H. B. Law
R. R. Law
Vincent Learned
M. T. Lebenbaum
W. R. Lepage
F. D. Lewis
W. D. Lewis
J. G. Linvill
F. B. Llewellyn
S. P. Lloyd
A. W. Lo
J. R. MacDonald
Nathan Marchand
Nathan Marcuvitz
F. L. Marx
W. P. Mason
G. L. Matthaei
W. J. Mayo-Wells
E. D. McArthur
D. O. McCoy
Knox McIlwain
Brockway McMillan
R. E. Meagher
T. H. Meisling
Pierre Mertz
H. R. Mimno
S. E. Miller
A. R. Moore
Norman Moore
G. E. Mueller
E. J. Nalos
H. Q. North
K. A. Norton
W. B. Nottingham
B. M. Oliver
H. F. Olson
G. D. O'Neill
P. F. Ordung
C. H. Page
R. M. Page
R. C. Palmer
C. H. Papas
M. C. Pease, III
R. W. Peter
H. O. Peterson
W. H. Pickering
J. A. Pierce
W. J. Poch
A. J. Pote
R. L. Pritchard
C. F. Quate
W. H. Radford
J. R. Ragazzini
J. A. Rajchman
H. J. Riblet
D. H. Ring
Stanley Rogers
T. A. Rogers
H. E. Roys
V. H. Rumsey
J. D. Ryder
R. M. Ryder
Vincent Salmon
A. L. Samuel
H. A. Samulon
O. H. Schade
S. W. Seeley
Samuel Seely
O. G. Selfridge
Samuel Sensiper
R. F. Shea
R. E. Shelby
Donald Shuster
W. M. Siebert
D. B. Sinclair
George Sinclair
David Slepian
R. W. Slinkman
C. E. Smith
O. J. M. Smith
L. D. Smullin
R. A. Soderman
A. H. Sommer
R. C. Spencer
J. R. Steen
Leo Storch
A. W. Straiton
D. E. Sunstein
Charles Susskind
G. C. Sziklai
G. K. Teal
J. C. Tellier
E. R. Thomas
H. P. Thomas
H. E. Tompkins
J. G. Truxal
D. F. Tuttle, Jr.
L. C. Van Atta
K. S. Van Dyke
E. K. Van Tassel
S. N. Van Voorhis
O. G. Villard, Jr.
R. L. Wallace, Jr.
L. G. Walters
C. C. Wang
D. A. Watkins
D. K. Weaver, Jr.
S. E. Webber
W. M. Webster
P. K. Weimer
Louis Weinberg
J. R. Weiner
H. G. Weiss
J. O. Weldon
J. M. West
G. W Wheeler
H. A. Wheeler
J. R. Whinnery
W. D. White
J. B. Wiesner
Irving Wolff
G. O. Young
L. A. Zadeh

Education

Samuel Seely, *Chairman*

V. A. Babits
A. B. Bereskin
E. M. Boone
C. C. Britton
J. N. Dyer
I. O. Ebert
W. A. Edson
C. L. Foster
Ferdinand Hamburger, Jr.
C. D. Harp
A. E. Harrison
H. E. Hartig
E. W. Herold
G. B. Hoadley
T. A. Hunter
S. B. Ingram
T. F. Jones
Jerome Kurshan
C. R. Moe
H. A. Moench
A. D. Moore
P. H. Nelson
R. E. Nolte
J. M. Pettit
J. L. Potter
H. W. Price, Jr.
G. A. Richardson
J. D. Ryder
George Sinclair
H. H. Stewart
Donald V. Stocker
A. W. Straiton
O. I. Thompson
W. N. Tuttle
David Vitrogan
D. L. Waidelich
J. R. Whinnery
D. G. Wilson
A. L. Winn
M. E. Zaret

Finance

W. R. G. Baker, *Chairman*

J. T. Henderson
A. V. Loughren
Haraden Pratt
J. D. Ryder

History

Haraden Pratt, *Chairman*

Melville Eastham
Lloyd Espenschied
Keith Henney
H. W. Houck
L. E. Whittemore

Nominations

J. D. Ryder, *Chairman*

S. L. Bailey
J. T. Henderson
E. W. Herold
A. V. Loughren
J. W. McRae
K. V. Newton
H. W. Wells
J. R. Whinnery

Policy Advisory

C. F. Wolcott, *Chairman*

J. F. Byrne
J. N. Dyer
A. W. Graf
E. W. Herold
A. B. Oxley
F. A. Polkinghorn
Samuel Seely

Professional Groups

W. R. G. Baker, *Chairman*
A. W. Graf, *Vice-Chairman* (Central Div.)
M. E. Kennedy, *Vice-Chairman* (*Western Div.*)
Ernest Weber, *Vice-Chairman* (*Eastern Div.*)

Victor Azgapetian
M. S. Corrington
J. E. Eiselein
R. M. Emberson
D. G. Fink
R. A. Heising
J. T. Henderson
T. A. Hunter
A. V. Loughren
C. J. Marshall
W. J. Morlock
J. D. Noe
C. H. Page
A. C. Peterson, Jr.
Leon Podolsky
W. M. Rust, Jr.
J. D. Ryder
J. S. Saby
L. C. Van Atta
Lewis Winner

Chairmen of Professional Groups, *ex officio*.

Tellers

G. P. McCouch, *Chairman*

T. N. Anderson
C. G. Gorss, Jr.
P. G. Hansel
R. J. Keogh
G. F. Maedel
David Sillman
Ned A. Spencer

Special Committees

Armed Forces Liaison Committee

G. W. Bailey, *Chairman*

IRE-IEE International Liaison Committee

F. S. Barton
Ralph Bown
R. H. Davies
Willis Jackson
F. B. Llewellyn
C. G. Mayer
R. L. Smith-Rose
J. A. Stratton

Professional Recognition

G. B. Hoadley, *Chairman*

C. C. Chambers
H. F. Dart
W. E. Donovan
C. M. Edwards

Technical Committees

20. Standards Committees

M. W. Baldwin, Jr., *Chairman*
C. H. Page, *Vice-Chairman*
R. F. Shea, *Vice-Chairman*
L. G. Cumming, *Vice-Chairman*

J. Avins
W. R. Bennett
J. G. Brainerd
D. R. Brown
T. J. Carroll
P. S. Carter
A. G. Clavier
G. A. Deschamps
S. Doba, Jr.
J. E. Eiselein
D. Frezzolini
E. A. Gerber
A. B. Glenn
H. Goldberg
V. M. Graham
R. A. Hackbusch
H. C. Hardy
D. E. Harnett
A. G. Jensen
I. M. Kerney
J. G. Kreer, Jr.
W. A. Lynch
A. A. Macdonald
Wzyne Mason
D. E. Maxwell
H. R. Mimno
G. A. Morton
J. H. Mulligan, Jr.
W. Palmer
R. L. Pritchard
P. A. Redhead
R. Serrell
H. R. Terhune
W. E. Tolles
J. E. Ward
E. Weber
W. T. Wintringham

20.5 Definitions Coordinating

C. H. Page, *Chairman*
P. S. Carter, J. G. Kreer, Jr., E. A. Laport

20.8 Basic Terms

J. G. Brainerd, *Chairman*
M. W. Baldwin, Jr., C. H. Page

20.11 Coordination of Comments on International Standard Proposals

L. G. Cumming, *Chairman*

20.12 Ad Hoc Committee on Envelope Delay

P. S. Christaldi, *Chairman*

A. J. Baracket, W. L. Behrend (alt.), John Bullock, S. Doba, Jr., A. D. Fowler, G. L. Fredendall, L. A. Looney, Ralph Kennedy (alt.), N. J. Oman, J. R. Popkin-Clurman, J. Tillman, W. T. Wintringham

2. Antennas and Waveguides

G. A. Deschamps, *Chairman*
A. A. Oliner, *Vice-Chairman*
K. S. Packard, *Secretary*

J. Blass, P. S. Carter, M. J. DiToro, H. A. Finke, P. W. Hannan, W. C. Jakes, Jr., Henry Jasik, D. J. LeVine, P. A. Loth, R. L. Mattingly, D. C. Ports, W. Sichak, G. Sinclair, P. H. Smith, K. Tomiyasu, W. E. Waller, M. S. Wheeler

2.4 Waveguide and Waveguide Component Measurements

A. A. Oliner, *Chairman*
P. A. Loth, K. Packard, W. E. Waller

2.5 Methods of Antenna Measurement

R. L. Mattingly, *Chairman*
W. C. Jakes, Jr., D. J. LeVine, W. Sichak

3. Audio Techniques

Iden Kerney, *Chairman*
D. S. Dewire, *Vice-Chairman*

A. A. Alexander, C. A. Cady, R. H. Edmondson, A. P. Evans, F. K. Harvey, F. L. Hopper, A. H. Lind, A. A. McGee, R. C. Moody, F. W. Roberts, L. D. Runkle, R. E. Yaeger

3.1 Audio Definitions

D. S. Dewire, *Chairman*

W. E. Darnell, W. F. Dunklee, C. W. Frank, A. A. McGee, L. D. Runkel, R. E. Yaeger

3.3 Methods of Measurement of Distortion

R. C. Moody, *Chairman*

L. H. Bowman, F. Coker, J. French, L. D. Grignon, F. Ireland, E. King, J. J. Noble, E. Schreiber, R. Scoville, K. Singer, A. E. Tilley, P. Vlahos, P. Whister

3.4 Methods of Measurement of Noise

F. K. Harvey, *Chairman*

A. A. Alexander, C. A. Cady, A. P. Evans, H. A. Gauper, Jr., J. P. Smith

4. Circuits

W. A. Lynch, *Chairman*
J. T. Bangert, *Vice-Chairman*

W. R. Bennett, J. G. Brainerd, A. R. D'Heedene, T. R. Finch, R. M. Foster, W. H. Huggins, R. Kahal, H. L. Krauss, S. J. Mason, C. H. Page, E. H. Perkins, E. J. Robb, J. J. Suran, W. N. Tuttle, L. Weinberg

4.2 Linear Lumped-Constant Passive Circuits

L. Weinberg, *Chairman*

J. A. Aseltine, R. Kahal, G. L. Matthaei, J. G. Truxal

4.3 Circuit Topology

R. M. Foster, *Chairman*

R. L. Dietzold, S. Goldman, E. A. Guillemin, J. Riordan

4.4 Linear Varying-Parameter and Nonlinear Circuits

W. R. Bennett, *Chairman*

J. G. Kreer, Jr., C. H. Page, J. R. Weiner

4.7 Linear Active Circuits Including Networks with Feedback Servomechanism

E. H. Perkins, *Chairman*

E. J. Angelo, Jr., W. A. Lynch, J. M. Manley, C. F. Rehberg

4.8 Circuit Components

A. R. D'Heedene, *Chairman*

4.9 Fundamental Quantities

H. L. Krauss, *Chairman*

P. F. Ordung, J. D. Ryder

4.10 Solid State Circuits

J. J. Suran, *Chairman*

R. H. Baker, E. Gonzalez, R. A. Henle, J. G. Linvill, A. W. Lo, R. D. Middlebrook, D. O. Pederson, A. K. Rapp, G. H. Royer, R. R. Webster

4.11 Signal Theory

W. H. Huggins, *Chairman*

6. Electroacoustics

H. C. Hardy, *Chairman*
H. S. Knowles, *Vice-Chairman*

B. B. Bauer, M. Copel, W. D. Goodale, Jr., C. J. LeBel, H. F. Olson, V. Salmon, F. M. Wiener, A. M. Wiggins, P. B. Williams

7. Electron Tubes

(Chairman to be appointed)
G. A. Espersen, *Vice-Chairman*

J. R. Adams, E. M. Boone, A. W. Coolidge, W. S. Cranmer, P. A. Fleming, K. Garoff, T. J. Henry, E. O. Johnson, W. J. Kleen, P. M. Lapostolle, R. M. Matheson, G. D. O'Neill, A. T. Potjer, H. J. Reich, H. Rothe, W. G. Shepherd, E. S. Stengel, R. G. Stoudenheimer, W. W. Teich, B. H. Vine, R. R. Warnecke, S. E. Webber

7.1 Tubes in Which Transit-Time Is Not Essential

W. S. Cranmer, *Chairman*

T. A. Elder, W. T. Millis, E. E. Spitzer, A. K. Wing, A. H. Young

7.2 Cathode-Ray and Storage Tubes

J. R. Adams, *Chairman*

R. Dressler, H. J. Evans, J. T. Jans, L. T. Jansen, R. Koppelon, J. C. Nonnekens, G. W. Pratt, D. Van Ormer

7.2.2 Storage Tubes

A. S. Luftman, *Chairman*
J. A. Buckbee, *Secretary*

A. Bramley, A. E. Beckers, Joseph Burns, G. Chafaris, C. L. Corderman, M. Crost, D. Davis, Frances Darne, M. D. Harsh, B. Kazan, H. Hook, J. A. McCarthy, W. E. Mutter, D. L. Schaefer, H. M. Smith, W. O. Unruh

7.3 Gas Tubes

A. W. Coolidge, *Chairman*

J. H. Burnett, E. J. Handley, R. A. Herring, D. E. Marshall, G. G. Riska, W. W. Watrous, A. D. White, H. H. Wittenberg

7.3.1 Methods of Test for TR and ATR Tubes

L. W. Roberts, *Chairman*
A. Marchetti, *Secretary*

N. Cooper, L. Gould, H. Heins, F. Klawsnik, I. Reingold, R. Scudder, E. Vardon, R. Walker

7.4 Camera Tubes, Phototubes, and Storage Tubes in Which Photoemission is Essential

R. G. Stoudenheimer, *Chairman*

M. Adelman, H. H. Brauer, S. F. Essig, G. W. Iler, F. W. Schenkel, A. H. Sommer

7.5 High-Vacuum Microwave Tubes

E. M. Boone, *Chairman*

J. H. Bryant, R. L. Cohoon, H. W. Cole, G. A. Espersen, M. S. Glass, P. M. Lally, R. A. LaPlante, A. W. McEwan, R. R. Moats, H. L. McDowell, M. Nowogrodzki, S. E. Webber

7.5.1 Non-Operating Characteristics of Microwave Tubes

M. Nowogrodski, *Chairman*
R. L. Cohoon, *Secretary*

M. S. Glass — E. D. Reed
R. C. Hergenrother — F. E. Vacarro

7.5.2 Operating Measurements of Microwave Oscillator Tubes

R. R. Moats, *Chairman*
R. A. LaPlante, *Secretary*

T. P. Curtis — J. T. Sadler
G. I. Klein — M. Siegman
W. W. Teich

Consultants

A. E. Harrisan — J. S. Needle
J. F. Hull — E. C. Okress
T. Moreno — W. G. Shepherd

7.5.3 Operating Measurements of Microwave Amplifier Tubes

H. L. McDowell, *Chairman*
R. C. Knechtli, *Secretary*

J. Berlin — H. J. Hersh
M. R. Boyd — L. M. Holmbloe
H. W. Cole — A. W. McEwan
H. Einstein — S. E. Webber
G. Weibel

7.6 Physical Electronics

R. M. Matheson, *Chairman*

R. W. Atkinson — H. B. Frost
J. G. Buck — P. N. Hamblenton
L. Cronin — J. M. Lafferty
J. E. White

7.6.2 Noise

H. A. Haus, *Chairman*

W. B. Davenport — S. W. Harrison
W. H. Fonger — E. K. Stodola
W. A. Harris — T. E. Tapley

7.8 Camera Tubes

B. H. Vine, *Chairman*

B. R. Linden — D. H. Schaeffer
M. Rome — C. E. Thayer

8. Electronic Computers

D. R. Brown, *Chairman*
R. D. Elbourn, *Vice-Chairman*

S. N. Alexander — J. A. Rajchman
W. T. Clary — R. Serrell
M. K. Haynes — Q. W. Simkins
L. C. Hobbs — R. L. Snyder, Jr.
J. R. Johnson — W. H. Ware
M. Middelton, Jr. — C. R. Wayne
C. D. Morrill — J. R. Weiner
G. W. Patterson — C. F. West
Way Dong Woo

8.3 Static Storage Elements

M. K. Haynes, *Chairman*

H. R. Brownell — J. Rajchman
T. G. Chen — E. A. Sands
J. D. Lawrence — R. Stuart-Williams
W. Olander — D. H. Toth
C. B. Wakeman

Consultants

R. R. Blessing — C. C. Horstmann
R. O. Endres — M. F. Littmann
N. B. Saunders

8.3.1 Methods of Measurement of Bobbin Cores

C. B. Wakeman, *Chairman*

L. R. Adams — R. Kodis
N. Cushman — H. A. Lewis
B. Falk — C. Lufcy
A. Fitzpatrick — R. W. Olmsted
E. A. Gaugler — W. Schaal
M. Geroulo — W. Sielbach
J. R. Jaquet — E. Sommerfield
C. Williams

8.4 Definitions (Eastern Division)

R. D. Elbourn, *Chairman*

J. R. Johnson — R. P. Mayer
G. W. Patterson

8.5 Definitions (Western Division)

W. H. Ware, *Chairman*

L. C. Hobbs — W. E. Smith
H. T. Larson — W. S. Speer
R. Thorensen

8.6 Magnetic Recording for Computing Purposes

S. N. Alexander, *Chairman*

8.8 Analog Computers—Definitions and Symbols

C. D. Morrill, *Chairman*

Stanley Fifer — W. G. McClintock
Howard Hamer — T. A. Rogers

8.9 Digital Computer Logical and Block Diagram Symbols

G. W. Patterson, *Chairman*
J. S. Murphy, *Vice-Chairman*

C. F. Lee — R. J. Nelson
M. P. Marcus — A. J. Neumann
R. P. Mayer — J. J. O'Farrell
G. E. Poorte

9. Facsimile

D. Frezzolini, *Chairman*
P. Mertz, *Vice-Chairman*

H. F. Burkhard — L. R. Lankes
A. G. Cooley — R. N. Lesnick
D. K. DeNeuf — K. R. McConnell
J. Hackenberg — G. G. Murphy
J. R. Hancock — M. P. Rehm
J. V. Hogan — H. C. Ressler
B. H. Klyce — R. B. Shanck

26. Feedback Control Systems

J. E. Ward, *Chairman*
E. A. Sabin, *Vice-Chairman*

M. R. Aaron — J. C. Lozier
G. S. Axelby — T. Kemp Maples
V. B. Haas, Jr. — W. M. Pease
R. J. Kochenburger — P. Travers
D. P. Lindorff — R. B. Wilcox
W. K. Linvill — S. B. Williams
D. L. Lippitt — F. R. Zatlin

26.1 Terminology for Feedback Control Systems

F. Zweig, *Chairman*

G. R. Arthur — J. S. Mayo
C. F. Rehberg

26.2 Methods of Measurement and Test of Feedback Control Systems

V. Azgapetian, *Chairman*

R. Gordon — M. Matthews
A. F. Stuart

10. Industrial Electronics

J. E. Eiselein, *Chairman*
E. Mittelmann, *Vice-Chairman*

R. E. Anderson — H. R. Meahl
W. H. Brearley, Jr. — J. H. Mennie
G. P. Bosomworth — W. D. Novak
R. I. Brown — H. W. Parker
Cledo Brunetti — S. I. Rambo
E. W. Chapin — E. A. Roberts
R. D. Chipp — R. J. Roman
C. W. Frick — W. Richter
R. A. Gerhold — C. E. Smith
H. C. Gillespie — C. F. Spitzer
G. W. Jacob — L. W. Thomas
E. A. Keller — W. R. Thurston
T. P. Kinn — M. P. Vore
E. W. Leaver — J. Weinberger
V. Wouk

10.1 Definitions

R. J. Roman, *Chairman*

W. H. Brearley, Jr. — C. W. Frick
D. W. Cottle — W. Hausz
J. E. Eiselein — E. Mittelmann
C. F. Spitzer

10.3 Industrial Electronics Instrumentation and Control

E. Mittelmann, *Chairman*
W. H. Brearley, Jr., *Vice-Chairman*

R. E. Anderson — E. A. Keller
S. F. Bartles — D. Krett
R. I. Brown — C. W. Miller
D. Esperson — J. Niles
E. A. Goggio — W. D. Novak
C. E. Jones — C. F. Spitzer
N. P. Kalmus — L. W. Thomas
W. A. Wildhack

11. Information Theory and Modulation Systems

J. G. Kreer, Jr., *Chairman*
P. Elias, *Vice-Chairman*

P. L. Bargellini — S. Goldman
N. M. Blachman — H. W. Kohler
W. R. Bennett — E. R. Kretzmer
T. P. Cheatham, Jr. — N. Marchand
L. A. DeRosa — L. Meacham
M. J. E. Golay — J. F. Peters
D. Pollack

11.1 Modulation Systems

D. Pollack, *Chairman*

11.2 East Coast Information Theory

P. Elias, *Chairman*
R. M. Fano

11.3 West Coast Information Theory

N. M. Blachman, *Chairman*
J. H. Tillotson

25. Measurements and Instrumentation

J. H. Mulligan, Jr., *Chairman*

C. D. Owens, *Vice-Chairman*

M. J. Ackerman — G. B. Hoadley
P. S. Christaldi — G. A. Morton
J. L. Dalke — M. C. Selby
G. L. Fredendall — R. M. Showers

25.1 Basis Standards and Calibration Methods

M. C. Selby, *Chairman*

S. L. Bailey — G. L. Davies
F. J. Gaffney

25.2 Dielectric Measurements

J. L. Dalke, *Chairman*

C. A. Bieling — F. A. Muller

25.3 Magnetic Measurements

C. D. Owens, *Chairman*

W. E. Cairnes — R. C. Powell
D. I. Gordon — J. H. Rowen
P. H. Haas — E. J. Smith

25.4 Audio-Frequency Measurements

R. Grim — R. A. Long

25.5 Video Frequency Measurements

J. F. Fisher — H. A. Samulon
C. O. Marsh — W. R. Thurston

25.6 High Frequency Measurements

G. B. Hoadley, *Chairman*

R. A. Braden — E. W. Houghton
I. G. Easton — D. Keim
F. J. Gaffney — B. M. Oliver
B. Parzen

25.8 Interference Measurements

R. M. Showers, *Chairman*

H. E. Dinger — F. M. Greene
C. W. Frick — A. W. Sullivan

25.9 Measurement of Radio Activity

G. A. Morton, *Chairman*

25.10 Oscillography

M. J. Ackerman, *Chairman*

F. J. Bloom — G. R. Mezger (alternate)
W. G. Fockler — M. S. Rose
C. F. Fredericks — A. L. Stillwell
H. M. Joseph
H. Vollum

29. Medical Electronics

W. E. Tolles, *Chairman*

A. M. Grass — T. F. Hueter
J. P. Hervey — L. H. Montgomery, Jr.

16. Mobile Communication Systems

A. A. Macdonald, *Chairman*
W. A. Shipman, *Vice-Chairman*

N. Caplan — J. C. O'Brien
D. B. Harris — N. H. Shepherd
N. Monk — D. Talley
T. W. Tuttle — W. C. Vergara
A. Whitney

12. Navigation Aids

W. Palmer, *Chairman*
H. I. Metz, *Vice-Chairman*

A. M. Casabona — H. R. Mimno
D. G. C. Luck — A. G. Richardson
L. M. Sherer

12.2 Standard DF Measurements

E. D. Blodgett, *Chairman*
J. Kaplan, *Vice-Chairman*
R. Silberstein, *Secretary*

A. D. Bailey — W. M. Richardson
H. I. Butler — J. A. Solga
J. J. Kelleher — J. O. Spriggs
F. M. Kratokvil — C. A. Strom, Jr.
A. A. Kunze — S. R. Thrift
J. T. Lawrence — J. H. Trexler
H. R. Mimno — H. W. von Dohlen

12.3 Measurement Standards for Navigation Systems

F. Moskowitz, *Chairman*
S. B. Fishbein, *Secretary*

P. Adams — G. Litchford
R. Alexander — J. T. MacLemore
S. Anderson — G. E. Merer
R. Battle — J. S. Pritchard
S. D. Gurian — P. Ricketts
P. Hansel — Abe Tatz
V. Weihe

13. Nuclear Techniques

G. A. Morton, *Chairman*

R. L. Butenhoff — R. W. Johnston
D. L. Collins — T. R. Kohler
D. C. Cook — W. W. Managan
Louis Costrell

14. Piezoelectric and Ferroelectric Crystals

E. A. Gerber, *Chairman*
I. E. Fair, *Vice-Chairman*

J. R. Anderson — Hans Jaffe
J. H. Armstrong — E. D. Kennedy
H. G. Baerwald — T. M. Lambert
R. Bechmann — W. P. Mason
W. G. Cady — W. J. Merz
W. A. Edson — C. F. Pulvari
W. D. George — P. L. Smith
R. L. Harvey — R. A. Sykes
E. J. Huibregtse — K. S. VanDyke

14.1 Ferroelectric Crystals

J. R. Anderson, *Chairman*

J. H. Armstrong — E. D. Kennedy
E. J. Huibregtse — Walter Merz
C. Pulvari

14.2 Piezoelectric Crystals

R. Bechmann, *Chairman*

I. E. Fair — W. D. George
C. R. Mingins

14.4 Definitions for Magnetostriction

S. L. Ehrlich, *Chairman*

H. G. Baerwald — P. L. Smith
R. L. Harvey — R. S. Woollett

14.5 Piezoelectric Ceramics

H. Jaffe, *Chairman*

D. Berlincourt — T. Lambert
T. Kinsley — D. Schwartz

27. Radio Frequency Interference

A. B. Glenn, *Chairman*

C. C. Chambers — N. Flinn
J. F. Chappell — E. C. Freeland
E. W. Chapin — W. F. Goetter
K. A. Chittick — S. D. Hathaway
L. E. Coffey — J. B. Minter
M. S. Corrington — W. E. Pakala
H. E. Dinger — W. A. Shipman
R. J. Farber — R. M. Showers

27.1 Basic Measurements

M. S. Corrington, *Chairman*

E. W. Chapin — E. O. Johnson
F. M. Greene — V. Mancino
W. S. Skidmore

27.2 Definitions

C. W. Frick — R. M. Showers

27.3 Radio and TV Receivers

R. J. Farber, *Chairman*

A. Augustine — W. G. Peterson
E. W. Chapin — C. G. Seright
M. S. Corrington — P. Simpson
E. C. Freeland — W. S. Skidmore
R. O. Gray — M. Soja
E. O. Johnson — D. G. Thomas
W. R. Koch — A. E. Wolfram
R. S. Yoder

27.4 Radio Transmitters

W. F. Goetter, *Chairman*

H. S. Walker — V. Mancino

27.5 Industrial Electronics

27.7 Mobile Communications Equipment

W. Shipman, *Chairman*

K. Backman — J. R. Neubauer
W. M. Cagney — N. Sheppard
J. F. Chappell — B. Short
S. I. Conn — R. C. Stinson

27.12 Navigational and Communication Equipment

17. Radio Receivers

D. E. Harnett, *Chairman*
W. O. Swinyard, *Vice-Chairman*

J. Avins — G. S. Ley
K. A. Chittick — I. J. Melman
L. E. Closson — G. Mountjoy
A. S. Goldsmith — J. N. Phillips
D. J. Healey III — L. Riebman
J. J. Hopkins — J. D. Reid
K. W. Jarvis — L. M. Rodgers
J. K. Johnson — S. W. Seeley
W. R. Koch — F. B. Uphoff
R. S. Yoder

17.8 Television Receivers

W. O. Swinyard, *Chairman*

W. R. Alexander — C. E. Dean
J. Avins — E. Floyd
J. Bell — E. C. Freeland

W. J. Gruen
W. R. Koch
C. O. Marsh
I. J. Melman
B. S. Parmet
E. Pufahl
G. F. Rogers
S. P. Ronzheimer

17.10 Automatic Frequency and Phase Control

F. B. Uphoff, *Chairman*

R. Davies
K. Farr
W. J. Gruen
W. R. Koch
R. N. Rhodes
D. Richman
L. Riebman

17.11 AM-FM Broadcast Receivers

Alan Goldsmith, *Chairman*

John Merklenger
Richard Farber
Edward Cornet
Ralph Brown

15. Radio Transmitters

H. Goldberg, *Chairman*
A. E. Kerwien, *Vice-Chairman*

J. H. Battison
M. R. Briggs
A. Brown
H. R. Butler
T. Clark
W. R. Donsbach
L. K. Findley
H. E. Goldstine
F. B. Gunter
R. N. Harmon
J. B. Heffelfinger
P. J. Herbst
L. A. Looney
J. F. McDonald
S. M. Morrison
J. Ruston
G. W. Sellers
B. Sheffield
J. B. Singel
B. D. Smith
M. G. Staton
V. E. Trouant
I. R. Weir
V. Ziemelis

15.1 FM Transmitters

J. Ruston, *Chairman*

J. Bose
J. R. Boykin
N. Marchand
P. Osborne
H. P. Thomas

15.2 Radio-Telegraph Transmitters up to 50 MC

B. Sheffield, *Chairman*

J. L. Finch
J. F. McDonald
F. D. Webster
I. R. Weir

15.3 Double Sideband AM Transmitters

J. B. Heffelfinger, *Chairman*

W. T. Bishop, Jr.
E. J. Martin, Jr.
D. H. Hax

15.4 Pulse-Modulated Transmitters

B. D. Smith, *Chairman*

R. Bateman
L. V. Blake
L. L. Bonham
H. Goldberg
G. F. Montgomery
W. K. Roberts

15.5 Single Sideband Radio Communication Transmitters

J. B. Singel, *Chairman*

W. B. Bruene
J. P. Costas
H. E. Goldstine
L. Kahn
A. E. Kerwien
E. A. Laport

15.6 Television Broadcast Transmitters

R. N. Harmon, *Chairman*

E. Bradburd
W. F. Goetter
L. A. Looney
J. Ruston
F. E. Talmage

19. Recording and Reproducing

D. E. Maxwell, *Chairman*
R. C. Moyer, *Vice-Chairman*

M. Camras
W. R. Chynoweth
F. A. Comerci
E. W. D'Arcy
A. W. Friend
C. J. LeBel
W. E. Stewart
L. Thompson
T. G. Veal

19.1 Magnetic Recording

R. C. Moyer, *Chairman*

J. S. Boyers
M. Camras
F. A. Comerci
E. W. D'Arcy
W. H. Ericson
O. Kornei
K. I. Lichti
C. B. Pear
E. Schmidt
W. T. Selsted
T. L. Vinson
R. A. VonBehren

19.2 Mechanical Recording

L. Thompson, *Chairman*

W. S. Bachman
S. M. Fairchild
A. R. Morgan
R. C. Moyer
F. W. Roberts
A. S. R. Tobey

19.3 Optical Recording

T. G. Veal, *Chairman*

P. Fish
J. A. Maurer
E. Miller
C. Townsend

19.5 Flutter

F. A. Comerci, *Chairman*

S. M. Fairchild
U. Furst
C. J. LeBel

28. Solid State Devices

R. L. Pritchard, *Chairman*
W. M. Webster, *Vice-Chairman*
V. P. Mathis, *Secretary*

J. B. Angell
S. J. Angello
Abraham Coblenz
L. Davis, Jr.
J. M. Early
J. J. Ebers
H. Epstein
H. Goldberg
J. R. Hyneman
J. P. Jordan
N. R. Kornfield
A. W. Lampe
L. T. MacGill
W. J. Mayo-Wells
C. W. Mueller
W. J. Pietenpol
R. H. Rediker
J. R. Roeder
C. A. Rosen
B. J. Rothlein
R. M. Ryder
J. Saby
B. R. Shepard
S. Sherr
C. F. Spitzer

28.4 Semiconductor Devices

S. J. Angello, *Chairman* (AIEE)
J. M. Early, *Chairman* (IRE)

George Abraham
J. B. Angell
R. L. Bright
E. N. Clarke
A. Coblenz
S. K. Ghandi
J. D. Johnson
C. H. Knowles
R. M. LeLacheur
B. R. Lester
L. T. MacGill
H. T. Mooers
C. W. Mueller
R. L. Pritchard
B. J. Rothlein
H. N. Sachar
A. C. Scheckler
A. P. Stern
R. L. Trent

28.4.2 Methods of Test for Transistors for Linear CW Transmission Service

A. Coblenz, *Chairman*

28.4.3 Definitions and Letter Symbols of Semiconductors

B. J. Rothlein, *Chairman*

28.4.4 Methods of Test for Semiconductor Devices for Large-Signal Applications

R. L. Trent, *Chairman*

A. W. Berger
C. Huang
R. M. LeLacheur
R. L. Wooley

28.4.5 Methods of Test for Bulk Semiconductors

E. N. Clarke, *Chairman*

D. C. Cronemeyer
I. Drukaroff
J. R. Haynes
A. Kestenbaum
M. F. Lamorte
B. J. Rothlein
K. W. Uhler

28.4.7 Transistor Internal Parameters

R. L. Pritchard, *Chairman*

R. B. Adler
J. B. Angell
J. M. Early
W. M. Webster

28.4.9 Semiconductor Diode Definitions

C. H. Knowles, *Chairman*

L. D. Armstrong
D. C. Dickson
F. F. Finnegan
B. Jacobs
J. D. Johnson
R. P. Lyon
E. M. Pollard
R. H. Redicker
B. Seddon
D. R. Smith
E. L. Steele
J. R. Thurell

28.5 Dielectric Devices

H. Epstein, *Co-Chairman* (AIEE)
C. A. Rosen, *Co-Chairman* (IRE)

J. H. Armstrong
W. D. Bolton
J. Bramley
R. B. Delano, Jr.
H. Diamond
D. P. Faulk
R. Gerson
R. B. Gray
F. P. Hall
S. R. Hoh
H. F. Ivey
B. Jaffee
N. R. Kornfield
E. E. Loebner
E. F. Mayer
A. Myerhoff
H. I. Oshry
C. F. Pulvari
N. Rudnick
E. A. Sack
E. Schwenzfeger
F. A. Schwertz
G. Shaw
B. R. Shepard
C. F. Spitzer
L. E. Walkup

28.5.1 Nonlinear Capacitor Definitions

E. A. Sack, *Chairman*

28.5.2 Dielectric Electro-Optic Definitions

E. E. Loebner, *Chairman*

J. Bramley
F. Gordon
R. E. Halsted
H. L. Ivey
H. Kaulman
D. Livingston
R. Rulon
E. A. Sack
F. A. Schwertz
C. F. Spitzer
L. E. Ullery

28.5.3 Definitions, Formation and Utilization of Electrostatic Images

F. A. Schwertz, *Chairman*

28.6 Magnetic Devices

R. W. Rochelle, *Chairman* (IRE)
D. G. Scorgie, *Chairman* (AIEE)

A. Applebaum
D. R. Brown
T. H. Crowley
R. L. Harvey
C. L. Hogan
M. L. Kales
H. W. Katz
C. A. Maynard

T. R. McGuire
J. A. Osborn
G. F. Pittman
J. A. Rajchman
J. B. Russell
M. Sirvetz
H. F. Storm
V. C. Wilson

21. SYMBOLS

H. R. Terhune, *Chairman*
R. T. Haviland, *Vice-Chairman*

H. W. Becker
E. W. Borden
D. C. Bowen
M. C. Cisler
W. A. Ford
I. L. Marin
C. D. Mitchell
E. W. Olcott
M. B. Reed
C. F. Rehberg
R. V. Rice
M. P. Robinson
M. S. Smith
R. M. Stern
H. P. Westman

21.3 FUNCTIONAL REPRESENTATION OF CONTROL, COMPUTING AND SWITCHING EQUIPMENT

E. W. Olcott, *Chairman*

R. E. Buscher
T. G. Cober
H. J. Elschner (alt.)
H. F. Herbig
E. W. Jervis, Jr.
R. Knox
H. P. Kraatz
W. G. McClintock
F. T. Meyer
J. S. Osborne
T. J. Reilly
A. C. Reynolds, Jr.
R. C. Stiles
George Tranfield

21.5 NEW PROPOSALS AND SPECIAL ASSIGNMENTS

M. P. Robinson, *Chairman*

21.7 LETTER SYMBOLS

C. F. Rehberg, *Chairman*

M. C. Cisler
G. A. Deschamps
A. C. Gilmore, Jr.
R. M. Stern

22. TELEVISION SYSTEMS

W. T. Wintringham, *Chairman*
W. F. Bailey, *Vice-Chairman*

M. W. Baldwin, Jr.
J. E. Brown
K. A. Chittick
C. G. Fick
D. G. Fink
P. C. Goldmark
R. N. Harmon
J. E. Hayes
A. G. Jensen
I. J. Kaar
R. D. Kell
D. C. Livingston
H. T. Lyman
L. Mautner
J. Minter
A. F. Murray
D. W. Pugsley
D. B. Smith
A. J. Talamini, Jr.

22.2 TELEVISION PICTURE ELEMENT

D. C. Livingston, *Chairman*

J. B. Chatten
A. V. Bedford
P. W. Howells
P. Mertz

23. VIDEO TECHNIQUES

S. Doba, Jr., *Chairman*
G. L. Fredendall, *Vice-Chairman*

I. C. Abrahams
S. W. Athey
A. J. Baracket
J. M. Barstow
J. H. Battison
E. E. Benham
K. B. Benson
E. M. Coan
L. B. Davis
V. J. Duke
J. R. Hefele
J. L. Jones
R. T. Petruzzelli
W. J. Poch

23.1 DEFINITIONS

G. L. Fredendall, *Chairman*

I. C. Abrahams
R. F. Cotellessa
S. Deutsch
W. C. Espenlaub

23.3 VIDEO SYSTEMS AND COMPONENTS: METHODS OF MEASUREMENT

I. C. Abrahams, *Chairman*

G. M. Glassford
J. R. Hefele
A. Lind
N. E. Sprecher
E. Stein
W. B. Whalley

23.4 VIDEO SIGNAL TRANSMISSION: METHODS OF MEASUREMENT

J. M. Barstow, *Chairman*

A. B. Ehlinger (Alternate for W. B. Whalley)
R. D. Chipp (Alternate for H. Mate)
M. H. Diehl
H. P. Kelly
H. Mate
R. M. Morris
J. R. Popkin-Clurman
E. B. Pores
E. H. Schreiber
L. Staschover
J. W. Wentworth
W. B. Whalley

24. WAVE PROPAGATION

T. J. Carroll, *Chairman*

H. H. Beverage
H. G. Booker
K. Bullington
C. R. Burrows
A. G. Clavier
A. B. Crawford
J. T. deBettencourt
J. H. Dellinger
F. H. Dickson
H. Fine
I. H. Gerks
W. D. Hershberger
M. Katsin
M. Kline
M. G. Morgan
H. O. Peterson
M. L. Phillips
J. A. Pierce
J. C. W. Scott
J. C. Simon
R. J. Slutz
R. L. Smith-Rose
J. B. Smyth
A. W. Straiton
O. G. Villard, Jr.
J. P. Voge
J. R. Wait
A. T. Waterman
A. H. Waynick

IRE REPRESENTATIVES IN COLLEGES

Adelphi College: I. Feerst
*Agricultural and Mechanical College of Texas: H. C. Dillingham
*Akron, Univ. of: P. C. Smith
*Alabama Polytechnic Institute: H. M. Summer
**Alabama, Univ. of: P. H. Nelson
Alaska, Univ. of: R. P. Merritt
*Alberta, Univ. of: J. W. Porteous
*Arizona State College: C. H. Merritt
*Arizona, Univ. of: J. L. Knickerbocker
*Arkansas, Univ. of: W. W. Cannon
Augustana College: V. R. Nelson
*Bradley Univ.: P. Weinberg
Bridgeport, Univ. of: D. M. Silverstone
Brigham Young University: D. Bartholomew
*British Columbia, Univ. of: A. D. Moore
*Polytech. Inst. of Bklyn. (Day Div.): M. V. Joyce
*Polytech. Inst. of Bklyn. (Night Div.): G. J. Kent
Brooklyn College: E. H. Green
*Brown University: C. M. Angulo
*Bucknell University: H. Webb
Universidad de Buenos Aires: A. DiMarco
Buffalo, Univ. of: M. Hettinger
*Calif. Institute of Technology: H. C. Martel
*Calif. State Polytech. College: H. Hendriks
*Calif. University of: H. J. Scott
California, Univ. of at L.A.: W. L. Flock
Capitol Radio Eng. Inst.: L. M. Upchurch, Jr.
*Carnegie Inst. of Tech.: J. B. Woodford, Jr.
*Case Inst. of Tech.: J. R. Martin
Catholic University of America: G. E. McDuffie, Jr.
*Central Technical Institute: J. E. Lovan
*Cincinnati, Univ. of: A. B. Bereskin
*Clarkson College of Tech.: W. J. Strong
*Clemson College: L. C. Adams
*Colorado Agri. and Mech. College: C. C. Britton
*Colorado, Univ. of: C. T. Johnk
*Columbia University: P. Mauzey
*Connecticut, Univ. of: H. W. Lucal
*Cooper Union School of Eng.: J. B. Sherman
*Cornell University: T. McLean
Dartmouth College: M. G. Morgan
*Dayton, Univ. of: L. H. Rose
*Delaware, Univ. of: L. P. Bolgiano, Jr.
*Denver, Univ. of: E. Vance
*Detroit, Univ. of: G. M. Chute
DeVry Technical Inst.: W. B. McClelland
*Drexel Inst. of Tech.: H. H. Sun
Duke University: H. A. Owen, Jr.
Evansville College: M. S. Caslen
*Fenn College: K. S. Sherman
*Florida, Univ. of: H. M. Latour
Fordham University: D. F. McDonald
*George Washington Univ.: G. Abraham
*Georgia Inst. of Tech.: P. T. Hutchison
Gonzaga University: H. J. Webb
Harvard University: C. L. Hogan
Hofstra College: B. Zeines
Houston, Univ. of: W. L. Anderson
*Howard University: W. K. Sherman
*Illinois Inst. of Tech.: G. T. Flesher

Colleges with approved student branches.

*Illinois, Univ. of: P. F. Schwarzlose
Institute Technologico De Aeronautica: Chen To Tai
*Iowa State College: G. A. Richardson
*Iowa, State Univ. of: J. E. Frankhauser
*John Carroll University: W. F. O'Hearn, Jr.
*Johns Hopkins University: W. H. Huggins
*Kansas State College: K. W. Reister
*Kansas, Univ. of: D. Rummer
*Kentucky, Univ. of: N. B. Allison
*Lafayette College: F. W. Smith
*Lamar State College of Tech.: F. M. Crum
LaSalle College: D. T. Best
*Laval University: J. E. Dumas
*Lehigh University: L. G. McCracken
*Louisiana Polytechnic Inst.: D. L. Johnson
*Louisiana State Univ.: L. V. McLean
*Louisville, Univ. of: S. T. Fife
Lowell Technological Institute: C. A. Stevens
Loyola University: J. H. Battocletti
McGill University: F. S. Howes
*Maine, Univ. of: L. W. Bowles
*Manhattan College: C. J. Nisteruk
Manitoba, Univ. of: H. Haakonsen
*Marquette Univ.: To be appointed
*Maryland, Univ. of: H. W. Price
*Mass. Inst. of Tech.: J. F. Reintjes
*Mass., Univ. of: J. W. Langford
*Miami, Univ. of: F. B. Lucas
*Michigan College of Mining and Tech.: R. J. Jones
*Michigan State University: L. O. Ebert
*Michigan, Univ. of: J. E. Rowe
Milwaukee School of Eng'g.: T. I. Lyon
*Minnesota, Univ. of: L. T. Anderson
*Mississippi State College: H. H. McCown
Mississippi, Univ. of: A. B. Cullen
*Missouri School of Mines and Metallurgy: R. E. Nolte
*Missouri, Univ. of: J. C. Hogan
Mohawk Valley Tech. Inst.: W. R. Pulhamus
*Montana State College: R. C. Seibel
*Nebraska, Univ. of: W. C. Robison
*Nevada, Univ. of: To be appointed
*Newark College of Eng'g.: D. W. Dickey
*New Hampshire, Univ. of: A. L. Winn
*New Mexico College of A and M Arts: H. A. Brown
*New Mexico, Univ. of: B. M. Fannin
*New York, College of the City of: H. Wolf
*New York Univ. (Day and Eve. Div.): L. J. Hollander
*North Carolina State College: E. G. Manning
*North Dakota Agri. College: E. M. Anderson
*North Dakota, Univ. of: C. Thomforde
*Northeastern University: R. S. Rochefort
*Northwestern University: To be appointed
*Norwich University: R. F. Marsh
*Notre Dame, Univ. of: C. Hoffman
Oberlin College: C. E. Howe
*Ohio Northern Univ.: R. H. Nau
*Ohio State Univ. W. C. Davis
*Ohio University: D. B. Green
*Oklahoma State Univ.: H. T. Fristoe
*Oklahoma, Univ. of: C. E. Harp
*Oregon State College: A. L. Albert
Oregon Tech. Inst.: D. B. Orrell
Ottawa, Univ. of: L. A. Beauchesne
Pacific Union College: I. R. Neilsen
*Pennsylvania State University: H. J. Nearhoof
*Pennsylvania, Univ. of: R. Berkowitz
*Pittsburgh, Univ. of: J. Brinda, Jr.
*Pratt Institute: D. Vitrogan
*Princeton Univ.: J. B. Thomas
Providence College: E. B. Halton
Puerto Rico, Universidad de: B. Dueno
*Purdue University: W. H. Hayt, Jr.
Queen's University: H. H. Stewart
RCA Institutes, Inc.: P. J. Clinton
*Rensselaer Polytechnic Inst.: H. D. Harrit
*Rhode Island, Univ. of: M. J. Prince
*Rice Institute: C. R. Wischmeyer
Rochester Inst. of Tech.: C. F. Piotraschke
Rochester, Univ. of: C. H. Dawson
*Rose Polytechnic Institute: P. D. Smith
Royal Military College of Canada: W. D. Ryan
Royal Tech. Univ. of Denmark: G. Bruun
*Rutgers University: C. V. Longo
Ryerson Inst. of Tech.: V. J. Byers
*Saint Louis University: G. E. Dreifke
*San Diego State College: C. R. Moe
*San Jose State College: H. Engwicht
*Santa Clara, Univ. of: H. P. Nettesheim
Saskatchewan, Univ. of: A. M. Michalenko
*Seattle University: F. P. Wood
*South Carolina University: R. G. Fellers
*South Dakota State College of Agriculture and Mechanic Arts: J. N. Cheadle
*South Dakota School of Mines & Technology: D. R. Macken
*Southern Calif., Univ. of: R. W. Winchell
*Southern Methodist University: P. Harton
Southern Technical Institute: R. C. Carter
*Southwestern Louisiana Inst.: G. B. Bliss
*Stanford University: V. R. Eshleman
*Stevens Inst. of Technology: E. Peskin
*Swarthmore College: C. Barus
*Syracuse University: R. E. Gildersleeve
Tennessee A. & I. State University: F. W. Bright
*Tennessee, University of: F. M. McClelland
*Texas College of Arts and Industries: E. Korges
*Texas Technological College: C. Houston
*Texas, University of: W. H. Hartwig
Texas Western College: T. G. Barnes
*Toledo, Univ. of: D. J. Ewing
*Toronto, Univ. of: G. Sinclair
*Tufts Univ.: A. L. Pike
*Tulane University: J. A. Cronvich
Tulsa, Univ. of: H. M. Zenor
*Union College: R. B. Russ
*U. S. Naval Postgrad. School: G. R. Giet
*Utah State Agricultural College: W. L. Jones
*Utah, University of: D. K. Gehmlich
Valparaiso Technical Institute: E. E. Bullis
*Valparaiso University: W. Shewan
*Vanderbilt University: P. E. Dicker
*Vermont, University of: A. R. Eckels
*Villanova University: J. A. Klekotka
*Virginia Polytechnic Institute: R. R. Wright
*Virginia, Univ. of: W. P. Walker
*Washington, State College of: R. D. Harbour
*Washington University: H. A. Crosby
*Washington, University of: F. D. Robbins
Washington & Lee University: To be advised
*Wayne University: D. V. Stocker
*Wentworth Institute: T. A. Verrecchia
Wesleyan University: K. S. VanDyke
Western Ontario, Univ. of: E. H. Tull
*West Virginia University: C. B. Seibert
Wichita, Univ. of: A. T. Murphy
*Wisconsin, Univ. of: G. Kochler
*Worcester Poly. Inst.: H. H. Newell
*Wyoming, Univ. of: E. M. Lonsdale
*Yale University: J. G. Skalnik

IRE REPRESENTATIVES ON OTHER BODIES

ASA Conference of Executives of Organization Members: G. W. Bailey, L. G. Cumming, alternate

ASA Standards Council: E. Weber, A. G. Jensen, alternate, L. G. Cumming, alternate

ASA Electrical Standards Board: M. W. Baldwin, L. G. Cumming, E. Weber, A. G. Jensen, alternate

ASA Acoustical Standards Board: E. Weber, L. G. Cumming, alternate

ASA Graphic Standards Board: H. R. Terhune, R. T. Haviland, alternate

ASA Nuclear Standards Board: G. A. Morton, W. E. Shoupp, alternate, L. G. Cumming, alternate

ASA Sectional Committee (C16) on Radio: (Sponsored by IRE) E. Weber, Chairman, D. E. Harnett, M. W. Baldwin, Jr., L. G. Cumming, Secretary

ASA Sectional Committee (C39) on Electrical Measuring Instruments: J. H. Mulligan, C. D. Owens, alternate

ASA Sectional Committee (C42) on Definitions of Electrical Terms: M. W. Baldwin, Jr., J. G. Brainerd, A. G. Jensen, J. G. Kreer, Jr.

ASA Subcommittee (C42.1) on General Terms: J. G. Brainerd

ASA Subcommittee (C42.6) on Electrical Instruments: R. F. Shea

ASA Subcommittee (C42.13) on Communications: J. C. Schelleng

ASA Subcommittee (C42.14) on Electron Tubes: P. A. Redhead

ASA Sectional Committee (C60) on Standardization on Electron Tubes: R. L. Pritchard, P. A. Redhead

ASA Sectional Committee (C61) on Electric and Magnetic Magnitudes and Units: S. A. Schelkunoff, J. W. Horton, E. S. Purington

ASA Sectional Committee (C63) on Radio-Electrical Coordination: A. B. Glenn, R. M. Showers

ASA Sectional Committee (C67) on Standardization of Voltages—Preferred Voltages—100 Volts and Under: No IRE Voting Representative: Liaison: J. R. Steen

ASA Sectional Committee (C83) on Components for Electronic Equipment: P. K. McElroy

ASA Sectional Committee (C85) on Terminology for Automatic Controls: J. E. Ward, E. A. Sabin

ASA Sectional Committee (Y1) on Abbreviations: H. R. Terhune, R. T. Haviland, alternate

ASA Sectional Committee (Y10) on Letter Symbols: H. R. Terhune, R. T. Haviland, alternate

ASA Subcommittee (Y10.9) on Letter Symbols for Radio: C. F. Rehberg

ASA Subcommittee (Y10.14) on Nomenclature for Feedback Control Systems: J. E. Ward, W. A. Lynch, E. A. Sabin

ASA Sectional Committee (Y14) on Standards for Drawing and Drafting Room Practices: Austin Bailey, K. E. Anspach, alternate

ASA Sectional Committee (Y15) on Preferred Practice for the Preparation of Graphs, Charts and other Technical Illustrations: C. R. Muller, M. P. Robinson, alternate

ASA Sectional Committee (Y32) on Graphical Symbols and Designations: Austin Bailey, A. G. Clavier, A. F. Pomeroy, alternate

ASA Sectional Committee (Z17) on Preferred Numbers: H. R. Terhune

ASA Sectional Committee (Z57) on Sound Recording: (Sponsored by IRE) H. E. Roys, Chairman, F. A. Comerci, Representative, A. W. Friend, alternate, L. G. Cumming, Secretary

ASA Sectional Committee (Z58) on Standardization of Optics: T. Gentry Veal, E. Dudley Goodale, alternate

American Association for Advancement of Science: J. G. Brainerd

*International Radio Consultative Committee of U. S. Delegation: A. G. Jensen, Ernst Weber, L. G. Cumming, alternate

*Joint IRE-RETMA-SMPTE-NARTB Committee for Inter-Society Coordination (Television) (JCIC): W. J. Poch, M. W. Baldwin, L. G. Cumming, alternate

National Bureau of Standards Technical Advisory Committee: H. G. Booker, Chairman, W. L. Everitt, S. L. Bailey, H. W. Wells, J. B. Wiesner, A. H. Waynick

National Research Council—Div. of Eng. and Indus. Research: H. F. Wells

National Electronics Conference: J. J. Gershon

*U. S. National Committee of the International Electrotechnical Commission: M. W. Baldwin, Ernst Weber, L. G. Cumming, A. G. Jensen, alternate

*U. S. National Committee of the International Scientific Radio Union (URSI) Executive Committee: S. L. Bailey, Ernst Weber, alternate

* Submitted for approval of the Executive Committee.

Abstracts and References

Compiled by the Radio Research Organization of the Department of Scientific and Industrial Research, London, England, and Published by Arrangement with that Department and the *Electronic and Radio Engineer*, incorporating *Wireless Engineer*, London, England

NOTE: The Institute of Radio Engineers does not have available copies of the publications mentioned in these pages, nor does it have reprints of the articles abstracted. Correspondence regarding these articles and requests for their procurement should be addressed to the individual publications, not to the IRE.

The number in heavy type at the upper left of each Abstract is its Universal Decimal Classification number and is not to be confused with the Decimal Classification used by the United States National Bureau of Standards. The number in heavy type at the top right is the serial number of the Abstract. DC numbers marked with a dagger (†) must be regarded as provisional.

The Index to the Abstracts and References published in the PROC. IRE from February, 1956 through January, 1957 is published by the PROC. IRE, May, 1957, Part II. It is also published by *Electronic and Radio Engineer*, incorporating *Wireless Engineer*, and included in the March, 1957 issue of that journal. Included with the Index is a selected list of journals scanned for abstracting with publishers' addresses.

ACOUSTICS AND AUDIO FREQUENCIES

534.2-14 2652

On Wave Propagation in a Randon Inhomogeneous Medium—D. S. Potter and S. R. Murphy. (*J. Acoust. Soc. Amer.*, vol. 29, pp. 197–198; February, 1957.) A derivation of the coefficient of variation of intensity.

534.2-14-8 2653

Double Relaxation Effects—R. T. Beyer. (*J. Acoust. Soc. Amer.*, vol. 29, pp. 243–248; February, 1957.) Expressions are derived for the velocity of ultrasonic waves in fluid media and the excess absorption coefficient assuming two relaxation processes. The results are discussed for several special cases.

534.2:621.395.623.52 2654

Analysis of the Wave Parameters of the Exponential Horn—J. Kacprowski. (*Arch. Elektrotech.*, vol. 5, pp. 719–755; 1956. English summary, pp. 757–758.) The wave parameters of an exponential horn of finite length are evaluated on the basis of the general theory of four-terminal networks using matrix algebraic methods, and the results obtained are extrapolated for horns of infinite length. The concept of wave impedance of a horn is discussed. The transformation properties of the horn are analyzed.

534.24 2655

On Scattering and Reflection of Sound by Rough Surfaces—V. Twersky. (*J. Acoust. Soc. Amer.*, vol. 29, pp. 209–225; February, 1957.) A detailed analysis which extends the original work of Rayleigh and the previous work of the author (*e.g.*, *J. Appl. Phys.*, vol. 24, pp. 659–660; May, 1953.)

534.24 2656

On the Reflection of Sound at an Interface of Relative Motion—J. W. Miles. (*J. Acoust. Soc. Amer.*, vol. 29, pp. 226–228; February, 1957.) An analysis of reflection of a plane wave at an interface between two perfect fluids. The errors and limitations of previous work are discussed.

534.52 2657

Scattering of Sound by Sound—P. J. Westervelt. (*J. Acoust. Soc. Amer.*, vol. 29, pp. 199–203; February, 1957.) The effects of interaction are calculated by means of a scattering source function.

534.6:534.241 2658

The Development of "Echo-Parameter" Measuring Equipment—H. Niese. (*Nachr-Tech.*, vol. 6, pp. 545–552; December, 1956.) This parameter was defined earlier (670 of 1957) as the ratio of disturbing sound energy to total sound energy (useful+disturbing) received at the point of observation. A source of sound pulses (see 2324 of 1957) and special microphone are used to produce automatically an echo oscillogram from which the parameter can be derived.

534.78 2659

Note on the Design of "Terminal-Analogue" Speech Synthesizers—J. L. Flanagan. (*J. Acoust. Soc. Amer.*, vol. 29, pp. 306–310; February, 1957.) The synthesis of vowel sounds by lumped-constant electrical networks having transfer functions similar to the transmission properties of the vocal tract is considered.

534.86:534.76 2660

Influence of Noise upon the Equivalence of Intensity Differences and Small Time Delays in Two-Loudspeaker Systems—D. M. Leakey and E. C. Cherry. (*J. Acoust. Soc. Amer.*, vol. 29, pp. 284–286; February, 1957.) The effect is measured with speech and wide-band noise.

621.395.613.386 2661

Ear-Insert Microphone—R. D. Black. (*J. Acoust. Soc. Amer.*, vol. 29, pp. 260–264; February, 1957.) Results are presented of an investigation of factors which make possible the use of a microphone in the ear to pick up the voice of the wearer.

621.395.614 2662

Piezoelectric Ceramic "Bimetal" Strips used as Electroacoustic Transducers: Microphones—J. Peyssou. (*Ann. Radioélect.*, vol. 12, pp. 33–44; January, 1957.) A formula is derived for the emf generated by a cantilever formed by a twin strip of piezoelectric materials which is subjected to a bending moment. This effect is utilized in a form of microphone and various means of modifying its impedance are discussed. A circular "biceramic" diaphragm is designed, but the rectangular strip used as cantilever with its free end acting on the metal diaphragm of a microphone is a more efficient transducer.

621.395.614:546.289 2663

Piezoresistive Semiconductor Microphone—F. P. Burns. (*J. Acoust. Soc. Amer.*, vol. 29, pp. 248–253; February, 1957.) Design and constructional data are given for a germanium rod microphone. Performance is compared with that of a standard carbon button transmitter.

621.395.616:534.612.2 2664

Condenser Microphones for Measurement of High Sound Pressures—J. K. Hilliard and W. T. Fiala. (*J. Acoust. Soc. Amer.*, vol. 29, pp. 254–260; February, 1957.)

621.395.625.3 2665

The Characteristics of Magnetic Recording Heads and Tapes—H. P. Spring. (*J. Brit. IRE*, vol. 17, pp. 217–233; April, 1957.) The fundamental principles, operating conditions, and limitations are discussed. Some novel designs are described and the effect of head and tape wear on frequency response is measured.

ANTENNAS AND TRANSMISSION LINES

621.372.2:621.385.16 2666

The Attenuation of the Helical Wire Line—G. Schiefer. (*Arch. elekt. Übertragung*, vol. 11, pp. 35–40; January, 1957.) The propagation of an infinite number of partial modes along an inhomogeneous delay line based on Sensiper's model (1247 of 1955) is considered so as to determine the attenuation constant of the helical line. Some of the results calculated differ considerably from previous solutions obtained by considering the fundamental mode only. Diagrams are given for finding the attenuation constant as a function of line dimensions, wavelength, and wire conductivity.

621.372.2.029.6 2667

The Mode Conversion Phenomena of Laminated Transmission Lines and Their Influence on the Transmission by Single or Coupled Sections—H. E. Martin. (*Arch. elekt. Übertragung*, vol. 11, pp. 7–16 and 81–96; January/February, 1957.) The problem is considered of coupling power from coaxial into laminated lines, and vice versa, using graded potentials to reduce mode conversion losses [see also 328 of 1955 (Kaden and Martin)]. The influence of the dimensions and the transitions is investigated and methods of measuring transmission characteristics are discussed. Approximate for-

mulas are derived for transmission coefficients of an arrangement consisting of several series-connected laminated line sections.

621.372.21:621.315.213 2668
Theory of the Microstrip—T. T. Wu. (*J. Appl. Phys.*, vol. 28, pp. 299–302; March, 1957.) A discussion of the current distribution of the lowest mode of a transmission line consisting of a thin metallic strip pasted on the dielectric coating of a second and extensive conductor.

621.372.22 2669
Computation of the Impedances of Non-uniform Lines by a Direct Method—L. A. Pipes. (*Commun. & Electronics*, no. 27, pp. 551–554; November, 1956.) The impedances are computed by solving first-order nonlinear differential equations of the Riccati type. Special cases which include the uniform line, the Bessel line, and the Heaviside-Bessel line are discussed.

621.372.8:538.566.2 2670
Orthogonality Relation for Gyrotropic Waveguides—L. R. Walker. (*J. Appl. Phys.*, vol. 28, p. 377; March, 1957.) A generalization of a simpler theorem which is applicable to guides partially filled with ferrite or plasma.

621.372.8:621.317.352 2671
Equipment for Measuring Attenuation of the H_{01} Wave in Short Sections of Waveguides by the Cavity Resonance Method—V. M. Vakhnin and T. F. Kolodina. (*Radiotekhnika i Elektronika*, vol. 1, pp. 1485–1491; December, 1956.) A method is described of measuring the attentuation in cylindrical waveguides, with diameters of 50 mm, at a wavelength of 3.2 cm. The method is based on a comparison of the resonance curve of the measured volume with the frequency characteristic of an integrating *RC* circuit. Random errors are less that 1 per cent. The equipment is suitable for the determination of the influence of various factors, such as surface treatment, on the attenuation. A section drawing and photograph of the resonator are shown and a block diagram of the *Q* meter is given.

621.396.674.1 2672
Impedance of Thin-Wire Loop Antennas—J. E. Storer. (*Commun. & Electronics*, no. 27, pp. 606–619; November, 1956.) Hallén's rigorous Fourier-series solution is modified to avoid convergence difficulties. Calculated loop impedances for various wire gauges and antenna circumferences up to $2\frac{1}{2}\lambda$ are tabulated, and curves for the computation of field patterns and current distribution are given.

621.396.677 2673
A Limiting Case in the Design of an Excited-Reflector Antenna—V. A. Krishnaswamy. (*J. Inst. Telecommun. Eng., India*, vol. 3, pp. 38–42; December, 1956.) A discussion of a limitation in the use of an excited reflector in a two-element broadside array.

621.396.677:621.396.933.2 2674
D.F. Antenna System for Decimetre Wavelengths—C. Clarke. (*Electronic Radio Eng.*, vol. 34, pp. 238–245; July, 1957.) The development and performance of two antenna systems, for vertically and horizontally polarized waves, respectively, are described. They are designed to work with a twin-channel cr-tube instrument having an azimuthal coverage limited to a selected 90° sector.

621.396.677.3:523.16:523.72 2675
Interferometer for the Study of Localized Solar Sources of Centimetre Waves—Alon, Kundu, and Steinberg. (See 2733.)

621.396.677.833:523.16 2676
A New Form for a Giant Radio Telescope—Head. (See 2736.)

621.396.677.833.012.12 2677
A Method of Measuring the Directivity Characteristics of Radiotelescopes with High Resolving Power—N. A. Esepkina. (*C.R. Acad. Sci. U.R.S.S.*, vol. 113, pp. 94–96; March 1, 1957. In Russian.) Equations given relate the directivity characteristic of a system comprising a primary radiator at the focus of a parabolic mirror to that of a system in which the radiator is displaced from the focus along the axis of the mirror. Results are given of an experimental verification on a system comprising a primary radiator of 3-cm-λ radiation and a parabolic mirror with aperture 150 cm and focal length 50 cm; directivity curves obtained from measurements at a distance of 150 m with the primary radiator at the focus agree closely with those obtained at 13 m with the primary radiator displaced by 3 cm.

621.396.677.833.2:621.396.96 2678
A New Type of Surveillance [radar] Antenna: a Paraboloid Illuminated by a Slotted Waveguide—L. Thourel. (*Ann. Radioélect.*, vol. 12, pp. 3–13; January, 1957.) The production of a radiation pattern of given shape by means of a paraboloidal reflector illuminated by an equiphase linear source, such as a slotted waveguide, is described. Calculation and construction methods are indicated. The gain obtained with a reflector 1.8 m high is comparable to that of a double curvature reflector of 2.5-m height.

AUTOMATIC COMPUTERS

681.142 2679
The Principles of Universal Numerical Computers—F. H. Raymond. (*Onde élect.*, vol. 36, pp. 838–841; October, 1956, and vol. 37, pp. 68–78; January, 1957.) Continuation and conclusion of paper included in the Electronic Computer issue of the journal (see 997 of 1957).

681.142 2680
Designing for Reliability—N. H. Taylor. (PROC. IRE, vol. 45, pp. 811–822; June, 1957.) A discussion of reliability as applied to digital computer technology. The choice of components, their application, and considerations of design are discussed in detail. The design of a high-speed, vacuum-tube flip-flop is considered as a practical example.

681.142 2681
Punched-Card Transcriber for Automatic Computers—(*Tech. News Bull. Nat. Bur. Stand.*, vol. 41, pp. 38–39; March, 1957.) The unit described is intended for use with the SEAC computer (see 385 of 1951).

681.142 2682
Magnetic Data Recording Theory: Head Design—A. S. Hoagland. (*Commun. & Electronics*, no. 27, pp. 506–512; November, 1956.) The relation of the read-back waveform to bit density is examined and basic theoretical expressions are derived. The design of a recording head for magnetic disks is discussed with the aid of experimental results.

681.142 2683
Number Systems for Computers—I. J. Gabelman. (*Electronic Ind. Tele-Tech.* vol. 15, pp. 32–33, 118; December, 1956.) Decimal, binary, octal, bi-quinary, coded-decimal, and excess-three systems are considered.

681.142:519.283 2684
The Generation of Random Numbers on Automatic Computers—S. von Hoerner. (*Z. angew. Math. Phys.*, vol. 8, pp. 26–52; January 25, 1957.) Some mathematical methods are summarized and a new one, which avoids the formation of stable cycles and degeneration, is discussed. The theory of random-number generation using γ radiation is confirmed by means of the experimental arrangement described.

681.142:621.374.5.001.4 2685
Locating "Open Heaters" in Computer Circuitry—R. L. Ives. (*Electronic Ind. Tele-Tech.*, vol. 15, pp. 46–47, 102; December, 1956.)

681.142:621.374.32:621.314.7 2686
Computer Switching with Micro-alloy Transistors—J. B. Angell and M. M. Fortini. (*Electronic Ind. Tele-Tech.* vol. 15, pp. 38–39, 126; December, 1956.) Transistor characteristics are discussed in relation to flip-flop circuits.

CIRCUITS AND CIRCUIT ELEMENTS

621.3.011.21 2687
Contribution on the Calculation of the Total Impedance of Parallel-Connected Impedances—F. R. Belot. (*Rev. gén. Élect.*, vol. 65, pp. 675–676; December, 1956.) Outline of a slightly modified version of Boesch's method (991 of 1956) and description of a purely graphical method for rapidly obtaining results of adequate accuracy.

621.3.049 2688
High-Temperature Subassembly Design—R. B. Kieburtz. (*Electronics*, vol. 30, pp. 158–161; May 1, 1957.) A component-by-component survey of the problems involved and progress to date in achieving reliable operation at 500°C.

621.314.26 2689
Frequency Conversion by means of a Special Electronic Device—V. P. Tychinski. (*Radiotekhnika i Elektronika*, vol. 1, pp. 1525–1526; December, 1956.) The changes of frequency produced by the application of a modulating voltage to the helix of a traveling-wave tube [1808 of 1956 (Beck)] are discussed with reference to the application of this phenomenon in a frequency changing device.

621.372.22 2690
Theory of Inhomogeneous Transmission Lines—S. I. Orlov. (*Zh. Tekh. Fiz.*, vol. 26, pp. 2361–2372; October, 1956.) An expression is derived for the coefficient of reflection at the input of an arbitrary inhomogeneous line connected to an arbitrary complex impedance. For small inhomogeneities in a lossless line the problem of determining the law of change of the wave impedance along the line, is approximately solved, given the reflection coefficients at the input and output of the line as functions of frequency. The analysis is based on the classical theory of inhomogeneous transmission lines.

621.372.412 2691
Crystal-Controlled Oscillators—G. Becker. (*Arch. elekt. Übertragung*, vol. 11, pp. 41–47; January, 1957.) The characteristics of a number of oscillator circuits are discussed with reference to the criteria for the basic series-resonance and parallel-resonance types (see also 2048 of 1957).

621.372.5/.6 2692
Topological Analysis of Linear Nonreciprocal Networks—S. J. Mason. (PROC. IRE, vol. 45, pp. 829–838; June, 1957.)

621.372.5 2693
Time and Frequency Characteristics of Linear Pulse Systems with Variable Parameters—G. P. Tartakovski. (*Radiotekhnika i Elektronika*, vol. 1, pp. 1463–1473; December, 1956.) Theoretical paper. The application of the concepts introduced is illustrated by a discussion of a RC circuit under the influence of a pulsed fm signal.

621.372.5:512.9 2694
Circuit Analysis by Normalization—J. J. Hupert. (*Electronic Eng.*, vol. 29, pp. 226–230; May, 1957.) A method of network analysis

based on a normalization procedure similar to that used in the concept of the normalized resonance curve.

621.372.6 2695
The Interconnection of Two Multipoles—W. Ruppel. (*Arch. elekt. Übertragung*, vol. 11, pp. 33–34; January, 1957.) A method is described of determining the scattering matrix of a $2n$-terminal network consisting of two parts, if the matrices of the partial $2n$-terminal networks are known.

621.373+621.375.9]:538.561.029.6 2696
Negative-Temperature Reservoir Amplifiers—Motz. (See 2726.)

621.373:621.396.822 2697
Noise in Nonlinear Oscillators—M. A. Garstens. (*J. Appl. Phys.*, vol. 28, pp. 352–356; March, 1957.) An approximate solution is obtained of a nonhomogeneous nonlinear differential equation of van der Pol type for a noise driven oscillator.

621.373.029.42 2698
A Two-Phase Low-Frequency Oscillator: Part 2—E. F. Good. (*Electronic Eng.*, vol. 29, pp. 210–213; May, 1957.) Part 1: 2372 of 1957.

621.373.4 2699
Oscillators Unaffected by Load Impedance—F. Frisch and W. Herzog. (*Nachrichtentech. Z.*, vol. 10, pp. 35–38; January, 1957.) Oscillator circuits with frequency and amplitude independent of load impedance are examined (see also 1367 of 1957). Measurements on two experimental 100-kc oscillator circuits show that frequency changes are of the order of 0.1 per cent and do not exceed 0.35 per cent irrespective of load impedance.

621.373.421 2700
Investigations of the Nyquist Effect—H. Barkhausen and E. G. Woschni. (*Hochfreq. und Elektroakust.*, vol. 64, pp. 180–184; May, 1956.) Results of theoretical and experimental investigations on a Hartley-type oscillator are discussed.

621.373.421.11 2701
Variable-Frequency Generator of High Frequency Stability—S. Ryżko, R. Nowak, and J. Fórmaniak. (*Arch. Elektrotech.*, vol. 5, pp. 759–766; 1956. English summary, p. 767.) An oscillator for the 1.5–3-mc frequency range is designed on the basis of Groszkowski's analysis (2337 of 1956) of the Gouriet-Clapp oscillator (1627 of 1950 and 3170 of 1954). The temperature coefficient of frequency is $+4\times10^{-6}$/°C, and short-period frequency fluctuations are less than $\pm3\times10^{-6}$.

621.373.421.14:621.372.413 2702
Excitation of Oscillations in a High Q-Cavity Resonator by an Oscillator—A. P. Fedotov and B. K. Shembel'. (*Radiotekhnika i Elektronika*, vol. 1, pp. 1474–1477; December, 1956.) A calculation of an antiparasitic ('quenching') resistor in the line connecting the oscillator with the high-Q cavity resonator is presented.

621.373.444.1 2703
A Millimicrosecond Timebase—M. W. Jervis and R. T. Taylor (*Electronic Eng.*, vol. 29, pp. 218–219; May, 1957.) Circuit and performance of a hard-tube timebase producing a rate of change of voltage of 5×10^{11}v/sec are described.

621.373.52 2704
Transistor Relaxation Oscillations—F. J. Hyde and R. W. Smith. (*Electronic Eng.*, vol. 29, pp. 234–236; May, 1957.) The continuous relaxation oscillations occurring in a point-contact transistor circuit using a cr combination in shunt with the emitter input are studied as functions of emitter bias and ambient temperature. A method of temperature compensation is described.

621.373.52:621.373.431.1 2705
Multivibrator with Point-Contact Semiconductor Triode—K. S. Rzhevkin and M. A. Abdyukhanov. (*Radiotekhnika i Elektronika*, vol. 1, pp. 1478–1484; December, 1956.) The operation of a transistor multivibrator is briefly analyzed and design formulas are given. Calculated and experimental values are tabulated for comparison.

621.374.3:621.314.7 2706
Transistorized Low-Level Chopper Circuits—R. B. Hurley. (*Electronic Ind. Tele-Tech.*, vol. 15, pp. 42–43, 112; December, 1956.) Improved performance is obtained by the use of stabilizing and compensating resistances in collector and emitter circuits.

621.374.32:621.316.8.012.7 2707
Tolerance Limit of Resistors in Binary Scaling Units—B. M. Banerjee and S. Choudhury. (*Electronic Eng.*, vol. 29, pp. 237–241; May, 1957.) An experimental investigation shows that limits of ±20 per cent are permissible if optimum values are chosen for the cathode resistor.

621.374.33 2708
Linear Gate of 200 Millimicrosecond Duration—E. L. Garwin and A. S. Penfold. (*Rev. Sci. Instr.*, vol. 28, pp. 116–119; February, 1957.) The circuit gives an inverted output with a gain very close to unity and has a linearity within 1 per cent for pulses in the range 1 to 70 v.

621.375.2 2709
Operation of a Valve in a Grounded-Grid Circuit—A. Smoliński. (*Arch. Elektrotech.*, vol. 5, pp. 621–642; 1956. English summary, pp. 643–644.) Theoretical analysis.

621.375.3 2710
Magnetic-Amplifier Control of Switching Transistors—H. W. Collins. (*Commun. & Electronics*, no. 27, pp. 585–589; November, 1956.) The circuits described use a magnetic amplifier to control the average output power of switching transistors by pulse-width modulation combined with high-gain amplification.

GENERAL PHYSICS

535.13:537.122 2711
Particle Aspect of the Electromagnetic Field Equations—R. H. Good, Jr. (*Phys. Rev.*, vol. 105, pp. 1914–1919; March 15, 1957.) Maxwell's theory of the electromagnetic field in vacuum can be stated in a form closely similar to Dirac's theory of the electron.

536.7 2712
Fluctuations and Irreversible Thermodynamics—L. Tisza and I. Manning. (*Phys. Rev.*, vol. 105, pp. 1695–1705; March 15, 1957.) The theory of kinetic (time-dependent) fluctuation problems is developed on the basis of the kinetic analog of the Boltzmann-Einstein principle given by Onsager and Machlup (*ibid.*, vol. 91, pp. 1505–1515; September 15, 1953.)

537.122:539.15:621.315.61 2713
Effective Mass Approximation for Excitons—G. Dresselhaus. (*Phys. Chem. Solids*, vol. 1, pp. 14–22; September/October, 1956.)

537.221 2714
Contact Electrification across Metal/Dielectric and Dielectric/Dielectric Interfaces—G. S. Rose and S. G. Ward. (*Brit. J. Appl. Phys.* vol. 8, pp. 121–126; March, 1957.) The transfer of charge, across the interface produced when spherical and planar specimens are pressed into contact, has been measured.

537.31 2715
A [dielectric] Cylinder in the Field of a Point Source of Electric Current—B. P. D'yakonov. (*Bull. Acad. Sci. U.R.S.S., sér. géophys.*, no. 1, pp. 116–121; January, 1957. In Russian.) Theoretical calculation of the effect of an infinitely long cylinder of conducting dielectric embedded in a medium containing the point source of current.

537.311.1 2716
Electron and Lattice Conduction in Metals—I. I. Hanna and E. H. Sondheimer. (*Proc. Roy. Soc. A*, vol. 239, pp. 247–266; February 26, 1957.) Simple expressions are derived for the conduction magnitudes which are exact at high and low temperatures and are assumed to be approximately valid for all temperatures.

537.312.62 2717
Superconductivity—(*Wireless World*, vol. 63, pp. 326–330; July, 1957.) A discussion of the principles and applications.

537.52:621.317.382.029.63/.64 2718
Effect of Microwave Signals Incident upon Different Regions of a D.C. Hydrogen Glow Discharge—Udelson. (See 2866.)

537.525 2719
On the Measurement of Ionic Densities in Electric Discharges at High Frequency by means of Perforated Probes—A. Pozwolski. (*C.R. Acad. Sci., Paris*, vol. 244, pp. 1744–1746; March 25, 1957.) Measurements on hydrogen and argon discharges show negative and positive currents rising to a maximum at a pressure of about 0.05 mm Hg and dying away asymptotically as the pressure rises.

537.533.72:621.385.833 2720
Graphical-Analytical Construction of Space Trajectories of Charged Particles in Electrostatic Fields by the Method of Radii of Curvature—N. I. Shtepa. (*Zh. Tekh. Fiz.*, vol. 26, pp. 2281–2286; October, 1956.)

537.533.8.08 2721
Reverse Current in Apparatus of the Spherical-Capacitor Type—M. Ya. Mandel'shtam. (*Zh. Tekh. Fiz.* vol. 26, pp. 2234–2242; October, 1956.) In investigations of the energy distribution of secondary electrons by bombardment of a target in a spherical collector, elastically reflected electrons may cause secondary electron emission from the collector; in investigations of the photoemissive effect emission may occur from the collector due to diffusely scattered light. The dependence of the reverse current on the potential difference between the collector and the target is calculated.

538.2:621.318.134 2722
Dispersion Relations for Tensor Media and their Application to Ferrites—B. S. Gourary. (*J. Appl. Phys.*, vol. 28, pp. 283–288; March, 1957.) "The well-known Kronig-Kramers integral relations between the real and imaginary parts of the susceptibility are generalized to the case where the susceptibility is a tensor. The consequences of the principle of energy conservation are discussed. The case of a ferrite is discussed in some detail."

538.221 2723
Criterion for Uniform Micromagnetization—W. F. Brown, Jr. (*Phys. Rev.*, vol. 105, pp. 1479–1482; March 1, 1957.) An initial uniform state is compared with all neighboring states, uniform or nonuniform, as an initially large applied field decreases.

538.221:538.569.4 2724
Ferromagnetic Relaxation by the Exchange Interaction between Ferromagnetic and Conduction Electrons—A. H. Mitchell. (*Phys. Rev.*, vol. 105, pp. 1439–1444; March 1, 1957.) The relaxation time calculated from this mechanism is too long to account for the observed

line width in nickel. The exchange reaction may be dominant in other materials having narrower lines than nickel.

538.56:535.42 2725
Extension of Babinet's Principle to Absorbing and Transparent Materials, and Approximate Theory of Back-Scattering by Plane, Absorbing Disks—H. E. J. Neugebauer. (*J. Appl. Phys.*, vol. 28, pp. 302–307; March, 1957.) Calculations are made for circular disks of various reflection coefficients from zero to unity. Experimental results of Severin and v. Baeckmann (2693 of 1951) support the theory.

538.561.029.6:[621.373+621.375.9 2726
Negative-Temperature Reservoir Amplifiers—H. Motz. (*J. Electronics*, vol. 2, pp. 571–578; May, 1957.) Theoretical discussion of the principles of maser operation, with application to the conditions for oscillation in a cavity and for amplification in a transmission line.

538.569.4:535.33/.34 2727
Plane Parallel Plate-Transmission-Line Stark Microwave Spectrograph—S. A. Marshall and J. Weber. (*Rev. Sci. Instr.*, vol. 28, pp. 134–137; February, 1957.)

538.569.4:621.372.029.64 2728
Molecules and Microwaves—(*Electronic Radio Eng.*, vol. 34, pp. 254–257; July, 1957.) The basic principles of molecular absorption and emission of energy with particular reference to ammonia is discussed and the operation of molecular amplification by stimulated emission of radiation is described.

538.569.4.029.6:621.372.413 2729
A Precision Paramagnetic-Resonance Spectrometer—K. D. Bowers, R. A. Kamper, and R. B. D. Knight. (*J. Sci. Instr.*, vol. 34, pp. 49–53; February, 1957.) An accuracy within 3 parts in 10^6 is claimed.

537/539 2730
Solid-State Physics [Book Review]—F. Seitz and D. Turnbull (eds.). Publishers: Academic Books, London; vol. 1, 469 pp., 1955; vol. 2, 469 pp., 1956. (*Phys. Chem. Solids*, vol. 1, p. 128; September/October, 1956.) First of a series of volumes reviewing progress in different fields and planned to appear initially twice a year.

GEOPHYSICAL AND EXTRATERRESTRIAL PHENOMENA

523.16 2731
A Survey of Cosmic Radio Emission at 600 Mc/s—J. H. Piddington and G. H. Trent. (*Aust. J. Phys.*, vol. 9, pp. 481–493; December, 1956.) The celestial sphere was surveyed at Sydney, Australia, between declinations 90° S and 51° N using a 3.3° wide beam. When reduced to isophotes and plotted in celestial coordinates (epoch 1955), the results determined a galactic pole at $l \approx 330°$, $b - 89.1°$ (Lund coordinates) with the sun at about 50 parsecs north of the galactic plane. See also 2707 of 1956.

523.16 2732
An Investigation of the Radio Source 06N2A in Gemini—H. Rishbeth. (*Austr J. Phys.*, vol. 9, pp. 494–504; December, 1956.) During a lunar occulation the intensity of the source was reduced by over one fifth. The emission at meter wavelengths is mainly nonthermal.

523.16:523.72:621.396.677.3 2733
Interferometer for the Study of Localized Solar Sources of Centimetre Waves—I. Alon, M. R. Kundu, and J. L. Steinberg. (*C.R. Acad. Sci., Paris*, vol. 244, pp. 1726–1729; March 25, 1957.) The interferometer has two antennas 60 m apart on an east-west line. It was used for observations at 3.23 cm λ. Sources have an apparent diameter of 1 foot.

523.16:523.74 2734
Observation of Radio-Frequency Solar Storms by means of the Great Nançay Interferometer—Y. Avignon, E. J. Blum, A. Boischot, R. Charvin, M. Ginat and P. Simon. (*C.R. Acad. Sci., Paris*, vol. 244, pp. 1460–1463; March 11, 1957.) The diameter, duration, altitude, and conditions of formation were established by daily observations. See also 3644 of 1956 (Blum, *et al.*).

523.16:551.510.535:538.566 2735
Refraction of Extraterrestrial Radio Emission in the Atmosphere—W. A. Belyaev. (*Astronom. Zh.*, vol. 32, pp. 359–372; July/August, 1955.) Refraction due to a quiet unperturbed ionosphere and atmosphere is considered assuming that the electron-density height distribution in the layers is parabolic. Calculations indicate that below about 100 mc ionospheric refraction exceeds molecular refraction.

523.16:621.396.677.833 2736
A New Form for a Giant Radio Telescope—A. K. Head. (*Nature, London*, vol. 179, pp. 692–693; April 6, 1957.) The main reflector is a hemisphere of 250-foot radius which may be partly below ground. A small reflector designed to focus beams from the main reflector rotates in equatorially mounted bearings which are supported by a tripod and mounted at the center of the hemisphere. This form is claimed to be easier to construct than the usual steerable parabolic reflector of 250 feet or larger diameter.

523.5:621.396.67.012.12:621.396.11.029.62 2737
Height-Gain in the Forward-Scattering of Radio Waves by Meteor Trails—Hines and O'Grady. (See 2892.)

523.53:621.396.96 2738
Radio Echo Observations of Meteor Activity in the Southern Hemisphere—C. D. Ellyett and C. S. L. Keay. (*Aust. J. Phys.*, vol. 9, pp. 491–480; December, 1956.) Most meteoric matter incident on the southern hemisphere down to magnitude +4.5, is confined to direct orbits closely following the plane of the ecliptic. Increase of observation sensitivity shows that many of the meteors previously regarded as sporadic represent the upper limit of showers of minor-sized particles, which are present during months normally regarded as devoid of showers.

523.72 2739
Solar Radiation and Atmospheric Attenuation at 6-Millimetre Wavelength—R. N. Whitehurst, J. Copeland, and F. H. Mitchell. (*J. Appl. Phys.*, vol. 28, pp. 295–298; March, 1957.) A Dicke-type radiometer was used. The total vertical attenuation on clear summer days is 1.2 db and is 1 db higher for a thin overcast. The effective solar temperature in mid 1956 was 4500°K.

523.74/.75 2740
Determination of the Velocity of Corpuscles, Ejected from the Active Regions of the Sun, from the Time of Delay of Phenomena on the Earth—V. A. Petukhov. (*Bull. Acad. Sci. U.R.S.S., sér. géophys.*, no. 1, p. 124; January, 1957. In Russian.) Brief note drawing attention to the fact the corpuscles are not necessarily ejected radially from the sun.

523.74+523.72]:551.510.535 2741
Relations between the Sun and the Ionosphere—(*Nature, London*, vol. 179, pp. 804–806; April 20, 1957.) Summarized report of a discussion at the Royal Astronomical Society on February 22, 1957, where short papers were read dealing with the great solar flare of February 23, 1956 and the solar-cycle variation of the sun's ionizing radiation.

550.37/.38:35.083 2742
Experimental Investigation of the Natural Electromagnetic Field of the Earth in the Frequency Spectrum from 2 to 300 c/s—B. S. Enenshtein and L. E. Aronov. (*Bull. Acad. Sci. U.R.S.S., sér. géophys.*, no. 1, pp. 62–70; January, 1957. In Russian.) Apparatus for the determination of the horizontal electric and the three magnetic components is described and its use in field measurements is outlined. Oscillograms of some typical records are shown. The field strength varied considerably with time with a mean value of about 30–50 μv/km for the horizontal components of the electric field; the field strength of the horizontal magnetic components was of the order of 10^{-9} oersted.

550.371:523.5 2743
Influence of the Meteoric Stream of the Perseids on the Electric Field of the Earth's Atmosphere—M. V. Okhotsimskaya. (*Bull. Acad. Sci. U.R.S.S., sér. géophys.*, no. 1, pp. 122–123; January, 1957. In Russian.) Records at the Alma-Ata station situated at a height of 1800 m above sea level indicate that the percentage decrease of the potential gradient on August 18–19 relative to the normal value was 28 per cent in 1952, 31 per cent in 1953, 10 per cent in 1954, and 24 per cent in 1955. The observed effect may be due to processes occurring in the *E* layer by telemeteorites or by their screening effect.

551.510.5:551.593:537.5.08 2744
A Spectrophotometric Investigation of the Air Afterglow—D. T. Stewart. (*J. Atmos. Terr. Phys.*, vol. 10, pp. 318–319; 1957.) Further evidence that the spectral continuum having a short-wavelength limit at 3700 Å can be attributed to the nitrogen dioxide molecule.

551.510.5:551.594.5 2745
The Red and Near Infrared Auroral Spectrum—A. Omholt. (*J. Atmos. Terr. Phys.*, vol. 10, pp. 320–331; 1957.) The results of intensity measurements in the range 5400–8800 Å.

551.510.5:551.594.5:621.396.822 2746
Low-Frequency Radio Emission from Aurorae—G. R. Ellis. (*J. Atmos. Terr. Phys.*, vol. 10, pp. 302–306; 1957.) A possible contribution to the level of continuous noise observed at hundreds of kc may be Cherenkov radio emission originating from the incidence of auroral particles on the upper ionosphere. If the Cherenkov process is valid, the frequency range of the emission would extend from a few hundred kc to the low-audio frequencies.

551.510.535 2747
The Present State of Knowledge concerning the Lower Ionosphere—A. H. Waynick. (PROC. IRE, vol. 45, pp. 741–749; June, 1957.) A review of recent progress resulting from radio measurements and rocket sounding. Seventy-eight references.

550.510.555 2748
Analysis of Fading Records from Four Spaced Receivers for Ionospheric Wind Measurements—M. S. Rao and B. R. Rao. (*J. Atmos. Terr. Phys.*, vol. 10, pp. 307–317; 1957.) The advantages of a four-receiver system and an improved method of analyzing results are discussed.

551.510.535 2749
Diffraction Microscopy and the Ionosphere—G. L. Rogers. (*J. Atmos. Terr. Phys.*, vol. 10, pp. 332–337; 1957.) Improvements in the interpretation of existing Mitra fading patterns, used in the determination of ionospheric movement, through the application of diffraction microscopy technique are shown to be slight;

but with antenna spacings of 3–10 λ improvements might be substantial.

551.510.535 2750

Movements of Ionospheric Irregularities Observed Simultaneously by Different Methods—I. L. Jones, B. Landmark, and C. S. G. K. Setty. (*J. Atmos. Terr. Phys.*, vol. 10, pp. 296–301; 1957.) Horizontal movements of large F-layer and E-layer irregularities were traced by recording "bursts" of amplitude received from three transmitters about 15 km apart, and by other methods. It was concluded that the large irregularities had the same movements as those irregularities producing ordinary fading.

551.510.535 2751

Motion in the Night-Time E_s Region at Brisbane—J. A. Thomas and M. J. Burke. (*Aust. J. Phys.*, vol. 9, pp. 440–453; December, 1956.) Speeds of movement are grouped about 70 m, and the winds are predominantly towards the north.

551.510.535 2752

Double-Layer Phenomena in the E_s Region—J. A. Thomas. (*Aust. J. Phys.*, vol. 9, pp. 574–577; December, 1956.) *P'f* and *P'f* records are shown on which both "sequential E_s" and constant-height E_s are present. Occasional records also show "stacks" of E_s echo traces which are attributed to multiple hops between the E_s layers.

551.510.535 2753

The Behaviour of a Chapman Layer in the Night F_2 Region of the Ionosphere, under the Influence of Gravity, Diffusion, and Attachment—R. A. Duncan. (*Aust. J. Phys.*, vol. 9, pp. 436–439; December, 1957.) "It is shown that, in the presence of diffusion, gravity, and attachment, a Chapman layer, no matter what its height, maintains its shape, decaying uniformly with an effective attachment coefficient equal to the true attachment coefficient at the height of the electron density maximum; and that, at the same time, the layer drifts bodily towards an equilibrium height. It is then shown that a uniform vertical tidal drift will alter the equilibrium height of a Chapman layer."

551.510.535:621.396.11 2754

Reflection at a Sharply-Bounded Ionosphere—I. W. Yabroff. (PROC. IRE, vol. 45, pp. 750–753; June, 1957.) "A quantitative description of the waves transmitted into and reflected from a sharply-bounded, anisotropic ionosphere with losses is given. Given curves show the effects of the earth's field and losses for a particular model of the nighttime E layer at vlf."

551.594.22 2755

The Dependence of Point-Discharge Currents on Wind as Examined by a New Experimental Approach—M. I. Large and E. T. Pierce. (*J. Atmos. Terr. Phys.*, vol. 10, pp. 251–257; 1957.) "Experiments are described in which a metal point mounted in the open air is artificially raised to a high potential V and the resulting point-discharge current I is measured. The relation $I=A(V-V_0)(W^2+c^2V^2)^{\frac{1}{2}}$, where A and c are constants, W the wind speed, and V_0 the onset potential, is found to fit the results reasonably well."

551.594.22 2756

Point Discharge from an Isolated Point—J. R. Kirkman and J. A. Chalmers. (*J. Atmos. Terr. Phys.*, vol. 10, pp. 258–265; 1957.) The discharge current I from a point mounted on a mast was measured and related to wind speed W and natural potential gradient F. The results and those of earlier workers are shown to fit a formula $I=K(W+c)(F-M)$, where c and M are constants.

551.594.6 2757

Relations between the Character of Atmospherics and their Place of Origin—J. Chapman and E. T. Pierce. (PROC. IRE, vol. 45, pp. 804–806; June, 1957.) Waveforms of atmospherics from similar distances but different directions have been found to differ even when the ionospheric conditions along the two paths were apparently similar. The different conductivities of land and sea offer one humble explanation.

551.594.6 2758

Atmospheric Waveforms with Very-Low-Frequency Componants below 1 kc/s known as Slow Tails—F. Hepburn. (*J. Atmos. Terr. Phys.*, vol. 10, pp. 266–287; 1957.) Observed characteristics are explained by a critical application of Hales' waveguide theory (2888 of 1948) for propagation between the earth and a homogeneous layer with a lower boundary. The height of this boundary during the day is different from that at night.

551.594.6:621.317.35 2759

A Technique for the Rapid Analysis of Whistlers—J. K. Grierson. (PROC. IRE, vol. 45, pp. 806–811; June, 1957.) A proposal for a machine in which the whistlers are recorded magnetically, and successive small samples are played back repeatedly, at high speed, through a filter of rapidly varying frequency.

551.594.6:621.396.11.029.45 2760

Very-Low-Frequency Radiation from Lightning Strokes—E. L. Hill. (PROC. IRE, vol. 45, pp. 775–777; June, 1957.) Derivation of the frequency spectrum and total radiated power from an idealized model of the return stroke.

551.594.6:621.396.822 2761

Noise Investigation at V.L.F. by the National Bureau of Standards—W. Q. Crichlow. (PROC. IRE, vol. 45, pp. 778–782; June, 1957.) A brief description of new equipment for the measurement of atmosphereic noise, and a discussion of the most recent presentation of data on a world-wide basis.

551.594.6:621.396.822 2762

Some Recent Measurements of Atmospheric Noise in Canada—C. A. McKerrow. (PROC. IRE, vol. 45, pp. 782–786; June, 1957.) Measurements of noise power at 10 kc and 107 kc, and a comparison with previous data. Highest noise levels were in summer, but a smaller maximum occurred in winter.

551.594.6:621.396.822 2763

Characteristics of Atmospheric Noise from 1 to 100 kc/s—A. D. Watt and E. L. Maxwell. (PROC. IRE, vol. 45, pp. 787–794; June, 1957.) The frequency spectrum of the radio energy of a lightning flash is derived from the waveform of the current distribution. The results are combined with propagation data to determine the field at a distance. Amplitude probability distributions of received noise are plotted.

523.78:551.510.535 2764

Solar Eclipses and the Ionosphere [Book Review]—W. J. G. Beynon and G. M. Brown (eds.). Publishers: Pergamon Press, London and New York, 330 pp., 1956. (*Nature, London*, vol. 179, p. 711; April 6, 1957.) An account of the proceedings at a symposium held in London, August, 1955, giving fifty-three formal papers in full, brief accounts of discussions, and a comprehensive bibliography.

LOCATION AND AIDS TO NAVIGATION

621.396.933 2765

Automatic Position Plotting—(*Engineer, London*, vol. 203, p. 344; March 1, 1957.) A system of automatic triangulation of a number of bearings by means of luminous traces on a glass screen to determine the position of aircraft is briefly described. High-intensity projection cr tubes are used and the bearing information can be transmitted via telephone circuits or radio links.

621.396.933.2:621.396.677 2766

D.F. Aerial System for Decimetre Wavelengths—Clarke. (See 2674.)

621.396.96:621.396.677.833.2 2767

A New Type of Surveillance [radar] Aerial: a Paraboloid Illuminated by a Slotted Waveguide—Thoural. (See 2678.)

621.396.96:621.396.822:621.317.3 2768

Measurement of Noise Factor in Centimetric Radar—N. N. Patla. (*J. Inst. Telecommun. Eng. India*, vol. 3, pp. 32–37; December, 1956.) A description of methods in which the noise factors of the IF amplifier and the complete receiver are measured by means of noise diodes and gas-discharge tubes, respectively.

621.396.962.21 2769

Note on an Approximation Method of Forecasting the Distortion of Equiphase Hyperbolae where they Cross Coast Lines—P. Hugon. (*Ann. Radioélect.*, vol. 12, pp. 78–83; January, 1957.) Approximate formulas for the coastline correction were applied to a provisional Decca chain in Southern France; fair agreement with practical measurements was found.

621.396.963.083.7 2770

Remote Presentation of Radar Information by Microwave Link—G. J. Dixon and H. H. Thomas. (*J. Brit. IRE*, vol. 17, pp. 193–209; April, 1957.) The basic problems and possible systems are reviewed. An equipment operating at 4 kmc using pulse time modulation is described in detail.

621.396.965.088:621.396.677.859 2771

Measuring Radome Tracking Error—J. B. Damonte and A. F. Gaetano. (*Electronic Ind. Tele-Tech.*, vol. 16, pp. 66, 128, 132; January, 1957.) A quick and accurate method of measuring the error.

MATERIALS AND SUBSIDIARY TECHNIQUES

535.215:546.368.63 2772

The Characterization and Crystal Structure of Caesium Antimonide, a Photoelectric Surface Material—K. H. Jack and M. M. Wachtel. (*Proc. Roy. Soc. A*, vol. 239, pp. 46–60; February 12, 1957.) X-ray investigation shows that it is a "normal-valency" intermetallic compound with a small range of homogeneity near to the composition Cs_3Sb. The atomic arrangement is pseudo-body-centered cubic with a defect structure based upon the B32 sodium thallide type (NaTl).

535.215:546.471.241 2773

CdS-Type Photoconductivity in ZnTe Crystals—R. H. Bube and E. L. Lind. (*Phys. Rev.*, vol. 105, pp. 1711–1715; March 15, 1957.) Photoconductivity measurements on ZnTe single crystals show that the mechanism proposed for photoconductivity phenomena in CdS and CdSe may also be applied to ZnTe.

535.215:[546.817.231+546.817.241 2774

PbSe and PbTe Infrared Detectors—T. Piwkowski. (*Acta Phys. Polon.*, vol. 15, pp. 271–274; 1956. In English.) PbTe photoconductive and photovoltaic layers prepared by a known evaporation method retain their properties when exposed to the air but similar PbSe layers do not. A new evaporation method of preparing PbSe layers overcomes this disadvantage. Nineteen references.

535.215:546.817.231 2775

Photoconductivity of Lead Selenide: Theory of the Mechanism of Sensitization—J. N. Humphrey and R. L. Petritz. (*Phys. Rev.*, vol. 105, pp. 1736–1740; March 15, 1957.) Various models for the mechanism of photoconductivity are examined in relation to experimental results on the sensitization of

PbSe films by O, S, Se ,and the halogens. It is concluded that the only satisfactory model is one in which minority-carrier traps are introduced and the majority-carrier lifetime increased by the sensitizing agent.

535.37 2776

A Note on the Diffusion-Controlled Processes in Luminescent Solutions—A. Jabłoński. (*Acta Phys. Polon.*, vol. 15, pp. 263–266; 1956. In English.)

535.37:[546.472.21+546.482.21 2777

De-excitation of ZnS and ZnCdS Phosphors by Electric Fields—H. Kallmann and P. Mark. (*Phys. Rev.*, vol. 105, pp. 1445–1450; March 1, 1957.) The effect of strong applied ac and dc fields on the rise and decay of photoconductivity in ZnS and ZnCdS phosphors is described. The electron fields accelerate the de-excitation process. This phenomenon is attributed to the reduction of retrapping of excited electrons.

535.37:546.561–31 2778

A New Luminescence Emission in Cu_2O—J. Bloem, A. J. Van der Houven van Oordt, and F. A. Kröger. (*Physica*, vol. 22, pp. 1254–1256; December, 1956.) Infrared luminescence characteristics measured at 77° and 20°K are shown as a function of oxygen pressure during preparation.

535.376 2779

Electroluminescence Deterioration—W. A. Thornton. (*J. Appl. Phys.*, vol. 28, pp. 313–316; March, 1957.) The slow decrease in luminescence with time has been studied in conjunction with various associated effects. The observations are consistent with trap and donor depletion by electrolysis.

535.376 2780

Crystal Mount and Techniques for Measuring High-Frequency-Induced Electroluminescence—G. G. Harman. (*Rev. Sci. Instr.*, vol. 28, pp. 127–129; February, 1957.) The apparatus includes a simple optical system for irradiation and for separation of excitation and luminescence spectra. Excitation frequencies ranging from dc to to 400 mc, and also in selected microwave bands, may be used.

537.226/.227:546.431.824–31 2781

Activation Field and Coercivity of Ferroelectric Barium Titanate—H. H. Wieder. (*J. Appl. Phys.*, vol. 28, pp. 367–369; March, 1957.) Measurements obtained from hysteresis loop data may be used to calculate the activation field. The fields calculated lead to conclusions relating to the properties of the crystals.

537.226/.227:547.476.3 2782

Electric Strength of Rochelle Salt Crystals at a Constant, Alternating (50 c/s) or Pulse Voltage of 10^{-4}–10^{-7} sec Duration—K. M. Kevroleva. (*Zh. Tekh. Fiz.* vol. 26, pp. 2243–2247; October, 1956.) The dependence of breakdown voltage gradient on the thickness of the crystals, crystal axis, temperature, and time was investigated experimentally. Results show that the breakdown strength decreases with increasing thickness, that it is independent of temperature in the range −60°C to 50°C, and no changes occur at the Curie temperatures (−18°C and +24°C), that it is independent of the crystallographic axis, and that it increases with decreasing pulse duration.

537.226.3 2783

Mechanism of Dielectric Relaxation Losses in Crystals with Polar Molecules—I. Ts. Lyast. (*Zh. Tekh. Fiz.*, vol. 26, pp. 2293–2301; October, 1956.) The complex permittivity is calculated assuming the following mechanism: the relaxation dielectric losses are connected with the migration of polar molecules to unoccupied positions; this movement is, in general, accompanied by rotation of the polar molecule, resulting in relaxation polarization of the crystal. Theoretical and experimental results are compared for gypsum.

537.226.31 2784

Dielectric Losses in Dense Amorphous Structures—V. Kh. Kozlovski. (*Zh. Tekh. Fiz.*, vol. 26, pp. 2254–2258; October, 1956.) The losses are considered theoretically taking into account the inertia of ions. The frequency characteristic of the real and imaginary parts of the dielectric constant is calculated for particular cases.

537.227/.228:061.3(47) 2785

1st Conference on Ferroelectricity (Leningrad, 19th–24th June 1936)—(*Bull. Acad. Sci. U.R.S.S., sér. phys.*, vol. 21, pp. 233–292; February, 1957. In Russian.) Texts are given of the following five papers presented at the conference:

Brief Review of Some Results of Investigations of Ferroelectrics in Recent Years—G. A. Smolenski (pp. 233–263).

Orientation of Domains and Macrosymmetry of Properties of Ferroelectric Single Crystals—I. S. Zheludev and L. A. Shuvalov (pp. 264–274).

Crystal Chemistry of Ferroelectrics with Perovskite-Type Structure—Yu. N. Venevtsev and G. S. Zhdanov (pp. 275–285).

The Characteristic of the Change of Domain Structure of Rochelle Salt in Alternating Electric Fields—I. S. Zheludev and R. Ya. Sit'ko (pp. 286–288).

Some Details of Domain Structure of Rochelle Salt Crystals (from Optical Observations)—M. A. Chernysheva (pp. 289–292).

537.227:546.431.824–31 2786

Infrared-Absorption Studies on Barium Titanate and Related Materials—J. T. Last. (*Phys. Rev.*, vol. 105, pp. 1740–1750; March 15, 1957.) Absorption bands, arising from normal vibrations of the TiO_3 group, have been measured; they are centered on wave numbers of 495 cm^{-1} and 340 cm^{-1}.

537.311.31:538.63 2787

Magnetoresistance Effects in the Group I Metals at High Fields—R. G. Chambers (*Proc. Roy. Soc. A*, vol. 238, pp. 344–357; January 8, 1957.) Resistivity and Hall coefficient were measured in Cu, Ag, and Au at 4°K in fields up to 25 kg.

537.311.31:538.63 2788

Magnetoresistance—New Tool for Electrical Control Circuits—R. K. Willardson and A. C. Beer. (*Elec. Mfg.*, vol. 57, pp. 79–84; January, 1956.) Review of principles and applications.

537.311.33 2789

General Semiconductor Junction Relations N. H. Fletcher. (*J. Electronics*, vol. 2, pp. 609–610; May, 1957.) General carrier density relations are derived for an abrupt junction between two sections of semiconductor with arbitrary impurity contents and with an arbitrary applied bias.

537.311.33 2790

Drift of Minority Carriers in the Presence of Trapping—A. K. Jonscher. (*Proc. Phys. Soc., London*, vol. 70, pp. 223–229; February 1, 1957.) Expressions are derived for the densities of free carriers, N, and trapped carriers, N_t, as functions of distance and time, ignoring the effects of diffusion. The N/time-response curve depends critically on the steady-state carrier lifetime, the trapping time constants, and on the distance of the collector from the emitter.

537.311.33 2791

Diffusion of Minority Carriers in the Presence of Trapping—A. K. Jonscher. (*Proc. Phys. Soc., London*, vol. 70, pp. 230–234; February 1, 1957.) For constant-level carrier density, the diffusion is little affected by trapping in extrinsic material; if the density varies sinusoidally the effective diffusion length is the same as for the trap-free case at low and high frequencies but is appreciably less at intermediate frequencies.

537.311.33 2792

Possible Mechanism for Radiationless Recombination in Semiconductors—L. Bess. (*Phys. Rev.*, vol. 105, pp. 1469–1478; March 1, 1957.) Two Auger-type processes are described and evaluated whereby the trapping of a hole or electron results in the emission of an energetic hole or electron instead of a photon. These radiationless processes predominate over the radiative process under nearly all operating conditions for a wide class of semiconductors.

537.311.33 2793

Fluctuations in the Number of Electrons and Holes in a Semiconductor—D. J. Oliver. (*Proc. Phys. Soc., London*, vol. 70, pp. 244–247; February 1, 1957.) Statistical mechanics are used to extend previous work [793 of 1956 (Burgess)] to include semiconductors in which electrons and/or holes form a degenerate assembly.

537.311.33 2794

Theory of Semiconductors of Type $A^{III}B^{V}$—A. I. Gubanov (*Zh. Tekh. Fiz.*, vol. 26, pp. 2170–2178; October, 1956.) Critical comment on Seraphin's theory (1379 of 1955). A semiquantitative model is presented clarifying the widening of the forbidden zone in compounds of the $A^{III}B^{V}$ type in comparison with isoelectron elements of Group IV.

537.311.33 2795

Electronic Properties of Aromatic Hydrocarbons: Part 3—Diffusion of Excitons—O. Simpson. (*Proc. Roy. Soc. A.*, vol. 238, pp. 402–411; January 8, 1957.) A method is described by which the migration of excitons in anthracene can be observed. For Parts 1 and 2, see 2093 of 1956.

537.311.33:061.3(47) 2796

8th All-Union Conference on Semiconductors (Leningrad, 15th–21st November, 1955)—(*Bull. Acad. Sci. U.R.S.S., sér. phys.*, vol. 20, pp. 1467–1580; December, 1956; vol. 21, pp. 1–159, and pp. 161–224; January, February, 1957. In Russian.) Texts are given of papers presented in the following sections: a) electrical and thermal properties of semiconductors, b) theory of semiconductors, c) chemistry of semiconductors, and d) semiconductor catalysis. The papers include:

Thermal Equilibrium of Electrons in Surface and Bulk Levels in a Semiconductor—V. E. Lashkarev (pp. 1469–1478).

Thermoelectric Phenomena in Semiconductors with a Non-equilibrium Concentration of Current Carriers—Ya. Tauts [Taue] (pp. 1479–1483).

Appearance of Photoelectromotive Force in an Illuminated Semiconductor in an Inhomogeneous Magnetic Field—Ya. Tauts [Taue] (pp. 1484–1485).

Structure and Electrical Properties of Indium Antimonide in Thin Layers—I. D. Konozenko and S. D. Mikhnovski (pp. 1486–1490).

Investigation of the Peltier Effect and Thermoelectromotive Forces in Germanium—M. Shtenbek and I. I. Baranski (pp. 1491–1493).

New Vitreous Semiconductors—N. A. Goryunova and B. T. Kolomiets (pp. 1496–1500).

Semiconductor Properties of Magnesium—Bismuth Alloys—A. K. Kikoin and G. D. Fedorov (pp. 1501–1508).

Electrical Properties of Manganese-Germanium Alloys—I. G. Fakidov, N. P. Grazh-

dankina, and V. N. Novogrudski (pp. 1509–1518).

New Type of Thermal Acceptors in Germanium—V. A. Zhidkov and V. E. Lashkarev (pp. 1521–1525).

Diffusion of Antimony and Zinc from the Vapour Phase into Germanium—V. E. Kosenko (pp. 1526–1532).

Thermomechanical Phenomena in Thin Layers of Semiconductors—I. G. Nerkashevich (pp. 1533–1540).

Temperature Dependence of the Electrical Conductivity of Organic Semiconductors—A. T. Vartanyan (pp. 1541–1547).

Dependence of the Mobility of Current Carriers in Germanium on the Concentrations of Antimony and Phosphorus—P. I. Baranski (pp. 1548–1549).

Theory of Electric Strength of Germanium and Silicon—V. A. Chuenkov (pp. 1550–1552).

Electron Density Distribution and Electrical Conductivity of Cadmium Sulphide Crystals—Yu. N. Shuvalov (pp. 1553–1559).

An Attempt to Determine the Increase of Current Carrier Temperature Caused by an Electric Field in Germanium—M. Shtenbek (pp. 1560–1562).

Formation of Vacancies in a Crystal Lattice—N. P. Kalabukhov (pp. 1563–1568).

Production of Phosphors by means of Recrystallization in Electron Migration—Z. D'yulai (pp. 1569–1570).

Electrical Properties and Uses of Silicon Carbide—N. P. Bogorodlitski, V. V. Pasynkov, G. F. Kholuyanov, and D. A. Yaskov (pp. 1571–1580).

Spur Method for Conduction Electrons in Semiconductors: Part 1—Weak Interaction of Electrons with Oscillations. Part 2—Variational Method—M. A. Krivoglaz and S. I. Pekar (pp. 3–32).

Influence of the Polaron Effect on the Thermodynamics of Conduction Electrons in Semiconductors—M. A. Krivoglaz and S. I. Pekar (pp. 33–36).

Interaction of Excitons with a Molecular Lattice—E. I. Rashba (pp. 37–47).

Investigation of Crystal Micro-theory—K. B. Tolpygo (pp. 48–64).

Theory of Excitons in Ionic Crystals—I. M. Dykman (pp. 65–67).

Interaction of Localized Electrons with Acoustic Vibrations in Homopolar Crystals—M. F. Deigen (p. 68).

Recombination in a Collision of Current Carriers in Semiconductors—L. Sosnovski [Sosnowski] (pp. 70–73).

Excited States of Two-Electron Colour Centres in Ionic Crystals of α and β Bands—O. F. Tomasevich (pp. 74–77).

Energy Spectrum of Exciton in Ionic Crystal—I. P. Ipatova (pp. 78–86).

A Recombination Mechanism of Current Carriers in Strongly Alloyed Semiconductors—V. L. Bonch-Bruevich (pp. 87–96).

Some Peculiarities in the Thermodynamics of the Phonon and the Electron Gas in a Solid Body—Yu. N. Obraztsov (pp. 97–102).

Mean Free Path of an Electron in Liquid and Amorphous Conductors—A. I. Gubanov (p. 104).

Interaction of Electrons of a Semiconductor with Lattice Vibrations at Very Low Temperatures—L. E. Gurevich (pp. 105–111).

Some Electroacoustic Effects—L. E. Gurevich (pp. 112–119).

Some Problems of the Crystal Chemistry of Compounds with Zinc Blende Structure—N. A. Goryunova (pp. 120–132).

Theory of Phases [of compounds] of Variable Composition with Zinc Blende Structure (Investigation of Possible Range of Homogeneity of Type $A^{III}B^{V}$ Compounds)—B. F. Ormont, N. A. Goryunova, I. I. Ageeva, and N. N. Fedorova (pp. 133–140).

Physico-chemical Analysis of some Semiconductor Systems—N. Kh. Abrikosov (pp. 141–145).

Crystallization of Single-Crystal Layers of Silicon and Germanium from the Gaseous Phase—N. N. Sheftal', N. P. Kokorish, and A. V. Krasilov (pp. 146–152).

Production of Single-Crystal Specimens of Cuprous Oxide—Yu. I. Gritsenko (pp. 153–157).

Investigation of the Coefficients of Self-Diffusion of I and K Ions in Alkali-Halide Crystals Irradiated by X Rays—V. V. Mumladze (pp. 158–159).

Effect of Adsorption on the Electrical Conductivity and Work Function of a Semiconductor—V. B. Sandomirski (pp. 211–219).

Absorption of Light in Crystals of Mercury Halides—E. F. Gross and A. A. Kaplyanski (pp. 220–224).

537.311.33:535.215 2797

Kinetics of the Bipolar Photo-e.m.f. in a Semiconductor with Metal Electrodes—E. I. Kaplunova and K. B. Tolpygo. (*Zh. Tekh. Fiz.*, vol. 26, pp. 2165–2169; October, 1956.)

537.311.33:535.34 2798

The Anomalous Skin Effect and the Optical Absorptivity of Semiconductors: Part 2—R. B. Dingle. (*Physica*, vol. 22, pp. 1237–1241; December, 1956.) More general expressions are derived by solving the integro-differential equation of the anomalous skin effect. Part 1: 1116 of 1957.

537.311.33:537.324:546.87.24.23 2799

Solid Solutions Bi_2Te_3—Bi_2Se_3 as Materials for Thermoelements—S. S. Sinani and G. N. Gordyakova. (*Zh. Tekh. Fiz.*, vol. 26, pp. 2398–2399; October, 1956.) Brief note. The solid solutions, with various impurities, have a conductivity σ 490–900 $\Omega^{-1}\cdot cm^{-1}$, thermoelectric coefficient $-\alpha$ 225 to $-180\mu V/°C$, and thermal conductivity χ $2.6-3.0\times10^{3}$ $cal\cdot cm^{-1}deg^{-1}\cdot s^{-1}$.

537.311.33:538.21 2800

Magnetic Properties of Pure and *n*-Type Germanium at Liquid-Helium Temperatures—F. T. Hedgcock. (*J. Electronics*, vol. 2, pp. 513–528; May, 1957.) Susceptibility measurements at temperatures between 4.2°K and room temperature are reported for *n*-type Ge samples of various charge-carrier densities. In high-purity material an anomalous low-temperature paramagnetism was observed. For nondegenerate samples in a particular impurity concentration range, the results are consistent with the usual activation process, but below this concentration it seems necessary to suggest the existence of conduction in an impurity band.

537.311.33:538.6 2801

D.C. Magnetoconductivity and Energy Band Structure in Semiconductors—R. M. Broudy and J. D. Venables. (*Phys. Rev.*, vol. 105, pp. 1757–1763; March 15, 1957.) A general method is described for experimentally obtaining all components of the magnetoresistivity and hence the magnetoconductivity tensor. Expressions for determining the mass ratio K have been derived. The known band structures of *n*-type Ge and Si have been verified by the method and K has been determined for Ge from 65°K to 200°K.

537.311.33:538.6 2802

The Galvanomagnetic and Thermomagnetic Effects in Semiconductors—R. Mansfield. (*Proc. Phys. Soc., London*, vol. 70, pp. 240–243; February 1, 1957.) The values of the coefficients are calculated for a semiconductor in which the charge centers are scattered by ionized impurity centers.

537.311.33:538.63 2803

Theory of the Hall and Nernst Effects in a Semiconductor with an Impurity Zone—M. I. Klinger, V. G. Novikova, and V. N. Agarkova. (*Zh. Tekh. Fiz.* vol. 26, pp. 2185–2194; October, 1956.) The Hall effect, R, and the Nernst effect, Q, are first considered for a metal with a narrow conduction zone and then for a semiconductor with an impurity zone. The functions $R(T)$ and $Q(T)$ are investigated and experimental results are compared with theory.

537.311.33:538.63 2804

Measurement of Gauss Effect in Various Semi-conductors at 10,300 and 600 Mc/s—P. Ramer, M. J. O. Strutt, and F. K. von Willisen. (*Arch. elekt. Übertragung*, vol. 11, pp. 1–7; January, 1957.) The Gauss effect is a galvanomagnetic effect in which the resistance of a semiconductor increases in a transverse magnetic field; it is directly connected with the Hall effect. Measurements on samples of InAs, InSb, and Ge show a slight decrease in galvanomagnetic effects at 10 mc and very pronounced falls at 300 and 600 mc compared to the values obtained at zero frequency. The experimental methods and errors and the limitations of existing theory are discussed.

537.311.33:538.632 2805

A Simple Graphical Method of Calculating the Density of Current Carriers in a Semiconductor from the Hall Coefficient—T. S. Robinson, M. Smollett, and R. G. Pratt. (*Brit. J. Appl. Phys.*, vol. 8, pp. 130–131; March, 1957.)

537.311.33:[546.28+546.289 2806

Energy Band Structure in *p*-type Germanium and Silicon—E. O. Kane. (*Phys. Chem. Solids*, vol. 1, pp. 82–99; September/October, 1956.) Energy-band calculations are made for the three valence bands in Si and Ge in terms of the cyclotron resonance parameters. The energy in the band measured from $k=0$ is not assumed small compared with the spin-orbit splitting. Matrix elements for direct optical transitions between valence bands and the free-carrier absorption are calculated.

537.311.33:546.28 2807

Energy Levels in Electron-Bombarded Silicon—G. K. Wertheim. (*Phys. Rev.*, vol. 105, pp. 1730–1735; March 15, 1957.) "Electron bombardment of *n*- and *p*-type silicon reduces the lifetime of minority carriers and decreases the carrier concentration. This paper presents evidence that: 1) an electron trapping level is located 0.16 ev below the conduction band and a hole-trapping level 0.29 ev above the valence band, 2) the recombination centers responsible for the reduction of lifetime in *n* type are located 0.31 ev from a band edge, and those in *p* type approximately 0.24 ev from a band edge, 3) lattice imperfections are produced at a rate of 0.18 per electron-cm of bombardment at 700 kev."

537.311.33:546.28 2808

Electrical and Optical Properties of Heat-Treated Silicon—W. Kaiser. (*Phys. Rev.*, vol. 105, pp. 1751–1756; March 15, 1957.) The effects of oxygen impurity in Si crystals pulled from a quartz crucible have been investigated by optical and electrical means after heat-treatment at 450°C and 1000°C.

537.311.33:546.28 2809

Absorption Spectra of Impurities in Silicon: Part 1—Group III Acceptors—E. Burstein, G. Picus, B. Henvis, and R. Wallis. (*Phys. Chem. Solids*, vol. 1, pp. 65–74; September/October, 1956.) The spectra give information about the ionization energies and excited states of the impurity centers. The results are compared with a simple theoretical model.

537.311.33:546.28 2810

Absorption Spectra of Impurities in Silicon: Part 2—Group V Donors—G. Pincus, E. Burstein, and B. Henvis. (*Phys. Chem. Solids*,

vol. 1, pp. 75–81; September/October, 1956.) These spectra were measured at liquid helium temperature, and ionization energies and term schemes for these materials have been determined from the data. Part 1: 2809 above.

537.311.33[546.28+546.289]:536.21 2811
The Thermal Conductivity of Germanium and Silicon between 2 and 300°K—J. A. Carruthers, T. H. Geballe, H. M. Rosenberg, and J. M. Ziman. (*Proc. Roy. Soc. A*, vol. 238, pp. 502–514; January 29, 1957.) Measurements on single crystals of pure *n*-type and *p*-type Ge containing from 10^{14} to 10^{19} Group III impurity atoms per cm³ and on pure *n*-type and gold-doped *p*-type Si are reported.

537.311.33:546.281.26:535.3 2812
Absorption of Light in Alpha SiC Near the Band Edge—W. J. Choyke and L. Patrick. (*Phys. Rev.*, vol. 105, pp. 1721–1723; March 15, 1957.)

537.311.33:546.289 2813
Vacuum Technology for Germanium—Z. Majewski. (*Arch. Elektrotech.*, vol. 5, pp. 769–779; 1956.) The technological process used in the production of metallic Ge from the oxide of Polish origin is described and the equipment used in the production of single crystals is discussed. The methods of resistivity and lifetime measurement used in various stages of manufacture are briefly described and the results are given.

537.311.33:546.289 2814
Thermal Acceptors in Germanium—H. Letaw, Jr. (*Phys. Chem. Solids*, vol. 1, pp. 100–116; September/October, 1956.) Thermal acceptors in Ge are identified as vacancies with an energy of formation of 2 ev. In the annealing of Ge divacancies are initially formed, followed by clusters of higher order.

537.311.33:546.289 2815
Storage of Injected Carriers at Surfaces of Germanium—B. H. Schultz. (*Philips Res. Rep.*, vol. 12, pp. 82–96; February, 1957.) The effects of surface storage are calculated using standard space-charge theory. Measurements of the relaxation of photoconductance show the storage to be appreciable although the surface layer is very thin. The results are in qualitative agreement with theory.

537.311.33:546.289 2816
Investigation of Surface Conductivity and Surface Recombination in Germanium Specimens—A. V. Rzhanov, I. G. Neizvestnyi, and V. V. Roslyakov. (*Zh. Tekh. Fiz.*, vol. 26, pp. 2142–2153; October, 1956.) Results of an experimental investigation are reported. A correlation is established between the changes in surface conductivity and the surface recombination velocity in Ge specimens in various gas media. This correlation is shown to be connected with changes in the surface potential which is evaluated.

537.311.33:546.289 2817
Field Effect on an Illuminated Ge Surface and Investigation of the Surface Recombination Process—S. Wang and G. Wallis. (*Phys. Rev.*, vol. 105, pp. 1459–1464; March 1, 1957.) From measurements of surface conductivity and photoconductivity on an etched Ge sample in the Brattain-Bardeen ambient cycle, values of surface potential and surface recombination velocity were derived. Dominant recombination centers with discrete levels were found near the center of the gap with a ratio of hole to electron capture probabilities of 9. The effect of a normal electric field was also studied and good agreement between theory and experiment obtained. This effect can be used as an additional tool to study the surface recombination centers.

537.311.33:546.289 2818
Recombination Radiation from Deformed and Alloyed Germanium *p-n* Junctions at 80°K—R. Newman. (*Phys. Rev.*, vol. 105, pp. 1715–1720; March 15, 1957.) The recombination radiation from Ge *p-n* junctions shows an intrinsic band, peaked at 0.7 ev, and also a band peaked at about 0.5 ev which is attributed to mechanical strain. Junctions containing Cu show a radiation band at 0.59 ev.

537.311.33:546.289:537.32 2819
Some Aspects of Peltier Heating at Liquid /Solid Interfaces in Germanium—W. G. Pfann, K. E. Benson, and J. H. Wernick. (*J. Electronics*, vol. 2, pp. 597–608; May, 1957.) Uses of Peltier heating in growing single crystals, in producing *n-p-n* and *n-p-n-p* junctions in semiconductors, and in temperature-gradient zone melting, are discussed. The Peltier coefficient at the interface between the solid and liquid phases of a substance, may be determined from the velocity of interface movement due to Peltier heating.

537.311.33:546.289:538.639 2820
Nernst-Ettingshausen Effect in Germanium—R. I. Bashirov and I. M. Tsidil'kovski. (*Zh. Tekh. Fiz.*, vol. 26, pp. 2195–2199; October, 1956.) Measurements on specimens of *n*- and *p*-type Ge in the temperature range 125–650°K are reported and the results are discussed.

537.311.33:546.289:545.7 2821
Determination of Gaseous Impurities in the Surface Layers of Germanium—S. M. Fainshtein and V. I. Fistul'. (*Zh. Tekh. Fiz.*, vol. 26, pp. 2162–2164; October, 1956.) A mass-spectrometer used in conjunction with a vacuum extraction system was used. The method used and results obtained are briefly described.

537.311.33:546.561–31 2822
Diffusion of Chemical Admixtures in Cuprous Oxide and their Influence on its Rectification Properties—A. V. Sandulova and A. I. Andrievski. (*Radiotekhnika i Elektronika*, vol. 1, pp. 1492–1502; December, 1956.) Results are presented of an experimental determination of the diffusion coefficients for P^{32}, S^{35}, I^{131}, and Au^{198} in cuprous oxides with various structures and of the influence of Ag^{110}, S^{35}, and I^{131} impurities and of excess oxygen on the electrical parameters of cuprous oxide rectifiers.

537.311.33:546.621.86 2823
Electrical and Optical Properties of Aluminium Antimonide; Action of Lithium—F. Kover and A. Quilliet. (*C.R. Acad. Sci., Paris*, vol. 244, pp. 1739–1741; March 25, 1957.) Alloying Li to the pure substance greatly increases the resistivity. It is suggested that the pure substance is composed of slightly more atoms of Al than of Sb and that Li atoms may fill the resulting gaps in its structure. See also 178 of 1957 (Kover).

537.311.33:546.681.23.19 2824
Arsenoselenides of Gallium—N. A. Goryunova and V. S. Grigor'eva. (*Zh. Tekh. Fiz.*, vol. 26, pp. 2157–2161; October, 1956.) Brief report on X ray, surface microstructure, and quantitative analysis of compounds in the *m* GaAs. $(1-m)Ga_2Se_3$ system. An electrical-conductivity/composition curve is also given.

537.311.33:546.682.86:535.215 2825
Theory of the Spectral Distribution of Recombination Radiation from InSb—T. S. Moss. (*Proc. Phys. Soc., London*, vol. 70, pp. 247–250; February 1, 1957.) The theory explains satisfactorily the observed spectral distribution and indicates that 20 per cent of the total recombinations are radiative.

537.311.33:548.0:621.385.833 2826
The Examination of *p–n* Junctions with the Scanning Electron Microscope—C. W. Oatley and T. E. Everhart. (*J. Electronics*, vol. 2, pp. 568–570; May, 1957.) A technique for showing up junctions is described, with discussion of factors affecting contrast.

537.311.33:549.351.12 2827
Measurement of Electrical Conductivity of Crystals. Case of Chalcopyrite—M. Wintenberger. (*C.R. Acad. Sci., Paris*, vol. 244, pp. 1801–1803; March 25, 1957.) Valdes' four-probe method for measuring conductivity (1502 of 1954) is applied to study the anisotropy of resistivity in $CuFeS_2$. It is suggested that this increases with purity.

537.533.8:546.331.31 2828
Secondary Electron Emission from a NaBr Single Crystal—T. L. Matskevich. (*Zh. Tekh. Fiz.*, vol. 26, pp. 2399–2400; October, 1956.) The secondary emission coefficient σ was determined at 20, 50, and 300°C at normal primary electron beam incidence and at 20°C also at an angle of incidence of 50°. At 20°C, normal incidence and primary electron potential U_p 1800 V, $\sigma_{max}=24\pm2$, at 20°C, 50° incidence, $U_p\geq3000$ V, $\sigma_{max}>30$. The coefficient is strongly temperature dependent.

537.533.8:546.77+546.74 2829
Secondary Electron Emission of Nickel and Molybdenum at Low Primary Electron Energies—A. R. Shul'man and E. I. Myakinin. (*Zh. Tekh. Fiz.*, vol. 26, pp. 2223–2233; October, 1956.) Results show that there is a threshold value for secondary electron emission close to the work function. At primary electron energies $V_p>\phi$ secondary electrons appear, their average energy increasing with increasing V_p. This can be explained by assuming spherically symmetric; scattering at low V_p values; *i.e.*, different from the distribution at higher V_p values.

537.58:546.832 2830
Thermionic Constants and Sorption Properties of Hafnium—H. D. Hagstrum. (*J. Appl. Phys.*, vol. 28, pp. 323–328; March, 1957.)

538.221 2831
Analysis of Ferromagnetic and Antiferromagnetic Second-Order Transitions—J. A. Hofmann, A. Paskin, K. J. Tauer, and R. J. Weiss. (*Phys. Chem. Solids*, vol. 1, pp. 45–60; September/October, 1956.) Gives methods of separating the magnetic contribution to the specific heat of these materials.

538.221 2832
Effect of the Interaction between Magnetic Particles on the Critical Single-Domain Size—A. H. Morrish and L. A. K. Watt. (*Phys. Rev.*, vol. 105, pp. 1476–1478; March 1, 1957.)

538.221 2833
The Electronic Properties of Nickel-Palladium Alloys—E. P. Wohlfarth. (*Phys. Chem. Solids*, vol. 1, pp. 35–38; September/October, 1956.) Theoretical predictions are made about the specific heat of these alloys, their electrical and magnetic properties, and the effect of compression on their Curie point.

538.221 2834
Reproducing the Properties of Alnico Permanent-Magnet Alloys with Elongated Single-Domain Cobalt-Iron Particles—F. E. Luborsky, L. I. Mendelsohn, and T. O. Paine. (*J. Appl. Phys.*, vol. 28, pp. 344–351; March, 1957.) A description of the synthesis of the magnetic properties of alnico alloys using fine-particle compacts.

538.221 2835
Magnetic Alloy of High Permeability and Low Hysteresis Loss—(*Engineer, London*, vol. 203, p. 427; March 15, 1957.) Note of the

magnetic properties of "supermendur," an alloy of 49 per cent Fe, 49 per cent Co, and 2 per cent Va developed by Bell Laboratories. Maximum permeability is 66000 at 20 kg, remanence 21.5 kg, and coercive force 0.26 oersted.

538.221 2836
Dynamax, a New Crystal and Domain-Oriented Magnetic Core Material—G. H. Howe. (*Commun. & Electronics*, no. 27, pp. 548–550; November, 1956. Discussion p. 551.) The high-permeability material described contains approximately 65 per cent Ni, 2 per cent Mo, and 33 per cent Fe. It is available as thin tape for toroidal cores; its dynamic characteristics are superior to those of other commercial rectangular-loop materials. The best values obtained are 1780000 maximum permeability, 11.95 kg residual flux density, and 0.0053 oersted coercive force.

538.221 2837
Superposed Magnetic Fields in Materials with Rectangular Hysteresis Loops—C. B. Wakeman and F. J. Beck. (*Commun. & Electronics*, no. 27, pp. 562–569; November, 1956.) Report of experimental investigations of tubular, tape-wound specimens of Ni-Fe alloys, one containing 50 per cent Ni, and the other 79 per cent Ni and 4 per cent Mo.

538.221:621.317.411.029.63 2838
On the Complex Permeability of Iron-Nickel Alloys at High Frequencies—J. C. Anderson and B. Donovan. (*Proc. Phys. Soc.*, vol. 70, pp. 186–191; February 1, 1957.) The internal resonance frequency in the anisotropic field varies with the composition; it is a minimum for 70 per cent Ni. The resonance curve for pure Ni has multiple peaks.

538.221:621.318.124 2839
Ceramic Magnets—R. A. Scholten. (*Product Eng.*, vol. 27, pp. 143–148; December, 1956.) The characteristics and unit costs of barium ferrite magnets and the various grades of alnico magnets are tabulated for comparison. Some data are given on ceramic-magnet applications, particularly those utilizing their high coercivity.

538.221:621.318.124 2840
Magnetic-Induction and Coercive-Force Data on Members of the Series $BaAl_xFe_{12-x}O_{19}$ and Related Oxides—L. G. Van Uitert. (*J. Appl. Phys.*, vol. 28, pp. 317–319; March, 1957.) The anisotropy field of the series increases with Al content causing ferromagnetic resonance to move to higher frequencies. Materials with extremely high coercive forces can thus be realized.

358.221:621.318.134 2841
Magnesium-Copper-Manganese-Aluminium Ferrites for Microwave Applications—L. G. Van Uitert. (*J. Appl. Phys.*, vol. 28, pp. 320–322; March, 1957.) The preparation of these ferrites is discussed and data presented on the saturation inductions, Curie temperatures, densities, and dc resistivities.

538.221:621.385.833:548.0 2842
Observation of the Domain Structure of a Ferromagnetic Material by means of Photoelectrons—G. V. Spivak, T. N. Dombrovskaya, and N. N. Sedov. (*C.R. Acad. Sci. U.R.S.S.*, vol. 113, pp. 78–81; March 1, 1957. In Russian.) A photoelectron microscope and its applications are briefly described. The image on the fluorescent screen is obtained by magnetically focused photoelectrons emitted by the illuminated antimony-caesium film which covers the ferromagnetic material.

538.245 2843
Spontaneous Magnetization and Magnetic Susceptibilities of an Antiferromagnetic with Foreign Ions in Both Sublattices—K. F. Niessen. (*Phillips Res. Rep.*, vol. 12, pp. 69–81; February, 1957.)

538.245 2844
Formation of Magnetic Texture by a Magnetic Field in Thin Layers of Iron Obtained by the Electrolytic Method—N. V. Kotel'nikov. (*C.R. Acad. Sci. U.R.S.S.*, vol. 113, pp. 97–99; March 1, 1957. In Russian.)

538.632 2845
The Hall Effect in the Silver-Palladium Alloy System—A. I. Schindler. (*Phys. Chem. Solids*, vol. 1, pp. 42–44; September/October, 1956.)

538.65 2846
The Interrelation of Magnetomechanical Phenomena and their Practical Applications—P. Ross. (*Rev. gén. Elect.*, vol. 65, pp. 689–694; December, 1956.) After summarizing the theory underlying these effects, the conditions are derived for obtaining the maximum magnetoelastic sensitivity and magnetomechanical coupling coefficient for a given ferromagnetic material.

539.23:537.311.3 2847
Influence of the Support on Electrical Conductivity of Very Thin Films of Gold. Measurement of the Condenstation Factor—Sen-Sik Minn and S. Offret. (*C.R. Acad. Sci., Paris*, vol. 244, pp. 1624–1626; March 18, 1957.) An experimental study using supports of bismuth oxide, MgF_2, and glass.

539.23:546.87:538.63 2848
Magnetoresistance of Thin Bismuth Films—P. Huet and A. Colombani. (*C.R. Acad. Sci., Paris*, vol. 244, pp. 1626–1629; March 18, 1957.) Experimental results are given in graphical form for fields up to 35 000 oersted and thicknesses between 25 and 2 800 Å. See also 2532 of 1957 and back references.

621.315.5/.6:539.16 2849
Designing Electronics to Resist Nuclear Energy—H. L. Morgan. (*Electronics*, vol. 30, pp. 155–157; May 1, 1957.) Materials and components must be selected that will function under conditions of high nuclear radiation and temperature, and low susceptibility to secondary radiation is essential to permit servicing of equipment. The properties of some materials are tabulated and discussed.

621.315.611:546.623-31 2850
Electric Strength of Thin Layers of Aluminium Oxide—S. N. Koikov and A. N. Tsikin. (*Zh. Tekh. Fiz.*, vol. 26, pp. 2248–2253; October, 1956.) An experimental investigation is reported of the dependence of electric strength on 1) the polarity of electrodes, 2) thickness of the oxide film in the range 15–30 μ, and 3) temperature in the range 300–2000°K. The breakdown of the oxide in air at normal temperatures is probably due to the breakdown of the air in the pores of the film; in vacuum the breakdown occurs 1) in the vacuum in the pores of the film and 2) along the surface of the pores. A thermal breakdown mechanism may be operative above 1300–1400°K.

621.315.612.6:537.52 2851
The Electric Strengths of Glasses with Different Sodium Contents—J. Vermeer. (*Physica*, vol. 22, pp. 1247–1253; December, 1956.)

621.315.612.6:537.52 2852
The Electrical Conduction of Glass at High Field Strengths—J. Vermeer. (*Physica*, vol. 22, pp. 1257–1268; December, 1956.) The dc ionic conductivity of four kinds of glass has been measured at different temperatures. Above ~100 kv/cm the final conductivity increased exponentially with field strength.

621.315.612.6:537.52 2853
On the Relation between Ionic Conductivity and Breakdown Strength of Glass—J. Vermeer. (*Physica*, vol. 22, pp. 1269–1278; December, 1956.)

MATHEMATICS

517.9:519.47 2854
Relation between a Criterion of Realizability and Functional Transformations—I. Gumowski. (*C.R. Acad. Sci., Paris*, vol. 244, pp. 1466–1468; March 11, 1957.) See also 1674 of 1957.

519.272 2855
A Scatter Diagram which Gives the Complex Correlation Coefficient for Normal Variables—N. F. Barber. (*N.Z.J. Sci. Tech. B.*, vol. 38, pp. 366–374; January, 1957.) "The correlation coefficient between two complex variables $u(t)$ and $v(t)$ can, in certain cases, be estimated by forming a scatter diagram of the variable $[u^x(t)+v(t)]$. An experimental example is given."

MEASUREMENTS AND TEST GEAR

526.2:535.22 2856
Precision of the Geodimeter as Affected by the Speed of Light in Air—D. T. Williams and J. R. Williams. (*Rev. Sci. Instr.*, vol. 28, pp. 108–115; February, 1957.) An analysis of the limitations imposed by uncertainties in the velocity of propagation of light in the atmosphere.

536.531:546.289 2857
Germanium Resistance Thermometers Suitable for Low-Temperature Calorimetry—J. E. Kunzler, T. H. Geballe, and G. W. Hull. (*Rev. Sci. Instr.*, vol. 28, pp. 96–98; February, 1957.) Details are given of their construction including the preparation of the crystal "bridges" and their manner of mounting inside a platinum capsule. The measured electrical properties of several samples are also given.

621.3.018.41(083.74)+529.786]:538.569.4 2858
Frequency Shift in Ammonia Absorption—K. Matsuura, Y. Sugiura, and G. M. Hatoyama. (*J. Phys. Soc. Japan*, vol. 11, p. 1301; December, 1956.) A shift in the frequency of the center of a microwave absorption line of ammonia was observed with change of state of the gas.

621.3.018.41(083.74):621.396.11.029.45 2859
Intercontinental Frequency Comparison by Very-Low-Frequency Radio Transmission—J. A. Pierce. (PROC. IRE, vol. 45, pp. 794–803; June, 1957.) Discussion of the frequency stability of a 16-kc signal over paths 5 200 km and 18 700 km long. Measurements accurate to a few parts in 10^9 are possible in less than an hour.

621.317.2:621.373.421.13.029.63 2860
A Crystal-Controlled Signal Generator—M. T. Stockford. (*Electronic Eng.*, vol. 29, pp. 202–205; May, 1957.) Detailed description of equipment with an output of 5 w at 937.5 mc designed to drive a klystron Type VX8175 [2915 of 1956 (Norris)].

621.317.3:621.314.63 2861
Dynamic Methods of Testing Semiconductor Rectifier Elements and Power Diodes: Part 2—A. H. B. Walker and R. G. Martin. (*Electronic Eng.*, vol. 29, pp. 220–224; May, 1957.) "Approximate" methods using normally available instruments are described. Direct comparison is made in certain cases between these measurements and those using the specialized equipment described in Part 1 (2544 of 1957). A useful test summary is tabulated.

621.317.3:621.396.822:621.396.96 2862
Measurement of Noise Factor in Centimetric Radar—Patla. (See 2768.)

621.317.34.029.62 2863
Measurement of Group Delay in the 95- to 115-Mc/s Band—A. C. H. Borsboom. (*Philips Telecommun. Rev.*, vol. 17, pp. 90–99; January, 1957.) Description of an instrument measuring delay variations with an accuracy of 10^{-9} sec.

621.317.35:551.594.6 2864
A Technique for the Rapid Analysis of Whistlers—Grierson (See 2759.)

621.317.35.029.426 2865
A Continuous Amplitude/Time Analyser—W. A. P. Young. (*Electronic Eng.*, vol. 29, pp. 206–209; May, 1957.) A twin-channel amplifier and integrator for the band 16–30 cps for analyzing encephalographic records.

621.317.382.029.63/.64:537.52 2866
Effect of Microwave Signals Incident upon Different Regions of a D.C. Hydrogen Glow Discharge—B. J. Udelson. (*J. Appl. Phys.*, vol. 28, pp. 380–381; March, 1957.) The change in voltage drop across a series resistor might be used to measure microwave power.

621.317.42 2867
Instrument for Relative Measurements of Constant Magnetic Fields—I. S. Shpigel', M. D. Raizer, and E. A. Myae. (*Radiotekhnika i Elektronika*, vol. 1, pp. 1515–1519; December, 1956.) The instrument which utilizes the magnetic resonance absorption phenomenon, is designed for relative measurements of weakly inhomogeneous magnetic fields. The maximum measurable difference in the magnetic field is $\Delta H_{max} = \pm 5$ per cent, where H is the field strength. The error in ΔH is ± 3–4 per cent. Measurements were made of the injection-field distribution ($H_0 = 150$ oersted) of the new 10-kmeV synchrophasotron of the Acedemy of Sciences.

621.317.726:621.385.832 2868
The Measurement of Peak Voltage using a Cathode-Ray Tube—E. S. Fairley. (*Brit. J. Appl. Phys.*, vol. 8, pp. 101–102; March, 1957.) A null method is used, a balance against an accurately determined direct voltage being achieved.

621.317.75:538.569.4 2869
Direct Measurement of the Characteristic Moments of the Line Structure in Paramagnetic Resonance: Sinusoidal Sweep and Harmonic Analysis of the Signal—J. Hervé (*C.R. Acad. Sci., Paris*, vol. 244, pp. 1475–1478; March 11, 1957.)

621.317.755:621.385.029.63/.64 2870
The Wamoscope—a Microwave Display Device—D. E. George. (*Sylvania Technologist*, vol. 10, pp. 5–7; January, 1957.) The "wamoscope" is a traveling-wave tube combined with a cr tube screen in such a way as to make the brightness at the screen a function of the microwave power input.

OTHER APPLICATIONS OF RADIO AND ELECTRONICS

621.365.92 2871
Radio-Frequency Carbonization—S. W. Taylor. (*Research, London*, vol. 10, pp. 108–115; March, 1957.) Apparatus for rf heating giving an extremely uniform distribution of heat is briefly described and results of experiments on various coals are given.

621.384.612 2872
Strong Focusing in Particle Accelerators: Alternating-Gradient Synchrotrons—P. Lapostolle. (*Onde élect.*, vol. 37, pp. 4–47; January, 1957.) Outline of underlying principles and brief description of 200-m diameter, 25-kmev synchrotron for CERN in Geneva [see also 3371 and 3372 (Grivet) of 1955].

621.384.622.1:535.42 2873
Linear Accelerator with Preliminary Electron Bunching: Application to Electron Diffraction between 0.5 and 1 MeV—M. Papoular. (*Ann. Phys., Paris*, vol. 13, pp. 914–958; November/December, 1956.) Detailed description of the development and construction of a particle accelerator which incorporates a special device for preliminary bunching by velocity modulation to improve the energy spectrum (see also 1267 of 1957). Its application in electron diffraction techniques is outlined and illustrated by experimental results.

621.384.622.2 2874
The 28-MeV Electron Accelerator Project for the Nuclear Research Centre at Saclay [France]—H. Leboutet, E. Picard, and J. Vastel. (*Onde élect.*, vol. 37, pp. 28–35; January, 1957.) Basic design data of the linear accelerator and general description of the installation.

621.385.832 2875
Tristable Gate moves C.R.O. Line Drawings—P. A. Ryan. (*Electronics*, vol. 30, pp. 178–180; May 1, 1957.) A means for producing simple contours on the face of a conventional cro.

621.385.833 2876
Properties of Two-Aperture Electron Lenses—G. D. Archard. (*Brit. J. Appl. Phys.*, vol. 8, pp. 127–130; March, 1957.) "Spherical and chromatic aberrations and focal properties of two-aperture ('immersion') electron lenses are investigated theoretically, and the results are presented graphically as functions of lens geometry and voltage ratio."

621.398:621.396.934 2877
Missile Telemeter uses Transistor Amplifier—J. H. Porter. (*Electronics*, vol. 30, pp. 170–171; May 1, 1957.) "Chopper-type dc amplifier uses available channels to indicate missile temperatures in an airborne telemetering system. Unit has voltage gain of 1000 with 5-v dc output and linearity within 2 per cent over the full output range. Input impedance is 100 Ω and response is flat from zero to 10 cps. Stability is within 2 per cent up to 10 *g* vibration at 1000 cps or over temperature range from −65°C to 85°C."

642.6:681.142 2878
Some of the Engineering Aspects of the Machine Translation of Language—R. E. Wall, Jr. (*Commun. & Electronics*, no. 27, pp. 580–584; November, 1956. Discussion, p. 585.)

621.385.833+537.533.72 2879
Proceedings of the Third International Conference on Electron Microscopy, London, 1954. [Book Review]—R. Ross (ed.). Publishers: Royal Microscopical Society, London, 705 pp.; 1956. (*Nature, London*, vol. 179, pp. 797–798; April 20, 1957.)

PROPAGATION OF WAVES

621.396.11 2880
Radio Propagation Fundamentals—K. Bullington. (*Bell Sys. Tech. J.*, vol. 36, pp. 593–626; May, 1957.) Nomograms and graphs are included which permit numerical estimates of field strength to be made. All frequency bands of practical importance are discussed. Thirty-four references.

621.396.11 2881
Spectrum of Turbulent Fluctuations Produced by Convective Mixing of Gradients—A. D. Wheelon. (*Phys. Rev.*, vol. 105, pp. 1706–1710; March 15, 1957.) The spectrum is calculated on the basis of the turbulent mixing of an established gradient of a passive scaler quantity (*e.g.*, electronic density). The resulting expression is consistent with experimental results on radio wave scattering by tropospheric and ionospheric irregularities.

621.396.11 2882
A Reflection Theory for Propagation Beyond the Horizon—H. T. Friis, A. B., Crawford, and D. C. Hogg. (*Bell Sys. Tech. J.*, vol. 36, pp. 627–644; May, 1957.) The atmosphere is assumed to contain fairly sharp gradients of refractive index having limited dimensions and random positions and orientations. This model gives good agreement with experimental data.

621.396.11:551.510.535 2883
The Fading of Radio Waves Reflected from the E Layer—B. Landmark. (*J. Atmos. Terr. Phys.*, vol. 10, pp. 288–295; 1957.) Simultaneous measurement of phase path and amplitude of waves reflected vertically from the E region are analyzed. A temporary increase in phase path was associated with an enhancement of amplitude, indicating focusing by a moving concavity in the layer.

621.396.11:551.510.535 2884
High-Frequency Back-Scatter Observations at Salisbury, South Australia—C. G. McCue. (*Aust. J. Phys.*, vol. 9, pp. 454–470; December, 1956.) By measuring simultaneously angles of elevation and time delays of strobed back-scatter signals, seven different back-scatter modes were noted, of which the most frequent was the ground-scattered single F_2 hop. Transmissions directed to four characteristic types of scattering area showed that at low angles of elevation land is a more prominent source of back-scatter than sea, and that extremely larrge changes in land roughness result in increased back-scatter amplitude.

621.396.11.029.45:551.510.535 2885
The Geometrical Optics of V.L.F. Sky-Wave Propagation—J. R. Wait and A. Murphy. (Proc. IRE, vol. 45, pp. 754–760; June, 1957.) Data are tabulated to facilitate the computation of received field strengths by combining ground and ionospheric waves. Comparison of some calculated values with experimental results leads to values of ionospheric refractive index differing from those previously published.

621.396.11.029.45:551.510.535 2886
The Mode Theory of V.L.F. Ionospheric Propagation for Finite Ground Conductivity—J. R. Wait. (Proc. IRE, vol. 45, pp. 760–767; June, 1957.) A mathematical formulation of the theory and graphical presentation of typical conclusions. Good agreement between calculated and measured fields is shown.

621.396.11.029.45:551.510.535 2887
The Attenuation vs Frequency Characteristics of V.L.F. Radio Waves—J. R. Wait. (Proc. IRE, vol. 45, pp. 768–771; June, 1957.) Attenuation factors are presented graphically as a function of various ionospheric parameters.

621.396.11.029.45:551.510.535 2888
The "Waveguide Mode" Theory of the Propagation of Very-Low-Frequency Radio Waves—K. G. Budden. (Proc. IRE, vol. 45, pp. 772–774; June, 1957.) Some apparent discrepancies between previous treatments are shown to be due to differences in the assumed ionospheric parameters and in the terminology for the modes.

621.396.11.029.45:551.594.6 2889
Very-Low-Frequency Radiation from Lightning Strokes—Hill. (See 2760.)

621.396.11.029.45:621.3.018.41(083.74) 2890
Intercontinental Frequency Comparison by Very-Low-Frequency Radio Transmission—Pierce. (See 2859.)

621.396.11.029.53 2891
The Ionospheric Attenuation of Hectometric Wave Propagation (550–1600kc/s)—M. Scholz. (*Nachrichtentech. Z.*, vol. 10, pp. 6–11; January, 1957.) Field-strength curves for nighttime propagation in the medium-wave band ob-

tained from various sources covering the past 22 years are compared. Other data plotted for comparison and brief discussion are the statistical distribution of field-strength variations, seasonal fluctuations, and the mean fading rate.

621.396.11.029.62:523.5:621.396.67.012.12 2892

Height-Gain in the Forward Scattering of Radio Waves by Meteor Trails—C. O. Hines and M. O'Grady. (*Canad. J. Phys.*, vol. 35, pp. 125–127; January, 1957.) Calculated curves are presented which show the detection rate of meteors and the mean signal level for forward transmission. The quantities are given as a function of antenna height and meteor-formation height.

RECEPTION

621.376.2 2893

The Demodulation of Linearly Distorted A. M. Spectra—H. Schneider and G. Petrich. (*Nachr-Tech.*, vol. 6, pp. 552–556; December, 1956.) The effect of amplitude and phase changes on the demodulating action of a receiving diode is investigated theoretically; the results are discussed with reference to the tuned selective circuit and the purely inductive hf channel.

621.376.333 2894

Some Problems in the Theory of the Ratio Detector—I. Kesler. (*Arch. Elektrotech.*, vol. 5, pp. 591–619; 1956. English summary, p. 620.) Theoretical and practical aspects of compensating amplitude variations of the input signal are discussed.

621.396.62:621.314.7 2895

Portable Transistor Receiver—S. W. Amos. (*Wireless World*, vol. 63, pp. 241–246 and 340–346; May and July, 1957. Correction, *ibid.*, p. 377; August, 1957.) A discussion of general principles of design and a stage-by-stage examination of a complete circuit, full details of which are given.

621.396.621.54 2896

A New Approach in R.F. Front-End Design—B. B. Bycer. (*Electronic Ind. Tele-Tech.*, vol. 16, pp. 82–84, 141; January, 1957.) The design is based on permeability tuning and the use of a triode Type 6021 as a reactance modulator for operation at 205 mc.

621.396.812.3 2897

The Effect of the Recorder Time on the Apparent Speed of Fading of a Radio Signal—S. A. Bowhill. (*J. Atmos. Terr. Phys.*, vol. 10, pp. 338–339; 1957.)

621.396.822:551.594.6 2898

Noise Investigation at V.L.F. by the National Bureau of Standards—Crichlow. (See 2761.)

621.396.822:551.594.6 2899

Some Recent Measurements of Atmospheric Noise in Canada—McKerrow. (See 2762.)

621.396.822:551.594.6 2900

Characteristics of Atmospheric Noise from 1 to 100 kc/s—A. D. Watt and E. L. Maxwell. (See 2763.)

621.396.823:537.523.3 2901

The Radio Interference Produced by Corona Discharge—M. I. Large. (*J. Atmos. Terr. Phys.*, vol. 10, pp. 245–250; 1957.) The spectrum of interference observed on a receiver showed peaks of noise at harmonics of the corona pulse repetition frequency, these noise peaks merging above the tenth harmonic. The spectrum conforms to that expected for pulses of variable interval.

621.396.823:537.523.3 2902

A Relaxation Oscillation Maintained by Discharge Corona—M. I. Large. (*Nature, London*, vol. 179, pp. 707–708; April 6, 1957.) During an investigation of interference due to negative corona from a receiver antenna (2901 above), a fine wire point a few millimeters from a plane at high potential was observed to oscillate, producing in a receiver a musical tone at twice the frequency of mechanical oscillation.

STATIONS AND COMMUNICATION SYSTEMS

621.376.3/.4:621.396.822 2903

Power Spectrum of a Carrier Modulated in Phase or Frequency by White Noise—R. Hamer and R. A. Acton. (*Electronic Radio Eng.*, vol. 34, pp. 246–253; July, 1957.) "Measurement of the power spectrum of a carrier, modulated either in phase or in frequency by a uniform Gaussian noise signal, is described, and the results are interpreted in the light of existing theory. A combination of measured and theoretical results is used to prepare generalized curves of fm and phm noise spectra."

621.39.001.11 2904

Instantaneous Companding of Quantized Signals—B. Smith. (*Bell Sys. Tech. J.*, vol. 36, pp. 653–709; May, 1957.) An extension of the analysis of Panter and Dite (1488 of 1951) permits the calculation of the quantizing error power as a function of a number of parameters. These calculations lead to the proper combination of the number of digits per code group and companding characteristic for quantized speech communication systems. Theoretical and experimental studies are compared.

621.39.001.11 2905

Geometric Interpretation of some Results of Channel Capacity Calculations—C. E. Shannon. (*Nachrichtentech. Z.*, vol. 10, pp. 1–4; January, 1957.) Translated and amplified version of an English paper published in *Nachrichtentech. Fachberichte*, vol. 6, pp. 13–15; 1957. The capacity of discrete channels not containing memory devices is investigated.

621.396.2:551.510.52 2906

Communications Potentialities of Tropospheric Scatter—M. Telford. (*Point to Point Telecommun.*, vol. 1, pp. 29–52; February, 1957.) The calculation of received signal level is discussed and charts are given. FM, ssb, and diversity systems are considered together with an apraisal of the possibilities in relaying television.

621.396.4 2907

Introduction to Channelling Systems on H.F. Radio Circuits—A. W. Cole. (*Point to Point Telecommun.*, vol. 1, pp. 5–12; February, 1957.) The history and trends of development in frequency-division and time-division channeling are briefly reviewed as an introduction to later articles.

621.396.4:621.396.72.029.62 2908

Radio-System Surveying on Very High Frequencies—D. C. H. Mellon. (*Point to Point Telecommun.*, vol. 1, pp. 13–27; February, 1957.) Factors governing the choice of sites for multichannel vhf systems are considered, and site testing is discussed.

621.396.41:621.396.72 2909

Experience with Single-Sideband Mobile Equipment—R. Richardson, O. Eness, and R. Dronsuth. (PROC. IRE, vol. 45, pp. 823–829; June, 1957.) The performance of the equipment, designed to operate at 159 mc, is compared with that of narrow-band fm equipment.

621.396.61/.62:621.314.7:621.311.6 2910

Transistor Equipment using Freely Available Power Supplies—(See 2916.)

621.396.65.029.64 2911

The Use of the Lower Centimetric Wavelengths for Radio Communication—G. Megla. (*Hochfreq. und Elektroak.*, vol. 64, pp. 194–199; May, 1956.) An examination of the microwave absorption by atmospheric gases and precipitation indicates that attenuation is sufficiently low for radio links at wavelengths down to 2 cm. Systems operating at 4 cm λ over a 33-km path using various forms of guided transmission are compared with a free-space transmission system; the latter has great economic advantages.

SUBSIDIARY APPARATUS

621–526 2912

An Introduction to the Study of Nonlinear Control Systems—J. F. Coales. (*J. Sci. Instr.*, vol. 34, pp. 41–47; February, 1957.) The nonlinearities may be used to improve the system performance provided they occur in the forward loop outside the load and are instantaneous; *i.e.*, there is no applicable delay between input changes and output response.

621.3.064 2913

Activation of Electrical Contacts by Organic Vapours—L. H. Germer and J. L. Smith. (*Bell Sys. Tech. J.*, vol. 36, pp. 769–812; May, 1957.) Carbon from the decomposed vapors may make it impossible to protect contacts against arcing by conventional *RC* networks. The activation process is discussed.

621.3.078:621.316.825:621.383 2914

A Thermistor Device as Automatic Gain Control in Lamp-Photocell Transducer Systems—A. M. Hardie. (*J. Sci. Instr.*, vol. 34, pp. 58–62; February, 1957.) Stabilization to within 0.03 per cent is achieved if the light beam is modulated symmetrically.

621.311.6:621–526.001.4 2915

Power Amplifier for Servo Testing—J. M. Diamond. (*Electronics*, vol. 30, pp. 176–177; May 1, 1957.) A cathode follower supplies 90w at 400–2600 cps.

621.311.6:621.396.61/.62:621.314.7 2916

Transistor Equipment using Freely Available Power Supplies—H. E. Hollmann. (*Hochfreq. und Elektroak.*, vol. 64, pp. 168–180; May, 1956.) The equipment described includes portable transmitters and receivers drawing power from solar batteries, hand-driven dynamos, sound energy, and the rf energy of a local broadcasting transmitter. See also 1893 of 1957.

621.311.69:537.311.33:535.215 2917

Photoelectric Converters of Solar Energy of *p*-Type Silicon—Yu. P. Maslakovets, S. A. Poltinnikov, G. B. Dubrovski, and V. K. Subashiev. (*Zh. Tekh. Fiz.*, vol. 26, pp. 2396–2397; October, 1956.) Brief note on experimental results. Efficiencies up to 2.8 per cent were obtained.

621.311.69:621.362 2918

Conversion of Radiations into Electricity—V. B. Veinberg and Yu. V. Mal'tsev. (*Zh. Tekh., Fiz.*, vol. 26, pp. 2373–2377; October, 1956.) Calculation of the efficiency of converting solar radiation into electrical energy via a heat engine. Numerical data are tabulated for various heater systems; efficiencies 3–4 times greater than those of thermoelectric converters are indicated.

621.314.6+621.316.72 2919

The Valve in Power Supply Units—K. Steimel. (*Telefunkenröhre*, no. 34, pp. 1–246; December, 1956.) The problems of stability and stabilization in electronic voltage and current supplies are discussed in detail. A section deals with rectification as a function of different circuit characteristics; other chapters describe and compare numerous basic tube circuits

used for various stabilizing purposes including special applications of more elaborate circuitry.

TELEVISION AND PHOTOTELEGRAPHY

621.397.5 2920

Horizontal versus Vertical Resolution—L. C. Jesty. (*Wireless World*, vol. 63, pp. 304–306; July, 1957.) No data appear to be available which suggest that greater sharpness is desirable in one direction rather than any other. The vertical/horizontal resolution is discussed; the number of lines should be increased beyond 405 to achieve equal resolution in these two directions.

621.397.5:389.6 2921

The Results of the 8th General Assembly [of the C.C.I.R.] (Warsaw 1956) in the Field of Black-and-White Television—J. Müller. (*Nachrichtentech. Z.*, vol. 10, pp. 27–30; January, 1957.)

621.397.5:535.623 2922

The Information Content and Frequency Bandwidth of the Chrominance Signal in a Subcarrier System of Colour Television—P. Neidhart. (*Nachr-Tech.*, vol. 6, pp. 529–533; December, 1956.) Problems arising from the adaption of the NTSC system to the 625-line standard are considered.

621.397.5:535.623 2923

The Efforts of the C.C.I.R. concerning a European Standard for Colour Television—F. Kirschstein, J. Müller, and K. O. Schmidt. (*Nachrichtentech. Z*, vol. 10, pp. 1–4; January, 1957.) Report on the discussions of a CCIR study group and on its visit to the U.S.A., France, Great Britain, and the Netherlands.

621.397.5:535.623 2924

Colour TV in U.S.A.—C. G. Mayer. (*Wireless World*, vol. 63, p. 325; July, 1927.) A favorable review of the status of color television with respect to that of black-and-white, implies that there is no longer any basis for the "color-blindness" which seems to prevail in Britain today.

621.397.6.001.4:535.623 2925

Simultaneous Colour-TV Test Signal—R. C. Kennedy. (*Electronics*, vol. 30, pp. 146–149; May 1, 1957.) Differential gain, phase characteristic, flag-burst, and chroma amplitudes of monitor or receiver can be determined using a test signal transmitted simultaneously with the program. The signal occupies three horizontal lines, one line displaced above top of picture.

621.397.611.2 2926

Transmission Defects of the Image Orthicon Television Camera Tube—R. Theile and F. Pilz. (*Arch. elekt. Übertragung*, vol. 11, pp. 17–32; January, 1957.) The causes are investigated of the characteristic spurious signals originating in this type of tube which give rise to picture distortion and loss of definition. These defects are due to capacitive coupling between adjacent picture elements and the deflection of scanning electrons by the potential pattern of the stored charge. Modifications of the construction and operation of the tube are suggested.

621.397.62:535.8 2927

A New Optical Viewfinder for Television Cameras—P. Lindner and E. Kosche. (*Nachr-Tech.*, vol. 6, pp. 538–544; December, 1956.) Description of optical view-finder in which correctness of focusing is indicated over the whole image. Its advantages over electronic viewfinders are evident from a point-by-point comparison.

621.397.62:621.374.33 2928

Noise Gating Tube for A.G.C. and Sync—J. G. Spracklen, W. J. Stroh, and G. C. Wood. (*Electronics*, vol. 30, pp. 172–175; May 1, 1957.) "Single miniature tube performs entire functions of sync clipping, generating age voltage and giving high degree of noise immunity to both these sections of a television receiver. Type 6BU8 contains common cathode, grid, and screen with separate plates and no. 3 grids."

621.397.621:778 2929

Construction of Equipment for the Photography of Single Frames of Television Pictures—K. Kröner. (*Elektronik*, vol. 6, pp. 12–15; January, 1957.) The equipment described is based on the circuit of Dillenburger and Wolf (586 of 1956).

621.397.621.2:535.623 2930

The Choice of Colour Phosphors and the Occurrence of Colour Information Losses—I. Bornemann. (*Nachr-Tech.*, vol. 6, pp. 534–537; December, 1956.) The requirements governing the choice of phosphors for use in tricolor cr tubes are discussed. The use of the Valensi diagram for determining information losses is proposed.

621.397.74(44) 2931

The French Television Network—Leschi. (*Télé. Franc.*, no. 138, pp. 9–22; January, 1957.) Outline of the development planned by the RTF with lists of stations and maps showing their coverage; details of the individual transmitters are also given.

TUBES AND THERMIONICS

621.314.63+621.314.7 2932

The High Current Limit for Semiconductor Junction Devices—N. H. Fletcher. (PROC. IRE, vol. 45, pp. 862–872; June, 1957.) At very high current densities new formulas must be derived considering previously neglected effects. Predictions of the theory for particular devices are in good agreement with experiment and show how the available parameters should be varied to achieve specific results.

621.314.63 2933

The Forward Voltage/Current Characteristics of a Junction-Type Rectifier for Large Currents—E. I. Rashba and K. B. Tolpygo. (*Zh. Tekh. Fiz.*, vol. 26, pp. 1419–1427; July, 1956.) A theoretcial discussion is presented, in which an equation is derived for the voltage /current characteristic of a *p-n* junction-type diode of arbitrary thickness for large currents, on the assumption that the barrier layer is flooded with carriers and that the main voltage drop occurs in the bulk of the semiconductor. A numerical example showing the application of the equation to a germanium diode is included, and the accuracy of the method proposed is estimated.

621.314.63:537.311.33 2934

Theory of the Metal/Semiconductor Contact—S. U. Umarov and L. G. Gurvich. (*Zh. Tekh. Fiz.*, vol. 26, pp. 2179–2184; October, 1956.) A calculation of the current/voltage characteristics is presented, taking into account the current across the junction and the degree of ionization of the impurity centers. The calculation is approximate and does not take account of the influence of the change of the average kinetic energy of the electron gas under the influence of the electric field.

621.314.63:546.28:539.18 2935

Effects of Irradiation upon Diodes of the Silicon Junction Type—R. Gorton. (*Nature, London*, vol. 179, p. 864; April 27, 1957.) After irradiation by slow and fast neutrons, a progressive change in the forward characteristics occurred accompanied by a distinct reduction of minority-carrier storage. There was no significant change in the reverse characteristics.

621.314.63:546.289 2936

Measurements of Current as a Function of Temperature in Germanium *n-p* Junctions—H. Bernard. (*J. Electronics*, vol. 2, pp. 579–596; May, 1957. In French.) Measurements of reverse current in grown Ge *p-n* junctions at temperatures above 10°C agree well with Shockley's theory. Below 10°C the reverse current arises from electron-hole generation in the space-charge layer. This mechanism is also used to explain the forward current characteristics measured between −50°C and liquid-nitrogen temperatures.

621.314.63:546.289 2937

Some Properties of Diodes of Germanium with Gold Admixture—A. A. Lebedev, V. I. Stafeev, and V. M. Tuchkevich. (*Zh. Tekh. Fiz.*, vol. 26, pp. 2131–2141; October, 1956.) An experimental investigation of the *I/V* and breakdown-voltage characteristics at temperatures down to 78°K is reported.

621.314.63+621.314.7]:621.396.822 2938

Theory and Experiments on Shot Noise in Semiconductor Junction Diodes and Transistors—W. Guggenbühl and M. J. O. Strutt. (PROC. IRE, vol. 45, pp. 839–854; June, 1957.) A general theory of shot noise, for low-current densities, and its dependence on frequency in the lf and hf bands. Experimental results at low-level injection agree well with the theory, but some deviation is apparent at high levels.

621.314.63.012.8 2939

Theoretical Consideration of the Physical Basis for the Equivalent Circuit of Semiconductor Diodes at High Current Densities—W. Guggenbühl. (*Arch. elekt. Übertragung*, vol. 10, pp. 483–485; November, 1956.) Consideration of the transient response of junction diodes in the high-current region is based on Herlet's theory of their dc performance (*Z. Naturf.*, vol. 11a, pp. 498–510; June, 1956). This accounts for the inductive part of the ac characteristics of a *p-n*-junction diode at high-injection levels. Experimental results agree satisfactorily with theory.

621.314.7 2940

Transistor Circuit Symbols—E. H. Cooke-Yarborough. (*Wireless World*, vol. 63, pp. 333–334; July, 1957.) The need to use symbols which distinguish between point-contact and junction transistors (1942 of 1957) is emphasized, together with the need for keeping to the "negative down" polarity convention already established with tube circuits.

621.314.7:621.374.32:681.142 2941

Computer Switching with Micro-alloy Transistors—Angell and Fortini. (See 2686.)

621.314.7:621.375.4 2942

Transistor Operating-Point Stabilization—A. Cramwinckel. (*Philips Telecommun. Rev.*, vol. 17, pp. 100–107; January, 1957.) A method of stabilizing transistors against increased collector leakage current caused by a rise in temperature. A dc negative-feedback method is described which is effective up to about 80°C for Ge transistors.

621.314.7:621.375.4.029.5/.6 2943

Transistors in High-Frequency Amplifiers—W. Guggenbühl and M. J. O. Strutt. (*Electronic Radio Eng.*, vol. 34, pp. 258–267; July, 1957.) A discussion of the frequency dependence of transistor parameters is followed by a review of the qualities of hf transistors and of the various problems which arise in their use. Twenty-nine references.

621.314.7:621.396.822 2944

Abnormal Noise in Junction Transistors during Secondary Ionization—R. B. Jackson and A. K. Walton. (*Proc. Phys. Soc., London*, vol. 70, p. 251; February 1, 1957.)

621.314.7.002.2 2945

The Depth of Diffused Layers—W. L. Bond. (*Bell Lab. Rec.*, vol. 35, pp. 1–5; January, 1957.) An interference fringe technique is described for measuring the depth of con-

ductivity layers diffused into semiconductor crystals in transistor fabrication.

621.383.2 2946
On the Constancy of the Spectral Characteristics of Oxygen-Caesium and Antimony-Caesium Vacuum Photocells—V. S. Khazanov and S. G. Yurov. (*Zh. Tekh. Fiz.*, vol. 26, pp. 1170–1173; June, 1956.) The effect of the magnitude of the applied voltage on the spectral sensitivity of the photocell was investigated experimentally. The data so obtained are compared with those of other authors.

621.383.2 2947
The Energy Distribution of Photoelectrons in the External Photoeffect of the Antimony-Caesium Cathode—Yu. K. Shalabutov and N. S. Maslennikova. (*Zh. Tekh. Fiz.*, vol. 26, pp. 1166–1169; June, 1956.) Measurements of spectral response and energy distribution of photoelectrons are reported. The $(dN/dE)/E$ curves, where E is the energy, show maxima near 0·6 and 0·2 ev for photoelectrons liberated by 530-mμ irradiation.

621.383.27 2948
Fluctuations in Photomultipliers and Statistical Properties of Secondary Emission—P. Moatti. (*C.R. Acad. Sci., Paris*, vol. 244, pp. 1742–1744; March 25, 1957.) Statistical treatment to determine the number of electrons comprising an output pulse when emission is initiated by 1) a single electron, 2) a group of electrons with Poisson distribution.

621.383.27 2949
Synchronization Accuracy Obtainable with Multiplier Phototubes—L. Levi. (*Commun. & Electronics*, no. 27, pp. 603–606; November, 1956.) The jitter in photomultiplier synchronization systems is analyzed to determine the effect of bandwidth, type of photocell, and optical parameters.

621.383.4 2950
A New Photocell for Long-Wave Infrared Radiation—E. Suchel. (*Elektronische Rundschau*, vol. 10, pp. 296–298; November, 1956.) The characteristics of the PbS cell Type 61SV for use in the wavelength range 0·3–3·5 μ are given; its sensitivity is greatest at 2·5 μ. Some typical applications are indicated.

621.383.42 2951
Influence of Temperature on the Height of the Potential Barrier of Selenium Photocells—G. Blet. (*C.R. Acad. Sci., Paris*, vol. 244, pp. 1754–1756; March 25, 1957.) The barrier potential determined from measurements of the emf of a cell in vacuum is independent of temperature in the range 125°–300°K

621.383.5:546.23:621.396.822 2952
Flicker Effect in Selenium Photovoltaic Cells—M. Téboul and N. Nifontoff. (*C.R. Acad. Sci., Paris*, vol. 244, pp. 1631–1633; March 18, 1957.) To a first approximation the flicker effect does not appear to be influenced by the illumination of the cell when the voltage across the rectifying contact is held constant.

621.383.5:546.817.221 2953
A Single-Crystal Photodiode of Lead Sulphide—J. Starkiewicz, G. Bate, H. Bennett, and C. Hilsum. (*Proc. Phys. Soc., London*, vol. 70, pp. 258–259; February 1, 1957.) A photovoltaic cell with a time constant $< 1\mu$s.

621.385:621.396.822 2954
An Investigation into the Flicker Effect—A. M. Malakhov and V. E. Dubrovin. (*Zh. Tekh. Fiz.*, vol. 26, pp. 1451–1455; July, 1956.) The flicker voltage developed across a resistance in the anode circuit of the tubes was measured over a frequency range from 0.5 to 120 cps, and the spectral density of the fluctuations was determined. The dependence of the intensity of the flicker effect and the form of its spectrum on the operating conditions of the tube, and, in particular, on residual gas in the tube are briefly discussed. A theoretical interpretation of the results obtained is given.

621.385.001.4:534.1 2955
White-Noise Vibration Test for Electron Tubes—J. D. Robbins. (*Sylvania Technologist*, vol. 10, pp. 10–12; January, 1957.)

621.385.004.2 2956
The Effects of Overload and Operation at High Altitudes on Electron-Tube Life—H. C. Pleak and A. V. Baldwin. (*Sylvania Technologist*, vol. 10, pp. 2–4; January, 1957.)

621.385.029.6 2957
Interchannel Interference due to Klystron Pulling—H. E. Curtis and S. O. Rice. (*Bell Sys. Tech. J.*, vol. 36, pp. 645–652; May, 1957.) Expressions are derived for the magnitude of the interference when the speech load is simulated by random noise.

621.385.029.6 2958
The Measurement of Space-Charge Wavelength in an Electron Beam—D. Walsh. (*J. Electronics*, vol. 2, pp. 436–440; March, 1957.) "A method is described of measuring the wavelength of space-charge waves in an electron beam by comparing the klystron gain between cavities unequally spaced along the beam."

621.385.029.6 2959
On Space-Charge Waves—R. H. C. Newton. (*J. Electronics*, vol. 2, pp. 441–449; March, 1957.) The wave equation for an electron beam in a collimating magnetic field is derived. The analysis is applicable when there is no positive space charge and is not entirely restricted to small-signal conditions.

621.385.029.6 2960
High-Order Space-Charge Waves in Klystrons—A. H. W. Beck. (*J. Electronics*, vol. 2, pp. 489–509; March, 1957.) Theoretical expressions are obtained for cylindrical and annular beams focused with an infinite magnetic field. The calculations are simplified by the use of finite Hankel transforms. Beams in finite magnetic fields are closely similar provided that the focusing field is somewhat greater than the Brillouin field for the same current, voltage, and beam diameter.

621.385.029.6 2961
Space-Charge Waves along Magnetically Focused Electron Beams—J. Labus. (PROC. IRE, vol. 45, pp. 854–861; June, 1957.) Two procedures in the analysis of wave propagation along electron beams are compared by consideration of different displacements of the beam surface.

621.385.029.6 2962
Space Harmonics in Electron Streams—R. Müller. (*Arch. elekt. Übertragung*, vol. 10, pp. 505–511; December, 1956.) The formation is considered of space-charge waves in electron beams traveling along specially shaped paths or under periodically changing dc conditions. The application of this phenomenon for generating high-harmonic frequencies is briefly discussed.

621.385.029.6 2963
On the Spreading of Bunches of a Space Charge—O. P. Beguchev. (*Zh. Tekh. Fiz.*, vol. 26, pp. 1483–1486; July, 1956.) A rigorous mathematical description is given of the process of the spreading of bunches of an uncompensated space charge.

621.385.029.6 2964
On the Space Charge Affected by the Magnetic Field: Part 2—Y. Yasuoka. (*J. Phys. Soc. Japan*, vol. 11, pp. 1292–1295; December, 1956.) A more advanced treatment of Part 1 (2575 of 1956) taking into account the effect of the magnetic field on the scattered electrons. Better agreement is obtained with experimental values.

621.385.029.6 2965
On the Shape of Electron Trajectories in a Magnetron under Static Conditions—B. Ya. Moizhes. (*Zh. Tekh. Fiz.*, vol. 26, pp. 1836–1840; August, 1956.) The equation of motion of electrons in a cylindrical magnetron, with an anode-radius/cathode-radius ratio approaching unity is derived taking into account the space charge, and trajectories in magnetic fields exceeding the critical vaue are considered.

621.385.029.6 2966
Minimum Noise Coefficient of Double-Stream Valve—S. K. Lesota. (*Radiotekhnika i Electronika*, vol. 1, pp. 1288–1291; September, 1956.) The calculation presented takes into account the correlation of fluctuations of the current and voltage in the double electron stream. A linear approximation and lossless-multipole theory are used. Results show that the minimum noise coefficient is higher for the double-stream tube than for a traveling-wave tube operating under similar conditions for fluctuations in the potential minimum.

621.385.029.6 2967
Theory of Nonlinear Phenomena in Travelling-Wave Amplifiers—A. A. Vedenov. (*Radiotekhnika i Elektronika*, vol. 1, pp. 1377–1378; October, 1956.) The limitation of the increase in amplitude is deduced from general energy relations without recourse to a concrete model.

621.385.029.6 2968
Developments of the Strophotron—H. Höggblom and S. Tomner. (*Ericsson Tech.*, vol. 12, pp. 165–184; 1956.) This transit-time tube was originally described by Alfven and Romell (3398 of 1954). Experimental results are reported for different types including the coaxial strophotron and the simplified theory is outlined. Oscillator efficiencies of 30 per cent at 1000 mc and 10 per cent at 5000 mc have been achieved.

621.385.029.6:621.375.2:621.396.65 2969
Design Considerations for Output Stages, Travelling-Wave Valves in Radio-Link Equipment—M. Müller. (*Nachrichtentech. Z.*, vol. 10, pp. 11–15; January, 1957.) On the basis of theoretical considerations traveling-wave tube operating and design data are tabulated for mid-band frequencies of 2, 4, 6, and 10 kmc and outputs of about 1 to 200 w for a focusing field of 600 g.

621.385.029.63/.64 2970
A Study of the Broad-Band Frequency Response of the Multicavity Klystron Amplifier—K. H. Kreuchen, B. A. Auld, and N. E. Dixon. (*J. Electronics*, vol. 2, pp. 529–567; May, 1957.) "A theoretical method is described for the evaluation of the amplitude-frequency response of a stagger-tuned klystron amplifier. The practical verification of the theoretically predicted response was carried out on a demountable four-cavity S-band klystron amplifier."

621.385.029.63/.64:621.317.755 2971
The Wamoscope—a Microwave Display Device—George. (See 2870.)

621.385.029.63/.64:621.317.755:621.385.833 2972
Typical Applications of the Wamoscope—H. Briskin. (*Sylvania Technologist*, vol. 10, pp. 8–9; January 1957.) A radar receiver and microwave television receiver are discussed.

621.385.029.63/.64:621.376.3 2973
Voltage-Tuned Magnetron for F. M. Applications—T. R. Bristol and G. J. Griffin, Jr. (*Electronics*, vol. 30, pp. 162–163; May 1, 1957.) "Stacked metal-ceramic miniature magnetron operating in 2-kmc to 4-kmc range has average output power capabilities up to 10 w. Effects of operation in tapered S-band wave-

guide and ridged waveguide are given and normal operating characteristics, together with present and future applictaions, are discussed."

621.385.029.64 2974
Backward-Wave Oscillators for the 17- to 41-k Mc/s Band—J. A. Noland and R. E. Lepic. (*Sylvania Technologist*, vol. 10, pp. 13–16; January, 1957.) Two backward-wave oscillators for use as local oscillators are described; the frequency ranges covered are 17–27 kmc and 26.5–41 kmc.

621.385.032.2 2975
High-Perveance Electron Guns—R. Hechtel. (*Arch. elekt. Übertragung*, vol. 10, pp. 535–540; December, 1956.) Various methods of obtaining high perveance are outlined. Pierce's formula for calculating perveance was amplified to cover higher values and applied to a gun having a perveance of $5\mu A/V^{3/2}$; the calculated results were verified experimentally.

621.385.032.2:539.23:537.533.9 2976
The Electron Bombardment of Thin Barium Films—L. Jacob. (*Proc. Phys. Soc., London*, vol. 70, pp. 235–239; February 1, 1957.) Describes how barium is deposited as a thin film on a strontium oxide cathode by electron bombardment.

621.385.032.213 2977
Evaporation of Barium from Impregnated Cathodes—I. Brodie and R. O. Jenkins. (*J. Electronics*, vol. 2, pp. 457–476; March, 1957.) For cathodes impregnated with barium aluminate, the evaporation of barium increases rapidly when the barium-oxide/alumina molar ratio exceeds 3. The addition of calcium oxide inhibits the rate of evaporation.

621.385.032.213 2978
Studies on the Mechanism of Operation of the L Cathode: Part 1—E. S. Rittner, R. H. Ahlert, and W. C. Rutledge. (*J. Appl. Phys.*, vol. 28, pp. 156–167; February, 1957.) The emission, evaporation rate, evaporant composition, and constitution of the emitting surface were examined. Activation of the tungsten plug comes from strongly adsorbed BaO issuing from the pores. The active surface consists of a nearly complete oxygen monolayer covered by a complete barium monolayer. The emission approaches the maximum possible for a barium-activated tungsten dispenser cathode.

621.385.032.213 2979
Studies on the Mechanism of Operation of the L Cathode: Part 2—W. C. Rutledge and E. S. Rittner. (*J. Appl. Phys.*, vol. 28, pp. 167–173; February, 1957.) An experimental study including the chemistry of carbonate decomposition and barium generation, the origin of BaO in the evaporant, the barium transport mechanism through the porous plug, and the factors determining cathode life.

621.385.032.216 2980
Application of a Mass Spectrometer in an Investigation of the Process of Activation of an Oxide Cathode—N. D. Morgulis and G. Ya. Pikus. (*Zh. Tekh. Fiz.*, vol. 26, pp. 1174–1176; June, 1956.) A study of the activation processes by gas analysis is reported.

621.385.032.216:537.582:537.543.2 2981
An Investigation into the Distribution of the Work Function over the Surface of an Oxide Cathode—D. G. Bulyginski and L. N. Dobretsov. (*Zh. Tekh. Fiz.*, vol. 26, pp. 1141–1149; June, 1956.) A method is proposed for measuring the distribution of the work function in the case of heterogeneous cathodes, and a detailed report is presented on these measurements for various states of activation of an oxide cathode. The data obtained are sufficient for giving a quantitative indication of the maximum and minimum values of the work functions, their variation with temperature, etc. The local work functions have a positive temperature coefficient, the value of which is higher, the greater the work function itself.

621.385.2 2982
The Cylindrical Diode—D. A. Bell and H. O. Berktay. (*J. Electronics*, vol. 2, pp. 425–435; March, 1957.) The following features of the cylindrical thermionic diode are reviewed: 1) current density, with and without allowance for initial electron velocities, 2) the retarding-field characteristic, 3) shot noise under space-charge controlled conditions.

621.385.2 2983
Thermal Fluctuations in Space-Charge-Controlled Diodes—D. A. Bell. (*J. Electronics*, vol. 2, pp. 477–488; March, 1957.) If, in the analysis, the conservation of energy is taken into account when compounding the thermal and drift velocities of electrons in transit, then larger fluctuations are predicted than if thermal and drift velocities are linearly superimposed. For both planar and cylindrical diodes the former treatment is more nearly in accord with experimental observations.

621.385.2 2984
Initial Current Establishing Processes in a Planar Diode with an External Magnetic Field—Yu. V. Pimenov. (*Zh. Tekh. Fiz.*, vol. 26, pp. 1955–1965; September, 1956.) The initial build-up of current, under space-charge limit conditions, following the application of a pulse voltage to the anode, is considered theoretically.

621.385.3:621.373.4 2985
The Stability of Oscillations of a Triode—L. Sidériades. (*Onde élect.*, vol. 37, pp. 48–54; January, 1957.) The analysis outlined is based on the topological method applied to an equivalent dynamic system. By means of isoclines the cyclic limits of stable oscillation are found. Experimental verification is provided by the integral curves obtained on a cr tube screen.

621.385.3:621.373.421.14 2986
The High-Power Long-Pulse Triode Type TH470 and Associated Circuits—(*Rev. Tech. Comp. Franç. Thomson-Houston*, no. 24, pp. 9–29; December, 1956.)

Part 1—Special Problems of High-Frequency Pulse Generators Used in Particle Accelerators—E. P. Courtillot (pp. 11–12).

Part 2—Investigation of Valve Type TH470—J. Péhé (pp. 13–20).

Part 3—2-MW Peak Pulse Generator—J. Afanassieff (pp. 21–29).

621.385.3:621.373.421.14 2987
The Triode Type TH1500 M2—M. Descarsin. (*Rev. Tech. Comp. Franç. Thomson-Houston*, no. 24, pp. 31–39; December, 1956.) The tube described is used in 100- or 200-mc radar pulse generators.

621.385.4:546.817.221:621.396.822 2988
Investigation of the Noise of Lead Sulphide Photoresistors—A. I. Goryachev and K. A. Yumatov. (*Radiotekhnika i Elektronika*, vol. 1, pp. 1503–1514; December, 1956.) Results are presented of an experimental investigation of the dependence of noise on operational conditions and on the dimensions of the photoresistors. The results are tabulated and presented graphically.

621.385.83 2989
Systems with Centrifugal Electrostatic Focusing of the Electron Beam—Z. S. Chernov. (*Radiotekhnika i Elektronika*, vol. 1, pp. 1428–1434; November, 1956.)

621.385.832 2990
Errors of Magnetic Deflection: Part 1—J. Haantjes and G. J. Lubben. (*Philips Res. Rep.*, vol. 12, pp. 46–68; February, 1957.) A detailed analysis of the deflection errors in cr tubes. With the exception of those due to curvature of the image field, most errors can be reduced by suitable distribution of the deflecting field.

621.385.832 2991
Viewing Storage Tubes for Large Displays—H. O. Hook, M. Knoll, and R. P. Stone. (*RCA Rev.*, vol. 17, pp. 503–514; December, 1956.) Two experimental tubes are described. One provides a 10-inch-diameter display for direct viewing with 250 foot-lamberts highlight brightness; the second is a projection tube with a 4½-inch spherical luminescent screen providing more than 5000 foot-lamberts brightness. Resolution is better than 500 lines. For an earlier 4-inch half-tone viewing storage tube, see 308 of 1955 (Knoll, *et al.*).

621.385.832:621.397.6 2992
Calculation of Resolving Power of an Electron-Optical [image] Converter with Uniform Fields—B. E. Bonshtedt, T. G. Dmitrieva, and I. I. Tsakkerman. (*Zh. Tekh. Fiz.*, vol. 26, pp. 1966–1968; September, 1956.) Criticism of an assumption made by DeVore (2385 of 1948) and Wendt (1918 of 1956) in deriving an expression for the resolving power.

621.385.833.032.2 2993
A Contribution on the Triode System of the Cathode-Ray-Tube Electron Gun—M. E. Haine. (*J. Brit. IRE*, vol. 17, pp. 211–216; April, 1957.) An analysis of published experimental data suggests the system suffers from severe spherical aberration, arising from the field close to the cathode. If this limitation were overcome, a reduction in beam diameter and cathode loading would be possible.

621.387:621.318.57 2994
Cold-Cathode Gas Tubes for Telephone Switching Systems—M. A. Townsend. (*Bell Sys. Tech. J.*, vol. 36, pp. 755–768; May, 1957.)

MISCELLANEOUS

001.891:621.396(54) 2995
Programme for Radio Research in India—(*J. Sci. Indus. Res.*, vol. 15A, pp. 550–552; December, 1956.) Outline of a 5-year program drawn up on behalf of the Council of Scientific and Industrial Research, India.

061.4 2996
Instruments Electronics Automation Exhibition, 1957—Review of Equipment—(*Instr. Practice*, vol. 11, pp. 631–656; June, 1957.)

061.6 2997
Report of the Max Planck Society for the Advancement of Science, for the Period 1st April 1954 to 31st March 1936—*Naturwiss.*, vol. 43, pp. 545–580; December, 1956.) Summaries of the activities of the Institute for Ionospheric Research and of the Computer Group are included.

558.569.2.047 2998
Maximum Permissible Radiation Exposures to Man—(*Tech. News Bull. Nat. Bur. Stand.*, vol. 41, pp. 17–19; February, 1957.) A preliminary statement of the U. S. National Committee on Radiation Protection and Measurement on new safe limits. The recommendations on protection against betatron-synchrotron radiations up to 100 mev are published in *National Bureau of Standards Handbook* H55. A list of other handbooks is appended.

621.3.049.75 2999
Testing of Foil-Clad Laminates for Printed Circuitry—T. D. Schlabach, E. E. Wright, A. P. Broyer, and D. K. Rider. (*ASTM Bull.*, no. 222, pp. 25–30; May, 1957.) Methods of testing insulation resistance, peel strength, solder-dip resistance, water absorption, volume, and surface resistivity by means of specially designed test specimens are described and discussed. An arrangement of these specimens forming a composite test pattern has been developed for etching foil-clad laminates so that the various parameters can be tested on a given sample.